Developmental basis of the female excess in neural tube defects

Mohammad Raasib Mahmood

Thesis submitted to University College London for the degree of Doctor of Philosophy

2024

Developmental Biology of Birth Defects

Developmental Biology and Cancer Programme

UCL Great Ormond Street Institute of Child Health

Declaration of Contribution

I, Mohammad Raasib Mahmood, hereby confirm that the work presented in this thesis is my own. Where information has been derived from other sources, or carried out by other people, I confirm that this has been indicated in the thesis.

_____

Mohammad Raasib Mahmood

Acknowledgements

What. A. Journey. It. Has. Been. WOW! All good things come to an end, but it is the valuable lessons they leave behind that last a lifetime. How unbelievably grateful I am for the opportunities, of which I have had many, to help me get to where I am today. These opportunities and this journey is one I never thought in my wildest dreams that I would have achieved.

To the man I call THE BOSS – Prof Copp! Andy - how extraordinary lucky I have been for the opportunity to be under your mentorship and guidance. I have thoroughly enjoyed being able to work alongside you for the many years that have flown by and for the friendship we have created. Your kind nature, your calm demeanour and your thirst for research have really driven and allowed me to think in a novel and exciting way. I thank for always having an open-door policy, for putting up with all my craziness and ADHD and for being the most supportive and good human being through the tough times I have had. You really took me under your wing and helped me develop and progress at my own pace and for that I will forever be grateful. Thank you for always believing in me and for pushing me to be the best person I can be both within and also out of research. I have learnt more from you than you will ever know. I thank for all the opportunities and belief you have put in me and for sharing all your knowledge and wisdom – I sincerely hope I have done you proud, Boss.

To the man I call the OTHER BOSS – Prof Greene! Nick – my journey started with you when you took me on as your little innocent master's student. You were instrumental in fostering my love for research and for allowing me to believe in myself. Your enthusiasm and wittiness is something I truly cherish and is something I strive to be like! It been absolute honour be able to work alongside you for so many years and to be part of your group. I sincerely thank you for EVERYTHING you have done for me, you are a big reason for the person I am today and for that I thank you so dearly.

Chlo. None and genuinely I mean NONE of this would have been possible without you. You honestly have taught me every single thing I leave ICH with, and you are the

person I have worked so closely with over the past 7 years. Thank you for always being selfless, so generous, for always believing in me, for never giving up on me, for guiding me, for motivating me, for pulling me through, for encouraging me to carry on, for all the craziness I have put you through, for the countless breaks and lunches we have had, for the crazy late night phone calls, for your calming nature, for being my single-ist greatest support throughout all of this and for being my go-to person for every single thing over the past 7 years. Thank you for the laughs, jokes and giggles every day. How proud I am of everything you have achieved and how proud I am to call you family.

Dawn – the legend that is and the legend that will always be. I am so glad I met you and I am even more glad for the friendship we have made. Honestly, words cannot do justice for how I see you and how lucky I am to have worked alongside you. You have been so supportive throughout my time at ICH and have been so caring, careful, and all-around amazing throughout. You have always been there for me to vent to and to help navigate and guide me through all of this. I truly value all you have done for me and for always being there no matter what. I feel so privileged that we got to work closely together and that you were there for our countless discussions about the data, about science and about life in general!

To Makiiiii, Nads, Didi, Kit-Yi and Zo – you have all been such amazing people to be around and work with throughout my time at ICH. You have made work so fun and enjoyable and have driven me to always carry on. Without you guys I honestly do not know what I would have done – thank you for everything.

Mum, Dad, Ramsha, Raheem, Roha, Laiba and Aimen. The Family. My Family. The sacrifice, the pain, the sleepless nights, the vested interest, the commitment, the duty, the unconditional love, the never-ending support, the patience, the motivation, the unity, the stability, the constants, the calm in the storm, the togetherness, the belief, the support, the care. The struggles, the school runs, the life-changing events, the hardships. The love. Thank you for EVERYTHING. I hope I have made you ALL proud.

WE done it; WE made it.

Table of Contents

Abstract

Neural tube defects (NTDs) are severe congenital malformations affecting both cranial (anencephaly) and spinal (spina bifida) regions. Cranial NTDs are strongly female preponderant in humans and mice, whereas spinal NTDs show an equal sex ratio. This PhD project aimed to test the hypothesis that X-chromosome inactivation (XCI), the X-linked gene dosage compensation mechanism, is responsible for female predisposition to cranial NTDs. XCI consumes methyl groups and is proposed to limit their availability in female but not male cells. This reduced methylation potential limits epigenetic modification of macromolecules such as DNA, histone and non-histone proteins which puts events such as neural tube closure at risk, making females susceptible to additional genetic or environmental challenges. Culture of wild-type mouse embryos during neurulation in the presence of the methylation cycle inhibitor, cycloleucine, produced cranial NTDs that were female preponderant. However, co-culture with a further inhibitor, MGBG, which restored methylation potential, led to specific rescue of female cranial NTDs. Use of the DNA methylation inhibitor, Decitabine, induced cranial NTDs but these were not female preponderant, arguing against a major downstream role for DNA methylation. In contrast, protein methyltransferases, whose activities were predicted from measurements of methylation cycle intermediates, appeared more affected than DNA methyltransferases. Immunoblotting for SETD2-mediated trimethyl-lysine methylation, previously implicated in embryonic development, showed specific inhibition in female embryos with cranial NTDs. Combining low-dose Decitabine with cycloleucine treatment was found to rescue female embryos from cranial NTDs. This effect appeared likely to result from partial reactivation of an X-chromosome, as the rate of sex chromatin (Barr body) positive cells was reduced, and expression of X-linked genes was increased, specifically in rescued female embryos. This work supports the XCI-related hypothesis of female excess in cranial NTDs, and suggests a key role for protein methylation in the embryonic mechanism of cranial neural tube closure.

Impact statement

Sex differences in disease frequency and severity are common and can provide information on pathogenic mechanisms as well as having health care implications. While direct or indirect effects of the sex hormones are often implicated, it is striking that a sex bias can also occur in clinically important birth defects that arise before the stage of gonad development or onset of sex steroid secretion. Understanding how such early arising malformations affect the sexes differentially may provide significant insight into developmental and preventive mechanisms. Cranial NTDs, in the form of anencephaly, are a well-known example of a sex-biased birth defect. Females are 1.5-2 times more often affected by anencephaly than males, whereas the closely related defect spina bifida shows an equal sex ratio. In mice, exencephaly (the developmental forerunner of anencephaly) is also more common in females. Hence, the female excess in anencephaly may be a general mammalian phenomenon.

In this PhD, the first experimental testing of the X-inactivation epigenetic “methyl sink” hypothesis was performed, and many lines of evidence were found to support it. Findings from this study also discovered a regional sex difference in the brain regions affected, with most female mouse embryos failing to close the hindbrain whereas male embryos usually failed to close the forebrain. In humans, anencephaly can affect the whole brain (holoacrania) or can be partial (meroacrania), but the individual sex ratios of such anatomical variations are unknown. This PhD’s findings on regional brain defects will prompt comparable studies in humans in future.

For many decades, the best-known method for reducing the rate of anencephaly has been folic acid supplementation during pregnancy. Strikingly, a greater reduction in anencephaly among females versus males has been reported in human studies of folic acid usage. This PhD work suggests that folic acid may have a specific rescuing effect for females via stimulation of methylation cycle function, and provision of methyl groups. However, folic acid is an un-methylated, synthetic form that needs conversion to tetrahydrofolate (THF) to become active. In contrast, the naturally occurring folate,

5-MeTHF, and the 1-C donor betaine both donate methyl groups directly to homocysteine, forming methionine which stimulates the methylation cycle. 5-MeTHF (marketed as Metafolin), and choline the precursor of betaine, have been suggested as more bio-available alternatives to folic acid for NTD prevention. An extension of this PhD work could possibly assess the relative effects of 5-MeTHF and betaine and their effectiveness in preventing NTDs and overcoming the female excess, compared with folic acid.

This PhD may represent the first example of a basic science study that can explain a sex bias in an early-arising birth defect, anencephaly, before the development of gonad-derived sex steroids. It is possible that approaches used in this study may stimulate comparable approaches to understand sex bias in other developmental disorders, such as Hirschsprung Disease and Di George Syndrome, which are important causes of human disability and ill-health.

List of Figures

List of Tables

Abbreviations

1C – 1 carbon

5-methylTHF – 5 methyl tetrahydrofolate

ANP – anterior neuropore

APP-1 – amyloid precursor protein

BHMT – betaine-homocysteine methyltransferase

BMP – bone morphogenic protein

Bcl10 – B-cell lymphoma/leukemia 10

CBS – Cystathionine-β-synthase

CNCs – cranial neural crest cells

CNS – central nervous system

CO_2 – carbon dioxide

Cdc42 – Cell division control protein 42

Ct – curly tail

Cx43 – Connexin 43

DFMO – difluoromethylornithine

DLHP – dorsolateral hinge point

DMEM – Dulbecco's Modified Eagle Medium

DNA – deoxyribose nucleic acid

Dnmt – DNA methyltransferase

E – embryonic day

E-cadherin – Epithelial cadherin

ESCs – embryonic stem cells

ETDA - Ethylenediamine tetraacetic acid

Efna5 – ephrin A5

FB – forebrain

FBS – fetal bovine serum

FGF – fibroblast growth factor

G6pdx - glucose-6-phosphate dehydrogenase X-linked

Grhl3 – grainyhead like 3

HB – hindbrain

HNP – hindbrain neuropore

Hipk – homeodomain-interacting protein kinase

Hprt – hypoxanthine phosphoribosyltransferase 1

Inka – inka box actin regulator 1

K_i – inhibitor constant

K_m - Michaelis constant

LINE-1 – loong interspersed elements 1

MAT – methionine adenosyl transferase

MB – midbrain

MECP2 – methyl-CpG binding protein 2

MGBG – Methylglyoxal bis(guanylhydrazone)

MHP – medial hinge point

MS – methionine synthase

MTHFR – Methylenetetrahydrofolate reductase

Marcks – Myristoylated alanine-rich C-kinase substrate

Mid1- midline 1

Momme D1 – modifiers of murine metastable epiallele D1

Msx2 – Msh homebox 2

N-cadherin – neural cadherin

N_2 – nitrogen

N_2O – nitrous oxide

NCCs – neural crest cells

NTDs – Neural tube defects

Nf - Neurofibromatosis type

O_2 – oxygen

OD – optical density

ODC – ornithine decarboxylase

PAX – Paired-box

PBS – phosphate buffer saline

PCP - planar cell polarity

PCR – polymerase chain reaction

PEMT – Phosphatidylethanolamine N-methyltransferase

PNP – posterior neuropore

PRC1 - Polycomb Repressive Complex 1

PTCH1 – Protein patched homolog 1

PVDF – polyvinylidene fluoride

Pdn - Polydactyly Nagoya

Phactr4 – phosphatase and actin regulator

qPCR – quantitative polymerase chain reaction

RIPA – Radioimmunoprecipitation assay buffer

RNA – ribose nucleic acid

Rac1 – Rac Family Small GTPase 1

SAH – S-adenosylhomocysteine

SAM – S-adenosylmethionine

SAMDC – S-adenosylmethionine decarboxylase

SD – standard deviation

SDS-PAGE – sodium dodecyl sulfate–polyacrylamide gel electrophoresis

SEM – standard error of mean

47

SHH – sonic hedgehog

SMCDH1 – structural maintenance of chromosomes flexible hinge domain 1

SMO – Smoothened, Frizzled Class Receptor

Shroom4 – shroom family member 4

Sry – sex-determining region Y gene

TAE – Tris base, acetic acid and EDTA

TBS - Tris-buffered saline

TBST - Tris-buffered saline with 0.1% Tween

THF – tetrahydrofolate

Trp53 – transformation related protein 53

Twist – twist family bHLH transcription factor 1

WNT – Wingless-related integrations site

XCI – X chromosome inactivation

XCR – X chromosome reactivation

Xist – X-inactive specific transcript

ZIC – Zinc finger protein

Chapter 1. General Introduction

1.1 Neurulation: the development and closure of the neural tube

The formation and closure of the neural tube begins on embryonic day (E)8.5 in mouse and is completed by E10.5, the equivalent to 21-28 days post-coitum in humans. The formation and closure of the neural tube occurs via a process known as neurulation and is characterised by various changes in morphology and shape of the neural plate that cause the elevation and bending of the neural folds (Wallingford et al., 2013). Subsequently, these folds merge to create a hollow tube, the neural tube, that ultimately differentiates into the central nervous system's brain and spinal cord. The process of neurulation is complex and involves various intricate and finely tuned cellular and molecular processes (Wallingford et al., 2013).

1.2 Neural induction and convergent extension: the initiation of neural tube closure

The neurulation process initiates during the post-implantation stage following the establishment of germ layers. Neural induction, the initial step in neural tube formation, is triggered by "the node" or 'organiser' situated at the anterior end of the primitive streak. This node signals nearby ectodermal progenitors to differentiate into neural cells (neuroepithelium), while the remaining epithelial cells commit to forming the epidermis (surface ectoderm). Induced by morphogens like Sonic hedgehog (Shh) and Bone morphogenic protein (Bmp), the neuroepithelium undergoes significant changes, with Shh from the notochord inducing the ventral/midline neural tube to form and bend, and Bmp leading to cell proliferation and thickening of the dorsal neural ectoderm. The neural plate, initially a flat cell sheet, transforms into a pseudostratified columnar neuroepithelium, stretching over the notochord from the node to the prechordal plate, creating a midline neural groove depression.

Prior to the initiation of neural tube closure, the flat embryonic disc undergoes shaping, by a process known as convergent extension. This causes the neural plate, and underlying mesoderm to elongate in the anterior-posterior axis and to narrow in the medial-lateral direction. Convergent extension involves directional cell orientation, facilitating intercalation in the midline (Keller, 2002). This narrowing of the neuroepithelial cell layer is essential for its subsequent closure to form the neural tube. The changes in the positioning and behaviour of these cells is controlled by the non-canonical Wnt/planar cell polarity (PCP) signalling pathway which involves the interaction between genes encoding some of the major proteins involved in convergent extension: the 'core' pathway proteins and 'Fat-Dachsous' pathway proteins. The core proteins comprise the cytosolic proteins Scribble, Dishevelled, Prickle and Inversin, and a group of transmembrane receptors proteins such as: Vangl1/2, Frizzled and Celsr1/2/3 (Carvajal-Gonzalez et al., 2016; Nikolopoulou et al., 2017). In the Fat/Dachsous pathway, the cadherin proteins, Dachsous and Fat, form part of the signalling cascade that runs in parallel or upstream of the PCP core pathway (Carvajal-Gonzalez et al., 2016; Nikolopoulou et al., 2017).

1.3 The progression of mammalian neurulation

Once induced and established, the neural plate undergoes intricate morphological transformations to give rise to the hollow neural tube. In the primary neurulation process, the neuroepithelial layer experiences a sequence of elevation and folding events, facilitated by the adjacent paraxial mesoderm. These events cause the lateral edges of the neuroepithelial layer to elevate, forming paired parallel neural folds. Subsequently, through bending along the body axis, these folds appose and fuse at the dorsal midline, resulting in the formation of the neural tube. Once fused, the neural tube separates from the ectoderm layer, leaving a continuous surface ectoderm layer above the closed neural tube (Copp and Greene, 2010).

Neural tube closure in mice follows a discontinuous pattern and initiates at specific sites known as closure points. From these initiation sites, neurulation progresses through a 'zippering' mechanism, leading to the shortening and closure of open neural

fold regions called neuropores (Copp and Greene, 2003; Galea et al., 2017). The positioning and events of each closure point along the anterior-posterior axis are illustrated in Figure 1.1.

The first contact site, referred to as Closure 1, emerges at the hindbrain-cervical spine boundary at E8.5. From this site, zippering occurs bidirectionally, closing part of the hindbrain neuropore (HNP) rostrally and the spinal neural tube caudally, extending down to the posterior neuropore (PNP). Another initiation site, Closure 5, forms at E10.5 at the posterior end of the embryo, contributing to the completion of spinal closure (Galea et al., 2017). Closure 2, the second point of *de novo* contact, initiates at the forebrain-midbrain boundary at E9.0. Zippering from this site covers theforebrain rostrally and the midbrain and rostral part of the HNP caudally. The third initiation site, Closure 3, forms at the most rostral extremity, completing the closure ofthe anterior neuropore (ANP), with zippering progressing only in the caudal direction (Greene and Copp, 2010; Copp and Greene, 2013).

The closure of the forebrain, hindbrain and spinal neural tube occur in a zipper-like fashion; however, the closure of the midbrain region appears to occur via an alternative mechanism that is described as a ‘buttoning-up’ process (Pyrgaki et al., 2010). The cranial neural tube is closed by E9.5 in mouse whereas closure of the spinal neural tube is achieved by E10.5, thereby concluding primary neurulation. Secondary neurulation forms the most caudal part of the neural tube, from the mid- sacral to the coccygeal regions, by condensation of a population of tailbud-derived cells, which form the neural tube lumen by canalisation (Copp, Greene and Murdoch 2003; Greene and Copp, 2010, Greene and Copp, 2013).

The failure to form the initial contact points, or the failure of zippering to progress from these points, result in disruption of neurulation and leads to congenital malformations termed Neural Tube Defects (NTDs).

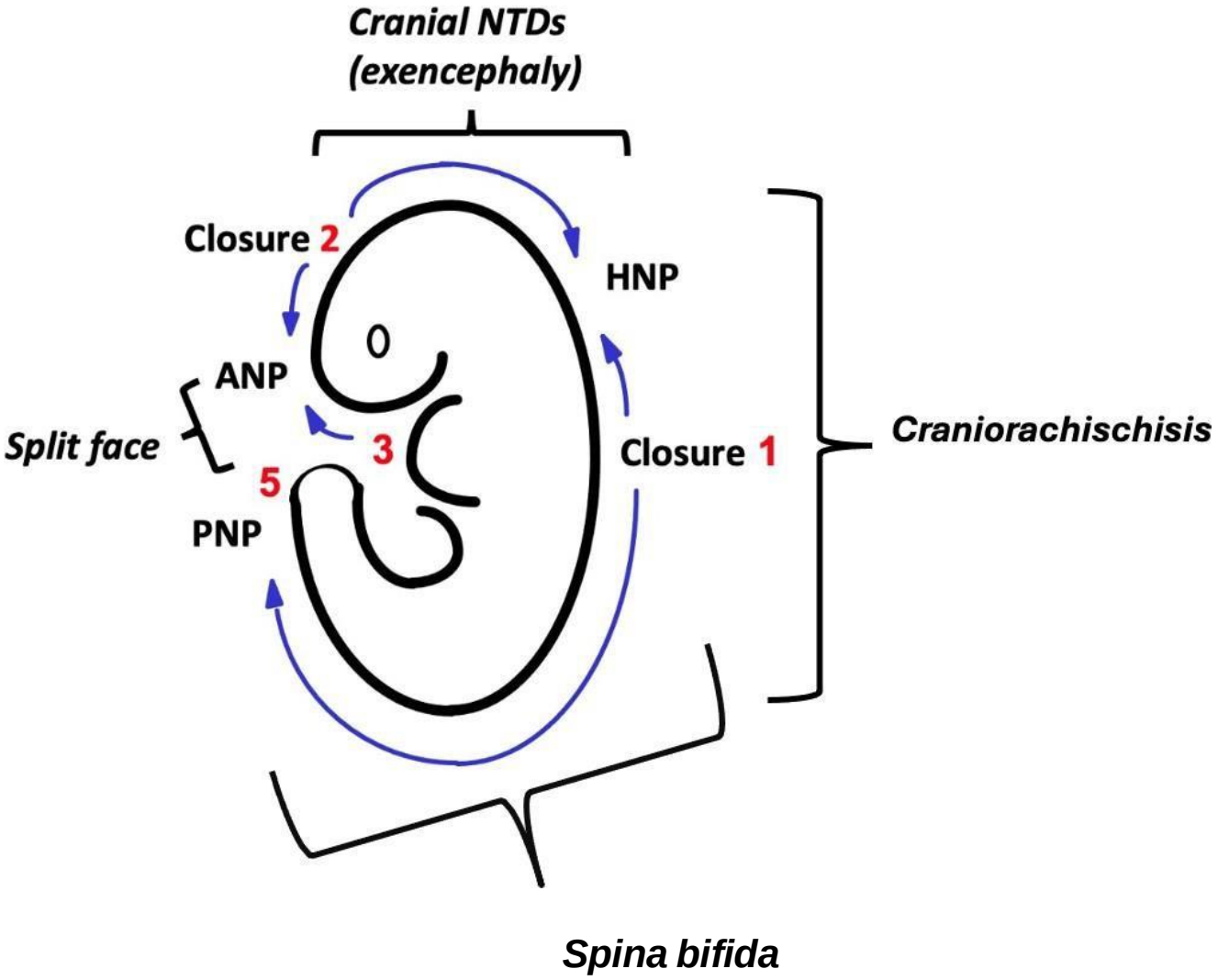

Figure 1.1. Mouse neurulation: the anterior-posterior position of closure points and zippering events that occur during neural tube closure and the consequential NTDs that arise when neural folds fail to close. Closure points, which are the initial sites of contact and fusion that occur during neural tube closure, are depicted with arrows showing the direction of closure from each initial contact point. Failed closure of the hindbrain neuropore (HNP) and the head region results in exencephaly, which in some cases is accompanied by split face when the anterior neuropore (ANP) fails to close. Failure to close the posterior neuropore (PNP) results in spina bifida.

1.4 The process of neural tube closure, with a focus on the cranial region

The closure of the cranial neural tube appears more complex than spinal closure and involves a number of specialised cellular, morphological, and molecular processes such as: the establishment of morphogenic signalling gradients, the formation of morphogen-induced hinge points, the specification and emigration of neural crest cells before closure, changes in mesenchymal cell density, cytoskeletal-mediated changes in cell shape, cell adhesion and fusion events and a balance between cell proliferation and apoptosis. This complexity may explain why failed cranial neural tube closure prevails in comparison to failed spinal neural tube closure amongst the many known genetic NTD mouse models (Harris and Juriloff, 2010). A summary of the morphogenetic processes involved in cranial neural tube formation is shown in Figure 1.2.

1.4.1 Morphogenic regulation

The control of cell behaviour and cell fate during embryonic development is governed by various cues, in particular morphogens, which are developmental signals vital in regulating various cellular events needed in establishing changes in tissue size and shape.

Morphogens are diffusible molecules that are secreted and expressed in a spatio-temporal gradient-like manner. In the context of neural tube closure, key morphogens include Shh, BMPs, fibroblast growth factors (FGFs), and Wingless-related integration sites (Wnts). Together, they play a crucial role in determining the dorso-ventral and rostro-caudal axes of the developing and neurulating embryo.

Shh is a ventralising morphogen that emanates from the notochord and the floor plate during neurulation, and which establishes a high-to-low gradient in the neural tube. Shh signalling induces formation of the neural groove and floor plate and therefore

influences neural fold elevation and bending. This process involves the binding of SHH protein to the transmembrane receptor Patched1 (PTCH1), activating SMO signalling and inducing GLI transcription factors. These factors translocate to the nucleus, regulating downstream target genes. One such target is the Pax3 gene, whose inhibition by SHH prevents dorsal identity in the ventral neural tube region (Carballo et al., 2018; Copp and Greene, 2013).

In contrast to Shh, BMP and Wnt signaling act as dorsalising factors, crucial for establishing the dorsal aspect of the neural tube. Wnts, secreted from the epidermal ectoderm adjacent to neural folds' dorsal tips, activate BMP and slug expression in presumptive neural crest cells (NCs). Wnts also contribute to maintaining Pax3 expression in the dorsal neuroepithelium, which is needed to maintain dorsal identity. BMPs, secreted from the non-neural ectoderm and roof plate, bind to BMP receptors, regulating downstream Smad protein expression. Smad protein complexes translocate to the nucleus, mediating the transcription of other genes (Bond et al., 2012).

The directional and axial establishment of the neural tube heavily relies on the role of morphogens. Mutations in morphogen genes or related genes in their signalling pathways can lead to NTDs due to the critical functions these signals perform during neural tube development (Murdoch and Copp, 2010).

1.4.2 Hinge point formation: the focal point of neural plate bending

In addition to orchestrating cellular events crucial for altering tissue size and shape, morphogenic signals also play a vital role in the formation of hinge points, specific sites on the neural plate – in some cases involving marked changes in cell shape – that are needed for bending of the neural plate and elevation of the neural folds.

The initiation of the first hinge point, known as the medial hinge point (MHP), is induced by Shh signalling from the notochord, an axial mesodermal structure underlying the

neural tube. Neuroepithelial cells at the midline undergo a slowdown in the cell cycle, resulting in a prolonged S-phase. Due to the pseudo-stratified nature of the neuroepithelium and its inter-kinetic nuclear migration, notochord signalling causes the nuclei of neuroepithelial cells to shift basally, while the apical cell borders constrict. This morphological change gives rise to wedge-shaped cells connected at narrow cell apices, forming the MHP along the neural plate's midline (Juriloff and Harris, 2018). This arrangement facilitates the elevation and midline apposition of the neural folds, particularly at upper spinal levels where the MHP serves as the only site for neural plate bending (Shum et al., 1996).

In addition to the MHP, bilateral hinge points, called dorsolateral hinge points (DLHPs), emerge approximately one-third of the way down from the dorsal neural fold tips in the dorso-ventral aspect. DLHP formation is crucial for the tips of the low spinal neural folds to come into close apposition for fusion and closure at the dorsal midline (Copp and Greene, 2003; Yamaguchi and Miura, 2013). DLHP-like bending points also arise in the cranial region, following an initial phase in which cranial mesodermal expansion leads to enlarged, convex cranial neural folds. In the second phase, DHLP-like bending begins, and converts the neural folds to concave structures, that are able to close in the midline (Morriss-Kay et al, 1981).

While a reduction in Shh expression does not cause NTDs, overexpression of Shh leads to NTDs due to the loss of Shh downstream negative regulators like Ptch1 and the inhibition of Noggin, an antagonist of Bmp expression which is crucial for DLHP formation (Murdoch and Copp, 2010). This regulatory network was identified in spinal neurulation (Ybot-Gonzalez et al., 2007) and, may also apply to the cranial region, although this remains unclear. However, mutations in dorsally expressed genes like Zic2 (*Kumba* mutant) and Pax3 (*splotch* mutant) result in both spinal and cranial NTDs and therefore suggest the existence of a similar dorso-ventral regulatory system in cranial neural tube closure (Epstein et al., 1991).

1.4.3 Apical constriction

Apical constriction is the process by which cytoskeletal proteins such as F-actin and myosin II accumulate at the subapical cortex and circumference of cells, arranged as microfilaments. Activation of myosin II leads to the contraction of the actomyosin apical network, inducing cell narrowing (Martin and Goldstein, 2014). This phenomenon is crucial in cranial neural tube closure, involving the presence of an actin cable at the boundary between the surface ectoderm and neuroepithelium, facilitating the complete closure of the hindbrain neural plate (HNP) (Nikolopoulou et al., 2017; Maniou et al., 2021). Myosin-driven contraction of cell apices at the medial hinge point (MHP) causes cells to adopt a wedge-shaped morphology, resulting in the bending of the neuroepithelium. The maintenance of actin cytoskeletal dynamics is indispensable for cranial neural tube closure but not for spinal neural tube closure as evidenced by the disruption caused by actin assembly-inhibiting drugs like cytochalasins, leading to cranial NTDs in cultured rodent embryos (Ybot-Gonzales and Copp, 1999) . Similarly, mice carrying mutations in genes encoding cytoskeletal proteins, such as vinculin, exhibit cranial NTDs (Morris-Kay and Tuckett, 1985; Xu et al., 1998).

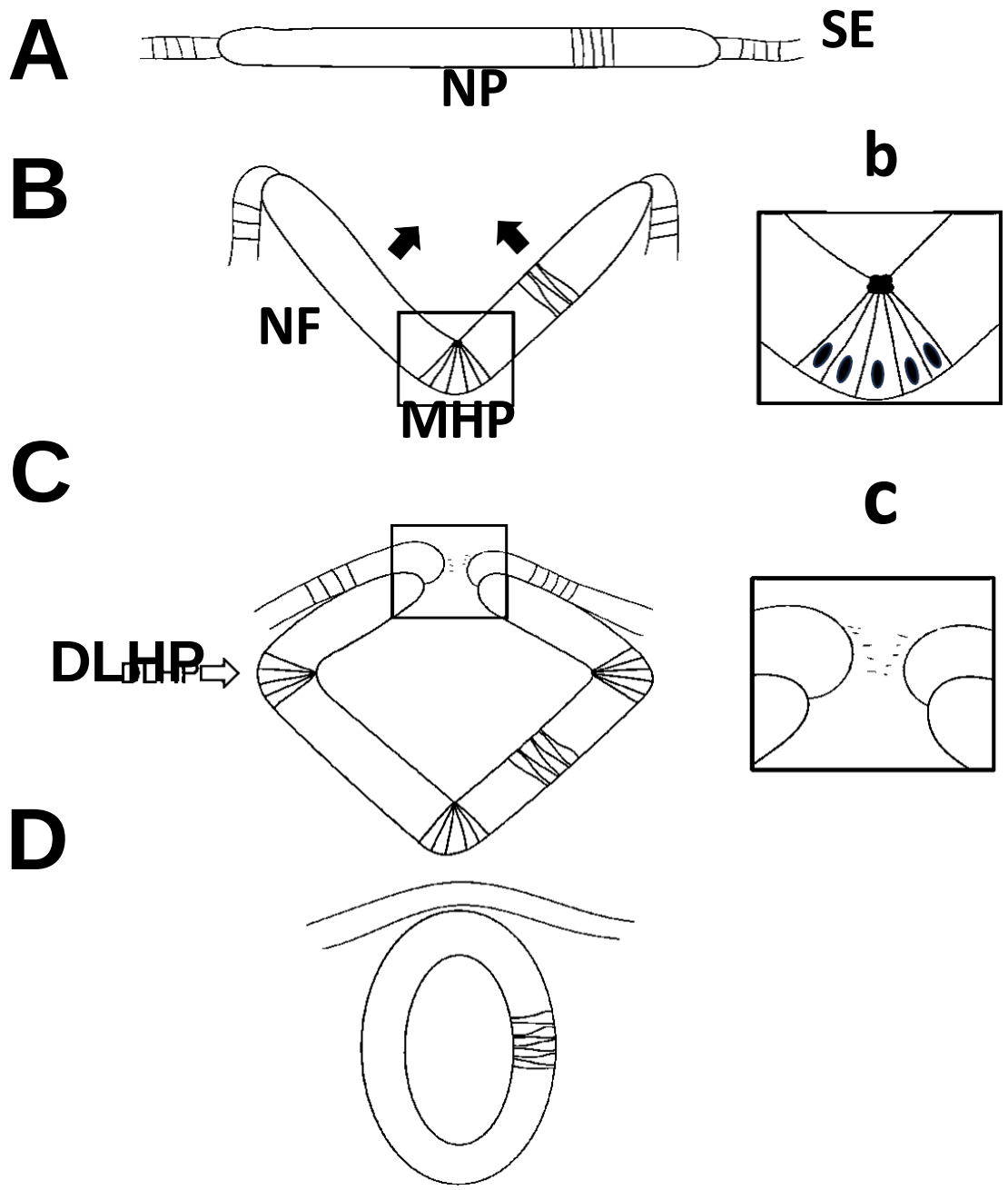

Figure 1.2. The stages of mammalian neurulation. Cross-sectional schematic showing the stages of cranial neurulation. **(A)** The flat neural plate and adjacent non-neural surface ectoderm. **(B)** The formation of the medial hinge-point formation results in a morphological change in shape of the neural groove and results in the elevation of the neural folds. **(b)** Illustration of midline neuroepithelial cells that undergo apical constriction which is mediated by actomyosin (actin and myosin) at their apex. **(C)** Dorso-lateral hinge-point formation results in the neural folds becoming close in apposition. **(c)** Filopodia and ruffles extensions establish the first contact points between the apposed neural fold with connection made across the dorsal midline. **(D)** The neural folds fuse medially, separating the epidermis from the neural tube. DLHP dorso-lateral hinge-point, MHP medial hinge-point, NF neural fold, NP neural plate, SE surface ectoderm. Image adapted from (Werner et al., 2020).

1.4.4 The expansion of the cranial mesoderm

Adjacent to the cranial neural tube is the paraxial cranial mesenchyme, a meshwork of connective tissue consisting of the cranial mesoderm and migrating cranial neural crest cells (cNCCs), once they have delaminated from the dorsal tips of the neural folds (Kinder et al., 1999). Changes in the cranial mesoderm are known to be essential for cranial neural tube closure: the reorganisation of the cranial mesoderm is thought to be essential in aiding and establishing the process of cranial neural fold elevation. The cranial mesenchyme undergoes expansion, driven by both mesenchymal cell proliferation and increased spaces between cells due to a higher concentration of hyaluronan, which absorbs water into the extracellular matrix of the cranial mesenchyme (Zohn and Sarkar, 2012). It is suggested that cells in the cranial mesenchyme become more densely packed in the lateral region and less dense in the medial region, changes in the cranial mesenchyme cell density that are thought to aid the transition of the cranial neural folds from its biconvex-to-biconcave morphology (Zohn and Sarkar, 2012; Morris-Wiman and Brinkley, 1990). Abnormalities in the cranial mesenchyme have been implicated as part of the process by which cranial NTDs are caused in several mouse models, including the *Inka* and *Twist* mutants. *Twist* encodes a transcription factor that is suggested to regulate cranial mesenchyme development. In *Twist* mutant embryos that present with cranial NTDs, the cell morphology in the cranial mesenchyme is abnormal with cells appearing more rounded with disrupted cell contacts, findings which suggest that abnormalities in the cranial mesoderm can result in abnormal closure of the cranial neural tube (Zohn and Sarkar, 2012).

1.4.5 Cranial Neural Crest Cells

Cranial NCCs are a subset of multipotent cells that form at the boundary of the neural plate where the dorsal neural fold tips of the neuroectoderm and non-neural surface ectoderm make contact (Kulesa et al., 2010). There is anterior-posterior variation in the origin of NCCs along the cranial region. In the midbrain, NCCs arise from all axial

levels whereas, in the hindbrain, NCCs arise from the neural folds primarily within even-numbered rhombomeres (2, 4 and 6). Rhombomeres 3 and 5 generate only sparse NCCs. Rhombomeres are the axial compartments of the hindbrain, defined by their patterns of Hox gene expression (Wilkinson et al., 1993). The anterior forebrain does not appear to produce any NCCs and, instead, NCCs migrate into the rostral forebrain from the caudal forebrain and midbrain.

A proposal in this thesis is that emigration of neural crest cells plays a direct role, and is required for, cranial neural tube closure. Evidence for this idea comes from the finding that NCCs detach from the midbrain and hindbrain neural fold apices prior to cranial neural tube closure. They are already migrating within the cranial mesenchyme, in both ventral and rostral directions, by the time the cranial neural folds approach each other for apposition and fusion (Santagati et al., 2003; Morriss-Kay and Tan, 1987). This differs from the spinal region where NCC emigration occurs some hours after closure is complete. Another line of evidence is that craniofacial defects, which often result from disrupted NCC migration, are associated with cranial NTDs in several mouse mutants (AP-2α, Cited2, Cx43, Laminin α5, Msx2 and Zic5).

It is possible that the decrease in cellular density from where the NCCs migrate allows for mechanical flexibility to mediate the inward bending of the neural fold tips, during cranial DLHP formation (Copp and Greene, 2013). Hence, delayed, or diminished migration of NCCs may disrupt the biomechanics of neural tube closure given NCC detachment and emigration is a cellular process that is a pre-requisite for cranial neural tube closure.

1.4.6 Neural fold adhesion and fusion

Cytoskeletal dynamics and processes are important in mediating the cellular adhesion and fusion events that occur during neural tube closure. Cytoskeletal dynamics and processes play a crucial role in facilitating cellular adhesion and fusion events during neural tube closure. Initial contact along the neural tube involves various cell

protrusion structures, such as lamellipodia, filopodia, and/or ruffles, under the control of small GTPases Rac1 and Cdc42 (Rolo et al., 2016). For the closure of the midbrain and hindbrain neural folds, the first point of contact made at closure 2 is by the non-neural surface ectoderm that overlies the tips of the neural folds (Massarwa and Niswander, 2012). Although the molecular basis governing the adhesion and fusion events of neural folds remains unknown, several cranial NTD mouse models have identified possible molecules that may be involved in this process.

One crucial player identified in regulating cell interaction during neural tube zippering at fusion sites is the cell adhesion cadherin protein. Cadherins are thought to mediate these effects either directly at the fusion site or indirectly by modulating the surface ectoderm (Nikolopoulou et al., 2019). N-cadherin is expressed in the neural ectoderm, while E-cadherin is predominantly expressed in the non-neural surface ectoderm. Studies have demonstrated that inhibiting or blocking the expression of N-cadherin or E-cadherin in the cranial neural folds, using antibodies or antisense oligonucleotides, can lead to cranial NTDs (Radice et al., 1997). These findings suggest that cell adhesion and fusion events at the foci of neural fold tips are crucial for cranial neural tube closure.

Other essential molecules involved in the adhesion and fusion of adjacent cranial neural folds include Ephrin ligands and their cell surface receptors, Ephs. Loss of ephrin-A5 and EphA7 in mouse embryos has been shown to result in cranial NTDs (Holmberg et al., 2000). Additionally, cranial NTDs have been observed in embryos with mutations in neurofibromatosis type 2 (*Nf2*). Nf2 mediates the assembly of neuroepithelial apico-lateral junction complexes. While these embryos complete primary neurulation as normal, the Nf2 deficiency disrupts the integrity of cell-cell adhesions, causing the cranial neural tube to re-open and resulting in cranial NTDs (McLaughlin et al., 2007). Apoptosis - the developmental process of programmed cell death - is mediated by cleaved caspases and results in the shrinkage and fragmentation of cells.

1.4.7 Apoptosis

Apoptosis has been observed in both the neural ectoderm and the non-neural surface ectoderm and more specifically in the dorsolateral bending regions of the neural plate and at the dorsal neural fold tips (Yamaguchi et al., 2013). Although it remains unknown what role apoptosis plays in cranial neural tube closure, apoptosis appears to coincide with the emigration of cranial NCCs at dorsolateral regions, which suggest that apoptosis may be essential in aiding the loosening of the neural tissue for the formation of the DLHPs and therefore the transition of neural folds to a biconcave shape. On the other hand, apoptosis at the neural fold tips may be required for the remodelling of the surface ectoderm and neuroepithelium when they separate into different layers after fusion, and therefore plays a role in finalising and remodelling the closure process (Copp, 2005). Both an excess and reduction of cell death have been associated with cranial NTDs, suggesting that the level and extent of apoptosis must be finely balanced in order for the cranial neural tube to close. For example, cranial NTDs have been observed in *Apaf-1* mouse mutants in which apoptosis is reduced (Honarpour et al., 2001) whereas the knockout of *Bcl10*, which encodes an anti-apoptotic protein, also results in increased cell death and the development of cranial NTDs, perhaps due to the disruption of the mechanical or functional integrity of the neuroepithelium (Copp and Greene, 2013). Despite this, the importance of apoptosis for cranial neural tube closure has not been recapitulated in vitro as pharmacological inhibition of apoptosis in culture experiments was not shown to cause NTDs, and so it remains unknown whether the suppression of apoptosis alone can cause NTDs (Massa et al., 2009).The in vivo versus in vitro difference in the role apoptosis may have in cranial neural tube closure may be a result of the exposure of embryos to inhibitory apoptotic signals. For instance, the exposed concentrations of drugs used to inhibit apoptosis may not accurately reflect physiological conditions and the distribution of these signals may be influenced by factors such as tissue barriers, metabolism, and pharmacokinetics. In addition, in vitro, the maternal immune system components are typically absent, which can significantly alter apoptotic processes since immune cells can induce or inhibit apoptosis given that immune system plays a crucial role in regulating apoptosis through the release of cytokines, direct cell-cell interactions, and phagocytosis of apoptotic cells.

1.4.8 Cell proliferation

The process of neurulation coincides with a period of rapid growth of the embryo, with the highest rate of proliferation being observed in the neuroepithelium and in the expanding underlying cranial mesoderm (Copp and Greene, 2013). A reduction in the rate of cell proliferation can therefore result in abnormal growth during neurulation and may disrupt the normal process of cranial neural tube closure. Diminished cell proliferation has been observed in the cranial neuroepithelium of *Pax3 Splotch* mutant embryos, which exhibit cranial NTDs, and this defect has been shown to be rescued by the addition of folic acid, possibly as a result of correcting downstream nucleotide biosynthesis cellular reactions (Sudiwala et al., 2019). On the other hand, excessive cell proliferation has also been associated with cranial NTDs in some mouse mutants though it remains unknown what the underlying mechanism in these mutants are. In the case of *Phactr4* mutants, excessive proliferation has shown to lead to an overgrowth of the neuroepithelium in the ventral aspect of the embryo, with failed closure of the cranial neural tube in these mutants. This is possibly caused by the increased mass and stiffness and thus reduced flexibility of the neuroepithelium to undergo the morphological changes in shape needed for closure (Kim et al., 2007).

1.5 Neural tube defects in humans and mice

1.5.1 Differences between cranial neurulation in human and mouse embryos

Cranial NTDs are more prevalent among the nearly 300 genes causing NTDs in mouse models, with an approximate ratio of 3:1 for cranial to spinal defects (Juriloff and Harris, 2018). In contrast, human NTD-affected cases show a similar occurrence of cranial and spinal defects (Zaganjor et al., 2016).

Although the process of neurulation is very similar in mouse and human embryos, noticeable differences do exist. As previously described, the process of neural tube closure in mouse initiates at three distinct closure sites. However, contradicting reports have appeared of whether closure 2 exists in human embryos. In one study, it was reported that multiple closure points, including a neurulation event that is like closure 2, do form in human embryos (Nakatsu et al., 2000). However, a later study that looked at almost twice the number of human embryo samples did not find a fusion event similar to closure 2 despite identifying closure points in the rhombencephalon and prosencephalon region, which correspond with mouse closures 1 and 3, respectively (O'Rahilly and Muller, 2002). This suggests that closure 2 may be absent from human neurulation, and so non-essential for neural tube closure. Interestingly, closure 2 has also been found to be omitted in embryos of the SELH/Bc mouse stock, a strain in which cranial NTDs only affect around a fifth of embryos. Despite omission of closure 2, the majority of SELH/Bc embryos still manage to complete cranial neural tube closure as a result of extending zippering in the caudal direction from closure 3 (MacDonald et al., 1989). The combined findings from human and mouse studies suggest that closure 2 may not be a critical factor for neural tube closure in mammals.

If closure 2 is indeed absent in human cranial neurulation, the question arises as to why. One dissimilarity between human and mouse embryos is the relative size of the cranial neural folds. In human embryos, the cranial region appears relatively smaller compared to the mouse embryo at the equivalent stage (Copp, 2005). This size difference may explain the higher number of mouse mutants with cranial NTDs. The cranial neural tube in human embryos might be mechanically easier to close than in mice, potentially leading to the evolutionary emergence of closure 2 in mouse development, which is absent in human neurulation.

1.5.2 Frequency of human NTDs

The average worldwide prevalence of NTDs is around 10 per 10,000 live births, although with marked geographical variations. In the US, from 2009 – 2011, the prevalence of NTDs was 6.5 births per 10,000 (Williams et al., 2015) and in Europe, 9 to 11.5 per 10,000. Higher rates such as 15.8 per 10,000 births in South-East Asia (Zaganjor et al., 2016) and 63.4 per 10,000 births in Ethiopia (Gedefaw et al., 2018) are often encountered in resource-poor countries. Among all categories of birth defects, NTDs are the second most common, after congenital heart defects.

1.5.3 Causation of NTDs

The aetiology of open NTDs is multifactorial. Although most NTDs are sporadic and do not show a Mendelian pattern of inheritance there are some NTDs that appear to have a genetic component, as is evidenced from the increased risk of NTD recurrence following a first affected pregnancy (Harris and Juriloff, 2007). Despite this, incomplete penetrance of NTDs has been observed in families in which both the parents and the child carries an NTD-associated genetic polymorphism, but the NTD does not present in both generations – findings which suggest that perhaps both genetic and environmental factors contribute to the penetrance of NTDs (Copp and Greene, 2013).

1.5.3.1 Genetic predisposition to NTDs

Evidence for a genetic contribution to NTDs has come from both population-based and family-based case studies. The recurrence risk of an NTD affected pregnancy following a previous affected pregnancy has shown to range from 2.3 - 6%, a risk that is 8-20-fold higher than the population risk of an NTD-affected pregnancy (Czeizel and Metneki, 1984; Cowchock, 1980; Elwood and Elwood, 1980), with a recurrence risk of 10% for women who have had multiple previously affected pregnancies (Rampersaud et al., 2006). An increased NTD-affected pregnancy risk has also been found in first- degree relatives of NTD cases (Toriello and Higgins, 1983). The risk in monozygotic twins exceeds that in dizygotic twins (Janerich and Piper, 1978; Elwood and Elwood, 1980).

In line with a genetic contribution to NTD risk, a number of genetic polymorphisms have been associated with NTD occurrence. One of the strongest associations is the C677T missense mutation in the *MTHFR* gene, which functions in folate one-carbon

metabolism, and has been shown to result in a 1.8-fold higher risk of an NTD-affected pregnancy in non-Hispanic populations (Yan et al., 2012; Amorim et al., 2007).

In addition to human studies, the large number of mouse mutants with NTDs also suggests a genetic component to the susceptibility of NTDs. Both single mutant genes and genetic (strain) backgrounds have been shown to contribute to the penetrance of NTDs in mice, with the background strain effect representing the occurrence of modifier genes. This latter concept may be especially relevant in human cases where a higher risk of NTDs may occur amongst certain populations and/or where NTDs result from the accumulation of several genetic risk factors that individually are insufficient to cause abnormalities (Copp and Greene, 2014).

1.5.3.2 Contribution of environmental factors to NTDs

Lower socioeconomic status correlates with an increased risk of human NTDs, a correlation that is thought to reflect the accessibility of individuals at high-risk of birth defects to nutritional factors. Lower blood levels of the B-vitamin folate have been observed in mothers of NTD foetuses (Smithells et al. 1976), a finding which prompted an investigation into whether the addition of a folic acid–containing multivitamin supplement could prevent the recurrence of NTDs (Smithells et al. 1980). A multicentre randomised controlled trial confirmed that maternal folic acid supplementation (at 4 mg per day) significantly reduced the recurrence risk (Wald et al. 1991) with other clinical trials providing evidence to also show a reduction in the occurrence risk of NTDs (Berry et al. 1999, Czeizel & Dudas 1992). Together, these findings show that environmental factors such as suboptimal nutritional factors, and more specifically folate-deficiency, can modify the prevalence of NTDs.

Various teratogenic agents have also been associated with NTDs (Copp & Greene 2010). These teratogens include the anticonvulsant drug valproic acid (Wlodarczyk et al. 2012) and the mycotoxin fungal product fumonisin (Missmer et al. 2006). In addition to these teratogenic agents, other nongenetic and environmental risk factors for NTDs

include maternal fever (Moretti et al. 2005), maternal obesity and maternal diabetes (Correa et al. 2003).

1.5.3.3 Gene – environment interactions

The causation of human NTDs follows a multifactorial model, whereby it is likely that NTDs arise from multiple heterozygous predisposing genetic factors, interacting with environmental factors, to determine individual NTD predisposition (Copp and Greene, 2014). Such interactions have been shown to result in an increased rate of NTDs in mice; for example, heterozygous *Splotch* (*Pax3*) mice do not usually develop NTDs, but can, in the presence of maternal folate deficiency, result in a low frequency of NTDs. Moreover, the frequency of cranial NTDs among *Pax3* null embryos is increased by maternal folate deficiency (Greene et al., 2009). It seems possible that almost every case of NTDs may represent a different combination of predisposing genetic and environmental factors, which is a special challenge for research in this area.

1.5.4 Pathology of NTDs

NTDs can be categorised into different three main groups: open, closed, or herniated NTDs. Open NTDs, resulting from impaired primary neurulation, exhibit termination of zippering at any point along the anterior-posterior axis. In contrast, closed NTDs manifest as skin-covered lesions due to failed secondary neurulation, often accompanied by subcutaneous lipomas or a distinctive hairy lesion at the affected lower spinal area. Herniated NTDs occur when the meninges, brain, or spinal cord protrude through an opening in the skull or vertebral column after completing primary neurulation.

The nature and severity of NTDs differs between the different forms and is determined by the stage and axial level at which neurulation fails (Copp and Greene, 2013). Figure

1 illustrates the types of NTDs observed along the anterior-posterior axis of the embryo.

The severest form of NTDs is the rarest and is referred to as craniorachischisis which manifests as splayed open neural folds throughout the midbrain, hindbrain and entire spinal region which is caused by failure to initiate closure 1 at the hindbrain/cervical boundary. In this condition, the forebrain region however develops normally as closures 2 and 3 fuse and undergo zippering events unperturbed (Copp et al., 2003; Copp and Greene, 2013).

Another NTD subtype that commonly presents is exencephaly, which arises when the anterior neural tube, the precursor of the future brain, fails to close, because of disrupted failure of rostral zippering from the site of closure 1. Exencephaly is the precursor phenotype to anencephaly which is how human cranial NTDs normally present and manifest at birth. The term exencephaly describes the exposed cranial neural folds that fail to fuse and instead become overgrown and everted which occurs when closure 2 fails either in addition to, or without, failure of closure 3, and single or multiple regions of the brain do not close. When there is an additional failure of closure 3, the forebrain anterior neuropore (ANP) remains open, and results in split face with exencephaly phenotype which present as craniofacial defects alongside NTDs. While the neuroepithelium can still develop neurons within the dorsally open brain, the failure to close the crania neural tube leaves the brain exposed to the surrounding amniotic fluid which at later stages leads to degeneration of the neural tissue, leading to the phenotype to progress to anencephaly. Open cranial NTDs are not compatible with life, and anencephaly-affected foetuses are either still-born or die very shortly after birth (Copp and Greene, 2013).

The other common NTD sub-type that manifests is spina bifida (myelomeningocele), which arises from the failure to close the PNP at the caudal end of the neural tube. It presents as defects in the vertebral arches that accompany the presence of open neural folds. Although compatible with life after birth, children affected by spina bifida suffer from severe neurological problems, kyphosis (spine curvature), impaired

bladder and rectal control, or often paralysis from the lesion down (Steifel et al., 2007; Copp and Greene, 2013).

1.5.5 Current treatments for NTDs

Over the past 20-30 years, the incidence of NTD-affected births has decreased in many countries, with primary prevention through folic acid playing a partial role. Additionally, the decline is attributed to the heightened use of prenatal diagnosis and the choice to terminate pregnancies affected by NTDs (Van Allen et al., 2006). For instance, in the UK, approximately 70-75% of NTD cases undergo termination, with only a minority progressing to full term (Broughan et al., 2023). In cases where NTD-affected pregnancies reach full term, there is currently no treatment available for anencephaly. However, for foetuses affected by spina bifida, the prevailing standard approach involves neonatal or foetal surgery. This procedure involves closing the lesion to protect exposed nervous tissue, preventing further damage to the spinal cord beyond that occurring in utero. In this regard, in utero surgery has been developed and utilised since the 1990s to cover the lesion well before birth. The Management of Myelomeningocele clinical trial demonstrated that in utero surgery improved patient neurological function, but its invasiveness can result in heightened maternal complications and premature birth (Adzick et al., 1998; Adzick et al., 2011). In utero surgery is increasingly offered to women with NTD pregnancies, including in the UK.

Advancements in biomaterials have led to the development of better patches and coverings for spina bifida. These materials aim to protect the exposed spinal cord and promote healing. For instance, new biodegradable material scaffolds provide temporary support to the developing spinal cord while minimizing the need for subsequent surgeries. Stem cell therapy has also shown promise in enhancing the outcomes of spina bifida repair. Stem cell patches aim to provide regenerative benefits that promote neural tissue repair and functional recovery. For instance, mesenchymal stem cells have been widely studied for their regenerative properties and ability to modulate inflammation whereas neural stem cells have the potential to differentiate into various neural cell types, offering a targeted approach to repairing spinal cord defects. Stem cells can be incorporated into patches applied directly to the defect site

during surgery. These patches provide a scaffold for stem cells to adhere to and promote tissue regeneration and hence provides opportunity to repair spinal NTDs.

1.5.6 Primary prevention of NTDs

The only existing primary preventive treatment for NTDs is the addition of folic acid either through fortification to foods such as wheat or grain or an increase in dietary intake (via supplementation). Despite increased folic acid intake having shown to reduce the occurrence and reoccurrence of NTDs it is not the complete answer, given that a large proportion of NTD cases are folate-resistant and folate-unresponsive (Schorah 2008, Smithells et al. 1981; Berry et al. 1999, Czeizel et al. 2011, Czeizel & Dudas 1992). A possible additional preventive approach is based on maternal supplementation with inositol, which was first shown to prevent NTDs in the *curly tail* (*Grhl3*) mutant mouse, an NTD model in which folic acid is ineffective (Greene et al., 1997). Subsequently, a pilot clinical trial was performed using inositol in addition to folic acid, and no cases of NTD recurrence were found in women who took both supplements (Greene et al., 2016). While inositol supplementation is not yet in widespread clinical usage, it is possible that this will lead to enhanced primary prevention of NTDs in future (D'Souza et al., 2021).

1.6 Female preponderance in cranial NTDs

One of the intriguing findings in the realm of NTD research is the discovery that cranial NTDs disproportionately affect a significantly higher number of females compared to males.

1.6.1 Sex ratio in human NTDs

The assessment of anencephaly in human populations from various geographical locations spanning over 60 years has consistently show an excess of females affected by anencephaly – an increase that represents almost up to two-thirds of all cases (refer to Table 1 in Juriloff et al., 2012). In these studies, the female-to-male ratio of anencephaly ranges between 1.2:1 and 2.1:1, and the majority of values have been found to be greater than 1.5:1, a sex ratio that significantly differs from the expected Mendelian 1:1 sex ratio with the eleven of the 13 studies having $p < 0.05$ and six studies showing $p < 0.0001$. Interestingly, the female excess in anencephaly has been found to be higher in regions of the world where the prevalence of NTDs is higher (e.g., Carter, 1974; Borman et al., 1986; Seller, 1987), and review of the human data in these regions suggest that these regions are not usually associated with any programmes or regimes of folic acid fortification or supplementation – findings which suggest that disrupted folate one-carbon metabolism reactions may be a downstream cellular pathway involved in determining the sex difference in cranial NTDs.

In contrast, no discernible increase in females is observed in human cases of spina bifida (refer to Table 1 in Juriloff et al., 2012). The female-to-male ratio in human spina bifida studies ranges from 1.4:1 to 1:1, with most values below 1.2:1, indicating no substantial difference in spina bifida rates between male and female embryos.

Human cases of craniorachischisis, characterised by the failure of closure of the hindbrain and entire spinal column, are extremely rare, and specific sex data for this NTD are typically unavailable. However, Seller (1987) reported a female-to-male ratio of 1.9:1 in 32 cases of craniorachischisis. Similarly, Shaw et al. (2003) reported that out of 16 cases, 12 were female, yielding a 3:1 ratio. Both studies demonstrate a female predominance comparable to that observed in anencephaly.

1.6.2 Female excess among cranial NTDs in mutant mouse embryos

In the almost ~200 mouse strains or stocks in which cranial NTDs are found embryonic sex has not been determined and therefore in the vast majority of cases it remains unknown whether a sex bias exists. In the 12 mouse strains or lines where cranial NTDs are observed and embryonic sex has been determined, a consistent pattern however emerges, whereby all these strains show a notable increase in the incidence of cranial NTDs among female embryos (refer to Table 2, Juriloff et al., 2012). These 12 mutants or strains can be categorised into two main groups: seven exhibit a female-to-male ratio of approximately 2:1 (*Cd, Efna5*, *Marcks*, *Hipk1/Hipk2*, *crn*, and *xn* mutants, and the SELH/Bc oligogenic strain), while five demonstrate that all or nearly all embryos affected by cranial NTDs are female (*Nf1*, *Pdn*, and *Trp53* mutants, the NZW-xid strain, and the ct mutant stock). Statistical analyses confirm the significance of this sex difference in the rate of cranial NTDs, with nine having $p < 0.05$ and three having $p < 0.0001$. Despite the selective increase in the rate of cranial NTDs among female embryos, the underlying mechanism for this sex difference in frequency remains unknown for these 12 mutant strains. Interestingly, in most mutants, the frequency of cranial NTDs in female embryos ranges from 20-30%, indicating a consistent rate regardless of the specific genetic mutation. Findings which suggest that the female preponderance in cranial NTDs may stem from an inherent predisposition that is common to all female embryos such as having two X chromosomes (Naggan et al., 1967; Carter et al., 1973a).

Among the eight mutants and strains where the mutant gene is known, no singular biochemical pathway is evident. Cd (Lrp6) results in the increased activity of the Wnt

signalling pathway (Carter, 2005), and Pdn (Gli3), is a mediator of Shh signalling (Hasenpusch-Theil et al., 2012). Efna5, is a cell surface molecule that is required for the adhesion of apposed neural folds during the closure process (Holmberg et al., 2000). Hipk1 and Hipk2 are involved in the regulation of transcription, proliferation, and apoptosis (Isono et al., 2006). Nf1 affects actin cytoskeleton organisation and dynamics (Boyanapalli et al., 2006), Marcks is an actin filament crosslinking protein (Hartwig et al., 1992; Stumpo et al., 1995), and Grhl3 (ct is a Grhl3 hypomorph), is a transcription factor, that can activate actin polymerisation (Yu et al., 2008). Trp53 is involved in DNA repair, cell-cycle arrest, and apoptosis (Armstrong et al., 1995; Sah et al., 1995). Though, given that the female excess in cranial NTDs has been observed across different mammalian species, including mice with various mutated genes and disrupted pathways, it seems that the female excess in cranial NTDs may be a general mammalian phenomenon with a fundamental reason why female embryos fail to close their cranial neural tube more commonly than male.

Unlike cranial NTDs in mouse embryos, for the two spina bifida mutants (Axd and ct) in which the sex has been reported and the sex ratio assessed have revealed no significant deviation from the 1:1 female-to-male ratio (Juriloff and Harris; Table 2) findings which suggest that for spina bifida in mouse mutants both male and female embryos are equally affected. For most of the approximately 15 mouse mutants reported with craniorachischisis (Harris and Juriloff, 2007, 2010), the penetrance is essentially complete (95–100%). For NTDs with such a high penetrance it is not possible to discern whether there is a relationship between embryo sex and NTD risk.

For most mouse mutants with cranial NTDs, embryonic sex has not been reported and so it remains unknown how many other mutants or strains may present with a female bias in cranial NTDs. Of the ~200 mouse mutants reported to date with cranial NTDs (with or without spina bifida) approximately 75% have incomplete penetrance (4–80% affected; Harris and Juriloff, 2007, 2010) such that it would be possible to assess whether a female excess among cranial NTDs also exists in these other strains. The non-routine nature of determining embryonic sex in NTD research has so far limited our understanding of the sex ratio in cranial NTDs, in both environmental and genetic studies, and it is possible that NTD researchers may be overlooking an entry point into

possible cellular and molecular mechanisms that may contribute to cranial NTDs in mammalian embryos. Future studies of mouse NTD mutants should compare sex ratios among cranial NTDs and non-penetrant mutant littermates, in order to help improve our understanding of why female embryos have an increased sensitivity to be affected by cranial NTDs.

To date, various hypothesis to explain the increased risk of female embryos developing cranial NTDs have been considered.

1.6.3 Sex differences in gonadal hormones

The process of cranial neural tube closure begins on E8.5 in mouse and is complete 24 hours later by E9.5, the equivalent to developmental days 21 - 24 in human embryos. The ovaries and testes, which produce steroid sex hormones, however, are not developed at the time of cranial neural tube closure and only become functional at E11.5 in mouse and days 44 - 48 of embryonic life in human embryos (Theiler, 1989). Given that the cranial neural tube closes several days (mouse) or weeks (human) before the gonads differentiate and start producing hormones, it seems very unlikely that sex differences in sex steroid secretion are present between female and male embryos at the time of cranial neural tube closure, and so can be discounted as a factor influencing sex bias in cranial NTDs.

1.6.4 Sex difference in the overall rate of embryonic development

A slower developmental rate at the time of cranial neural tube closure is expected to result in a longer time to complete cranial neurulation, thereby increasing the window of opportunity for predisposing environmental or genetic factors to perturb the process of cranial neural tube closure (Renwick et al., 1972; Golding et al., 1982; Seller et al., 1987). Studies in the *curly tail* mutant mouse strain, in which a female excess in cranial NTDs has been observed, has shown that, at the onset of cranial neural tube closure,

male embryos are larger and more developmentally advanced than female embryos (Seller and Perkins-Cole, 1987; Brook *et al*., 1994). However, careful analysis during the process of neural tube closure showed that the rates of growth and development do not differ between sexes (Brook et al., 1994). Hence, female embryos begin and end neurulation smaller and less advanced than males, with an identical rate of increase during the closure process. Moreover, in the SELH/Bc mouse strain, where there is also a female excess in cranial NTDs, female and male E9.5 embryos do not differ in either somite count or stage of cranial neural tube development (Juriloff, Harris, and Nishioka, unpublished 1989, Supplemental Table S3). This suggests that male and female embryos likely pass through each stage of the cranial neural tube closure process when they have the same number of somites. As a result, for both the *curly tail* and SELH/Bc models of cranial NTDs, no evidence exists to indicate that the rate of overall growth or neural tube development during cranial neurulation is the factor that may increase the susceptibility of female embryos to cranial NTDs.

1.6.5 Selective loss during pregnancy of cranial NTD-affected males

If male embryos with cranial NTDs experienced a preferential early demise during gestation before any sex assessment, it would result in a higher apparent occurrence of female embryos with cranial NTDs at the time of birth. However, investigations into the sex ratio of male and female embryos in four mouse mutants, strains, and stocks demonstrating a female preponderance of cranial NTDs found no indications that male embryos with cranial NTDs succumb before being evaluated for NTDs. The evaluation of embryo sex for the curly tail strain, the SELH/Bc strain, and the xn stock involved assessing gonadal morphology on E14 and E16 (xn), respectively. Results indicated a relative scarcity of cranial NTD-affected male embryos but did not show an overall insufficiency of male embryos (50%; Wallace et al., 1978; Copp and Brook, 1989; MacDonald et al., 1989). These outcomes align with a lower penetrance of cranial NTDs in male embryos but do not imply a difference in the overall proportion of female and male embryos in these mouse lines. For Trp53-null embryos, embryonic sex was determined through PCR analysis of embryonic DNA. The noticeable scarcity of male embryos among Trp53-null cranial NTD-affected embryos was detected as early as

E10.5 (Chen et al., 2008), and, in line with other studies, no overall deficit of male Trp53-null embryos and foetuses was observed at E12 - E18 (Armstrong et al., 1995; Chen et al., 2008).

1.6.6 Increased female risk in developing cranial NTDs is the result of having two X chromosomes

One notable distinction between male and female embryos during cranial neural tube closure lies in their respective sex chromosome compositions. Females possess two X chromosomes, while male embryos carry one X and one Y chromosome. This variation in sex chromosome complement could potentially be a decisive factor in elucidating the sex bias observed in cranial NTDs. It is plausible that the presence of the Y chromosome in male cells may act as a protective buffer, shielding male embryos from failed cranial neural tube closure, or conversely, that the existence of two X chromosomes in female embryo cells could heighten the susceptibility of female embryos to cranial NTDs.

A study conducted by Arnold and colleagues involving Trp53 mutant mice demonstrated that the heightened incidence of cranial NTDs in females is linked to the presence of two X chromosomes, and is and not influenced by the presence of a Y chromosome (Chen et al., 2008). Trp53, located on chromosome 11 in mice, segregates autonomously from the X and Y chromosomes. To explore which sex chromosome contributes to the augmented susceptibility to cranial NTDs, Chen et al. introduced the Trp53 null allele along with an atypical Y chromosome (Y*) that undergoes recombination with the normal X during gametogenesis in XY* males. This generates gametes that are either YR (recombinant), lacking the entire Y-specific region, or XR (recombinant), containing the complete Y-specific region, including the Sry testis-determining gene. Breeding pairs of XX females and XY* males were used to produce XX and XYR female embryos (both lacking Sry), and XY and XXR male embryos (both carrying Sry). Results indicated that half of XX (gonadal female) and XXR (gonadal male) embryos on the Trp53-null mutant background exhibited cranial NTDs, while all XY (gonadal male) and XYR (gonadal female) embryos developed without cranial NTDs. These findings suggest that the configuration of sex chromosomes, particularly the presence of two X chromosomes, rather than gonadal sex, plays a pivotal role in the increased risk of females developing cranial NTDs

1.6.7 X chromosome inactivation (XCI), a female-specific developmental process

If the heightened female susceptibility to cranial NTDs is linked to the presence of two X chromosomes in female cells, an evident inquiry arises: why and through what mechanism? One specific process unique to females that occurs early in the development of mammalian female embryos is X-chromosome inactivation (XCI). This dosage-compensatory mechanism ensures that one X chromosome per diploid set becomes silenced in every cell of the female embryo, ensuring equal X- linked gene dosage between XX females and XY male embryos. This mechanism prevents the potential toxicity of having twice as many expressed X-linked genes in female cells.

In mice, XCI unfolds in two developmental stages. The first, termed 'imprinted' XCI, transpires at the two-to-four-cell stage of embryonic development, resulting in the exclusive inactivation of the paternally inherited X chromosome (Xp) in embryos, while the maternally inherited X chromosome (Xm) remains active (Huynh et al., 2003; Okamoto et al., 2004). As the embryo progresses to the blastocyst stage, imprinted XCI is reversed in the inner cell mass through Xp-reactivation, while Xp remains silenced in extra-embryonic tissues like the yolk sac endoderm and trophoblast(Harper et al., 1982; Mak et al., 2004). Subsequently, a second round of XCI, specificto female embryos and referred to as 'random' XCI, is initiated just after implantation,around E5.5 (Okamoto et al., 2004; Mak et al., 2004). In this phase, one X chromosome in every cell of the developing female embryo becomes inactivated andsilenced, with a random chance of either Xp or Xm being inactivated. Using an heterozygous X-linked lacZ transgene, Tan et al. (1993) has shown that random XCI is established in the neural tube ectoderm by the time cranial neural tube closure begins. Subsequently, clonal expansion of cells in which Xp or Xm are active generates mosaicism in females for any gene that has different alleles on Xp and Xm.

Random XCI can be divided into three main phases: initiation, establishment, and maintenance (Barakat et al., 2010). In the initiation phase, the cell ensures one only

active X chromosome per diploid set of chromosomes is committed for silencing in a process that is regulated by activators and inhibitors of XCI and which leads to the monoallelic upregulation of the X-linked long noncoding RNA gene *Xist*. In the establishment phase, Xist RNA spreads and coats the entire future inactive X chromosome in *cis,* resulting in loss of active histone marks and the acquisition of inactive histone marks, which are crucial for the silencing process (Plath et al., 2003; O'Neill et al., 2008; Heard et al., 2001; Rougeulle et al., 2004). The final stage of XCI is the maintenance phase, in which the inactive state of the X chromosome remains and is clonally propagated to all daughter cells.

1.6.8 Initiation of XCI

In the initiation phase of XCI, the count of X chromosomes is conducted within each cell's genetic context, leading to the mono-allelic upregulation of Xist, the initiator of XCI, on one X chromosome per diploid set. This initiation process is a random and stochastic event, meaning that in every cell of the female embryo, either the maternal or paternal X chromosome has an equal chance and intrinsic probability of undergoing inactivation (Monkhorst et al., 2008). The selection of which X chromosome undergoes inactivation is governed by both X-encoded activators and autosomally encoded inhibitors of XCI. The delicate balance between these opposing factors determines the upregulation of Xist and dictates which X chromosome will experience XCI. While autosomally encoded XCI inhibitors are equally expressed in male and female cells, X-encoded XCI activators exhibit differential expression between male and female cells, enabling female cells to surpass the threshold for XCI set by the XCI inhibitors. XCI activators promote Xist expression, either directly or indirectly, by repressing Tsix expression, a negative regulator of Xist. Feedback during XCI is provided by the inactivation of X-encoded XCI activators. The inactivation of X chromosomes results in a decrease in the nuclear concentration of XCI activators, subsequently reducing the likelihood that the remaining X chromosome will initiate XCI. This ensures that only one active X chromosome per diploid set is preserved (Chureau et al., 2011; Tian et al., 2010).

1.6.9 Establishment of XCI

Following the initiation of XCI, Xist RNA spreads in *cis* across the 150-Mb mouse X chromosome, orchestrating various epigenetic and molecular processes that that result in inactivation and silencing of the X chromosome. As Xist RNA extends along the X chromosome, fundamental transcriptional machinery essential for gene expression, including RNA polymerase II, is excluded. Additionally, euchromatic modification marks such as histone H3 lysine 4 dimethylation and trimethylation (H3K4me2/me3), as well as histone H3 and histone H4 acetylation (H3/H4 Ac), promoting gene accessibility and expression, are lost (O'Neill et al., 2008; Heard et al., 2001; Goto et al., 2002). Upon losing these euchromatic marks, repressive and silencing epigenetic marks such as histone H3 lysine 9 dimethylation (H3K9me2) accumulate (Heard et al., 2001; Rogueulle et al., 2004), and enzymes such as the Polycomb complex 1 and 2 (PRC1 and PRC2) (Zhao et al., 2008; Plath et al., 2004; de Napoles et al., 2004; Schoeftner et al., 2006) are recruited and accumulate. These enzymes catalyse monoubiquitylation of lysine 119 of histone H2A (H2A119ub), histone H3 lysine 27 trimethylation (H3K27me3) (Rogueulle et al., 2004), and facilitate the incorporation of macroH2A (Costanzi et al., 2000; Mietton et al., 2009) to aid in the inactivation process. I As a final step in the establishment phase of XCI, accumulation of DNA methylation at CpG islands (Grant et al., 1992; Kaslow et al., 1997) on the X chromosome occurs, a epigenetic modification that silences X-linked gene expression and ensures the X chromosome is irreversibly inactivated and remains in a heritable silenced state. The establishment of XCI concludes with formation of a Barr body, a supercoiled and inaccessible heterochromatin structure with a collapsed nuclear compartment. This represents the inactive X chromosome in cytological preparations.

1.6.10 Maintenance and stabilisation of XCI

In the XCI maintenance phase, the inactive X chromosome remains in its inactive state and becomes clonally propagated throughout cell divisions to ensure only one active X chromosome persists in each female cell. Studies in differentiating mouse embryonic stem cells (ESCs) have shown that the switch from establishment to maintenance of XCI is characterised by a transition from Xist-dependent, reversible inactivation to an Xist-independent chromosomal silencing (Wutz et al., 2000).

The methylation of DNA at X-linked gene promoters is associated with repression and inactivation of the X chromosome during the maintenance phase. DNA methylation is an essential epigenetic process in the control of gene expression, which generally serves to silence gene expression. DNA methylation of the inactive X chromosome is enriched on gene promoters, so that hypermethylation is seen in gene-rich regions, whereas hypomethylation occurs in gene-poor regions (Hellman et al., 2007). The DNA methyltransferase 1, *Dnmt1*, which is needed to maintain DNA methylation marks, has shown to be essential for the stable maintenance of XCI in embryonic development. In mice, a mutation in *Dnmt1* leads to failure in the maintenance of gene silencing on the inactivate X chromosome and embryonic lethality at E9.5, findings which also indicate and support the important role DNA methylation has in stabilising and locking-in XCI in female cells.

1.6.11 Evidence for a role of XCI in the increased penetrance of cranial NTDs in female embryos

One mutant mouse model that presents with a female bias in cranial NTDs is the loss of the *Trp53* gene, which encodes the p53 tumour suppressor protein. Cranial NTDs occur in 17%–60% of female $p53^{-/-}$ embryos but in only 0–1% of $p53^{-/-}$ male embryos (Armstrong et al., 1995; Sah et al., 1995). It should be noted that this extreme sex bias in cranial NTDs is not typical of human anencephaly, nor of most mouse mutant in which sex ratios have been examined. When combined with the loss of one or both alleles of BIM, a BH3-only protein that inhibits all pro-survival BCL-2 family members (Czabotar et al., 2014; O'Connor et al., 1998), it was found that female embryos developed cranial NTDs with complete penetrance (Delbridge et al., 2016). This genetic system was used to prospectively isolate and study female $p53^{-/-}$ embryos destined to develop cranial NTDs and to assess the underlying mechanisms.

Female $p53^{-/-}$; $BIM^{-/-}$ knockout embryos showed a reduction in the percentage of nuclei with a detectable inactive X chromosome, as assessed by the absence of a Xist cloud or a H3K27me3 focus. They also showed a 2.3-fold enrichment of gene expression from the X chromosome and biallelic expression of the X chromosome genes, *Huwe1* and *Usp9x* which are usually subject to X inactivation. It was concluded that loss p53 results in a partial failure of XCI (Delbridge et al., 2019). In addition to defective XCI in $p53^{-/-}$; $BIM^{-/-}$ double knockout female embryos, Delbridge et al., 2019 also found that mouse embryos lacking the essential X chromosome inactivation protein SMCHD1 (Blewitt *et al*., 2008) which is essential for the epigenetic regulation of XCI, resulted in 5/6 female $Smchd1^{MD1/MD1}$ embryos presenting with cranial NTDs, whereas only 1/14 male $Smchd1^{MD1/MD1}$ embryos were affected (Delbridge et al., 2019). Together, these findings suggest that defects in XCI caused by loss of two unrelated proteins (SMCHD1 or p53) can lead to female specific NTDs with high penetrance and hence support the idea that the process of XCI may be involved in determining cranial NTD susceptibility.

The Delbridge et al (2019) study proposed that failure to undergo or complete XCI may be a mechanism underlying cranial NTD predisposition in female embryos. Alternatively, this may be a mechanism for the extreme female cranial NTD bias, as seen in the p53 model, but perhaps is not more generally applicable. Indeed, several lines of evidence suggest that the increased female risk to cranial NTDs is not caused by the failure of the XCI process itself. First, conditional deletion of *Xist* in the epiblast results in severely reduced fitness and survivability of female embryos (Yang et al., 2016). Hence, if XCI was to fail or become disrupted in female embryos at the early post-implantation stage it is likely that toxicity or severe developmental abnormalities would result, preventing survival to neurulation stages. Second, in the majority of mouse strains and stocks in which a female excess has been reported, no obvious association exists between the mutated gene and the process of XCI. The mutated genes disrupt a wide variety of cellular and molecular processes that directly affect cranial neural tube closure (see Section 1.6.2). Third, as noted above, cranial NTDs of the *p53* mutant model are almost totally female-preponderant, whereas in humans and most mouse cranial NTDs, there is a much less extreme sex bias.

1.6.12 An epigenetic “methyl sink” resulting from XCI

It seems likely that the process of XCI is involved in determining the increased rate of cranial NTDs in females, but perhaps not generally through failure of XCI. An alternative mechanism could involve a consequence of XCI, which may adversely affect female embryonic resilience during cranial neurulation. Although not sufficient to cause NTDs in otherwise normal embryos, such a mechanism could act as a modifier influence, so that in the presence of another genetic or environmental perturbation, female embryos are less able to compensate than are males.

XCI involves the silencing and inactivation of an X chromosome after every round of cell division in the developing female embryo. Methyl groups, together with other epigenetic complexes, are required to silence X-linked gene expression, through both DNA methylation and histone protein methylation, the latter reducing accessibility of

transcription factors to DNA. Given that XCI precedes cranial neural tube closure, it is suggested that the inactive X chromosome may act as an epigenetic “methyl sink”, leading to a relative shortage of methyl groups in female versus male cells (Juriloff and Harris, 2000, 2012). Since methylation reactions are very likely to be also essential for events of cranial neural tube closure, this relative lack of methylation potential may put female embryos at increased risk of cranial NTDs.

Methylation reactions are known to be essential for cranial neural tube closure, with NTDs occurring in rat embryos cultured in serum lacking methionine (the precursor of the universal methyl donor, s-adenosylmethionine, SAM), in embryos treated with N_2O to inhibit methionine synthase (Fujinaga et al., 1994; Coelho et al., 1989) and in mouse embryos cultured in ethionine, a methionine analogue that inhibits SAM production (Dunlevy et al., 2006). Methionine, a methyl group donor, is also known to be required for neural fold elevation (Coelho and Klein, 1990) and *Dnmt3b*, a methyltransferase responsible for *de novo* methylation of DNA has been found to be specifically and strongly expressed in elevating cranial neural folds, with its null mutation leading to failed cranial neural tube closure (Okano et al., 1999). These findings suggest that disruption of methylation cycle activity and a reduction in methyl group availability can affect cranial neural tube closure.

The concept that XCI can result in an epigenetic “methyl sink” and can also disrupt other methylation-dependent processes is supported by an analysis of epigenetic silencing. A panel of mice carrying random ENU-induced mutations was screened for a change in silencing of a non-X-linked reporter transgene (Blewitt et al., 2005; Ashe et al., 2008). One of the selected genes, Momme D1, is a null allele of *Smchd1* and is required for maintenance of gene repression on the inactive X chromosome (Blewitt et al., 2005; Blewitt et al., 2008). Mutation of *Smchd1* led to female-specific embryo lethality, reduced retrotransposon silencing (using the A^{vy} reporter strain), and reactivation of genes on the inactive X . In contrast, males were developmentally normal, and could survive to adulthood (Blewitt et al., 2005). Moreover, these processes of epigenetic silencing are dose-dependent, depending on the degree and availability of epigenetic complexes that are utilised (Ashe et al., 2008). Hence, common epigenetic mechanisms based on DNA methylation are shared between

diverse processes including XCI and silencing of transgenes and retrotransposons.

In relation to the XCI epigenetic “methyl sink” hypothesis, it is therefore plausible to assume that the extensive use of methyl groups, during inactivation of an X chromosome in every female cell, likely places a limit on availability of silencing complexes, particularly methyl groups, that are also needed for later developmental processes. This increase the risk of cranial closure failure in females, especially when other deleterious genetic or environmental influences co-exist in that embryo.

1.7 Folate one-carbon metabolism and the methylation of macromolecules

When considering the validity of the “methyl sink” hypothesis, it is important to consider the metabolic origin of methyl groups and their use in methylation reactions. This reveals an intriguing link with folic acid supplementation, a procedure already in clinical use to prevent a proportion of human NTDs.

1.7.1 Methylation Cycle

The methylation cycle, an integral component of folate one-carbon metabolism, is a universal metabolic pathway comprising a series of biochemical reactions with crucial roles in the regulation of cellular and epigenetic processes. These processes include the synthesis of the amino acid methionine, the formation of polyamines, DNA methylation essential for gene expression regulation (Friso and Choi, 2002), protein methylation reactions which influence protein function (Vafai and Stock, 2002), and the metabolism of the sulfur-containing compound homocysteine.

The methylation cycle begins at the point where a methyl group from 5-methyltetrahydrofolate (5-methylTHF) is transferred to homocysteine by the action of the methionine synthase enzyme (MS; Figure 3.1). This reaction converts 5-methylTHF to THF, and produces methionine. Subsequently, methionine reacts with

ATP, with the action of methionine adenosyltransferase (MAT; E.C.2.5.1.6), to form S-adenosylmethionine (SAM) (Figure 3.2) (Lombardini and Talalay, 1971). SAM is the universal methyl donor that catalyses the methylation of various downstream biomolecules including DNA, RNA, lipids, and proteins via methyltransferase-mediated reactions (Loenen, 2006). Decarboxylation of SAM by SAM decarboxylase (SAMDC; E.C.4.1.1.50) transfers its propylamine moiety for the synthesis of spermine and spermidine in polyamine synthesis reactions – with methylation reactions and polyamine synthesis functioning as the only downstream reactions of SAM.

The donation of a methyl group by SAM for downstream transmethylation reactions (Figure 1.3) results in the formation of S-adenosylhomocysteine (SAH), which is a potent product inhibitor of most methyltransferases (De Cabo et al., 1995). Hence, the ratio of SAM to SAH is crucial for the regulation of methylation and, to ensure SAM-mediated transmethylation reactions can occur, it is necessary that SAH is broken down. SAH must therefore be efficiently recycled, via the production of homocysteine, for methylation potential to be maintained (Finkelstein, 1998a; Scott, 1999). The breakdown and metabolism of SAH predominantly occurs via SAH hydrolase in a reversible reaction whose equilibrium favours the synthesis of SAH (Ueland, 1982). Therefore, active removal of SAH hydrolase products, homocysteine, and adenosine, are needed to ensure SAH removal, and to allow continued transmethylation reactions. The relative abundance of SAM to SAH is not only important for methylation, but can also influence flux through the folate cycle, since SAM inhibits 5,10-methylene tetrahydrofolate reductase (MTHFR; EC1.7.99.5) (Kutzbach and Stokstad, 1971) and therefore reduces the shunting of 1C units into the methylation cycle - instead tending to favour nucleotide synthesis within the folate cycle.

Once produced, homocysteine can be utilised in three metabolic reactions. First, it can be used to synthesise methionine in a reaction catalysed by the vitamin B_{12}-dependent MS enzyme that is present in all mammalian tissues. Methionine synthase utilises a newly formed methyl group from the 1C pool in the form of 5-methylTHF to convert homocysteine to methionine. This reaction is an important step in the recycling of intracellular folates as removal of the methyl group from 5-methylTHF produces THF which is then available for use in the folate cycle. Second, homocysteine can be

remethylated to methionine through the BHMT pathway in which homocysteine is used as a substrate for the oxidative catabolism of choline, through the action of betaine-homocysteine S-methyltransferease (BHMT) which utilises betaine as a methyl donor. BHMT activity is only found in liver and kidney tissue (Ericson, 1960; Finkelstein et al, 1971). Third, homocysteine can be utilised by cystathionine-β-synthase, a pyridoxal phosphate-dependent enzyme, which is the only reaction that removes homocysteine from the methionine cycle. This reaction, part of the transsulfuration pathway, involves a series of unidirectional steps that begin with homocysteine being condensed with serine to produce cystathionine and ends with the production of glutathione. The complete transsulfuration pathway is present in only four tissues (liver, kidney, small intestine, and pancreas).

Analysis of the enzymes involved in homocysteine metabolism during rat neurulation found that homocysteine catabolism occurs exclusively via the methionine cycle, and not through the transsulfuration pathway. The conservation of the homocysteinyl moiety in the homocysteine-methionine cycle perhaps may be the only route to breakdown homocysteine because of the absence of cystathionine-ß-synthase in the neurulating rat embryo (VanAerts et al., 1995) emphasising the importance of this cycle in embryonic development during neurulation. Despite this, Robert et al., 2003 has shown that CBS is expressed in the embryonic CNS of rat embryos and so whether or not the homocysteine-methionine cycle is the only pathway to remove homocysteine in rodents remains unclear (Robert et al., 2003). Neurulation coincides with a period of rapid protein synthesis and so a need to constantly supply methionine for embryonic growth or for conversion to SAM for either polyamine synthesis or to maintain transmethylation reactions. These findings may explain the greater activity of SAH hydrolase in the embryo proper and visceral yolk sac compared to placental and extraembryonic tissues as the embryo is likely to have a greater need to breakdown SAH to homocysteine to regenerate methionine to maintain the metabolic need of methylation reactions and subsequent downstream reactions.

1.7.2 Methylation cycle and NTDs

Several lines of evidence suggest that methylation cycle flux and integrity (Figure 1.3) plays a key role in determining susceptibility to NTDs. Risk factors for human NTDs include elevated levels of homocysteine and reduced levels of vitamin B_{12}, the co-factor for MS (Kirke et al., 1993; Steegers-Theunissen et al., 1994). In addition, a thermolabile polymorphic variant (C677T) of the enzyme MTHFR, which results in reduced catalytic activity and therefore an elevation of homocysteine, has also been associated with NTD patients and their mothers (Eskes, 1998). As homocysteine is the precursor for methionine, elevated levels of homocysteine could be linked with a limited production of methionine and therefore a reduction in methylation cycle flux. In humans, low dietary methionine intake has been reported to be associated with an increased risk of NTDs and hence it has been proposed that a high intake ofmethionine may be protective (Shoob et al., 2001).

Consistent with the importance of methylation reactions, the functioning of the methylation cycle has also been shown to be critical for cranial neural tube closure in rodent models. Cranial NTDs occur in rat embryos cultured in serum lacking methionine (the SAM precursor), in embryos treated with N_2O which inhibits methionine synthase (Fujinaga et al., 1994; Coelho et al., 1989) and in mouse embryos cultured in ethionine. The latter is a methionine analogue that is converted to S-adenosylethionine (SAE) which cannot be utilised by methyltransferases and which in turn acts as a competitive inhibitor of methionine adenosyltransferase (Dunlevy et al., 2006; Cox and Irving, 1977).

1.7.3 Folic acid effects on NTD sex ratio in humans

Evidence from population-based studies in South America (Poletta et al., 2018) and case-control studies in the US (Shaw et al., 2020) have shown a greater protective and preventive effect of folic acid supplementation on anencephaly rate in female foetuses, than in males. Given the multibranched nature of folate one-carbon metabolism reactions (Figure 1.3), it is possible that folic acid supplements may reduce the rate of cranial NTDs via shunting one-carbon units into the methylation cycle and thereby stimulating downstream cellular methylation reactions (Blom et al., 2006).

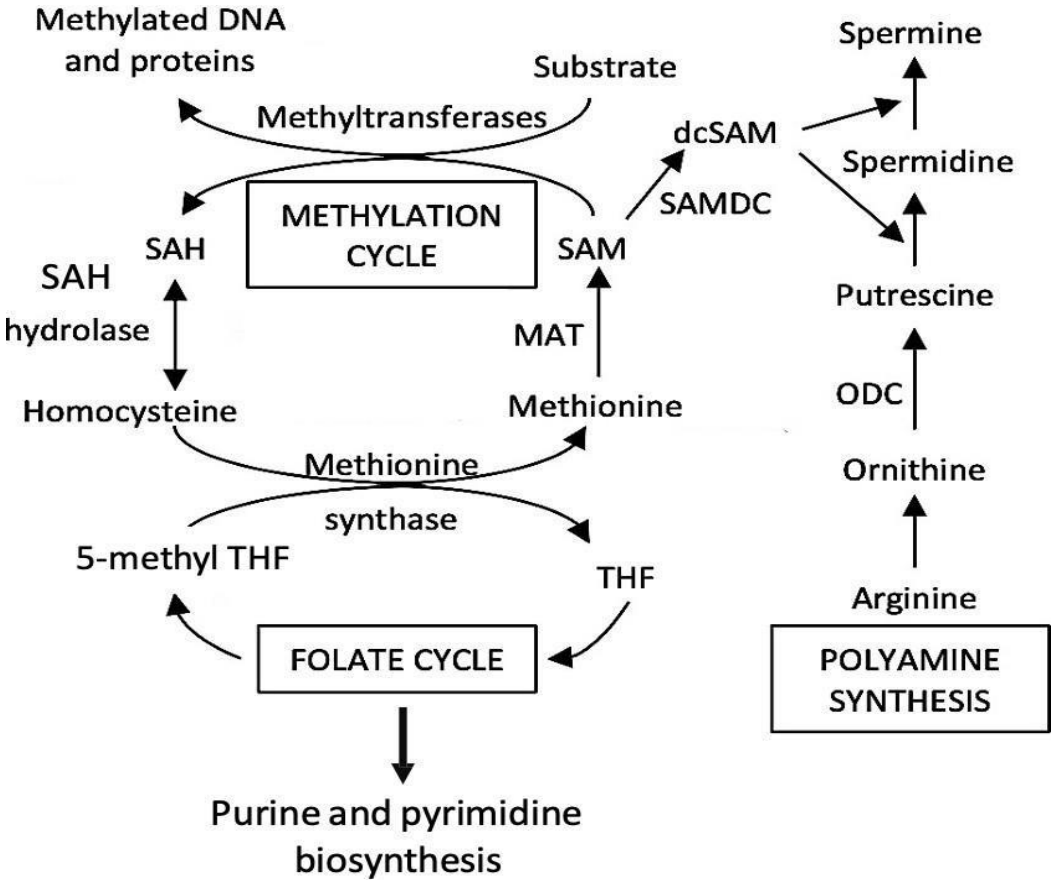

Figure 1.3. The methylation cycle and the major functional outputs of the key methylation cycle molecule, SAM. The methylation cycle begins via the production and shunting of the major 1C donor and form of folate, 5-methylTHF which is generated from 5,10-methylenetetrahydrofolate in the MTHFR-catalysed reaction (EC 1.5. 1.20), a reaction that links folate one-carbon metabolism to the methylation cycle by shunting 1C units (not shown). Once produced, 5-methyl THF donates its methyl group to homocysteine in a methionine synthase, vitamin B_{12}-dependent reaction which results in its re-methylation into methionine. Methionine is the precursor of the major product of the methylation cycle, SAM, which is produced by condensing and phosphorylating methionine by the use of ATP. Once produced, SAM can be retained in the methylation cycle and used as a methyl donor for the methyltransferase-catalysed reactions of downstream biomolecules. Alternatively, upon becoming decarboxylated by the action of SAMDC, SAM can be shunted for use in the synthesis of the polyamines spermidine and spermidine. The retention of SAM in the methylation cycle and its donation of the methyl group for downstream transmethylation reactions results in its conversion into SAH. SAH is rapidly broken down by SAH hydrolase into homocysteine and adenine (not shown), and it is at this point where a 1C donor is needed to remethylate homocysteine to restart the cycle and continue methylation cycle flux. MAT – methionine adenosyltransferase, SAMDC – SAM decarboxylase, ODC, ornithine decarboxylase, THF – tetrahydrofolate. 6Image adapted from (Greene et al., 2013).

1.8.1. DNA methylation

DNA methylation involves the attachment of a methyl group (provided by SAM) to the 5' carbon position of the cytosine nucleoside base, predominantly occurring within cytosine guanine dinucleotides (CpG) in the DNA sequence. CpG dinucleotide clusters, are commonly located in gene promoter regions known as "CpG islands," and utilise DNA methylation as a vital post-transcriptional epigenetic mechanism to modify gene transcription without altering the nucleotide base sequence (Oommen et al., 2005). Methylation of CpG islands, particularly at the site of transcriptional initiation, can effectively silence gene transcription either by directly blocking the binding of transcription factors or indirectly through the binding of methyl-binding proteins like MECP2. These proteins limit the access of transcription factors to the gene promoter or modify the chromatin structure to a repressive state (reviewed in Newell-Price et al., 2000; Van den Veyver, 2002).

DNA methylation is not only crucial for genes on autosomal loci but also for the methylation and silencing of scattered transposable DNA elements known as retrotransposons (Druker and Whitelaw, 2004; Cordaux and Batzer, 2009). Failure to silence these elements can lead to disruptions in gene expression or induce chromosome rearrangements (Yoder et al., 1997). Notably, it is interesting that in human cranial NTDs, LINE-1 retrotransposons and global genomic DNA have been reported to be hypomethylated when compared to control foetuses (Chen et al., 2010; Wang et al., 2010).

As a result, the disturbance and suppression of DNA methylation may impact the transcriptional control of key genes, resulting in the abnormal expression of various genes critical for the successful closure of the cranial neural tube. To this extent, inhibition of DNA methylation following genetic deletion of the DNA methyltransferase *Dnmt3b* has been shown to cause cranial NTDs in mouse embryos (Okano et al., 1999) and the DNA methylation cycle inhibitor, 5-azacytidine, used previously in

mouse studies, has also been shown to cause cranial NTDs in mouse embryos following administration in utero (Takeuchi and Takeuchi, 1985) and also when used in vitro (Burren et al., 2008).

1.8.2 Protein methylation

Protein methylation, catalysed by protein methyltransferase enzymes, involves the addition of the methyl-group provided by SAM to arginine or lysine amino acid residues within the protein sequence. This process plays a role in governing protein stability, influencing protein-protein interactions, and thereby impacting protein function (Grillo and Colombatto, 2005). In contrast, the methylation of histone proteins is linked to chromatin remodelling and the regulation of transcription (Martin and Zhang, 2005). As protein methylation can influence protein function, aberrant protein methylation is also a possible site that, if disturbed, could result in the failure of cranial neural tube closure. Cytoskeletal proteins such as β-actin and tubulin are known to become methylated during neurulation (Moephuli et al., 1997) and studies in which the cytoskeleton has experimentally been disrupted have shown that integrity of the cytoskeleton is essential for cranial neural tube closure (Matsuda and Keino, 1994; Smedley and Stanisstreet, 1986; Ybot-Gonzalez and Copp, 1999).

1.8.3 Lipid methylation

Lipids are also subject to methylation, through the action of phosphatidylethanolamine N-methyltransferase (PEMT), which is essential for the conversion of phosphatidylethanolamine to phosphatidylcholine, a key structural component of cell membranes (Hartz and Schalinske, 2006). As the period of cranial neural tube closure coincides with a period of rapid cell proliferation and division it is possible that a reduction in methyl group availability under any metabolic, genetic, or environmental constraint could impact cranial neural tube closure by affecting neuroepithelial cell integrity or number.

1.9. Aims of the thesis

The overall aim of the project was to experimentally test the XCI epigenetic “methyl sink” hypothesis, examining if female embryos' increased susceptibility to cranial NTDs results from reduced methyl group availability due to X chromosome inactivation (Figure 1.4).

Previous studies have noted a genetic sex difference and higher rates of cranial NTDs in female embryos. This study investigates whether environmental factors can also cause a skewed sex ratio and an increase in female cranial NTDs. To test this, wild-type embryos were cultured with cycloleucine, a MAT inhibitor, to potentially reduce methyl group availability and exacerbate any female methylation deficiency.

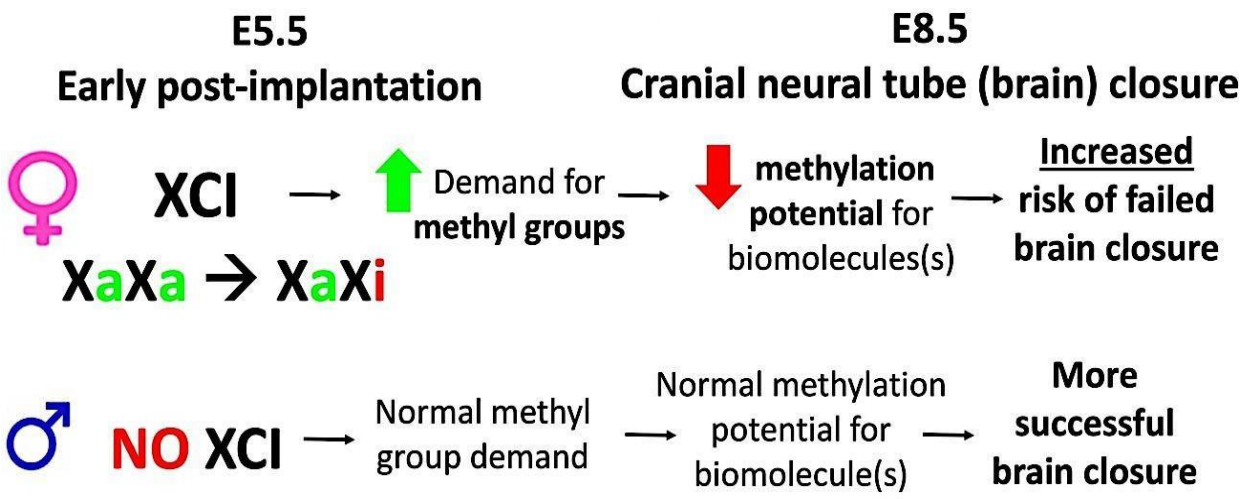

Figure 1.4. The proposed mechanism of the XCI epigenetic "methyl sink" hypothesis. Random XCI is a female-specific developmental dosage-compensatory process that occurs at the early post-implantation stage and results in the inactivation of one X chromosome in every cell of the developing female embryo. The process of XCI requires an extensive use of methyl groups which are likely utilised and needed for two main processes. That is, for the epigenetic control of DNA methylation-mediated X-linked gene silencing and for histone protein methylation, a modification that reduces the accessibility of transcription factors to DNA and thereby promotes gene silencing. As a result, the presence of the inactive X chromosome in every cell of the developing female embryos is likely to result in a "methyl drain" and therefore a reduction in the availability of methyl groups for the process of cranial neural tube closure which occurs three days later in mouse. It is thought the inactive X-"methyl drain" thereby reduces the methylation potential for downstream biomolecules such as DNA, proteins and lipids that may be essential for successful closure of the cranial neural tube. Thus, the reduced ability to undergo methylation reactions in female embryos at the time of cranial neural tube closure likely weakens and destabilises cranial neural fold elevation and thereby increases the susceptibility of female embryos to fail in cranial neural tube closure NTDs. On the other hand, however, because male embryos do not undergo XCI, no epigenetic "methyl sink" or drain in male embryos exist such that there is an adequate supply of methyl groups to meet the demand during the stages of cranial neural tube closure, which may explain why male embryos are more successfully able to close their cranial neural tube. Xa – active X chromosome, Xi – inactive X chromosome, XCI – X chromosome inactivation.

Aims of the project:

1. Test a specific prediction of the epigenetic XCI “methyl drain” hypothesis - that exacerbating the natural methylation difference between the sexes would reveal a female excess in cranial NTDs, whereas preserving methylation capacity in the same embryos would rescue the female excess.

In **Chapter 3**, a teratogen-based approach (cycloleucine) to inhibit methylation activity in wild-type embryo cultures is described. A female excess occurred among partially penetrant cranial NTDs, whereas use of a second inhibitor (MGBG), that preserved SAM and methylation potential, was able to specifically rescue females from cycloleucine-induced cranial NTDs. A male-female difference in location of NTDs between fore-, mid- and hindbrain was observed in this study. Preliminary data were also obtained that cycloleucine induces specific inhibition of protein methyltransferases.

2. Explore a possible role for DNA methylation, downstream of the methylation cycle, as a mechanism underpinning the increased risk and susceptibility of female embryos to cranial NTDs.

In Chapter **4**, wild-type embryo cultures were treated with the cytidine nucleoside inhibitor 5-aza-2’-deoxycytidine (Decitabine). While cranial NTDs were induced, there was no female excess, suggesting DNA methylation is not the primary methyl group-dependent process needed for cranial neural tube closure. Preliminary western blot data indicated reduced protein methylation specifically in cycloleucine-treated female embryos.

3. Reactivate the inactive X chromosome in female embryos, which should overcome the female excess in cranial NTDs, as a direct prediction of the XCI epigenetic “methyl sink” hypothesis.

In **Chapter 5**, low-dose Decitabine treatment was used as a means of reactivating the inactive X chromosome in wild-type cultured embryos. Evaluation by Barr body examination and X-linked gene expression confirmed at least partial X-reactivation in treated female embryos, and this was found to rescue cycloleucine-induced cranial NTDs specifically in female embryos, consistent with the “methyl sink” hypothesis.

Chapter 2. Methods

2.1 Mouse breeding

2.1.1 Maintenance of the CD1 mouse strain and generation of experimental litters

All animal experiments adhered to the guidelines outlined in Project Licence P8B3094F0, granted under the Animals (Scientific Procedures) Act 1986, and were carried out in accordance with the UK Medical Research Council's Responsibility in the Use of Animals for Medical Research Act (1993). Experimental litters were produced through carefully timed matings of random-bred non-mutant CD1 adult mice overnight (starting at 1600 hrs). The presence of a copulation plug in females was checked the following morning at 0900 hrs. Noon of the day the plug was found was designated as embryonic day 0.5 (E0.5)

2.1.2 Embryo collection and dissection

On embryonic day 8.5 (E8.5), the pregnant mouse was humanely euthanised through cervical dislocation, and the embryos within the uterus were carefully removed and placed in warm Dulbecco's Modified Eagle's medium with HEPES (DMEM, Gibco) supplemented with 10% foetal bovine serum (FBS) for subsequent dissection.

Throughout the dissection process, embryos were consistently kept in warm DMEM + FBS. Dissection procedures were conducted on a stereomicroscope stage (Zeiss, Stemi SV6) using fine forceps (Weiss, No. 5). The decidual swellings, each housing an embryo, were isolated from the uterus and transferred to a new petri dish (Greiner) containing DMEM + FBS (Figure 2.1A). Subsequently, the decidual layer was carefully

removed from each conceptus, revealing the trophoblast (Figure 2.1B), before proceeding with further dissection. The delicate 'elastic' Reichert's membrane, located just beneath the trophoblast layer, was then meticulously excised along with the mural trophoblast layer (Figure 2.1C). The resulting embryo, complete with yolk sac and intact ectoplacental cone, was prepared for whole embryo culture.

Once ready for culture, the embryos were ranked according to size (largest to smallest based on size and somite number) and allocated alternately into the treatment groups. While this is not 'random allocation', as recommended by the ARRIVE guidelines (https://arriveguidelines.org/), it is a preferred method to account for the intra-litter variation in embryonic development that is routinely encountered in mouse pregnancies. It ensured that groups for comparison began culture with as similar a range and mean embryonic stage as possible.

Embryos were cultured from E8.5 (~5-7 somites) given this is the 'head-fold' stage in mouse, the stage at which cranial neurulation begins. Embryos were cultured for a period of 24 hrs until E9.5 (~20 somites) given this is the stage at which cranial neurulation should be complete in mouse embryos and so any assessment of whether a cranial NTD is present can be made.

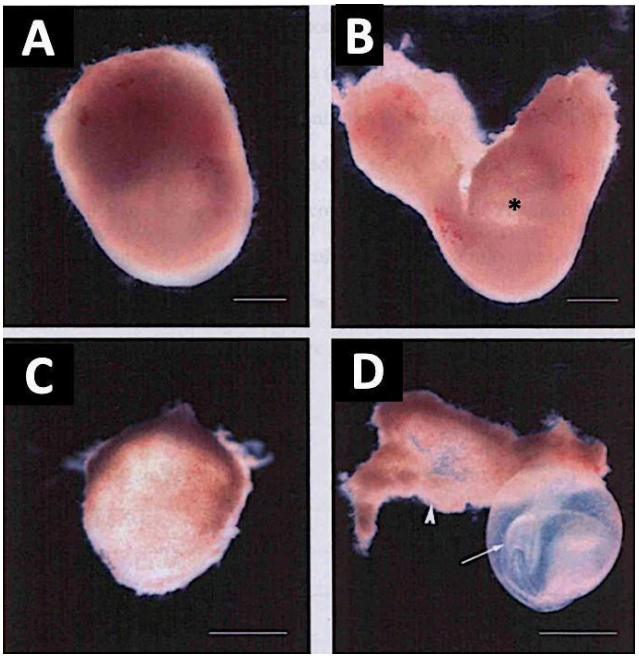

Figure 2.1.5 Dissection steps for whole embryo culture. Once removed from the uterus, the decidua (A) was opened by dissecting from the mesometrial side to reveal the trophoblast-enclosed embryo (* in B) which was then dissected free from decidual tissue (C). The trophoblast layer and underlying Reichert's membrane were then removed (white arrowhead in D) to reveal the embryo within the yolk sac (white arrow in F). Scale bars represent 1 mm. Images adapted from PhD thesis of Louisa Dunlevy, 2006.

2.2 Whole embryo culture

2.2.1 Preparation of rat serum

The Biological Services Unit at UCL prepared rat serum according to the method outlined by Cockroft (1990). Male Wistar rats were deeply anesthetized with isoflurane, followed by ventral dissection to expose the dorsal aorta for blood extraction using a syringe needle. Death was ensured by severing the diaphragm after exsanguination. The collected blood underwent immediate centrifugation for 5 minutes at 4000 rpm to separate red blood cells, and the resulting plasma and cells were left at room temperature for clotting. Serum was obtained by gently squeezing the fibrin clot with sterile forceps, maximising the serum collection. After additional centrifugation, the serum supernatant was transferred to a clean tube, and further centrifugation was performed to eliminate any remaining red blood cells, with the supernatant transferred to a new tube. The serum underwent heat inactivation at 56°C for 30 minutes with loosely secured lids to allow isoflurane evaporation. After cooling to room temperature, serum from multiple rats was pooled, pipetted into 2-3 ml aliquots in bijoux tubes, and stored at -20 °C.

2.2.2 Whole-embryo culture

The technique of sealed roller bottles, as described by New, Coppola, and Terry (1973), was employed for the cultivation of E8.5 mouse embryos. Prior to usage, rat serum was thawed, passed through a 0.45 µm filter (Millipore), and warmed to 38 °C using a rolling tube incubator. Vacuum grease (Glisseal, Borer Chemie) was applied to the rim of each NUNC culture tube to create an airtight seal. The tubes were gassed with an O_2, CO_2, and N_2 gas mixture (BOC) according to the embryonic stage.

Embryos with an intact yolk sac and ectoplacental cone were rinsed in PBS and transferred into the pre-warmed, pre-gassed rat serum (~ 1 embryo/ml) with a maximum of 3 embryos per tube. Special care was taken to minimise the transfer of DMEM + FBS into the rat serum. The culture tubes were positioned in the rolling tube incubator (approximately 30 rpm) at 38 °C. After 30 minutes, treatment or control solutions were introduced into the serum, and the tubes were returned to the rolling incubator for the entire culture duration. Each time the tubes were opened, they were re-gassed, and at least after 16 hours during the culture period. At E8.5, serum and embryos within the tube were equilibrated with the gas composition: 5% O_2, 5% CO_2, 90% N_2 and then at E9.25 with a gas atmosphere of 20% O_2, 5% CO_2, and 75% N_2.

Stock solutions of 0.5 M cycloleucine (Merck), 0.1 M decitabine (Merck) and 0.5 mM MGBG (Merck) were prepared by dilution in phosphate-buffered saline (PBS) and final concentrations were added as weight/volume additions to serum. PBS alone was added to control groups at the same volume as the teratogen or reagent being tested.

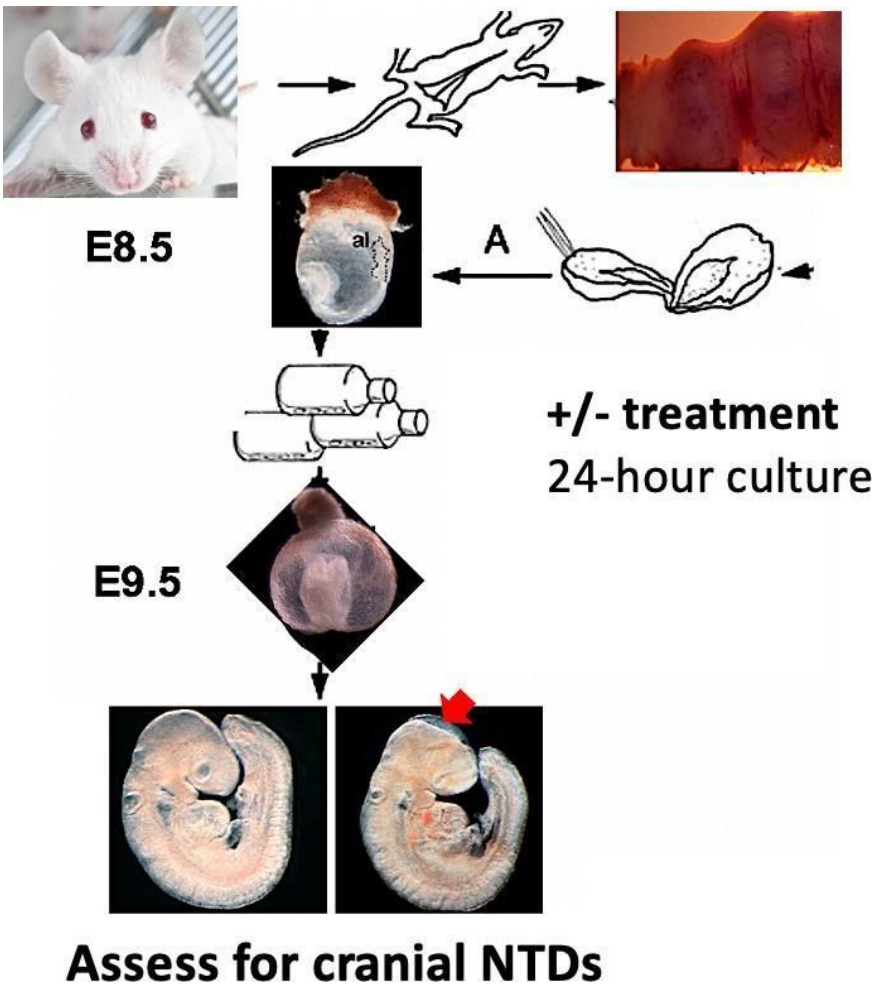

Figure 2.2. Overview of the whole embryo culture system. Pregnant CD1 female embryos were sacrificed eight days after the copulation plug was found to obtain embryos at E8.5, the stage at which cranial neurulation is beginning. To obtain the embryos, the uterus of the pregnant dam was removed and embryos which appear as decidual swellings in the uterus were taken out by fine microdissection that resulted in extraembryonic tissues including the trophoblast layer and Reichert's membrane being removed until the embryo in the yolk sac was isolated. The ectoplacental cone was kept intact. Embryos were then cultured whole using the rolling tube technique in rat serum for a period of 24 hrs with or without various treatments until embryos were E9.5, the stage at which cranial neurulation is complete. Embryos were then harvested and scored for various culture parameters such as embryonic viability, growth and developmental progression and scored for cranial NTDs. Exencephaly is indicated by the red arrow.

2.2.3 Post-culture embryo scoring

Following the completion of the 24-hour culture, embryos were taken out from the rat serum and transferred to warm DMEM + 10% FBS. Without removing the membranes, the circulation in the yolk sac was immediately evaluated using the Brown and Fabro scoring system (Brown & Fabro, 1981): a score of 0 indicated the absence of visible vitelline blood vessels and no discernible blood movement, a score of 1 signified the presence of blood islands with very slow circulation, a score of 2 denoted developed yolk sac vasculature with a steady and frequent heartbeat, and a maximum score of 3 indicated a fully vascularized appearance of the yolk sac with rapid blood circulation (Figure 3B).

After the yolk sac, ectoplacental cone, and amnion were removed, embryos were assessed for additional developmental parameters. The crown-rump length of each embryo was measured using an eyepiece graticule and stage micrometer on the stereomicroscope (Figure 3C). Calibration of the eyepiece graticule was conducted at each magnification using the stage micrometer. Other parameters included somite number, counted in a rostral to caudal direction along the dorsal length, and axial rotation or "turning," both indicative of developmental progression. Normally developing embryos exhibited complete turning with an entirely convex dorsal surface, while those with failed axial rotation displayed either a dorsally concave dorsal surface (complete turning failure) or a caudal region not positioned beside the head (partial turning failure). Visualisation and detailed assessment of the developmental parameters were in accordance with measurements as described previously (Culshaw et al., 2019; Copp et al., 2023).

Embryos were also assessed for developmental abnormalities, particularly cranial NTDs, which were assessed as the appearance of exposed and open cranial neural folds in embryos that had developed to at least the 16-somite stage.

The quantification of NTD severity was made by using the free hand tool in ImageJ software to measure the proportion of open and exposed neural folds as a percentage over total neural fold distance which was measured for each embryo individually in the anterior-posterior axis by measuring the total distance from the rostral extremity of the forebrain to the otic vesicle.

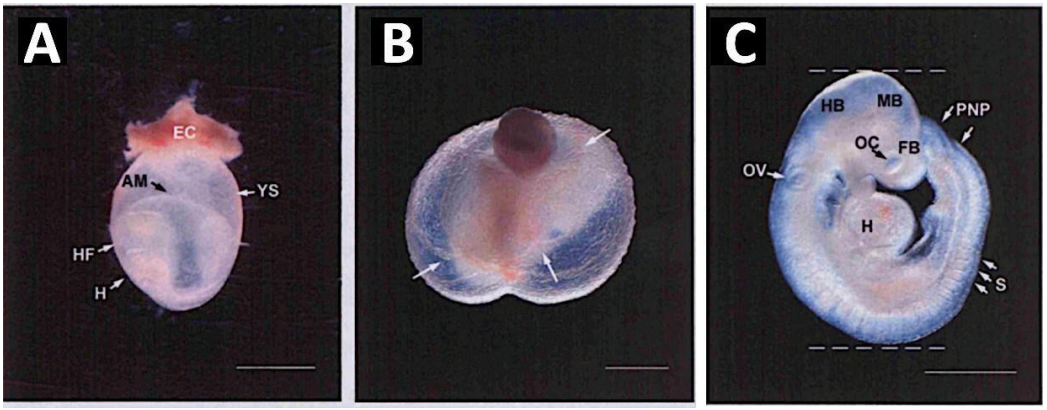

Figure 2.3. Embryo morphology and measurements pre- and post- whole embryo culture. (A) An E8.5 embryo that has been explanted and is ready for whole embryo culture with the with yolk sac (YS) and ectoplacental cone (EC) intact. (B) An E9.5 embryo after 24 hr culture; the YS circulation (white arrows in B) is obvious and is used to assess embryonic viability. (C). The E9.5 embryo after removal from its yolk sac and amnion, without any sign of developmental or growth abnormalities. The crown-rump length was measured between dotted lines in (C), as an indication of growth, and the number of somites was counted as an measure of developmental progression. Scale bar(s) in C represents 200 µm, A and C represent 500 µm, and B represents 1 mm. Abbreviations; AM, amnion; EC, ectoplacental cone; FB, forebrain; HB, hindbrain; H, heart; HF, head folds; MB, midbrain; OC, optic cup; OV, otic vesicle; PNP, posterior neuropore; S, somites. Image adapted from PhD thesis of Dunlevy, 2006.

2.2.4 Processing of embryos

Embryos were rinsed in PBS and fixed overnight in 4% PFA in DEPC-PBS, or frozen immediately in a minimal volume of PBS or rapidly frozen in a minimal PBS volume on dry ice and preserved at -80°C until required. Yolk sacs, intended for sex genotyping, were rinsed in PBS and stored at -20°C. Particular care was exercised to prevent the transfer of maternal tissue with the yolk sac during handling, as contamination could result in inaccurate genotyping.

2.3 Polymerase Chain Reaction (PCR) for identifying embryo sex

2.3.1 Extraction of DNA from yolk sac samples

Yolk sacs, previously kept at -20°C, underwent individual digestion using 10 µg/ml proteinase K (Invitrogen) in 50 µl PBS at 50°C overnight. The solution was then subjected to an incubation at 105 °C for 10 minutes to deactivate the proteinase K, followed by centrifugation at 14,000 rpm for 5 minutes to precipitate cell debris. A 2 µl portion of the resulting supernatant was utilised as the DNA source for the PCR reaction.

2.3.2 PCR protocol

A reaction mixture was prepared with 1 x PCR buffer (Bioline), 1.5 µl of 1.5 mM $MgCl_2$,5 µl of 0.25 mM of each deoxynucleoside triphosphate (dNTP), and 0.3 µl of 0.8 mM primers. The reaction mixture was kept on ice and immediately prior to use 1 unit in the volume of 0.25 µl of Taq polymerase (Bioline) per reaction was added followed by distilled deionised water to give a final volume of 45 µl for each reaction. The resulting

solution was mixed and 5 µl of yolk sac DNA solution was added. Controls were run with each PCR reaction; the negative control did not contain any DNA to ensure the reaction mixture was not contaminated, and the positive control used previously genotyped DNA of male and female embryos to determine embryonic sex of the sample mixture.

PCR amplification was conducted on a PTC-200 DNA Engine (MJ Research) and involved an initial denaturation followed by cycles of denaturation, annealing, and extension. The amplification cycle was repeated several times before concluding with a final extension step, as shown in Figure 2.4.

Embryo sex was determined by PCR using sex-specific primers to amplify the *Smcx* and *Smcy* genes (Agulnik et al., 1999). Male embryos were identified by two bands given both the *Smcx* and *Smxy* gene products, at molecular weights of 370 bp and 350 bp, whereas in female embryos only one 370 bp band was identified, corresponding to the Smcx gene product.

Forward Primer Sequence	5' CCTATGAAATCCTTTGCTGCACA 3'
Reverse Primer Sequence	5' AAGATAAGCTTACATAATCACAT 3'
PCR product size	Male allele 370 bp Female allele 350 bp
Initial Denaturation Step	95 ° C for 5 min
Amplification Cycle	Denaturation 92 °C for 1 min Annealing 60 °C for 1 min Extension 72 °C 2 min
Number of cycles	30
Final Extension Step	72 °C for 10 min

Figure 2.4. Primer sequences, product sizes and PCR conditions to determine embryo sex by genotyping.

2.3.3 Agarose gel electrophoresis

PCR products were detected and observed through horizontal agarose gel electrophoresis. To achieve this, a 2% agarose in 1x TAE (0.04 M Tris-acetate, 0.001 M EDTA) gel was created by melting the mixture in a microwave with occasional stirring. The gel was then left to cool, and approximately 0.5 mg/ml ethidium bromide was added. The resulting mixture was poured into a casting tray with combs and allowed to set at room temperature. Once the gel had solidified, it was positioned in a gel tank (Gibco BRL) containing 1x TAE, and 10 µl of the PCR products in 1x loading buffer (0.25% bromophenol blue, 0.25% Xylene cyanol FF, 15% Ficoll in water) was loaded into each well. A molecular weight marker (Hyperladder V, Bioline) was run in a lane parallel to the samples on each gel to facilitate the identification of the product sizes. Following electrophoresis at 120 volts for 30 minutes, the PCR products were visualised under UV light and captured using an alpha-imager system (Alpha Innotech).

2.4 Liquid Chromatography Tandem Mass Spectrometry (LC-MS/MS)

This procedure was performed by Dr Kit-Yi Leung, using a protocol described previously (Burren et al., 2006).

2.4.1 Preparation of samples

Embryos were immersed in 200 µl of ice-cold aqueous mobile phase containing 1 µM [$^{2}H_{3}$]-SAM and promptly sonicated at 12-micron amplitude for 10 seconds on ice to achieve a homogenous solution. A 10 µl aliquot was retained for determination of protein concentration. For sample preparation, the solution was heated at 80°C for 5

minutes to precipitate endogenous proteins, followed by immediate cooling on ice for 2 minutes and centrifugation for 15 minutes at 14,000 rpm to eliminate any particulate matter. The prepared samples were then promptly analysed using LC-MS/MS.

2.4.2 Calibration and quantification

In order to quantify endogenous levels of SAM and SAH in whole embryos, the "calibration curve method" was employed, utilising combined SAM and SAH calibrators composed of a pool of mouse embryos. Creating a calibration curve involved plotting the "peak area of the calibrator / peak area of the internal standard" against increasing concentrations of the calibrator spiked into the biological matrix. The resulting calibration curve allowed the determination of the endogenous metabolite level in the biological matrix by identifying the intercept on the x-axis when y = 0. To align the curve through zero on the x-axis, the endogenous metabolite level was subtracted from each calibrator. These working calibration curves were then used to quantify the levels of metabolites in samples. To quantify levels of SAM and SAH in neurulation stage embryos, calibrators containing 0.5, 1, 2.5, 5, 10, 25 µM of SAM and
0.01, 0.02, 0.05, 0.1, 0.2, 0.5 µM of SAH were utilised. All calibrators contained 1 µM of the internal standard, [$^{2}H_{3}$]-SAM.

2.4.3 LC-MS/MS Method

SAM, SAH and [$^{2}H_{3}$]-SAM were separated on a pentafluorophenylpropyl (PFPP)-bonded silica column (Discovery HS F5; 50 x 2.1 mm (i.d.); 5 pm bead size; Supelco, SigmaAldrich). Solvents for HPLC were: A, 100% methanol; B, 4 mM ammonium acetate, 0.1% formic acid, 0.1% heptafluorobutyric acid (pH 2.5). The F5 column was initially equilibrated with 40% A: 60% B, and the sample injection volume was set at 40 µl. The HPLC protocol consisted of 40% A: 60% B for 2 min, followed by a gradient of 40-100% A over a 2-min period. The column was then washed with 100% A for 4 min before re-equilibration for 7 min. The flow rate was maintained at 0.5 ml/min, and

the initial 72 seconds post-sample injection were diverted to waste to minimise the accumulation of endogenous compounds on the ionisation source, preserving the instrument's performance over time. The mass spectrometer was operated in positive-ion mode using the following settings: capillary 3.86 kV, cone voltage 20 V, collision energy 26V. A C8 reverse phase column (Discovery Hypurity C8; 10 x 2.1 mm (i.d.); 5 pm bead size) was also tested for its ability to retain SAM and SAH.

2.5 RNA-based assays

2.5.1 RNA extraction

RNA extraction from embryos was performed using the mini-RNeasy kit (cat. nos. 74104 and 74106, Qiagen). Embryos were lysed in 350 µl of RNeasy Lysis Buffer (RLT) for 5 minutes and gently centrifuged to ensure thorough extraction. An equal volume (1:1) of 70% ethanol was then added to the lysate and mixed by pipetting. The resulting sample volume (700 µl) was transferred to a RNeasy Mini spin column positioned in a 2 ml collection tube and centrifuged for 15 seconds at 14,000 rpm, discarding the flow-through. Subsequently, 350 µl of Membrane-bond RNA Wash Buffer (RW1) was added to the RNeasy column, which was then centrifuged for 15 seconds at 14,000 rpm. DNA digestion was carried out using an in-column DNAse 1 digestion kit (Qiagen). For this, 80 µl of the DNase I incubation mix, comprising 10 µl DNase I stock solution and 70 µl Buffer RDD, was directly applied onto the RNeasy column membrane, and the columns with the samples were incubated for 15 minutes at room temperature. Following this, the column was washed with 700 µl Purification RWT buffer for 15 seconds at 14,000 rpm, and twice with 500 µl RPE buffer for 15 seconds at 14,000 rpm. A final centrifugation for 1 minute at 14,000 rpm wasperformed without any buffer. The sample was then eluted in 30 µl of RNase/DNase-free water. RNA concentration was determined by measuring absorbance at 260 nm using a NanoDrop ND-1000 spectrophotometer.

2.5.2 cDNA synthesis

RNA was immediately reverse transcribed to cDNA using the First Strand cDNA Synthesis ProtoScript II Kit (New England Biolabs).

In a sterile microfuge tube, 2 µl of the 1 µg RNA solution was combined with 2 µl of Random primer mix at a concentration of 60 µM. To this mixture, 1 µl of 10 mM dNTP was added, and the volume was adjusted to 12 µl using nuclease-free water. The mixture was then heated for 5 minutes at 70 °C, briefly spun, and promptly placed on ice. Subsequently, 4 µl of 5X ProtoScript II RT Reaction Buffer, 2 µl of 0.1 M DTT, 1 µl of Murine RNase inhibitor (40 U/µl), and 1 µl of ProtoScript II Reverse Transcriptase (200 U/µl) were added to achieve a final volume of 20 µl. Following this, an incubation step was performed at 25°C for 4 minutes. The samples were then subjected to the thermocycler with the following reaction: 42°C for 1 hour and 80°C for 5 minutes to inactivate the enzyme. Samples were then stored at -20°C.

2.5.3 Quantitative real-time PCR

Primers for quantitative real-time PCR (qPCR) were ordered using the Harvard PrimerBank (https://pga.mgh.harvard.edu/primerbank/). Prior to each qPCR experiment, a melt curve analysis confirmed a single product was amplified. For each set of primers, a primer efficiency test was also performed. This experiment contained a standard curve of cDNA using a 3-fold serial dilution starting with undiluted cDNA.

The average Ct value was plotted against the Log(Sample quantity) and the gradient of the linear regression was converted into primer efficiency. Primers were only used if their efficiency was within 70 – 130%.

For qPCR analysis, the cDNA was initially diluted 1:10 in MilliQ water. Each 20 µl reaction in a 96-well PCR plate (Bio-Rad) consisted of 2 µl of diluted cDNA, 10 µl iTaq sybermix (Bio-Rad), 10 µM each of forward and reverse primers, and nuclease-free water. The plate was sealed with a Microseal 'B' Sealing Film (Bio-Rad) and loaded into a CFX Connect PCR machine (BioRad). The qPCR reaction was conducted with the following steps: 95°C for 2 min; 39 cycles of 95°C for 5 sec, 60°C for 30 sec; 95°C for 5 sec, followed by a melt curve with 0.5°C 5 sec increments from 65°C to 95°C.

Image analysis was carried out using CFX Manager (Bio-Rad). Relative gene expression was determined using the threshold cycle (Ct) method (Schmittgen and Livak, 2008), with 28S rRNA serving as the internal control gene. In this method, the Ct value represents the qPCR cycle at which the SYBR green signal crosses a threshold. Delta Ct (ΔCt) is calculated by subtracting the Ct of the target gene from the Ct of GAPDH. Subsequently, delta delta Ct (ΔΔCt) is determined by subtracting the ΔCt of the treated sample from the ΔCt of the control sample. The relative gene expression is then calculated using the formula: Fold change = $2^{-\Delta\Delta Ct}$.

Relative gene expression of X-linked genes was compared between male and female PBS control embryos and embryos that had been treated with cycloleucine, decitabine or co-treated with cycloleucine and decitabine embryos. All analysis was compared against X-linked expression found in PBS controls. In addition, autosomal gene expression was assessed and compared between cycloleucine and decitabine co-treated male and female embryos relative to expression in PBS controls to assess the effect, if any, co-treatment of cycloleucine and decitabine has on differentially affecting autosomal gene expression sex-specifically.

Primer	Forward Primer Sequence	Reverse Forward Primer Sequence
28S rRNA	5′ TGGGTTTTAAGCAGGAGGTG 3′	5′ GTGAATTCTGCTTCACAATG 3′
G6pdx	5′ CACAGTGGACGACATCCGAAA 3′	5′ AGCTACATAGGAATTACGGGCAA 3′
Hprt	5′ TCAGTCAACGGGGGACATAAA 3′	5′ GGGGCTGTACTGCTTAACCAG 3′
Mecp2	5′ CGTGACCGGGGACCTATGTAT 3′	5′ CCTCTCCCAGTTACCGTGAAG 3′
Gldc	5′ CTCCTGCCCAGACACGATG 3′	5′ GGACCGTCTTCTCGATGAGC 3′
Grhl3	5′ CCCGGCAAGACCAATACCG 3′	5′ AACCCCATGAATGCTCTCAAAT 3′

Figure 2.5. Primer sequences for genes assessed using qRT-PCR. Primers were obtained from: https://pga.mgh.harvard.edu/primerbank/

2.6 Protein assays

2.6.1 Protein extraction For Western blots

Protein extracts were acquired by utilising a 30 µl RIPA buffer (Sigma-Aldrich) comprising 150 mM NaCl, 1.0% IGEPAL CA-630, 0.5% sodium deoxycholate, 0.1% SDS, and 50 mM Tris, pH 8.0. Just before lysing, 82 mM of protease inhibitor cocktail mix (Roche), 1 mM sodium orthovanadate, and 1 mM sodium fluoride were incorporated into the lysis buffer. The embryos were sonicated, followed by centrifugation at 14,000 rpm for 15 minutes at 4°C. The resulting supernatants were withdrawn and stored in a clean 1.5mL tube, kept on ice, and either stored at -20°C if utilized the same day or returned to -80°C if not used immediately.

2.6.2 Bradford Assay - determination of embryonic protein content from embryo homogenates

The protein concentration was assessed using the Bradford assay. To achieve this, 5 µl of lysate was mixed with 995 µl of 25% (v/v) Coomassie brilliant blue G-250 dye (Bio-Rad, diluted at a 1:5 ratio in distilled water). Various dilutions (25:1, 50:1, 100:1, 200:1) of the homogenates were prepared to ensure samples fell within the range of the standard curve. Subsequently, the mixture was incubated at room temperature for 5 minutes, and the OD 562 nm for each sample was measured using the NanoDrop ND-1000 spectrophotometer. A standard curve was generated, and the protein concentration of the samples was determined using pre-installed software. For the conversion of absorbance to protein concentration, a range of standard protein solutions was created, spanning from 0 to 100 µg/ml, derived from an initial 0 mg/ml standard protein solution (bovine serum albumin) to 25 mg/ml (Bio-Rad).

2.6.3 Western blotting

After extracting protein from the samples and determining the concentration, the samples were prepared for SDS-polyacrylamide gel electrophoresis. An amount ranging from 15 to 30 µg of protein was combined with the loading buffer (125 mM Tris-base (pH 6.8); 10% (v/v) glycerol; 2% (w/v) SDS; 0.025% (w/v) bromophenol blue; 2.5% (v/v) β-mercaptoethanol) and heated for 5 minutes at 100°C before being directly loaded into a gel.

Polyacrylamide gels (1 mm thickness) were created by mixing 10% resolving gel solution (375 mM Tris-base (pH 8.8), 10% Acrylamide/bis; 0.1% (w/v) SDS; 0.075% (v/v) APS; 0.12% (v/v) TEMED). Once prepared and loaded, the gel was allowed to set and polymerise for 30 minutes. A 5% stacking gel was then prepared and added to the polyacrylamide gels by combining 125 mM Tris-base (pH 6.8); 5% Acrylamide/bis; 0.1% (w/v) SDS; 0.1% (v/v) APS; 0.12% (v/v) TEMED) and left to set. Gel sandwiches were placed in a vertical electrophoresis cell (Bio-Rad), and samples were loaded alongside a 7 µl Precision Plus Protein Standards (Bio-Rad). The tank was filled with running buffer (25 mM Tris-base; 192 mM Glycine; 0.1% (w/v) SDS), and electrophoresis was conducted at 100 V (constant voltage) for 105 minutes. After running, the proteins were transferred from the gel to an Immobilon-P PVDF membrane (Millipore) in a Mini Trans-Blot® Electrophoretic Transfer Cell (Bio-Rad). To facilitate this transfer, filter paper soaked in transfer buffer (25 mM Tris-base; 192 mM Glycine; 20% (v/v) methanol) and PVDF filters in 100% methanol were used.

In the cassette, the gel and PVDF membrane were sandwiched between six filter sheets and enclosed within fibre pads while submerged in the transfer buffer. An ice block was added to the cell, and the transfer ran at 100 V (constant voltage) for 1 hour. The membranes were then soaked in 100% methanol for 1 minute and washed twice for 5 minutes each in Tris-buffered saline (15.4 mM Trizma-HCL; 4.62 mM Tris-base, 150 mM sodium chloride; pH 7.6 using 2 M HCL (TBS) with 1% (v/v) Tween (TBST). Following this, the membranes were blocked in 10% (w/v) dried skimmed milk (Sigma-

Aldrich) in TBS for 1 hour and probed with the unconjugated Anti-Trimethyllysine Rabbit primary antibody in a diltution of 1:1000 and left overnight at 4°C (Catalog Number: PTM-601). The primary antibody was diluted in 5% (w/v) dried skimmed milk with 0.02% (w/v) sodium azide.

The next day, membranes were washed three times for 5 minutes each in TBST, followed by incubation in 0.2 µg/ml goat anti-rabbit antibody (Cat #31460 ThermoFisher Scientific) conjugated to HRP dissolved in 5% (w/v) dried skimmed milk for 1 hour. Washing steps were repeated, and membranes were incubated in TBS until detection. To detect the bound antibodies, 1.5 ml of Amersham ECL Prime Western Blotting Detection Reagent (GE Lifesciences) was added dropwise to the membrane and incubated in the dark for 5 minutes. Membranes were wrapped in clingfilm and exposed to Amersham Hyperfilm ECL (GE Lifescie nces) in an X-ray cassette(FUJI), followed by development in an Xograph Compact X4 processor.

Western blots were imaged on a Densitometer (Bio-Rad GS-800), and bands were quantified using Image Studio Lite software (Licor). During quantification, each sample and band was initially normalised to the β-actin loading control of PBS control embryos. Subsequently, samples were normalised to either the control lane or the blot average intensity.

2.7 Assessment of Barr body number

To count the number of Barr body positive cells in Chapter 5, several criteria and assessments were set out in order to establish the most robust and reducible method to count Body numbers. To help establish this criteria, the following assessments were conducted in collaboration with Dawn Savery and Jiaming Qian.

1. Assess the optimal source and type of embryonic tissue that could be used for analysis.

   Our findings revealed that the amnion layer of embryos appeared to be the most optimal tissue for Barr body analysis given it is relatively thin and was easily able

to be homogenised and give a good representation and number of cells in order to assess for Barr bodies. We found that other tissues such as the heart and tail bud were more stringent to breakdown and when using harsher conditions formed a cell suspension with too many cells such that it made it difficult to identify and count individual cells.

2. The dye used to stain for the Barr body and the best dilution that could be used to identify the Barr body. Various dyes such as crystal violet, Feulgen stain, haematoxylin and eosin and toluidine blue were tested, and it was found that 1% toluidine blue was the optimal dye and dilution to use given it provided the best contrast in nucleus and could most clearly stain and therefore identify the Barr body.

3. Identify the best way to prepare the slide for Barr body assessment.

   A comparison between gelatin-coated and uncoated slides was made with and without a cell border, a boundary that was made using a hydrophobic pen. Our findings revealed that coating slides with gelatin resulted in cell adhering too and therefore clumping together with the cell boundary resulting in difficulties in assessing for the number of cells with a Barr body given that the nuclei of cells could not be assessed individually and often presented layered upon one another. The optimal slide preparation therefore appeared to be using uncoated slides without a cell border boundary given this combination provided with the best cell spread which was arranged in a monolayer of cells and therefore enable nuclei to be counted individually.

4. Create a stringent and selective criterion in what is defined as a ‘Barr body+ cell’.

In order to determine what a Barr body positive cell looks like, various amnion samples from untreated PBS control male and female embryos were prepared and compared following the procedure as outlined above. The assessment and visualisation of numerous cells in these embryos was used to set-up the following criteria.

A Barr body+ cell is one in which:

- A densely and darkly stained structure is observed and situated at the periphery of the nuclear membrane.
- The structure appears greater than 0.8 × 1.1 microns.

With the exclusion criteria set up as follows:

1

- Only nuclei that appeared circular in appearance, as assessed by a length to width ratio were used given that differences in nuclei shape can alter the position of the Barr body within the nuclei.
- Only nuclei that were individually positioned and not sharing any boundaries with other nuclei were assessed.

2.8 Statistical analysis

The comparison between proportions of embryos affected and unaffected by cranial NTDs and by sex was conducted using a 2x2 Chi-square test with subsequent pair-wise comparisons through the Fisher exact test. Quantitative measurements underwent a comparison through one-way analysis of variance on ranks, and pair-wise comparisons were executed using the Mann–Whitney Rank Sum Test. The assessment of concentrations for S-adenosylmethionine (SAM) and S-adenosylhomocysteine (SAH) involved a comparison using One Way ANOVA. Ratios of SAM to SAH, both overall and within each sex, were subjected to comparison through t-tests. Student's t test was used to compare the means of different data sets. Statistical significance was considered for p-values less than 0.05.

Chapter 3. Treating cultured embryos with cycloleucine: a model to assess whether modulating methyl group availability causes a female excess in cranial NTDs

3.1 Introduction

The female excess in cranial NTDs has been known to exist for many decades (Carter et al., 1974) with thirteen studies in human cases over a 60-year period consistently showing that female foetuses are statistically more often affected with anencephaly than males, and representing up to two-thirds of all cases (Juriloff et al., 2012). Experimental mouse models have also shown a female preponderance in cranial NTDs, with twelve mutant models or strains in which cranial NTDs exist, and where embryo sex has been determined, all showing a clear female excess (Juriloff et al., 2012). Despite this, there is no established mechanism to explain why a sex difference in the rate cranial NTDs exists, either in humans or mouse genetic strains.

The female excess in cranial NTDs could be explained by a selective and preferential loss of cranial NTD-affected male embryos during pregnancy, and this is hard to exclude in human NTDs. However, in mice a female excess in cranial NTDs is observed from the stage of neurulation onwards, arguing strongly against a selective loss of males with cranial NTDs (Wallace et al., 1978; Copp and Brook, 1989; Macdonald et al., 1989; Chen et al., 2008; Armstrong et al., 1995). Hormonal differences between male and female embryos might also be implicated in the female excess, but this is unlikely given that the process of cranial neural tube closure is completed before the secretion of sex steroids begins: at ~24 days after the cranial neural tube closes in human embryos and three days after neurulation in mouse embryos.

Another proposed mechanism relates to sex differences in the rate of embryonic development during neurulation. In the *curly tail* mouse strain (*Grhl3* gene mutation), which has female preponderant cranial NTDs (Embury et al., 1979), female embryos

are retarded developmentally compared with males (Seller et al., 1987), and it was suggested that female embryos may be relatively immature during neurulation (Seller et al., 1987) and so predisposed to cranial NTDs. However, it was subsequently shown that female and male embryos develop at identical rates during neurulation, progressing and passing through each stage of cranial neural tube closure at the same somite stage. This is despite male embryos beginning neurulation some hours earlier than female embryos within a single litter (Copp and Brook, 1989). Hence, the female excess in cranial NTDs is unlikely to be due to sex differences in the 'maturity' of embryos at neurulation, nor in the 'window of teratogenic opportunity' during which genetic and environmental insults may act to disrupt cranial neural tube closure.

The question remains therefore – what is the mechanism that underpins the increased susceptibility of female embryos to cranial NTDs? One difference that is known to exist between male and female embryos is their complement of sex chromosomes: two X chromosomes in females, and one X and one Y chromosome in males. Two mechanisms relating to this sex chromosome difference might be relevant: either the presence of the Y chromosome could 'buffer' and protect male embryos from failed cranial neural tube closure, or the presence of two X chromosomes could increase female susceptibility to cranial NTDs.

The role of the Y chromosome was investigated in mice mutant for the *p53* (*Trp53*) gene, in which homozygous embryos develop partially penetrant cranial NTDs that are female preponderant (Chen et al., 2008). The 'four core genotypes' method was used, in which the testis-determining gene (*Sry*) is deleted from the Y chromosome and moved to an autosome, by insertion of an Sry transgene, thereby generating both XX and XY males, and XX and XY females (Arnold et al., 2020). Hence, determination of testis development occurs independently of the complement of X or Y chromosomes. When combined with homozygous loss of *p53*, embryos with two X chromosomes preferentially developed cranial NTDs irrespective of sex, whereas presence of a Y-chromosome provided no protection (Chen et al., 2008). This work suggests strongly that the sex difference in cranial NTDs is caused by differences in the number of X chromosomes, not by the presence or absence of a Y chromosome.

The finding that X chromosome number is the critical factor in determining predisposition to cranial NTDs points to a possible role for X chromosome inactivation (XCI). In this process, one X chromosome in every newly-generated female cell undergoes chromosome wide-gene silencing as a dosage-compensatory mechanism, to prevent the toxic effect of expressing twice as many X-linked genes as in male cells. XCI has its onset in the embryo proper at the early postimplantation stage, having begun in the extraembryonic tissues somewhat earlier in development (Lyon, 1999). Hence, by the time of neurulation, XCI is already established in most cell lineages of the female embryo (Tan et al., 1993). XCI requires both establishment of the inactive state, and its subsequent maintenance, each of which has multiple underpinning molecular mechanisms (Heard et al., 1997). One such mechanism is DNA methylation, which is known to be associated with repression of gene transcription, when it affects CpG islands that are often located within gene promoters (Deaton et al., 2011). CpG island methylation was found to be preferentially enhanced on the inactive X chromosome compared with the active X (Norris et al., 1991), providing evidence for a key role of DNA methylation in XCI.

These considerations led Juriloff and Harris (2012) to propose a mechanism for female preponderance in cranial NTDs related to the XCI process, which they termed the epigenetic ‘methyl sink’ hypothesis. This proposes that XCI in female cells reduces methyl group availability and thereby reduces methylation potential for epigenetic modification of DNA, RNA, proteins and lipids. Hence, neurulation stage female embryos are at a ‘methylation disadvantage’ compared with males, and this is proposed to adversely affect their ability to respond to challenges, such as the presence of NTD-predisposing gene mutations or environmental influences (Juriloff et al., 2012). While female embryos are ordinarily able to undergo normal development in the great majority of cases, a genetic or environmental challenge will preferentially affect females, as is seen with genetically-induced cranial NTDs in mice.

Studies in this Chapter were designed to begin to test the ‘methyl sink’ hypothesis in mouse embryos, using an environmental challenge rather than a genetic one, as in previous work. Embryos were treated with the methylation cycle inhibitor cycloleucine, which is a teratogen previously shown to cause cranial NTDs in mice (Dunlevy et al.,

2006). Cycloleucine is an inhibitor of methionine acetyltransferase (MAT) and so reduces supply of s-adenosyl methionine (SAM), the universal methyl donor (Figure 3.1). It was hypothesised that if female embryos are at an inherent methylation disadvantage, as a result of the 'methyl drain' resulting from XCI, then the addition of cycloleucine would further reduce methyl group availability and worsen the methylation potential in otherwise normal female embryos. It was predicted that this would result in a higher frequency of cranial NTDs in females, compared with male embryos.

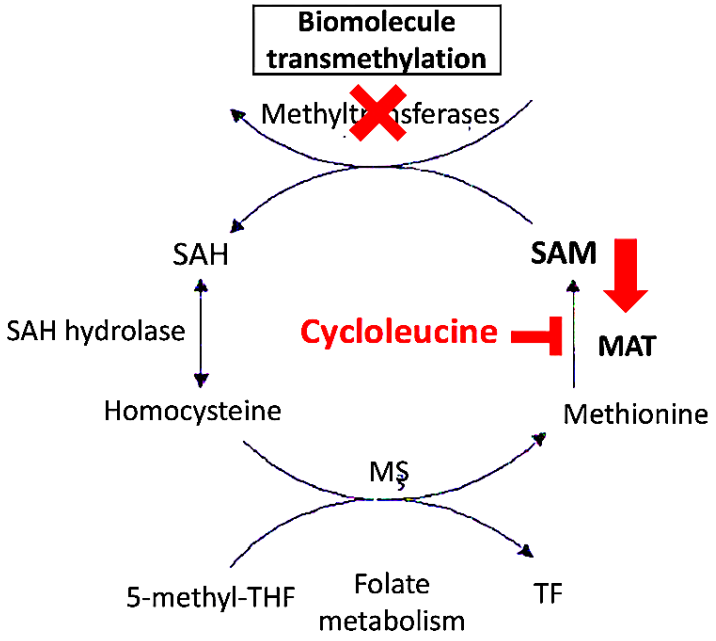

Figure 3.1. Mode of action of cycloleucine. Cycloleucine inhibits methionine adenosyltransferase (MAT) and thereby is expected to limit the synthesis and availability of s-adenosyl methionine (SAM) for downstream transmethylation reactions. MS, methionine synthase; TF, tetrahydrofolate; SAH, s-adenosyl homocysteine.

3.2. Results

CD1 embryos were treated with cycloleucine and cultured in rat serum for the period of cranial neural tube closure (E8.5-E9.5) using the whole embryo culture system (New DAT, 1978).

PBS was used as a vehicle control and embryos from within litters were allocate according to size/stage to make sure groups are balanced and to minimise any effect of litter-to-litter variation.

At the end of the culture period, embryos were harvested and assessed for cranial NTDs and scored for other developmental parameters including measures of embryo viability, embryonic growth, and development progression whilst the yolk sac was removed and used to determine embryonic sex by genomic PCR. Embryos were obtained from 21 litters.

3.2.1 Cycloleucine-treatment does not perturb embryonic viability or embryonic growth in CD1 mouse embryos

Exposure to cycloleucine at concentrations of up to 15 mM did not adversely affect embryonic viability as indicated by the mean yolk sac circulation scores at the end of the culture period which did not differ significantly between cycloleucine-treated and PBS-control embryos (Table 3.1). Crown-rump length (measure of growth) and somite number (measure of developmental progression) and occurrence of axial rotation were also not adversely affected in embryos cultured with cycloleucine (Table 3.1 and Figure 3.2). Hence, treating embryos with cycloleucine up to 15 mM does not have detectable embryotoxic effects.

Cycloleucine conc. (mM)	No. of embryos	Yolk sac circulation	Crown-rump length (mm)	No. of embryos with failed axial rotation (%)	No. of somites	No. of embryos with cranial NTDs (%)
0	28	2.73 ± 0.11	2.70 ± 0.12	0 (0)	20.68 ± 0.16	0 (0)
10	108	2.79 ± 0.15	2.57 ± 0.26	0 (0)	20.30 ± 0.23	62 (57.4)**
15	34	2.33 ± 0.21	2.37 ± 0.16	1 (2.9)	19.9 ± 0.25	25 (73.5)**

Table 3.1. Growth and development of CD1 mouse embryos cultured in the presence of cycloleucine. Non-viable embryos were identified by the absence of yolk sac circulation. Values for yolk sac circulation, somite number and crown-rump length are given as mean ± SEM. No significant difference between the developmental parameters assessed are found between cycloleucine-treated and PBS control embryos (0 mM; $p > 0.05$, as tested by Student's t-test). Data for failed axial rotation and cranial NTDs are presented as the number of embryos with percentage values in parentheses. Cycloleucine-treatment results in a significant increase in the rate of cranial NTDs; ** indicates $p < 0.0001$, as tested by Z-test.

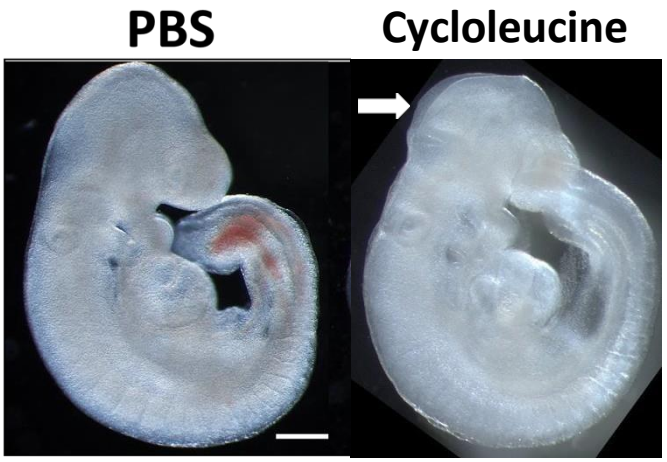

Figure 3.2. Representative image of a PBS control (left) and 10 mM cycloleucine-treated embryos (right). All embryos cultured without cycloleucine (PBS) show no sign of embryo toxicity, developmental delay, growth retardation and do not present with cranial NTDs (as shown by the closed head region). A proportion of embryos treated with 10 mM cycloleucine present with cranial NTDs as shown by the open cranial neural folds (white arrow). Scale bar represents 200 μM.

3.2.2 Cycloleucine causes cranial NTDs in CD1 mouse embryos

All embryos cultured from E8.5 for 24 h in the presence of cycloleucine progressed past the 16-somite developmental stage (Table 3.1), at which cranial neural tube closure is normally complete in CD1 mouse embryos. Hence all embryos in this experiment could be assessed for cranial NTDs.

The treatment of embryos with cycloleucine resulted in an increasing rate of cranial NTDs (Table 3.1 and Figure 3.2). A significant proportion of cycloleucine-treated embryos exhibited cranial NTDs: 57.4% at 10 mM ($p < 0.05$, tested by Z-test) and 73.5% at 15 mM ($p < 0.05$) when compared to PBS control embryos (Table 3.1 and Figure 3.2).

Since cycloleucine-treated embryos treated with up to 15 mM cycloleucine did not exhibit developmental or growth abnormalities (Table 3.1), these findings suggest that failure to close the cranial neural folds is a specific effect of cycloleucine, and not as part of a non-specific influence on development or growth.

3.2.3 Cycloleucine-treatment induces female preponderant cranial NTDs.

In order to detect a possible sex difference in the rate of cranial NTDs, cycloleucine at 10 mM was used as this gave an NTD rate of ~ 50% (Table 3.1). Hence, any increase or decrease in NTD rate in females versus males should be detectable.

The overall cranial NTD rate at 10 mM cycloleucine was 57.4% (62/108; Figure 3.3A), with female embryos (68.4% NTDs; 39/57) significantly more often affected than male embryos (45.1% NTDs; 23/51; Figure 3.3A). This represents a significant difference in the rate of cranial NTDs between sexes ($p = 0.0093$; as assessed by 2x2 Chi Square).

Quantifying by the proportion of embryos with or without cranial NTDs revealed that 63% of embryos with cranial NTDs were female whereas 37% were male. Conversely, 39% of non-NTD embryos were female whereas 61% were male (Figure 3.3B). The assessment of female-to-male sex ratio in cycloleucine-treated embryos was 1.5:1. Hence, 3 female embryos were affected with cranial NTDs for every two maleembryos.

The total number of female (n = 57) and male (n = 51) embryos that were cultured and harvested to score for cranial NTDs at 10 mM cycloleucine did not differ significantly (p = 0.2). Moreover, there was no ‘sex selection’ in these experiments, as embryos were harvested from the uterus and cultured blind to sex, which was determined after all other data were collected. Hence, the female excess in cranial NTDs in cycloleucine-treated embryos was not due to a selective absence or loss of male embryos.

In conclusion, the treatment of non-mutant CD1 embryos with cycloleucine in whole embryo culture reveals a female preponderance of cranial NTDs, closely paralleling the previous findings in humans and in mouse genetic models.

The female excess in cranial NTDs observed in cycloleucine-treated embryos is the first study to show that a female excess in cranial NTDs can also be caused by an environmental factor and more specifically one which is able to modulate methyl group availability.

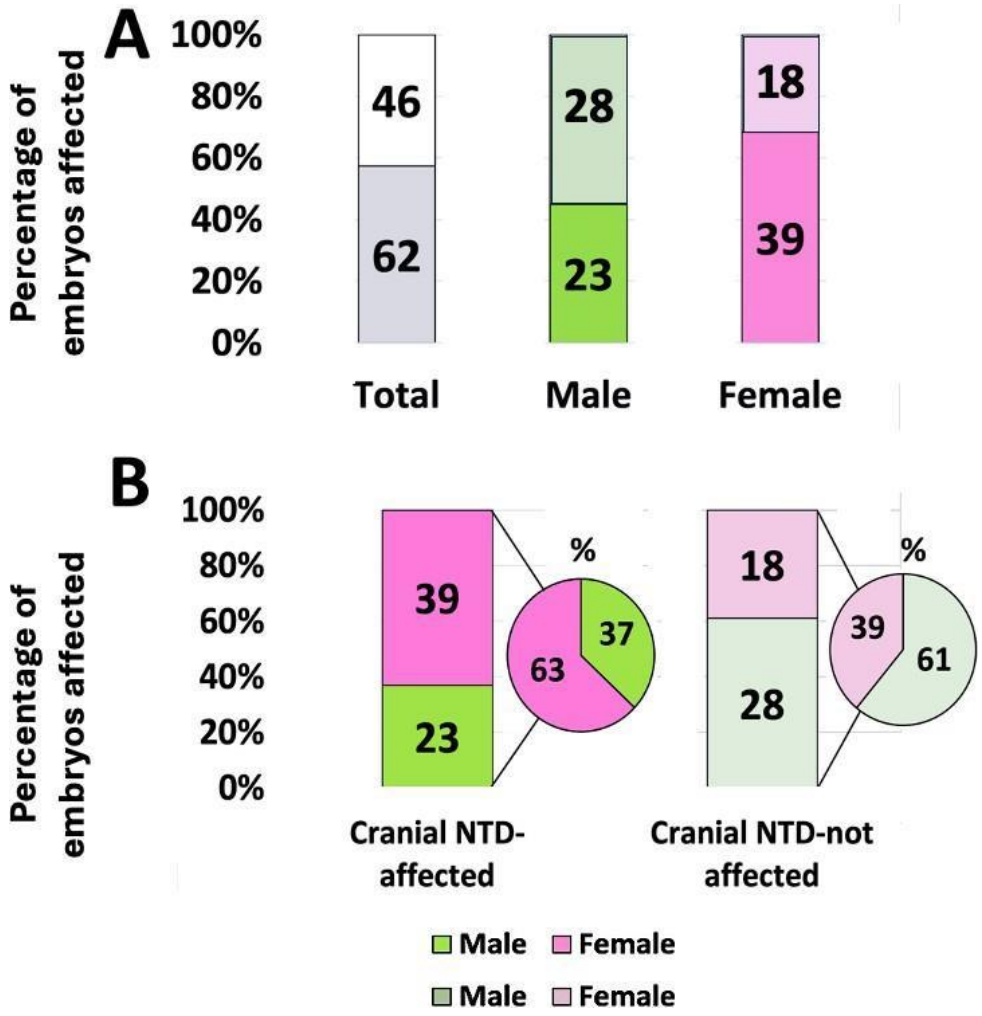

Figure 3.3 Cycloleucine-treatment results in female preponderant cranial NTDs. **(A)** At a dose of 10 mM, cycloleucine results in cranial NTDs in 57.4% (62/108) of treated embryos, with female embryos (68.4%; 39/57) significantly more often affected than male embryos (45.1%; 23/51). Cycloleucine- treatment results in a sex difference in the rate of cranial NTDs between sexes ($p = 0.01$) – a selective increase in the rate of cranial NTDs in female embryos that results in a distorted increase of the female- to-male ratio to 1.5:1. The colours in the stacked bar charts represent cranial NTD-affected embryos and the numerical values the number of embryos. **(B)** The distribution by sex between embryos affected and not affected by cranial NTDs. There is a significant difference between the number of embryos that present and do not present with cranial NTDs – which is skewed towards 1.7 times increase in cranial NTDs in female embryos (39/62; $p = 0.004$) and a 0.6x decrease in the number of female embryos that do not become affected with cranial NTDs (28/46; $p = 0.03$). The darker colours in the stacked bar charts represent cranial NTD-affected embryos whereas the lighter shades of colour represent embryos not- affected by cranial NTDs, with numerical values in the stacked bar charts representing the number of embryos. The pie charts represent the proportion and thus percentage of male and female embryos as extrapolated from the numerical embryo number values.

3.2.4 Cycloleucine results in a sex difference in the severity of cranial NTDs

Semi-quantitative assessment of the number of brain regions (i.e. forebrain, midbrain, hindbrain) affected in cycloleucine-treated embryos revealed that cycloleucine causes a more severe form of cranial NTDs in female embryos than in males. Female embryos most often had at least two brain regions affected, whereas one and two brain regions were equally often affected in male embryos (Figure 3.4A and 3.4B). The most severe form of cranial NTD, in which all three brain regions are affected, was found in five female embryos (12.8% of females) compared with one male embryo (4.3% of males). Nevertheless, these distributions do not differ significantly ($p > 0.05$; 3 x 2 chi-square test).

Quantitative assessment of the severity of cranial NTDs was performed by determining the proportion of cranial neural fold length that was open versus closed. Measurements were made from the rostral extremeity of the forebrain optic vesicle to otic vesicle along the body axis. On average the cranial neural tube region was open along 54.7 $\pm$ 12.1 % of the cranial region of cycloleucine-treated female embryos, compared with 37.6 $\pm$ 5.3 % in males ($p = 0.013$; Figure 3.5C). Hence, cycloleucine not only results in cranial NTDs more commonly in female embryos, but also causes a more severe form of cranial NTDs in affected females than males.

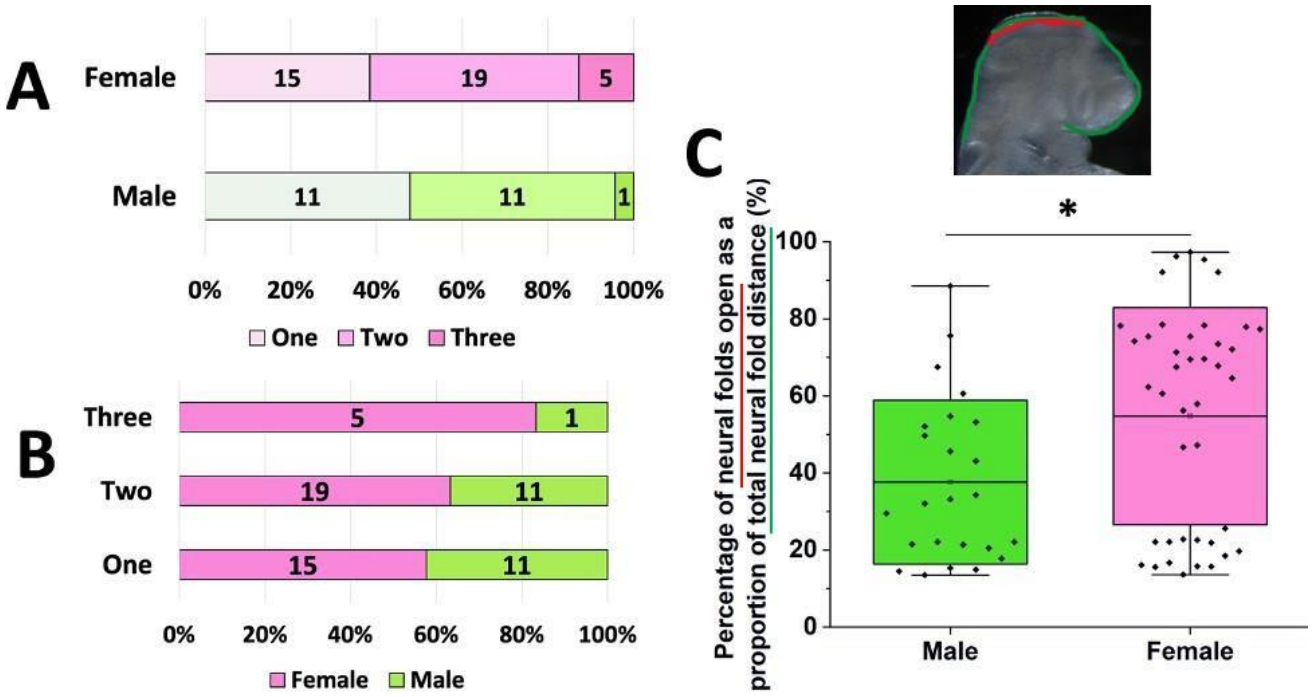

Figure 3.4. Cycloleucine results in a more severe form of cranial NTDs in female than male embryos. **(A)** The distribution of the number of brain regions that remain open per sex in embryos treated with cycloleucine. Female embryos present with an increased number of embryos that fail in cranial neural tube closure in all brain regions assessed, with most female embryos showing at least two brain regions affected. **(B)** A comparison by sex of the relative number of brain regions affected in cycloleucine-treated male and female embryos. There is an excess of female embryos that fail to close their cranial neural tube in all category groups with a clear excess in female embryos amongst the more severe (two brain region affected; two-third of female embryos affected vs one-third of male embryos) and the most severe form of cranial NTDs when the cranial neural tube completely fails to close (5:1). The numerical values in the stacked bar charts in (A) and in the bar charts in (B) represent the number of embryos. **(C)** Quantification of the severity of cranial NTDs in cycloleucine-treated male and female embryos. A sex difference between the percentage of neural folds open as a proportion of total neural fold distance exists whereby the extent and degree of failed cranial neural tube closure is significantly greater in female than male embryos ($p = 0.01$, two-tailed student's t test). Each point represents an embryo and values are plotted mean ± SD with the horizontal line representing the mean value.

3.2.5 Cycloleucine-treatment also results in a sex difference in the morphological appearance and pattern of brain regions affected.

In order to assess in more detail the inability of male and female embryos to close their cranial neural tube upon disruption of methylation cycle flux and that may predispose female embryos to increased failure, the specific regions of the cranial neural folds that were affected were recorded.

The comparison of brain regions open and therefore affected are between male and female embryos as assessed per brain region using chi-square tests. The null hypothesis would be that no difference would be expected from the 1:1 sex ratio.

Female embryos with a cranial NTD in only one brain region were significantly skewed towards a hindbrain defect (which was present in 53.3% of female embryos; Figure 3.5A), whereas a hindbrain-only defect was present in less than 10% of male embryos. In contrast, male embryos showed a preponderance of single forebrain defects (in 63.6% of male embryos; Figure 3.5A), whereas female embryos had forebrain-only defects in less than 10% of cases. This sex difference in the location of single open brain regions between the sexes is statistically significant ($p = 0.005$; 3x2 chi-square).

Embryos that showed exencephaly in at least two brain regions also showed a significant difference between sexes ($p < 0.001$). Females had an open midbrain + hindbrain in 79% (15/19) of embryos with two affected regions, whereas males showed a forebrain + midbrain preponderance in 82% (9/11) of such cases (Figure 3.5A). Overall, an affected hindbrain (+/- other regions) was present in 74% (29/39) of female embryos but in only 17% (4/23) of males, which is highly significant ($p = 0.000014$; 2x2 chi-square test), whereas an affected forebrain was present in 78% (18/23) of males but only 26% (10/39) of females: also highly significant ($p = 0.00058$). An affected midbrain was present in more equal numbers between the sexes: 74% (29/39) of females and 61% (14/23) of males, a non-significant difference ($p = 0.27$). Hence, cranial NTDs are predominantly hindbrain/midbrain in females but forebrain/midbrain in males.

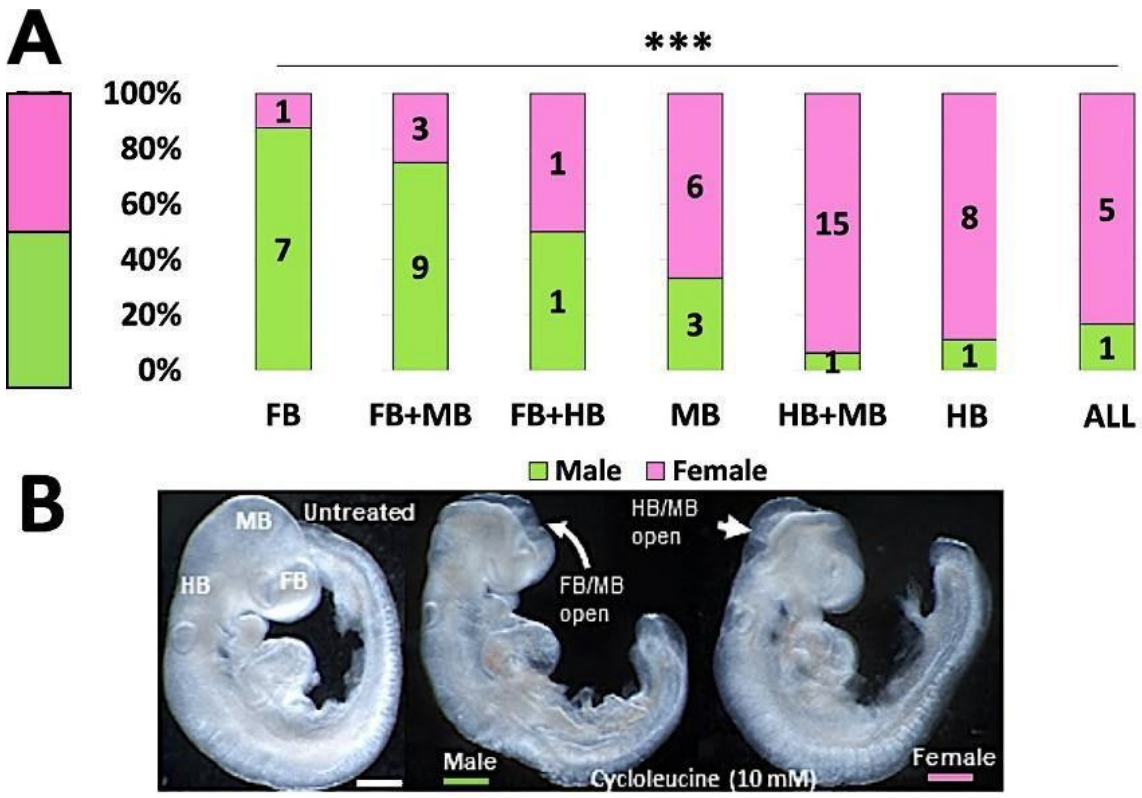

Figure 3.5. Cycloleucine-treatment results in a sex difference in the pattern and morphological appearance of cranial NTDs. (A) The distribution of cranial NTD the brain regions by embryonic sex. Male embryos show cranial NTDs of the FB/MB most often whereas HB/MB defects are most common in female embryos. The distribution of males and females between the seven different NTD regional combinations is significantly different (*** $p < 0.001$). Embryo numbers are shown on bars. **(B)** Representative embryos after 24 h culture from E8.5 without (left) or with 10 mM cycloleucine (mid and right). An open FB/MB defect can be seen in a male embryo (centre) and an open HB/MB in a female embryo (right). Scale bars represent 200 μm. Abbreviations: FB = forebrain, MB = midbrain and HB = hindbrain.

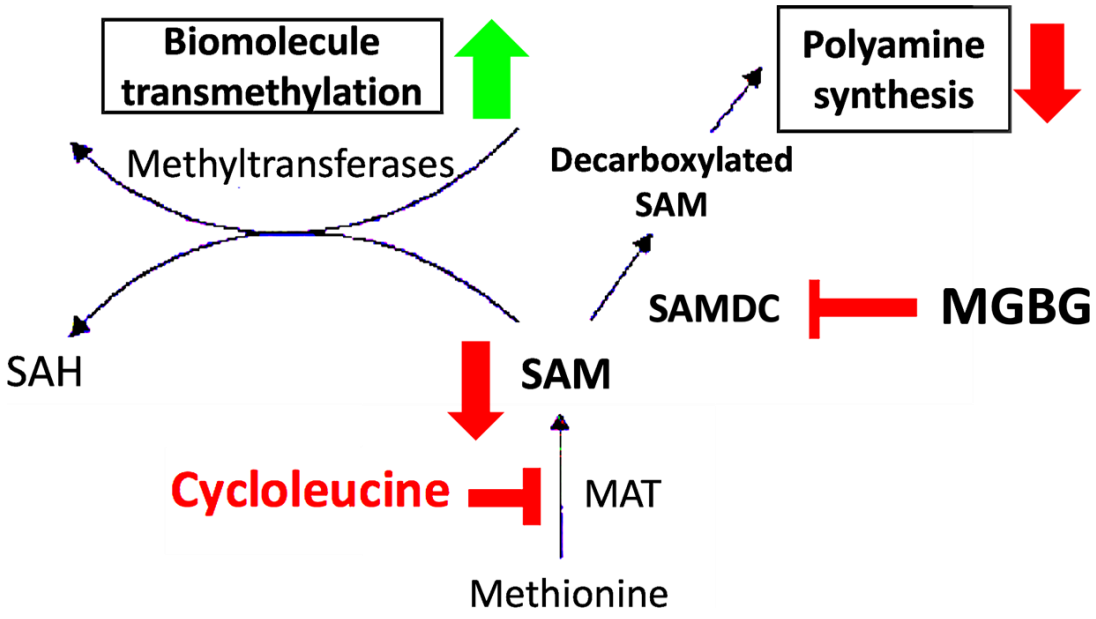

Figure 3.6. The proposed mechanism of MGBG action in maximising endogenous SAM for methylation reactions, by inhibiting SAMDC.

3.2.6 Blocking synthesis of the polyamines, spermidine and spermine, does not perturb normal embryonic development or cause cranial NTDs

The next step in this research was to assess whether retaining SAM in the methylation cycle, for use downstream methylation reactions, could prevent cycloleucine-induced cranial NTDs. For this purpose, embryos were cultured in the presence of MGBG (methylglyoxal-bis-guanyl hydrazone), an inhibitor of SAMDC (Figure 3.6). Embryos were obtained from 6 litters.

Initially, it was important to determine the effect of MGBG when added alone to CD1 embryo cultures from E8.5 for 24 h, as suppression of polyamine synthesis is reported to be detrimental to embryonic development at earlier stages (Fozard et al., 1980). Addition of MGBG up to a concentration of 10 μM did not affect embryo viability as judged by mean yolk sac circulation score, and there was also no effect on embryonic growth or developmental progression, as assessed by crown-rump length and somite number, respectively (Table 3.2; Figure 3.7). Moreover, no embryo at any concentration of MGBG presented with an open cranial neural tube, even though all embryos developed past the 16-somite stage (Table 3.2). MGBG-treated embryos had a closely similar morphology to PBS-treated controls (Figure 3.7). These findings suggest that MGBG is non-toxic for use in mouse whole embryo culture, and that spermidine and spermine biosynthesis from SAM is dispensable for embryonic development and cranial neural tube closure.

MGBG conc. (µM)	No. of embryos	Yolk sac circulation	Crown-rump length (mm)	No. of embryos with failed axial rotation (%)	No. of somites	No. of embryos with cranial NTDs (%)
0	6	3.00 ± 0.00	2.76 ± 0.16	0 (0)	20.0 ± 0.40	0 (0)
1	10	3.00 ± 0.00	2.71 ± 0.11	0 (0)	19.8 ± 0.37	0 (0)
2	8	3.00 ± 0.00	2.74 ± 0.14	0 (0)	19.6 ± 0.45	0 (0)
5	10	3.00 ± 0.00	2.66 ± 0.17	0 (0)	20.1 ± 0.48	0 (0)
10	12	3.00 ± 0.00	2.69 ± 0.13	0 (0)	19.4 ± 0.57	0 (0)

Table 3.2. Growth and development of CD1 mouse embryos cultured in the presence of MGBG alone. Values for yolk sac circulation, somite number and crown-rump length are given as mean ± SEM. No significant difference between any developmental parameters were found between MGBG-treated and PBS control embryos (0 µM; $p > 0.05$ as tested by Student's t-test). Data for failed axial rotation and cranial NTDs are presented as the number of embryos with percentage values in parentheses. MGBG treatment does not result in any growth or developmental abnormalities and does not cause cranial NTDs.

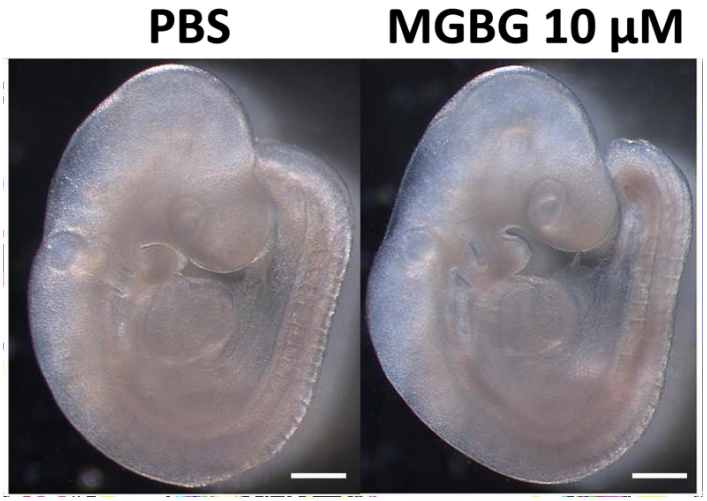

Figure 3.7. Normal development of neurulation stage embryos in the presence of MGBG. Representative images of embryos cultured for 24 h from E8.5 in the presence of PBS (left) and 10 µM MGBG (right). No signs of embryo toxicity, developmental delay, growth retardation or cranial NTD are visible in the MGBG-treated embryo (n = 12) compared with the PBS-treated control (n = 10). Scale bar represents 200 µM.

3.2.7 Retaining endogenous SAM in the methylation cycle prevents cycloleucine-induced cranial NTDs

Having established that MGBG is non-toxic for E8.5 embryos, it was next combined with cycloleucine in embryo cultures to test the prediction that MGBG would 'rescue' embryos from cranial NTDs induced by cycloleucine. The rationale was that inhibiting SAMDC will maximise SAM availability and so counteract the effect of cycloleucine in diminishing SAM abundance.

E8.5 embryos were co-treated with cycloleucine and MGBG in whole embryo culture, with the addition of an initial pre-loading period of 4 h in MGBG alone, to ensure increased SAM abundance before cycloleucine began its effect. Cycloleucine-treated embryos treated with MGBG in the 1-10 μM range showed no signs of generalised toxicity, growth abnormality or delay, as developmental parameters for embryonic viability, growth and developmental progression were comparable and did not differ significantly from PBS control embryos (Table 3.3).

Co-treatment with cycloleucine and varying concentrations of MGBG resulted in a dose-dependent decrease in the rate of cranial NTDs (Table 3.3). At 1 μM, MGBG had no protective effect (62.5% NTDs, 5/8 vs 61.1% NTDs in PBS control, 11/18), at 2 μM the rate of cranial NTDs reduced to 29% (30/103), and at 5 μM and 10 μM there was complete rescue of cranial NTDs (0/9 at each dose). Significant rescue in cycloleucine-treated embryos was observed at 2, 5 and 10 μM MGBG dose levels compared with cycloleucine-only treatment ($p < 0.01$; Table 3.3).

MGBG conc. (μM)	Cycloleucine conc. (mM)	No. of embryos	Yolk sac circulation	Crown-rump length (mm)	No. of embryos with failed axial rotation (%)	No. of somites	No. of embryos with cranial NTDs (%)
0.0	0.0	12	3.00 ± 0.00	2.74 ± 0.11	0 (0)	20.6 ± 0.17	0 (0)
0.0	10	18	2.84 ± 0.08	2.61 ± 0.16	0 (0)	20.1 ± 0.30	11 (61.1)
1.0	10	8	3.00 ± 0.00	2.56 ± 0.12	0 (0)	20.2 ± 0.32	5 (62.5)
1.5	10	14	2.78 ± 0.11	2.71 ± 0.14	0 (0)	19.4 ± 0.28	7 (50.0)
2.0	10	103	2.74 ± 0.21	2.51 ± 0.17	0 (0)	20.4 ± 0.67	30 (29.1)*
5.0	10	9	2.79 ± 0.10	2.48 ± 0.13	0 (0)	19.2 ± 0.43	0 (0)*
10.0	10	9	2.72 ± 0.17	2.42 ± 0.12	0 (0)	19.8 ± 0.38	0 (0)*

Table 3.3. Growth and development of CD1 mouse embryos cultured and co-treated with cycloleucine and MGBG. Non-viable embryos were identified by the absence of yolk sac circulation. Values for yolk sac circulation, somite number and crown-rump length are given as mean ± SEM. No significant difference between any developmental parameters were found between PBS control, cycloleucine-treated and cycloleucine and MGBG co-treated embryos ($p < 0.05$; as tested by Student's t-test). Data for failed axial rotation and cranial NTDs are presented as the number of embryos with percentage values in parentheses. The addition of MGBG to cycloleucine-treated embryos results in a dose-dependent decrease in the rate of cranial NTDs: 1 μM (no effect) to 5 μM (100% complete rescue) with no detectable toxicity or adverse effects. Cranial NTDs become significantly from doses of 2 μM MGBG ($p = 0.01$). * Indicates $p = 0.01$

3.2.8 MGBG abolishes the female excess in cycloleucine-induced cranial NTDs.

The next goal was to determine whether MGBG may affect the sex ratio of cycloleucine-induced cranial NTDs, as well as reducing the overall rate. The XCI hypothesis suggests that female embryos are predisposed to exencephaly because of an endogenous methyl drain. Hence, MGBG, by 'sparing' SAM for downstream methylation reactions, was predicted to reduce cranial NTD risk particularly in female embryos.

Cycloleucine-only treatment (10 mM) in the MGBG dose-response experiment produced a closely similar ($p > 0.05$) rate of cranial NTDs (61.1%, 11/18; Table 3.3) as in the earlier, larger-scale cycloleucine experiment (57.4% , 62/108; Table 3.1). Although a potential limitation of the work in order to provide greater statistical power for assessing the effect of MGBG on the sex difference in cranial NTDs, embryos co-treated with cycloleucine and 2 μM MGBG (n= 103) were subsequently compared with cycloleucine-only treated embryos from the larger previous study (n = 108). MGBG at 2 μM was chosen as this concentration significantly rescued cranial NTDs, compared with cycloleucine alone (Table 3.3), but the effect was partial, so that sufficient cranial NTDs remained to enable an accurate determination of embryonic sex ratio.

Co-culture of embryos in 2 μM MGBG and 10 mM cycloleucine resulted in a specific rescue of cranial NTDs among female embryos (Figure 3.8A,B), with a rate reduction of almost 2.5-fold (68.4% to 23.1%; $p < 0.00001$). In contrast, the rate of cranial NTDs in male embryos treated with MGBG was only 1.3-fold (45.1% to 35.3%; $p = 0.45$), a statistically non-significant change. Hence, the great majority of the MGBG-induced reduction in total cranial NTD rate is female-specific, with males showing a much smaller rescue effect (Figure 3.8C).

Presenting the data as number and proportion of embryos with or without cranial NTDs shows that the addition of MGBG to cycloleucine-treated embryos completely reverses the sex distribution. Hence, the 63% female: 47% male ratio among cycloleucine-induced NTDs is changed to a 40% female: 60% male ratio by addition of MGBG. This

had the effect of normalising the female: male sex ratio of cranial NTDs, from 1.5:1 in cycloleucine only-treated embryos to 0.7:1 in MGBG + cycloleucine ($p = 0.008$; comparison of the female: male ratio between cycloleucine-treated and co- treated embryos). A sex ratio that is significantly different ($p > 0.05$; Fisher's exact test)from the expected 1:1 ratio which suggest reversal of the female excess upon MGBG-cotreatment and highlights the increased sensitivity of female embryos to a reduced methylation capacity when compared with male embryos.

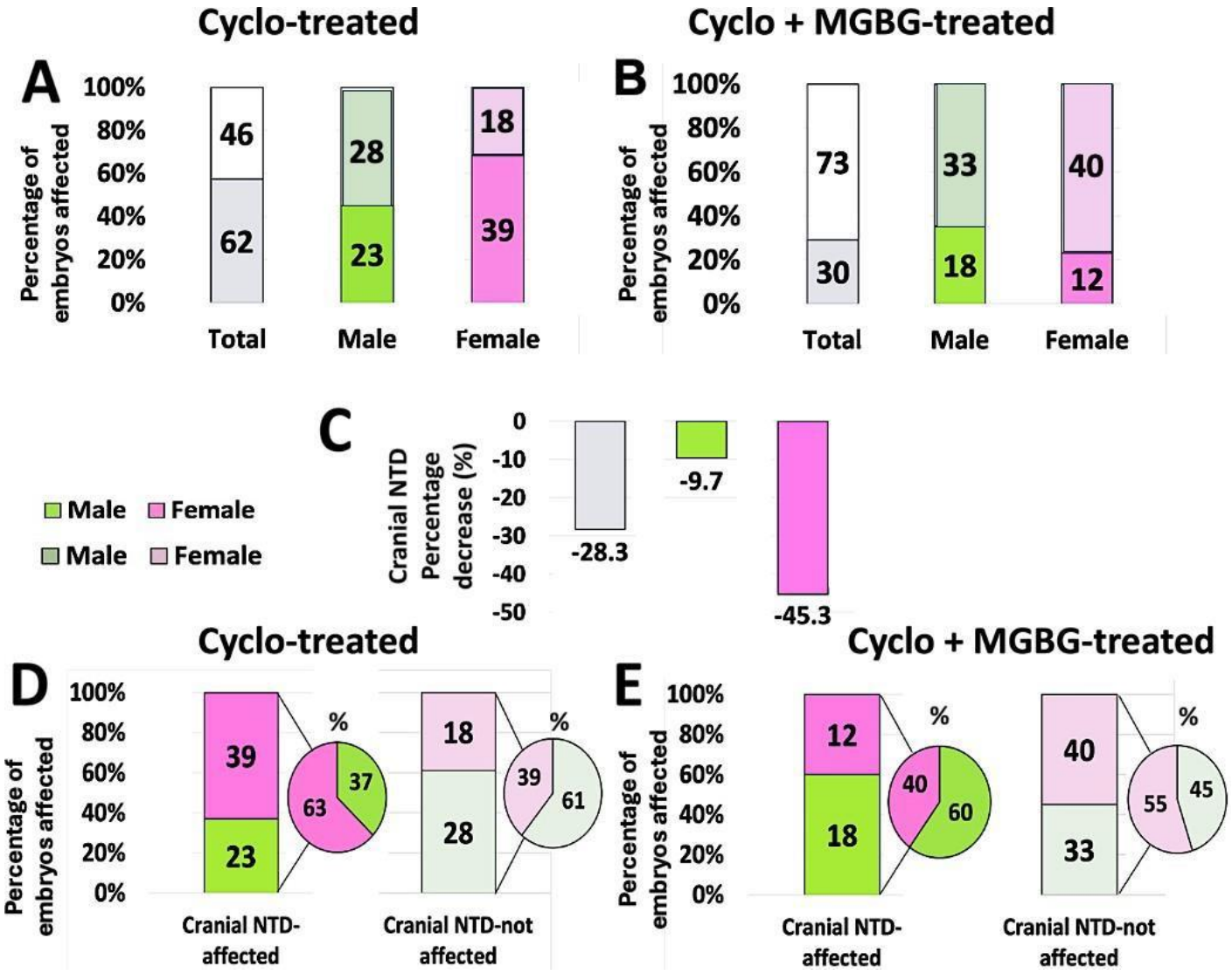

Figure 3.8. MGBG abolishes the female excess in cycloleucine-induced cranial NTDs. (A, B) Distribution of embryos between normal (open bar sectors) and cranial NTDs (filled bar sectors), in cultures with 10 mM cycloleucine only (A, data from Figure 3.3A) and with cycloleucine + 2 µm MGBG (B). Data are shown for total embryos (grey), males (green) and females (pink). Rate of cranial NTDs shows a significant reduction among MGBG-treated total embryos (57.4% to 29.1%; $p = 0.000035$) and female embryos (68.4% to 23.1%; $p < 0.00001$) but not male embryos (45.1% to 35.3%; $p = 0.45$). **(C)** The percentage change in NTD rate in cycloleucine + MGBG-treated embryos compared with cycloleucine-only cultures. Total (grey), male (green) and female (pink) embryo data are shown. The reduction in cranial NTD rate is almost five times greater in females than in males. **(D, E)** The distribution and proportion of embryos by sex that have (dark colours) or do not have (light colours) cranial NTDs when treated with cycloleucine only (D, data from Figure 3B) and with cycloleucine + MGBG (E). The female preponderance among cycloleucine-induced cranial NTDs is abolished by MGBG. Numbers of embryos are shown on bars. Pie charts represent the percentage values of male and female embryos in each category, as extrapolated from the numerical embryo number values.

3.2.9 Effect of cycloleucine and MGBG on SAM/SAH ratio: a marker of methylation cycle flux and activity

To assess the effect of cycloleucine treatment, with/without MGBG addition, on methylation cycle activity, total embryonic levels of SAM and SAH were measured using LC-MS/MS. SAM is the substrate for downstream methyltransferase enzymes while SAH is the product of SAM demethylation during methyl group donation to methyltransferases. SAH is a known potent inhibitor of downstream methylation reactions, with elevated intracellular levels of SAH being associated with global DNA hypomethylation (Caudill et al., 2001).

Cycloleucine treatment caused a statistically non-significant trend towards reduction of SAM concentration (Figure 3.9B) and a highly significant increase in SAH concentration, compared with PBS control embryos (Figure 3.9C; $p < 0.001$). SAM/SAH ratio is often reported as a measure of methylation cycle activity, with a reduced ratio indicating diminished methylation potential (James et al., 2002). As expected, given the reciprocal changes in SAM and SAH concentrations, cycloleucine-treated embryos exhibited a significantly reduced SAM/SAH ratio compared with PBS-treated controls (Figure 3.9A; $p < 0.001$).

Addition of MGBG to cycloleucine cultures did not result in a significant change in SAM/SAH ratio, nor in SAM level (Figure 3.9A,B), although there was a non-significant trend towards reduction of SAH concentration compared with cycloleucine only-treated embryos (Figure 3.9C). Strikingly, there was no significant difference in SAM or SAH concentrations, or in SAM/SAH ratio between cycloleucine-treated male and female embryos (Figure 3.9D). Although the SAM/SAH ratio was significantly reduced in embryos treated with cycloleucine +/- MGBG assessment no sex difference in the ratio was observed between pooled cycloleucine treated embryos male or female embryos (Figure 3.9E). Individual assessment of the metabolite levels of SAH (Figure 3.9F) and SAM (Figure 3.9G) also did not reveal a significant sex difference

These findings provide support for the idea that cranial NTDs in these experiments result from inhibition of the methylation cycle, consistent with previous findings for cycloleucine (Afman et al., 2005; Dunlevy et al., 2006). However, given its rescuing

effect on cycloleucine-induced NTDs, MGBG might have been expected to normalise the SAM/SAH ratio, although this was not detected in the current experiments. The comparison of SAM, SAH and SAM/SAH ratio between male and female embryos showed no sex differences. This argues that the predisposition of female embryos to

cranial NTDs does not result from a sex-specific difference in the potency of cycloleucine to disrupt methylation reactions. This is consistent with the ‘methyl sink’ hypothesis which proposes an inherent XCI-related methylation deficiency in female embryos, that is exacerbated by cycloleucine.

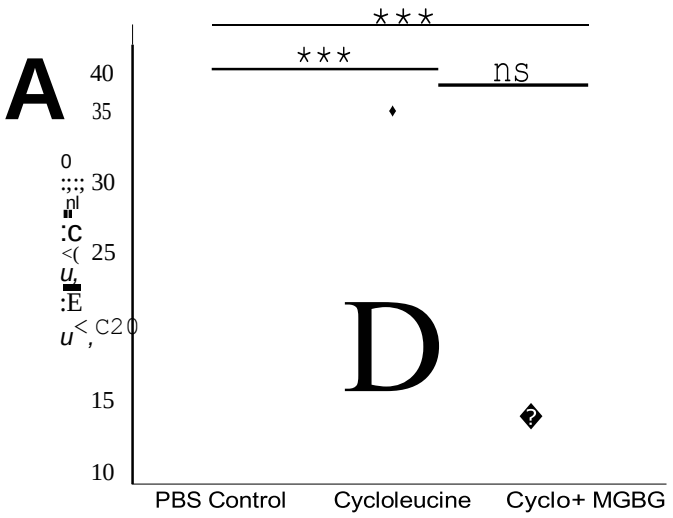
A
***
***
ns
40
35
30
25
20
15
10
D
PBS Control
Cycloleucine
Cyclo+ MGBG

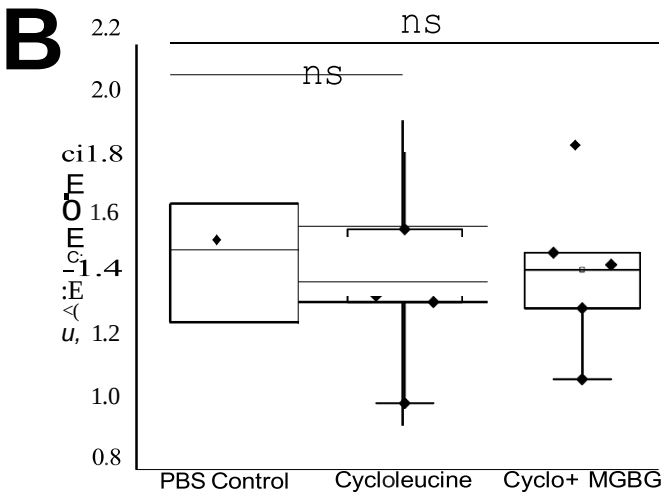
B
ns
ns
2.2
2.0
1.8
1.6
1.4
1.2
1.0
0.8
PBS Control
Cycloleucine
Cyclo+ MGBG

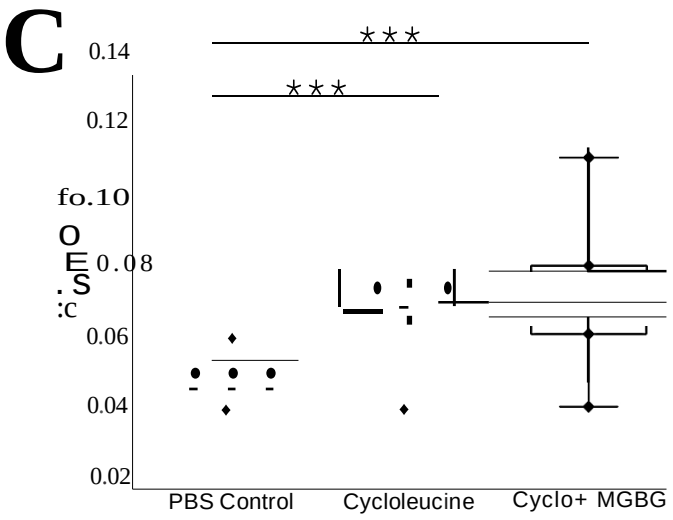
C
***
***
0.14
0.12
0.10
0.08
0.06
0.04
0.02
PBS Control
Cycloleucine
Cyclo+ MGBG

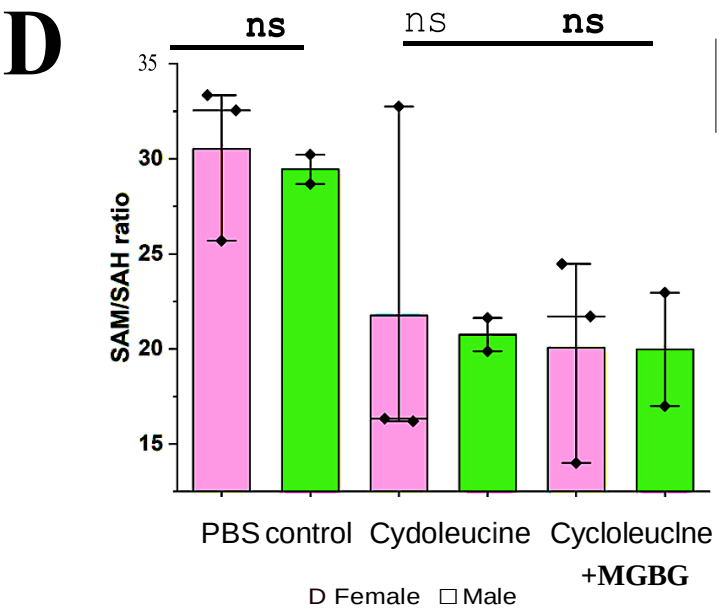
D
ns
ns
ns
SAM/SAH ratio
35
30
25
20
15
PBS control
Cydoleucine
Cycloleuclne
+MGBG
D Female
Male

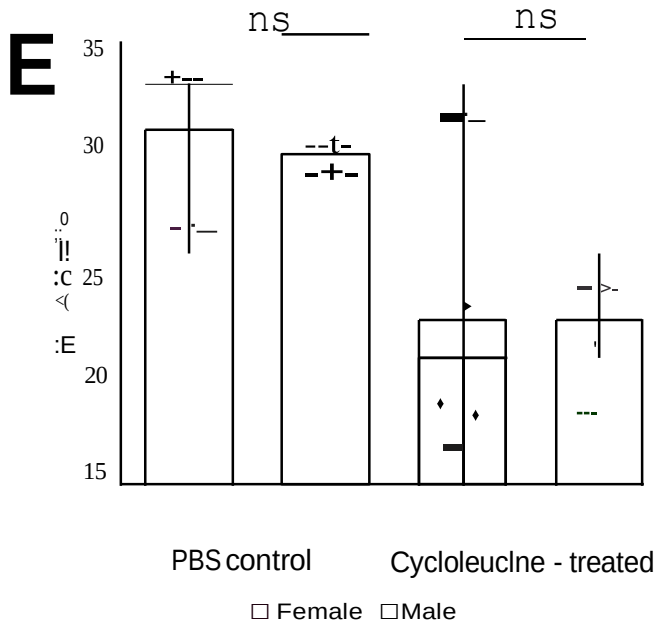
E
ns
ns
35
30
25
20
15
PBS control
Cycloleuclne - treated
Female
Male

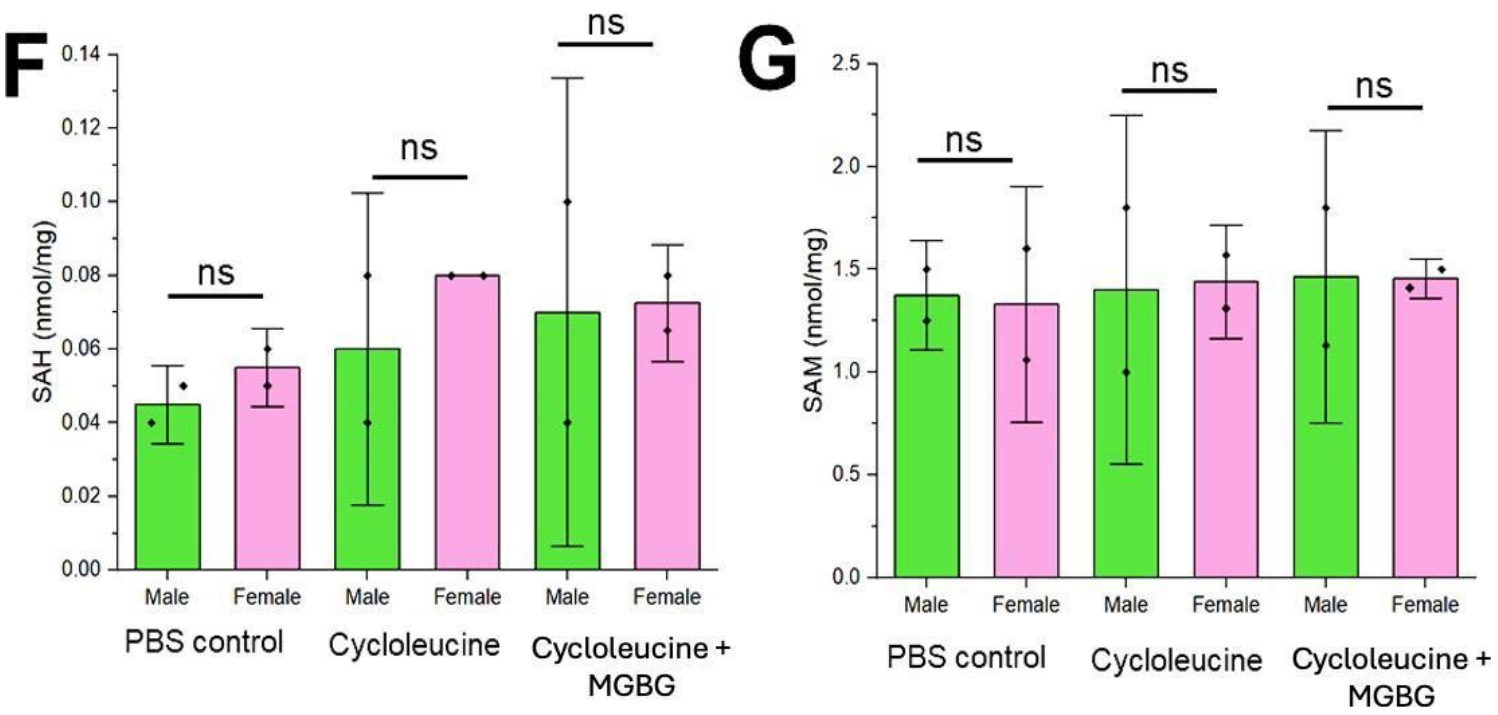

Figure 3.9. Determination of SAM and SAH concentrations, and SAM/SAH ratios, in PBS control, cycloleucine-treated and cycloleucine + MGBG co-treated embryos. (**A-C**) Concentrations of SAM (B) and SAH (C) were determined by LC-MS/MS assay of individual embryos, with calculation of SAM/SAH ratio (A), as a read-out of methylation cycle flux. While SAM shows a trend towards reduction in the cycloleucine-treated groups, compared with PBS controls, this is not statistically significant (B; $p > 0.05$). However, SAH concentration is significantly increased in both cycloleucine-treated groups (C; *** $p < 0.001$), and in consequence the SAM/SAH ratio is significantly reduced in these groups compared with PBS controls (A; *** $p < 0.001$). No differences were detected in SAM, SAH or SAM/SAH ratio between the cycloleucine and cycloleucine + MGBG groups ($p > 0.05$). **(D, E)** Comparison of SAM/SAH ratio in male and female embryos of the different treatment groups. **(F)** Comparison of the metabolite SAH and **(G)** SAM in male and female embryos of the different treatment groups. No sex difference in the SAM/SAH ratio or in SAM or SAH levels was found in any treatment group (D; $p > 0.05$), nor when the two cycloleucine-treated groups were combined (E; $p > 0.05$. Each data point represents a single embryo. Values are given as mean ± SD.

3.2.10 MGBG may increase downstream methyltransferase activity in cycloleucine-treated embryos

MGBG significantly diminishes the frequency of cycloleucine-induced cranial NTDs, particularly in females, and yet the expected increase of SAM/SAH ratio in co-treated embryos was not observed, raising the question of how MGBG exerts its preventive effect on NTDs. The hypothesis under test is that MGBG rescues female NTDs through enhancing their otherwise limited methylation capacity (compared with males).Hence, a further prediction of the hypothesis is that activity 1of downstream methyltransferase enzymes should be increased in MGBG + cycloleucine-treated embryos compared cycloleucine only-treated embryos.

Direct measurement of methyltransferase activity in cultured embryos was beyond the scope of this PhD project. However, the values of kinetic constants (K_m values for SAM and K_i values for SAH) are known for several mammalian methyltransferase enzymes (Carmel and Jacobsen, 2001, published in Clarke et al., 2001), and the wide range of K_i values (> 200-fold; Table 3.4) demonstrates that some methyltransferases are much more sensitive than others to the inhibitory action of SAH. The catalytic activity of each methyltransferase also depends on the concentration of SAM, since SAH acts as a competitive inhibitor. Using the published K_m values, it was previously possible (Katie Burren, 2007, unpublished PhD) to calculate relative enzyme activities of each methyltransferase in mouse embryos, using the Michaelis-Menten equation for competitive inhibition (Clarke & Banfield, 2001). This equation is:

Fraction of maximal enzyme velocity = [SAM] / (K_m + K_m [SAH]/K_i + [SAM])

Where [SAM] and [SAH] are SAM and SAH concentrations, K_m is the Michaelis constant for SAM for that enzyme, and K_i is the inhibition constant for SAH for the same enzyme.

The same method was employed here, using the measured SAM and SAH values (Figure 3.9B,C), to compute predicted methyltransferase activities for embryos cultured in PBS, cycloleucine, or cycloleucine + MGBG. SAM and SAH values for embryos treated with cycloleucine only generated a reduction, compared with PBS

controls, in functional activity of all downstream methyltransferase enzymes (Figure 3.10A). This is consistent with the known inhibitory effect of cycloleucine on SAM-dependent methylation reactions. In contrast, SAM and SAH values for embryos treated with MGBG + cycloleucine generated an increase in activity of most methyltransferases compared with cycloleucine only-treated embryos (Figure 3.10B), although the values were not fully restored to PBS control levels (Table 3.4). This is likely due to the small, although statistically non-significant, reduction in SAH levels in cycloleucine-treated embryos also exposed to MGBG (Figure 3.11C).

Of particular interest was calmodulin-lysine N-methyltransferase which showed the largest predicted reduction in activity in cycloleucine-treated embryos, and also the greatest percentage increase in MGBG-treated embryos (Figure 3.10A, 3.10B). Conversely no increase in the level of DNA (5' cytosine) or phosphatidylethanolamine (PEMT) methyltransferase activity was observed upon addition of MGBG. These findings could suggest that downstream protein methylation reactions are more sensitive to changes in SAM-dependent methylation potential than DNA or lipid methylation reactions.

SAM and SAH data for female and male embryos were also used in the Michaelis-Menten equation to predict methyltransferase activities. However, this generated only minimal female-male differences in any of the three treatment groups (Figure 3.11) suggesting that the female excess in cranial NTDs in cycloleucine-treated embryos, or its rescue after MGBG addition, are not caused by the differential ability of downstream methyltransferase enzymes to catalyse methylation reactions in embryos of the two sexes.

Methyltransferase	K_m for SAM	K_i for SAH	% activity of MT enzymes in PBS control embryos	% activity of MT enzymes in cycloleucine-treated embryos	% activity of MT enzymes in cycloleucine and MGBG co-treated embryos
DNA (cytosine 5-)	1.40	1.40	0.090	0.065	0.065
tRNA (cytosine 5-)	0.50	0.90	0.250	0.160	0.200
tRNA (guanine-N 1-)	3.00	0.11	0.040	0.027	0.030
tRNA (guanine-N 2-)	2.00	23.0	0.050	0.030	0.038
tRNA (adenine-N 1-)	0.30	0.85	0.420	0.260	0.310
rRNA (2'-ribose-O-)	0.24	0.17	0.530	0.330	0.390
Phosphotidylethanolamine (lipids)	18.2	3.80	0.006	0.004	0.004
Protein L-isoaspartate	2.00	0.08	0.060	0.040	0.050
Protein S-isoprenylcysteine	2.10	9.20	0.060	0.037	0.040
Protein Calmodulin-lysine N-	2.00	15.2	0.065	0.030	0.040
Protein histone-lysine N-	12.5	5.90	0.009	0.006	0.007
[Myelin basic protein]-arginine	4.40	1.80	0.030	0.018	0.020

Table 3.4. Fraction of maximal methyltransferase enzyme activity, as determined by SAM and SAH concentrations in embryos of the PBS, cycloleucine-only and MGBG + cycloleucine treatment groups. Predicted enzyme activities were calculated based on known K_m and K_i values (Clarke & Banfield, 2001), and using the Michaelis-Menten equation for competitive inhibition.

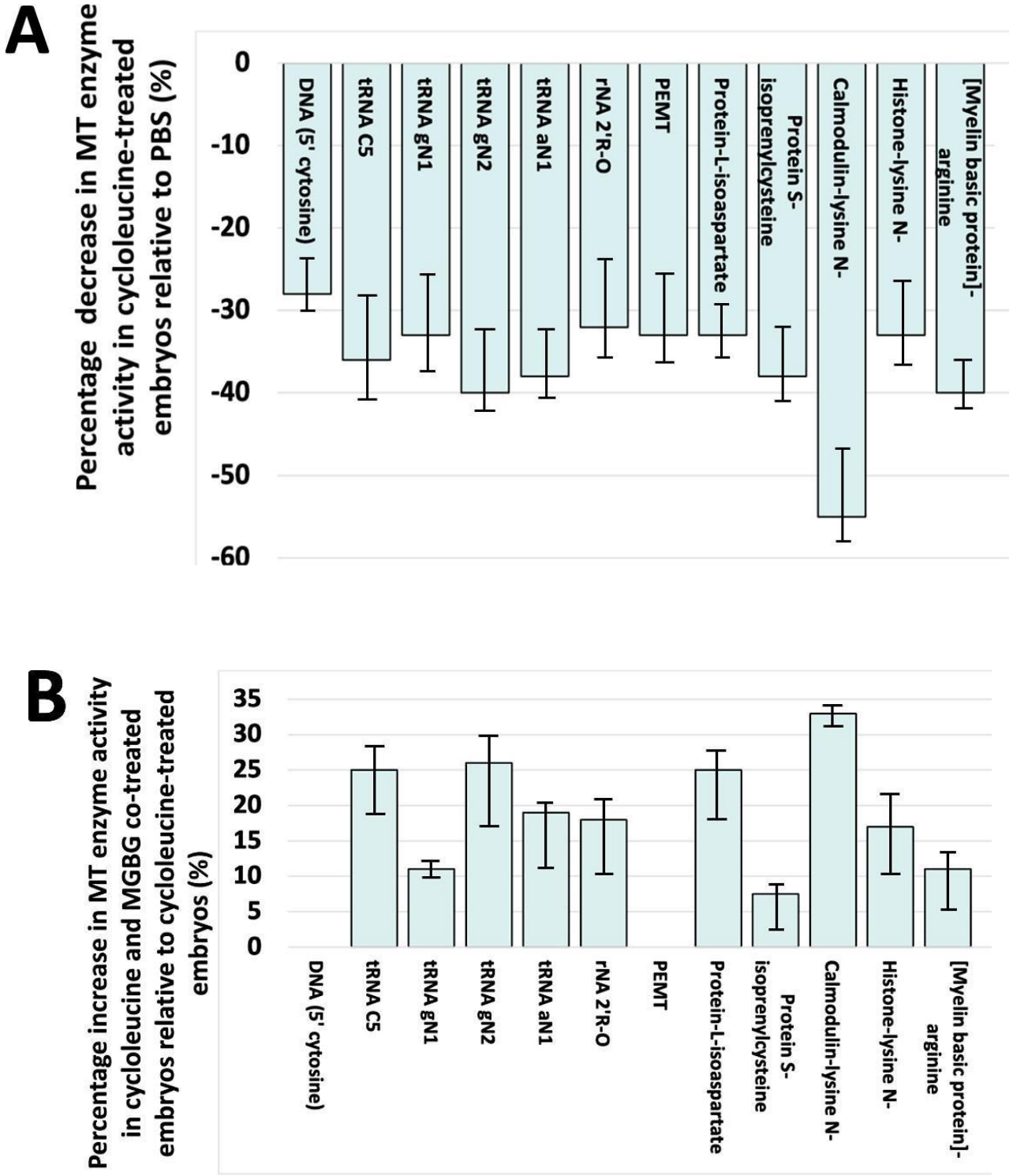
A
Percentage decrease in MT enzyme activity in cycloleucine-treated embryos relative to PBS (%)
0
-10
-20
-30
-40
-50
-60
DNA (5' cytosine)
tRNA C5
tRNA gN1
tRNA gN2
tRNA aN1
rNA 2'R-O
PEMT
Protein-L-isoaspartate
Protein S-isoprenylcysteine
Calmodulin-lysine N-
Histone-lysine N-
[Myelin basic protein]-arginine
B
Percentage increase in MT enzyme activity in cycloleucine and MGBG co-treated embryos relative to cycloleucine-treated embryos (%)
35
30
25
20
15
10
5
0
DNA (5' cytosine)
tRNA C5
tRNA gN1
tRNA gN2
tRNA aN1
rNA 2'R-O
PEMT
Protein-L-isoaspartate
Protein S-isoprenylcysteine
Calmodulin-lysine N-
Histone-lysine N-
[Myelin basic protein]-arginine

Figure 3.10. Percentage change of methyltransferase enzyme activity, as predicted for cycloleucine-treated embryos and cycloleucine and MGBG co-treated embryos, relative to PBS controls. Enzyme activity values were computed by insertion of measured SAM and SAH concentration values into the Michaelis-Menten equation, with use of published K_m and K_i values for each enzyme. **(A)** Cycloleucine-treatment is predicted to result in a decrease in the activity of all methyltransferase enzymes, with different enzymes exhibiting reductions in the range: 28-55%. **(B).** The addition of MGBG to cycloleucine-treated embryos results in an increase in the activity of almost all methyltransferase enzymes assessed, with 75% (9/12) enzymes showing an increase in activity of more than 10%. Calculated enzyme activities include the SD as shown by the error bars to show the variability between samples.

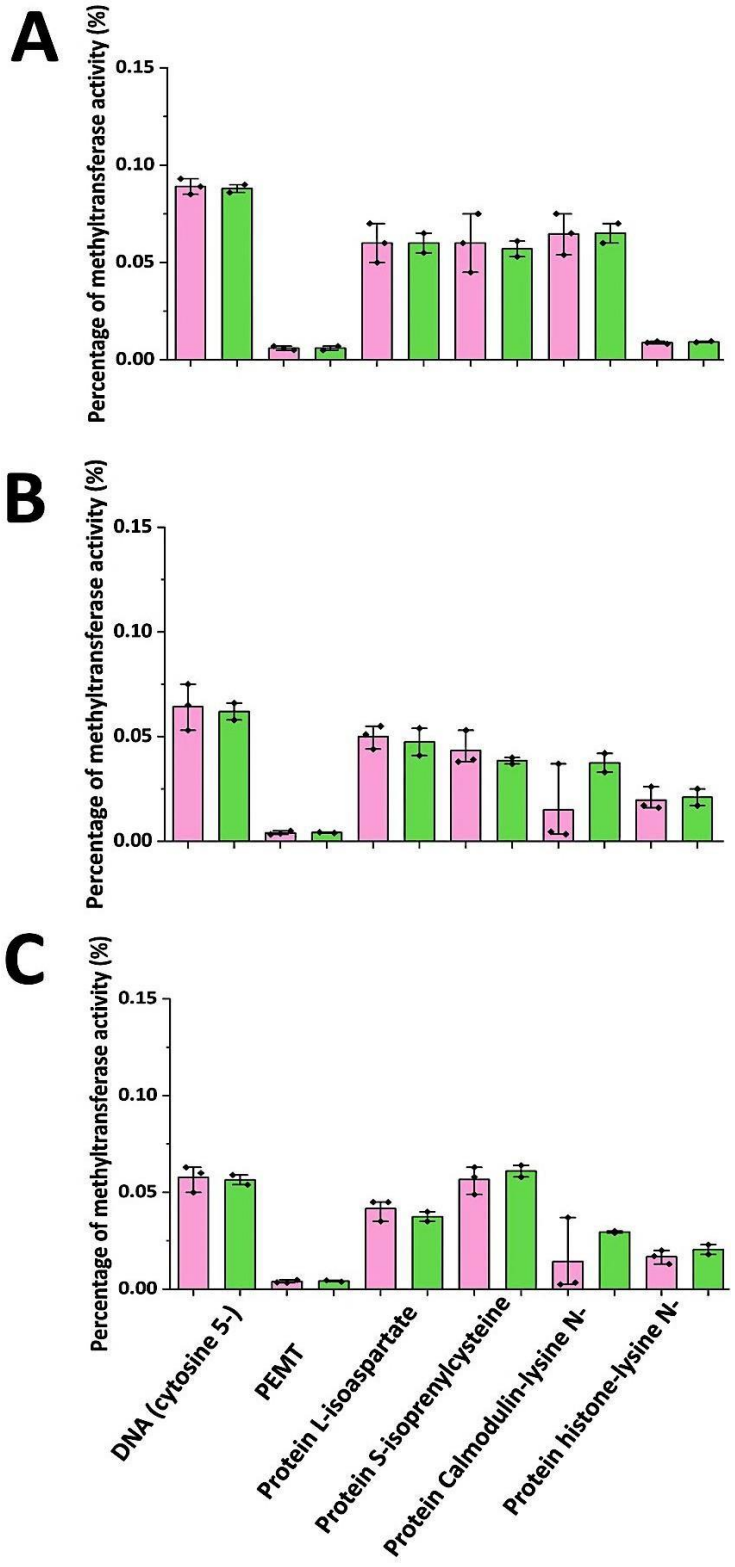

Figure 3.11. Percentage change of methyltransferase enzyme activity by sex in the different treatment groups. (A) PBS control embryos. (**B)** Cycloleucine-treated embryos. **(C)** Cycloleucine + MGBG co-treated embryos. No significant difference between methyltransferase enzyme activity was found between male and female embryos ($p > 0.05$; as assessed by unpaired t-test due to comparison of individual data by methyltransferase per sex) in all treatment groups. Each dot represents an individual embryo.

3.3 Discussion

This chapter represents the first experimental testing of the XCI epigenetic 'methyl sink' hypothesis to explain the increased susceptibility of female embryos to cranial NTDs (Juriloff & Harris, 2012). Despite inhibiting methylation cycle flux equally in both sexes, as judged by SAM/SAH ratio, the addition of the methylation cycle inhibitor, cycloleucine, results in a selective increase in the rate and severity of cranial NTDs in female embryos. These findings are consistent with the notion that closure of the cranial neural tube is more sensitive to disruption of methylation cycle flux in female than male embryos, due to an inherent reduction in methylation potential in females resulting from the proposed XCI-related methyl sink.

The results further show that retaining endogenous SAM in the methylation cycle, by MGBG action to inhibit SAM-dependent polyamine synthesis, is sufficient to abolish the female excess in cycloleucine-induced cranial NTDs. Whereas the SAM/SAH ratio is not restored to normal levels by addition of MGBG, there is a statistically non-significant trend towards reduced SAH concentration. Moreover, calculation of predicted downstream methyltransferase enzyme activity suggests that methylation activity is partially restored by MGBG, compared with cycloleucine-only treatment. Hence, a reduced risk of NTDs in female embryos is associated with an apparent increase in downstream methylation activity, consistent with the methyl sink hypothesis. If MGBG is predicted to restore downstream methylation activity why then is the SAM/SAH ratio not increased in co-treated embryos? One possibility for this is that the effect of MGBG on SAM/SAH is fast acting and time dependent. In our study, the assessment of the SAM/SAH ratio was made at the end of the culture period however it is possible that if embryos were harvested at different time points during the culture period i.e. 0, 2, 4 and 8 hrs after addition of the drug differences in the SAM/SAH ratio may have been detected given the measurements of metabolites may have been more reflective of drug-induced changes that occur in the embryo.

3.3.1 Cycloleucine and regulation of the methylation cycle

Cycloleucine regulates methylation cycle activity by irreversible inhibition of the enzyme methionine acetyltransferase, MAT, which synthesises SAM (Lombardini et al., 1971). Despite this, treatment of embryos with cycloleucine resulted in a non-significant decrease in abundance of SAM, although a highly significant increase in SAH concentration was observed. Of the three MAT isoforms, liver cells express MAT-I and MAT-III whereas the non-liver specific isoform MAT-II is expressed more widely (Finkelstein, 1990), including in embryos (Quere et al., 1999). SAM inhibits MAT-II at concentrations only slightly higher than normal SAM intracellular levels, ensuring cellular SAM levels are maintained relatively constant (Finkelstein, 1990). This can explain why cycloleucine treatment of cultured embryos did not result in a marked reduction in SAM levels. The clearance of SAH, however, is dependent on the rapid removal of homocysteine and adenosine. In the embryo, this may be a rate-limiting step as the methionine synthase-mediated reaction is the principal pathway for removing homocysteine from the cell, although the transsulphuration pathway via cystathione β-synthase is an alternative route, at least in adult tissues. Given that cycloleucine inhibits the production of SAM by blocking the MAT-catalysed conversion of methionine to SAM, cycloleucine is expected to result in a relative accumulation of methionine, which in turn would limit the re-methylation of homocysteine via methionine synthase. Delay in removal of homocysteine results in a build-up of SAH, as SAH-hydrolase catalyses a reversible reaction that favours the formation of SAH in the presence of homocysteine (Finkelstein, 1998a). These considerations can explain how the main effect of cycloleucine in the present study was to increase SAH, and so diminish the SAM/SAH ratio.

The equivalence of SAM/SAH ratio in female and male embryos in this study, with or without cycloleucine or MGBG treatment, provides evidence that the female excess of cranial NTDs does not result from sex differences in the methylation cycle itself. Hence, female and male embryos appear to generate SAM equally, and to stimulate downstream methyltransferase activity equally. This finding is consistent with the XCI-related methyl sink hypothesis, which suggests a sex difference at the level of methyl group availability for methyltransferase action, not at higher levels in the pathway

leading from the methylation cycle.

3.3.2 Cycloleucine effects on downstream methylation capacity

Given that cycloleucine results in only a small reduction in concentration of SAM – the universal methyl group donor – it might be argued that the effect of cycloleucine in inducing female preponderant cranial NTDs is not mediated through reduced methyl group availability. However, the significant increase in SAH and the overall decrease in the SAM/SAH ratio found in cycloleucine-treated embryos are more likely the key functional effects. The evidence for this is: (i) SAH is a potent product inhibitor of almost all methyltransferase enzymes (Zappia et al., 1969); (ii) elevated intracellular levels of SAH have been found to be a biomarker of global hypomethylation in methyl- deficient cystathionine-ß-synthase heterozygous mice (Caudill et al., 2001); (iii) a reduction in SAM/SAH ratio is indicative of poor downstream cellular methylation potential (Sibani et al., 2002).

To gain further insight into the likely downstream effects of cycloleucine, methyltransferase enzyme activities were predicted in cycloleucine-treated embryos, by entering the measured SAM and SAH concentration values into the Michaelis-Menten equation for enzymes with known K_m and K_i values (Clarke & Banfield, 2001). This predicts that cycloleucine-treated embryos exhibit a markedly reduced level of methyltransferase activity compared with PBS controls, as expected of a methylation cycle inhibitor. Importantly, MGBG, which was able to rescue female-specific cranial NTDs in the presence of cycloleucine, was associated with a predicted increase in most methyltransferase activities. Hence, predisposition to a female excess of cranial NTDs correlates with predicted downstream methylation capacity in this study.

The findings with predicted methyltransferase activity are subject to several important caveats. First, the K_m and K_i values for the methyltransferase enzymes were established in adult tissues of various types, and may not be directly applicable to embryos. Second, it is unclear whether the methyltransferases included in the present analysis are all expressed in neurulation stage embryos, or whether embryonic isoforms exist that may differ functionally. The developmental roles of DNA

methyltransferases are well established, with mammalian NTD phenotypes in genetic mutants (Chen et al., 2020). However, protein methyltransferases are less understood, although a few developmentally important enzymes, for example NSD3, have been found to participate in events such as neural crest migration (Jacques-Fricke et al., 2021).

A third consideration relates to the XCI-related methyl sink hypothesis, which predicts that methyl group usage (relatively compromised in females) is critical for one or more aspects of cranial neural tube closure. Hence, one or a few particular methyltransferases may be vital for this purpose. In this context, SAM/SAH data from MGBG + cycloleucine-treated embryos did not predict an increased activity of the DNA and lipid methyltransferase enzymes, perhaps suggesting that protein methyltransferases are more likely to be implicated in the female predisposition to cranial NTDs. Nevertheless, the identity of these 'neurulation critical' methyltransferases is currently unknown, and so it is impossible to predict their responses to the embryonic SAM and SAH concentrations. Clearly investigations of methyltransferase expression and activity in embryonic tissues is required to establish definitively how the activity of specific enzymes is affected by the treatments in the study.

3.3.3 Role of polyamine synthesis in induction of cranial NTDs

Once generated in the methylation cycle, SAM is primarily used for two main cellular processes: either as a methyl donor for downstream transmethylation reactions or, upon decarboxylation, as an aminopropyl donor for synthesis of the polyamines spermine and spermidine. In assessing MGBG for possible use in retaining SAM in the methylation cycle, embryos were first cultured in MGBG alone. This revealed no toxic effects at any concentration tested, demonstrating that SAM-dependent polyamine synthesis is not critical for neurulation-stage embryos. This contrasts with the essential role played by polyamines at earlier developmental stages where their growth-promoting properties are indispensable (Halloran et al., 2021; Pendeville et al., 2001). It seems likely that polyamines do indeed play a key role also at neurulation stages, but that SAM-dependent synthesis is not a critical part of the pathway.

A further possibility is that inhibition of spermine and spermidine synthesis is actually part of the 'NTD rescuing effect' of MGBG in these experiments. That is, a reduction of polyamine synthesis by MGBG counteracts the adverse effect of cycloleucine, for example by diminishing cell proliferation or other cellular processes that might be implicated in NTDs. To test this idea, embryos could be treated with an inhibitor of polyamine synthesis that is not SAM-related, and so intervenes at different point in the biosynthetic pathway. For example, the ornithine decarboxylase inhibitor difluoromethylornithine (DFMO) could be used to diminish polyamine synthesis (Fozard et al., 1980). If reduced polyamine concentration is able to ameliorate cycloleucine-induced female cranial NTDs, then DFMO should also show this effect.

On the other hand, if retaining SAM in the methylation cycle is the key 'rescuing' property of MGBG, then DFMO should not ameliorate female NTDs. Indeed, it might show considerable embryonic toxicity if polyamines are truly important for neurulation-stage development, by parallel with earlier embryonic events.

3.3.4 Other evidence for importance of methylation cycle flux in neural tube closure

Several lines of evidence from both human studies and experimental models of cranial NTDs have shown that methylation cycle flux is essential for cranial neural tube closure and, when perturbed, can increase the susceptibility of embryos to NTDs. Risk factors for human NTDs include elevated maternal plasma levels of homocysteine and reduced levels of vitamin B_{12}, the co-factor for methionine synthase (Kirke et al., 1993; Steegers-Theunissen et al., 1994). Additionally, the thermolabile polymorphic variant (C677T) of the enzyme MTHFR, which exhibits reduced catalytic activity, and therefore reduces the flux and commitment of one-carbon units between the folate and methylation cycles, is also a demonstrated genetic risk factor for NTDs (Amorim et al., 2007). To this extent, dietary studies in humans have recommended a high intake of methionine, the precursor of SAM (Shoob et al., 2001; Shaw et al., 1997) or an increased intake of choline, another methyl group donor (Shaw et al., 2004) to lower the risk of an NTD affected pregnancy.

Experimental models of cranial NTDs also show that disrupting methylation cycle activity can result in cranial NTDs. Neurulation-stage rat embryos cultured on blood sera from epileptic subjects failed to close their cranial neural tube unless the serum was specifically supplemented with methionine (Chatot et al., 1984).The sera from epileptic patients was found to be depleted of free methionine when compared with other sera that supported normal neural tube closure, suggesting that methionine, the precursor of SAM is an essential molecule for neural tube closure. Rat embryos cultured on bovine serum also failed to close the cranial neural tube, unless methionine was added to the culture; bovine sera also contain low or undetectable amounts of free methionine (Coelho et al., 1989). The methyl group from methionine appeared essential in preventing cranial NTDs given that only choline chloride, which can also act as a methyl group donor, could provide partial replacement of methionine. Failed closure of the cranial neural tube has also been found in embryos treated with N_2O, an inhibitor of methionine synthase (Coelho et al., 1989; Coelho and Klein, 1990), in mouse embryos cultured in ethionine, a methionine analogue that inhibits SAM production (Dunlevy et al., 2006), and in embryos treated with excess methionine that inhibits methylation cycle activity and results in reduced levels of SAM (Dunlevy et al., 2006). Chick embryos treated with methylation cycle inhibitors also exhibit neural tube defects (Afman et al., 2006). Furthermore, the perturbed metabolism and uptake of choline – the precursor of betaine, another methyl group donor – was also shown to cause cranial NTDs (Fisher et al., 2001; Fisher et al., 2002). Hence, a number of previous studies identify the critical role of the methylation cycle in neural tube closure. Nevertheless, the downstream methylated biomolecule(s) that are critical for embryos to undergo cranial neural tube closure have not been identified in these studies.

3.3.5 Conclusion

Overall, the findings from this study provide support for the epigenetic “methyl sink” hypothesis in explaining the female excess cranial NTDs. The results show that the addition of cycloleucine, an inhibitor of the methylation cycle causes a non-sex specific reduction in methylation cycle activity but results in a selective increase in the rate of cranial NTDs in female embryos – an increased sensitivity of disrupted methylation in

female embryos that likely reflects the inherently reduced availability of methyl groups that exist in female embryos. Consistent with the XCI epigenetic “methyl sink” hypothesis the findings reveal that downstream methylation reactions in cycloleucine-treated female embryos are reduced when compared to male embryos, findings which suggest that the reduced ability of female embryos to close the cranial neural tube is likely a result of the exacerbated reduction in the methylation potential in female embryos and the consequential disruption of downstream methylation reactions required for cranial neural tube closure. The female excess in cranial NTDs cycloleucine causes can be overcome by controlling the flux of SAM for downstream methylation reactions by co-treating cycloleucine-treated embryos with MGBG, an inhibitor of SAMDC, a female-specific rescue of cranial NTDs that is likely mediated by the increased availability of SAM for downstream methylation reactions. The specific rescue of cranial NTDs in cycloleucine-treated female embryos is as predicted by the XCI epigenetic “methyl sink” hypothesis. Our findings provide support for the idea that cycloleucine-induced cranial NTDs and the female excess it causes is as a result of cycloleucine exacerbating methyl group availability in female embryos and disrupting downstream transmethylation reactions. Given that female embryos are compromised in their availability of methyl groups as a result of the “methyl drain” the inactive X chromosome causes in female cells, our findings show that the further division and splitting up of SAM for downstream non-methylation is an additional factor which reduces SAM availability for downstream methylation reactions and puts female embryos at an increased risk of failed cranial neural tube closure. However, when methyl groups (SAM the major methyl group donor) are retained in the methylation cycle female embryos are protected from cycloleucine-induced cranial NTDs.

Chapter 4. Treating embryos with DNA methylation inhibitors: a model to assess whether downstream DNA methylation reactions underpin the female excess in cranial NTDs

4.1 Introduction

In the previous chapter, the availability of methyl groups, and thus methylationpotential during cranial neural tube closure, was found to be a critical factor in determining embryo risk for cranial NTDs. Cycloleucine, a well known inhibitor of methylation cycle flux, caused a selective increase in the rate of cranial NTDs in femaleembryos. These findings provide support for the XCI epigenetic 'methyl sink' hypothesis, which postulates a methylation capacity difference between the sexes asa basis for the greater susceptibility of female than male embryos to develop cranial NTDs.

As a first step towards understanding the critical downstream methylation reactions that may underpin cycloleucine-induced NTDs, predictions were made of the activity of downstream methyltransferase enzymes, using the SAM and SAH concentrations measured in cultured embryos (Chapter 3). Activity of all enzymes was predicted to be reduced in cycloleucine-treated embryos, whereas co-culture with the SAM decarboxylase inhibitor, MGBG, predicted an increased activity, particularly of protein methyltransferases. This may explain the observed MGBG-induced rescue of female embryos from cycloleucine-induced NTDs. However, these studies were indirect, and the specific downstream methylated biomolecule(s) targets that are critical for embryos to undergo cranial neural tube closure are yet to be identified.

The aim of this chapter was to assess more precisely which downstream methylation biomolecules/reactions may underpin the female excess in cycloleucine-treated cranial NTDs. Two approaches were taken: (i) a pharmacological approach to inhibit downstream DNA methylation reactions in cultured embryos, and (ii) use of

immunoblotting to determine the extent of a developmentally important category of protein methylation reactions in embryos treated with cycloleucine +/- MGBG.

The DNA methylation approach relies on the fact that all embryonic DNA methylation reactions are mediated by a small number of methyltransferases: the maintenance enzyme *Dnmt1*, and the de novo methyltransferases *Dnmt3a* and *Dnmt3b* (Jin et al., 2013). Hence, blocking these enzymes should reveal whether DNA methylation as a whole is essential for the female excess in cranial NTDs. Embryos were treated with the cytidine analogue inhibitors, 5-azacytidine and 5-aza-2'-deoxycytidine (Decitabine) to inhibit all DNA methylation reactions. 5-azacytidine has a broad spectrum of activity, with incorporation into both RNA and DNA (Raj et al., 2006), and hence is considered a relatively toxic drug. It was previously found to cause cranial NTDs in mice (Takeuchi and Takeuchi 1978, 1985). Decitabine on the other hand is incorporated into DNA only, not RNA (Jabbour et al., 2008), and so is expected to exhibit lower toxicity. Nevertheless, it is a known teratogen in mice, inducing limb and craniofacial defects (Mukhopadhyay et al., 2017; Rosen et al., 2002). Decitabine does not appear to have been tested for effects on mouse neurulation. It was hypothesised that, if the female excess in cranial NTDs in embryos treated with cycloleucine is the result of reduced availability of SAM for downstream DNA methylation reactions, then the addition of the cytidine analogue inhibitors would also result in a female excess of cranial NTDs.

Protein methylation, in contrast to DNA methylation, is catalysed by many methyltransferases which target a variety of amino acid residues within histone and non-histone proteins (Cornett et al., 2019). Nuclear histone methylation is critical for the regulation of gene expression, as evidenced by findings including knockout of Ezh2, a histone methyltransferase, which is lethal before gastrulation (O'Carroll et al., 2001). Of non-histone protein targets, SETD2 tri-methyl-lysine methylation has important developmental consequences. It is expressed in early mouse embryos, with exencephaly in knockout homozygotes (Hu et al., 2010). SETD2 trimethylates lysine in histones (H3K36me3), α-tubulin (a-TubK40me3) and F-actin (ActK68me3) (Seervai et al., 2020; Park et al., 2016). While α-tubulin is methylated in mitotic spindle microtubules, F-actin is methylated in cell protrusions, with loss of SETD2 leading to actin depolymerisation (reduced F/G actin ratio) and cell migration failure. Hence,

SETD2-tri-methyl-lysine methylation is a possible downstream candidate for involvement in cycloleucine-induced cranial NTDs.

The diversity of protein methyltransferases makes it difficult to block protein methylation reactions in an analogous way to the approach with DNA methylation. Indeed, there is no general inhibitor of protein methylation available (Kaniskan et al., 2018). Therefore, an alternative approach was adopted, in which the abundance of total cellular protein bearing SETD2-tri-methyl-lysine methylation marks was determined, using a specific antibody in Western blot experiments. This enabled female and male embryos to be compared, without or with cycloleucine +/- MGBG treatment.

4.2 Results

CD1 embryos were treated with the cytidine analogue inhibitors, 5-azacytidine and 5-aza-2'-deoxycytidine (Decitabine) for 24 h in whole embryo culture from E8.5 to E9.5. PBS served as vehicle control and embryos from within litters were allocate according to size/stage to ensure groups were balanced and to minimise effects of litter-to-litter variation. Embryos were obtained from 10 litters.

At the end of the culture period, embryos were harvested and assessed for cranial NTDs and scored for other developmental parameters including measures of embryo viability, embryonic growth, and development progression, as in Chapter 3. The yolk sac was removed and used to determine embryonic sex by genomic PCR.

4.2.1 Treating embryos with 5-azacytidine results in severe embryonic toxicity

Culture of embryos for 24 h in 5-azacytidine resulted in dose-dependent toxicity. At doses up to 0.075 μM, 5-azacytidine did not reveal any adverse effects as shown by the measures of viability, growth and developmental progression, compared with PBS-treated control embryos (Table 4.1). By contrast, in the dose range 0.1-0.5 μM, 5-azacytidine-treated embryos showed significantly reduced viability (yolk sac circulation), growth (crown-rump length) and developmental progression (axial rotation and somite number) compared with PBS controls (Table 4.1).

The critical issue in this experiment was whether 5-azacytidine-treated embryos would display cranial NTDs at sub-toxic dose levels, and so allow an assessment of sex ratio in viable NTD-affected embryos. However, no cranial NTDs were observed at 0.05 μM or 0.075 μM 5-azacytidine. Moreover, at higher doses, the majority of treated embryos failed to progress beyond the 16-somite stage, when normal cranial closure is complete, and so is the yardstick for determining the presence or absence of a cranial NTD. As these sub-viable embryos could not be assessed for cranial NTDs, 5-azacytidine did not prove to be a suitable agent for blocking DNA methylation in this study.

4.2.2 Decitabine induces cranial NTDs at sub-toxic dose levels

The exposure of E8.5 CD1 mouse embryos to Decitabine at concentrations up to 0.1 μM produced no detectable toxicity in terms of yolk sac circulation, crown-rump length or somite number, with no significant difference from PBS control embryos ($p > 0.05$; Student's t test for somite number and Z-test for other parameters). However, doses of 0.2 μM and above caused severe toxicity with a dramatic reduction in all embryonic parameters (Table 4.2). At concentrations of 0.5 μM and above, it was not possible to assess embryos for these parameters as a result of their severely perturbed morphology. Hence, the addition of Decitabine to neurulation stage embryos is less toxic and better tolerated than 5-azacytdine.

Importantly, Decitabine caused cranial NTDs at ~ 50% frequency at 0.075 and 0.1 μM: i.e. at dose levels that were not toxic (Table 4.2). No cranial NTDs were seen at the lowest dose, 0.05 μM, demonstrating a dose-response effect for this phenotype. At doses of 0.2 μM and above no assessment of cranial NTDs could be made as embryos did not progress beyond the 16 somite stage, which is the cut-off point for scoring cranial closure as complete or incomplete. Hence, Decitabine, which is known to blockDNA methylation, proved to be a suitable agent to induce cranial NTDs at dose levelsthat were not overtly toxic to the embryos.

5-azacytdine conc. (µM)	No. of embryos	Yolk sac circulation	Crown-rump length (mm)	No. of embryos with failed axial rotation (%)	No. of somites	No. of embryos with cranial NTDs (%)
0	14	3.00 ± 0.00	2.83 ± 0.13	0 (0)	20.4 ± 0.4	0 (0)
0.05	16	3.00 ± 0.00	2.73 ± 0.13	0 (0)	18.2 ± 0.3	0 (0)
0.075	10	2.50 ± 0.20	2.64 ± 0.24	0 (0)	17.1 ± 0.6	0 (0)
0.1	13	2.20 ± 0.18	2.21 ± 0.21*	2 (15.4)	15.1 ± 1.3**	1 (7.7)
0.15	10	1.50 ± 0.00**	1.83 ± 0.24**	4 (40)	13.6± 1.2***	-
0.2	12	1.00 ± 0.00**	1.36 ± 0.82**	15 (53.6)	10.8 ± 2.4***	-
0.5	8	-	-	-	-	-

Table 4.1. Growth and development of CD1 mouse embryos cultured with the cytidine analogue inhibitor, 5-azacytidine. 5-azacytidine resulted in a dose-dependent increase in embryonic toxicity with embryos showing no signs of embryonic viability at doses of 0.5 µM and above. At 0.1 µM only a single cranial NTD was observed, whereas crown-rump length and somite number are already significantly impaired at this dose. At doses of 0.15 µM and above, no embryos developed beyond the 16-somite stage, as needed to assess for cranial NTDs. There is a significant difference in all developmental parameters between 5-azacytidine-treated and PBS control embryos at doses of 0.1, 0.15 and 0.2 µM. The parameters could not be scored for embryos at 0.5 µM owing to the severity of abnormality. Data for failed axial rotation and cranial NTDs are presented as the number of embryos with percentage values in parentheses. Values for yolk sac circulation, somite number and crown-rump length are given as mean ± SEM. ** represents a p-value less than 0.01, and *** represents a p-value is less than 0.001 (as tested by Student's t-test for somite number and Z-test for all other parameters).

Decitabine conc. (µM)	No. of embryos	Yolk sac circulation	Crown-rump length (mm)	No. of embryos with failed axial rotation (%)	No. of somites	No. of embryos with cranial NTDs (%)
0	20	3.00 ± 0.00	2.72 ± 0.14	0 (0)	20.7 ± 0.2	0 (0)
0.05	25	2.86 ± 0.11	2.63 ± 0.26	0 (0)	20.3 ± 0.3	0 (0)
0.075	26	2.77 ± 0.10	2.59 ± 0. 24	0 (0)	20.1 ± 0.4	13 (50.0)**
0.1	50	2.65 ± 0.18	2.55 ± 0.38	0 (0)	19.8 ± 0.5	26 (52.0)**
0.2	28	1.48 ± 0.79	1.24 ± 0.82	16 (57.1)	13.6 ± 6.7**	-
0.5	10	1.00 ± 0.00	-	8 (80)	-	-
1	6	-	-	-	-	-
2	3	-	-	-	-	-

Table 4.2. Growth and development of CD1 mouse embryos cultured with Decitabine. No toxicity is detected for any of the parameters of viability, growth or developmental progression at doses up to 0.1 µM. However, at both 0.075 and 0.1 µM, cranial NTDs are induced in approximately half of all embryos. Decitabine at 0.2 µM causes significantly reduced somite number compared with PBS control embryos ($p = 0.004$; Student's t-test). Above this dose level, all parameters were adversely affected and at 1-2 µM embryos were severely abnormal and could not be scored. Data for failed axial rotation and cranial NTDs are presented as the number of embryos with percentage values in parentheses. Values for yolk sac circulation, somite number and crown-rump length are given as mean ± SEM. ** indicates $p < 0.001$, as tested by Z-test.

4.2.3 Effect of Decitabine on sex ratio in cranial NTDs

The next step was to assess whether inhibiting DNA methylation with Decitabine causes a sex difference in the rate of cranial NTDs. Decitabine resulted in 50% (13/26) NTDs at 0.075 µM and 52% (26/50) at 0.1 µM, giving a combined rate of 51.3% (39/76)in this dose-range. Embryos from these two concentration groups were pooled for subsequent analysis, in order to increase the power of the statistical tests. NTDs occurred in 57.8% (22/38) of female embryos and 44.7% (17/38) of male embryos, which is a statistically non-significant difference ($p = 0.35$, Fisher exact test). The female-to-male sex ratio of cranial NTDs in this experiment was 1.3:1 (Figure 4.1A). As a proportion of all embryos affected by cranial NTDs, females made up 56.4% (Figure 4.1B) and males 43.6%. Of embryos unaffected by cranial NTDs, females made up 43.2% whereas males made up 56.8% (Figure 4.1B).

These findings show that Decitabine-induced inhibition of DNA methylation is a potent cause of cranial neurulation failure in mouse embryos. Although this resembles previous findings with 5-azacytidine, the latter agent caused marked toxicity in NTD-affected embryos in vivo (Takeuchi and Takeuchi, 1985), whereas NTDs resulting from Decitabine treatment in embryo culture occurred at dose levels that appeared sub-toxic. Despite a trend towards more females than males being affected, the sex difference is not statistically significant, in contrast to the marked female excess observed with cycloleucine (Chapter 3). This argues that inhibition of downstream DNA methylation is unlikely to be the major factor leading to the sex difference in cranial NTDs, which is observed following inhibition of methylation cycle flux.

4.2.4 Sex difference in the regional morphology of Decitabine-induced cranial NTDs

Cycloleucine treatment revealed a sex difference in the brain regions that were primarily affected in NTDs: females had hindbrain/midbrain defects, whereas males

showed forebrain/midbrain defects (Section 3.2.5) A similar analysis was undertaken for embryos treated with Decitabine (Figure 4.2B), which also revealed a significantly different distribution of affected brain regions between the sexes ($p = 0.04$; 5 x 2 Chi-square test). Decitabine-induced NTDs affected the hindbrain (+/- other regions) in 50% (11/22) of female embryos but in no (0/17) males ($p = 0.02$) the midbrain (+/- other regions) was affected in 59% (13/22) of female embryos and 18% (3/17) of males ($p = 0.02$) and the forebrain (+/- other regions) was affected in 41% (9/22) of female embryos but 94% (16/17) of males ($p = 0.0007$) Hence, female embryos show defects in all regions, but especially in hindbrain and midbrain, whereas males almost exclusively show forebrain defects (Figure 4.2B). These findings are broadly similar to those obtained with cycloleucine treatment, and suggest the sex difference in brain region involvement is not directly related to a higher overall rate of cranial NTDs in females.

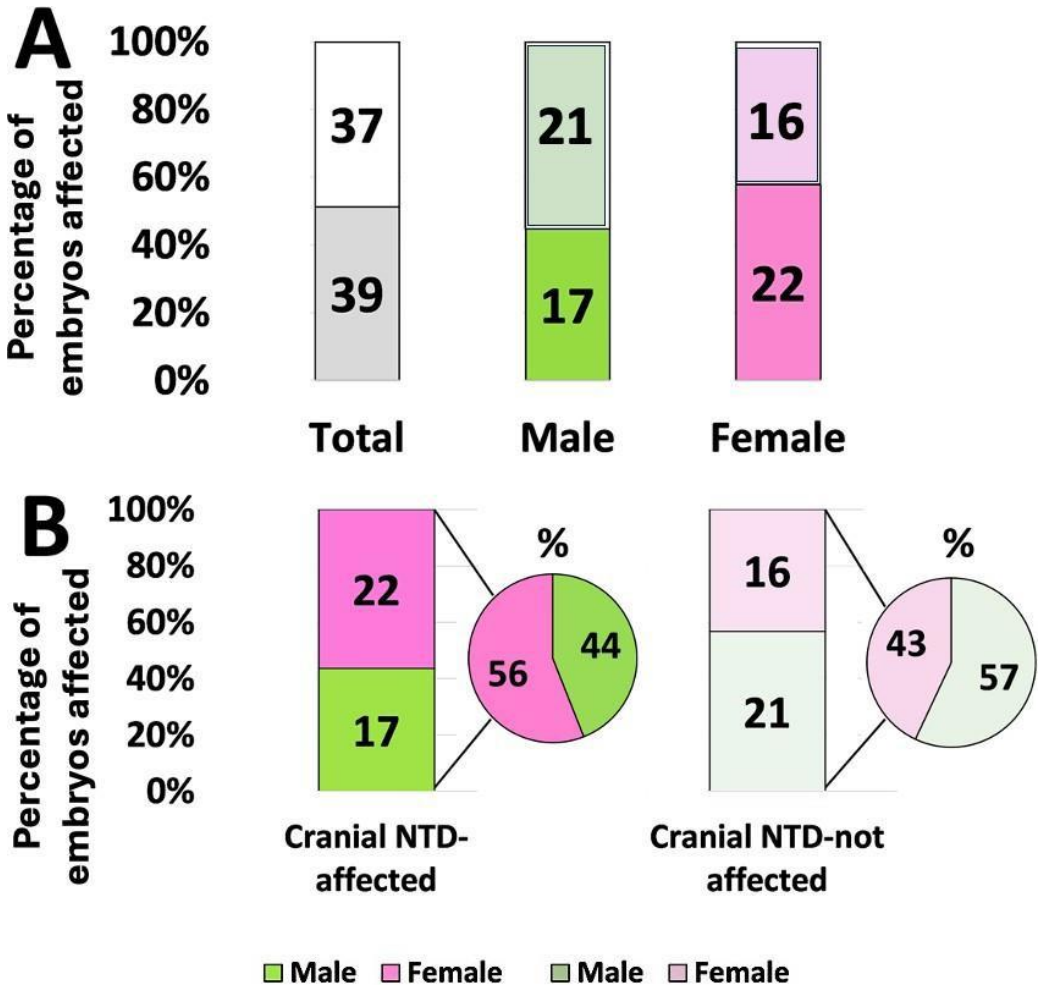

Figure 4.1. Decitabine-treatment does not result in a sex difference in cranial NTDs. (A) At a dose-range of 0.075-0.1 μM, Decitabine gives an overall rate of cranial NTDs of 51.3% (39/76), with females (57.8%; 22/38) and males (44.7%; 17/38) being almost equally affected. The female-to-male ratio is 1.3:1, and this sex difference is not significantly different ($p = 0.35$, Fisher's exact test). Coloured and white parts of the stacked bar charts represent cranial NTD-affected and -unaffected embryos respectively. Numerical values show the number of embryos in each group. **(B)** The distribution by sex between embryos affected and unaffected by cranial NTDs. Decitabine-treated female embryos show a slight but non-significant increase in the number of embryos affected by cranial NTDs as a proportion of all embryos and a slight but nonsignificant decrease in the number of embryos unaffected by cranial NTDs as a proportion of all embryos. Darker and lighter colours in the stacked bar charts represent NTD-affected and -unaffected embryos respectively. Numerical values represent the number of embryos in each group. Pie charts show the proportion (%) of male and female embryos as extrapolated from the numerical values.

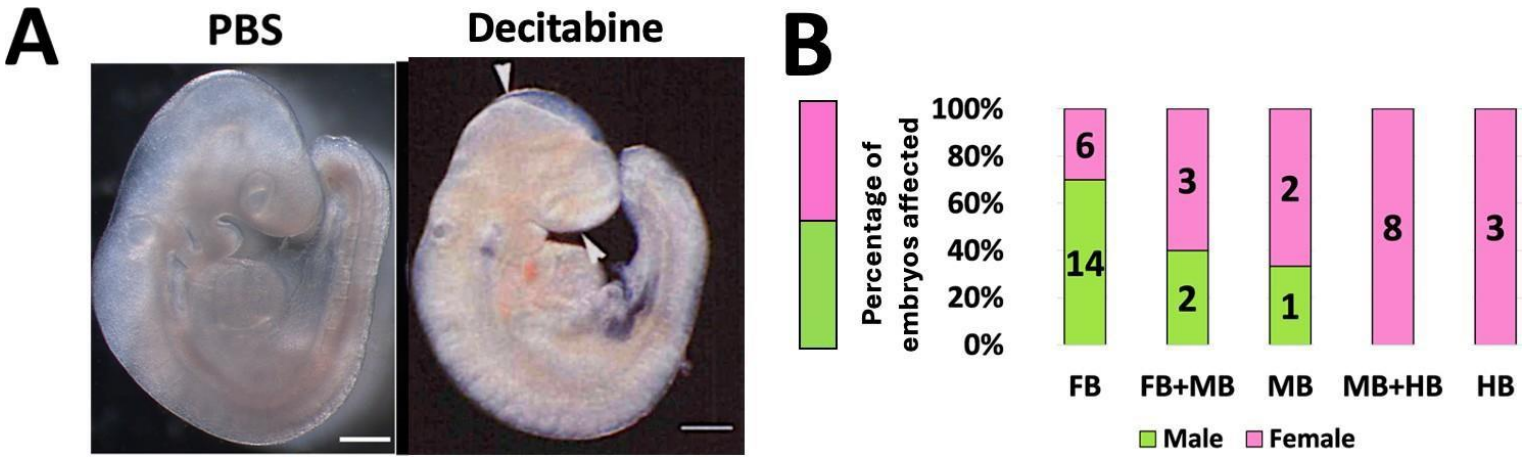

Figure 4.2. **(A)** Representative image of a PBS control (left) and a 0.1 μM Decitabine-treated embryo (right). PBS control embryo has developed normally, while the Decitabine-treated embryo has persistently open cranial neural folds (white arrow), representing a hindbrain/midbrain NTD. Scale bars: 200 μm for PBS-treated embryo; 150 μm for Decitabine-treated embryo. **(B)** Decitabine treatment results in a sex difference in the brain region primarily affected by NTDs. Male embryos most often show NTDs of the FB region whereas female embryos most commonly present with defects in the HB/MB region. This difference in distribution of male and female embryos between brain region categories is statistically significant ($p = 0.04$; 5 x 2 Chi-square test). Embryo numbers shown on bars. Representative image of exencephalic embryo as indicated by open brain region through arrowheads taken from the thesis of Louisa Dunlevy.

4.2.5 Effect of methylation cycle inhibition on downstream SETD2-tri-methyl-lysine protein methylation

Having assessed whether downstream DNA methylation is likely to underpin the female excess in cranial NTDs, the next step was to investigate the possible role of downstream protein methylation. Of particular interest is SETD2-mediated tri-methyl-lysine methylation, as this protein methyltransferase has been implicated in a number of developmentally important events (Roffers-Agarwa et al., 2021). Moreover, protein lysine methyltransferases showed the greatest predicted reduction in activity in cycloleucine-treated embryos, and the greatest predicted increase in MGBG + cycloleucine co-treated embryos (Figure 3.10).

An antibody specific for SETD2-tri-methyl-lysine methylation (PTM Biolabs) was used to probe Western blots of whole embryo extracts from cultures in cycloleucine +/- MGBG. This revealed a striking sex difference in cycloleucine-treated embryos. Female embryos showed a significant qualitative and quantitative decrease in SETD2-mediated tri-methyl-lysine methylation marks when compared to PBS control embryos ($p < 0.001$; unpaired t-test; Figure 4.3A and 4.3B). Co-culture in MGBG + cycloleucine significantly increased the level of SETD2-mediated tri-methyl-lysine methylation marks of all SETD2- tri-methyl-lysine methylated protein bands visible when compared to cycloleucine-treated embryos ($p = 0.04$; unpaired t test) an increase that was equivalent to ~50% increase in SET2D- tri-methyl-lysine levels between the treated and co-treated groups, findings which suggest that co-culture embryos in MGBG + cycloleucine can partially restore disrupted downstream SETD2- tri-methyl-lysine methylation marks that cycloleucine-treatment causes (Figure 4.3A and 4.3B). In contrast, male embryos did not show a significant reduction in SETD2-mediated tri-methyl-lysine methylation when cycloleucine-treated embryos were compared with PBS controls ($p = 0.06$; unpaired t-test), and there was no significant increase in MGBG + cycloleucine co-cultured embryos ($p = 0.3$; unpaired t test – Figure 4.3C and 4.3D).

These findings provide support for the idea that female embryos are predisposed to a downstream reduction in SETD2-tri-methyl-lysine methyltransferase activity, following methylation cycle inhibition by cycloleucine, whereas no such effect is seen in male embryos. Whether this effect also applies to other protein methyltransferases is not yet clear, and requires further analysis.

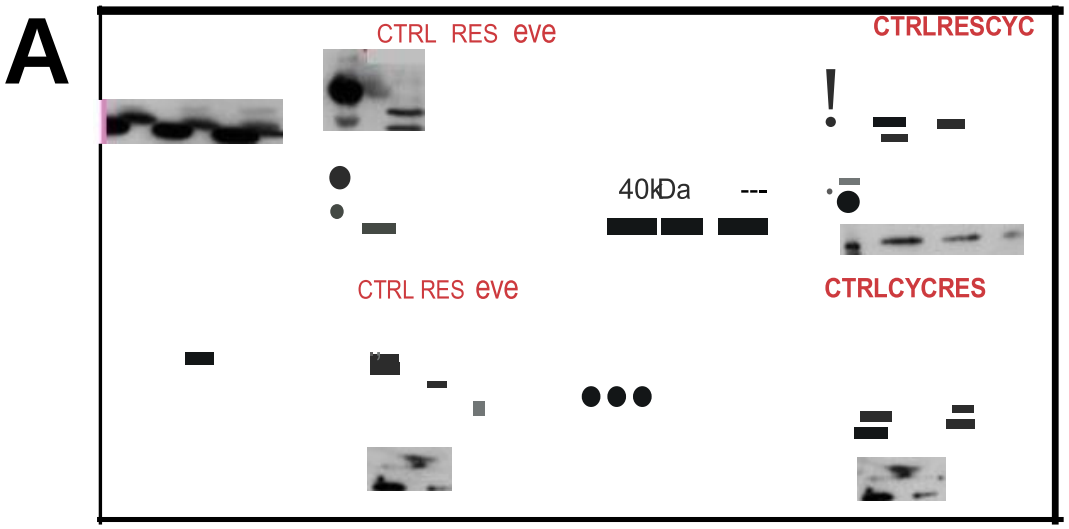
A
CTRL RES eve
CTRLRESCYC
40kDa
CTRL RES eve
CTRLCYCRES

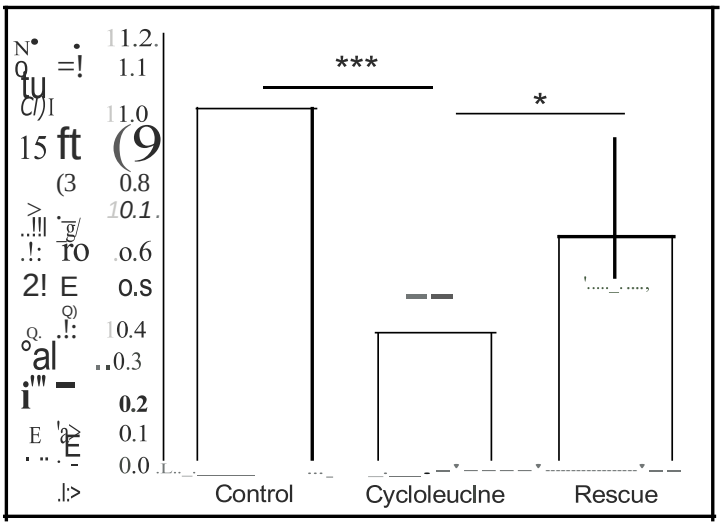
B
***
*
Control
Cycloleuclne
Rescue


C
RES eve
CTRL RESCYC

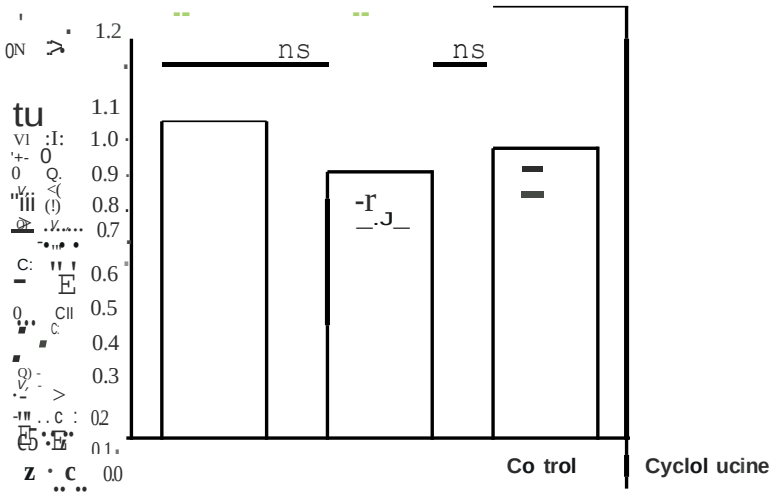
D
ns
ns
Co trol
Cyclol ucine

.

Rescue

Figure 4.3. Western blot analysis of SETD2-mediated tri-methyl-lysine methylation in cultured mouse embryos. (A) SETD2-mediated tri-methyl-lysine methylation marks in female embryos: cycloleucine-treated (CYC), cycloleucine + MGBG co-treated (RES), and PBS control (CTRL). **(B)** Methylation marks are significantly reduced in cycloleucine-treated embryos compared to PBS controls, whereas methylation levels are partially restored in MGBG co-treated embryos. **(C)** SETD2-mediated tri-methyl-lysine methylation marks in male embryos: cycloleucine-treated (CYC), cycloleucine + MGBG co-treated (RES), and PBS control (CTRL). **(D)** Comparable analysis in male embryos, in which SETD2-mediated tri-methyl-lysine methylation marks do not show any significant reduction in cycloleucine-treated male embryos (CYC) when compared to PBS control embryos (CTRL), with no significant change found in cycloleucine-treated male embryos co-treated with MGBG (RES). Data is shown as mean±SD with each data point representing an individual embryo. * $p < 0.05$; *** $p < 0.001$; ns non-significant.

4.3. Discussion

This chapter shows that sub-toxic dose levels of the DNA methylation inhibitor Decitabine result in cranial NTDs, with no significant skewing of the sex ratio among affected embryos. Another DNA methylation inhibitor, 5-azacytidine, produced no NTDs at sub-toxic doses and so could not be used to test for a female excess. Although a similar overall frequency of NTDs (50-60%) was observed in both Decitabine-treated and cycloleucine-treated cultures (Chapter 3), the female excess was only seen with cycloleucine. These findings suggest that perturbed DNA methylation is unlikely to be the main downstream methylation process responsible for the female excess in cranial NTDs.

4.3.1 5-azacytidine and NTDs

Previous studies have evaluated the effect of 5-azacytidine on mouse development both in vivo and in vitro. Injection of 1 mg/kg 5-azacytidine directly into pregnant dams at E7.5 produced cranial NTDs (exencephaly) in 91% of E18.5 fetuses (Takeuchi and Takeuchi, 1985), while another study found differential NTD susceptibility to 5-azacytidine in the dose range 0.1-1.0 mg/kg between two inbred mouse strains (Matsuda et al., 1990). Such in vivo studies are hard to compare with the embryo culture experiments in this thesis, as the involvement of maternal metabolism in vivo may affect the final concentration of 5-azacytidine, or even the metabolic form, as received by the embryos.

A previous study administered 5-azacytidine in whole embryo culture, using a final concentration of 0.8 µM in neurulation-stage rat embryo cultures. Cranial NTDs were observed in 74% of embryos, with relatively little embryotoxicity over a 24 h culture period (Matsuda et al. 1992). This contrasts with the present study in which 0.1 µM 5-azacytidine was already toxic to mouse embryos, with higher concentrations (up to 0.5 µM) leading to failure of embryonic growth and developmental arrest. As only a small proportion of embryos developed past the 16-somite stage, it was not possible to score for cranial NTDs. The greater toxicity of 5-azacytidine in the present study may be a

species difference, as mouse embryos were used, rather than rats as previously (Matsuda et al. 1992). Nevertheless, toxicity of 5-azacytidine is not unexpected, as it is known to depress DNA, RNA, and protein synthesis, as well as causing increased cell death and/or inhibition of cell proliferation (Li et al*.,* 1970; Constantinides et al*.,* 1978; Jones and Taylor, 1980).

4.3.2 Decitabine effects compared with 5-azacytidine

Despite also inhibiting DNA methylation, the use of Decitabine in embryo cultures provided a sub-toxic dose-range in which cranial NTDs were observed, in contrast to 5-azacytidine. This different response is likely to reflect the different inhibitory action of these cytidine analogues. Once taken into cells by the nucleoside transporters 1 and 2 (Rius et al., 2009), 5-azacytidine and Decitabine are modified by different metabolic pathways to achieve their active forms. The limiting step in this cascade is the ATP-dependent phosphorylation of the nucleoside to the monophosphorylated nucleotide, a reaction catalysed by uridine-cytidine kinase for 5-azacytidine and deoxycytidine kinase for Decitabine (Li et al., 1970). Subsequent phosphorylation by two different kinases yields the active metabolites: 5-aza-CTP for 5-azacytidine and 5- aza-dCTP for Decitabine. During DNA replication, 5-aza-dCTP (the active form of Decitabine) is completely incorporated into DNA, whereas only 10–20% of 5-aza-CTP (from 5-azacytidine) is incorporated into DNA, with 80–90% incorporated into RNA. Hence, unlike Decitabine, 5-azacytidine inhibits vital cellular processes such as tRNA methylation and processing (Lee et al., 1976), and tRNA methyltransferase levels and activity (Lu et al., 1980), which result in defective mRNA and tRNA production, and so protein synthesis inhibition (Schaefer et al., 2009). In conclusion, the differential sensitivity of mouse embryos to the two DNA methylation inhibitors in the present study, seems likely due to the DNA-only effects of Decitabine, in contrast to the DNA/RNA effects of 5-azacytidine (Li et al., 1970; Adams et al., 1982; Momparler et al., 1984; Momparler et al., 1984).

4.3.3 DNA methylation and cranial neural tube closure

DNA methylation is a major epigenetic modification of the genome that regulates gene expression (Mazzio et al., 2012). A methyl group is covalently attached at the cytosine-

5-carbon site of CpG dinucleotides, a reaction that is catalysed by the DNA. Multiple CpGs within ‘CpG islands’ (Gardiner-Garden et al., 1987) are present in the promoter regions of approximately 40% of mammalian genes (Larsen et al., 1992). Many studies have shown that the degree of methylation of CpG islands is directly related to the transcriptional activity of the RNA polymerase on that gene, with hypermethylation inhibiting gene expression and hypomethylation enabling transcription (Cain et al., 2022).

In relation to cranial neural tube closure, it was found that methylation of LINE-1 repetitive genomic elements is reduced in DNA of anencephalic but not spina bifida foetuses (Wang et a*l*., 2010). Moreover, folic acid, which significantly reduces the occurrence and recurrence of NTD-affected pregnancies (MRC Vitamin Study Research Group, 1991, Eichholzer et al., 2006), also has the effect of reversing DNA hypomethylation to varying degrees. In mouse models, the elevating cranial (but not spinal) neural folds express the *de novo* DNA methyltransferase enzyme, *Dnmt3b*, while mouse mutants of *Dnmt3b* present with cranial NTDs (Okano et al., 1999). Similarly, the maintenance methyltransferase *Dnmt1*, is required for embryo survival and cranial neural tube closure (Li et al., 1992). Hypomethylation of Caspase-8, part of the apoptosis pathway, and demethylation of nucleosome assembly protein 1-like 2 gene, important in chromatin structure, both lead to gene overexpression and NTDs in mice (Huang et al., 2019; Rogner et al., 2002). Increasingly, methylation defects (usually hypomethylation) are being described in relation to various human NTD-associated genes (Cao et al., 2022). Hence reduced DNA methylation is a general finding in NTDs, especially of the cranial region, and may be implicated via gene overexpression in their molecular pathogenesis.

4.3.4 Sex difference in brain regions affected in cranial NTDs

A striking finding of the experiments with cycloleucine (Chapter 3) and Decitabine (this Chapter) was the preponderance of forebrain cranial NTDs in males, and hindbrain (+/- midbrain) NTDs in females. This regional brain difference between the sexes appears irrespective of whether females have a higher rate of NTDs than males, as this was not observed in Decitabine-treated cultures. The data suggest that disruption

of DNA methylation reactions – caused indirectly by cycloleucine or directly by Decitabine – may be an important factor in determining the susceptibility of male embryos to forebrain NTDs, and female embryos to hindbrain/midbrain NTDs.

Several possible explanations for this phenomenon may be considered. In disorders that follow an X-linked inheritance pattern, males are more commonly and severely affected than females, as males are hemizygous (X^{-}/Y) for a mutant (-) gene, whereas females are most often heterozygous (X^{-}/X^{+}). For example, this is seen in X-linked Opitz G/BBB syndrome, a defect caused by mutation of the *MID1* gene, with birth defects of the midline including hypertelorism, cleft lip, laryngeal cleft, hypospadias, anorectal defects, agenesis of the corpus callosum, and conotruncal heart defects (Quaderi et al., 1997). However, Opitz G/BBB syndrome does not present with NTDs – a striking finding given that most other midline systems are affected. Indeed, such male-preponderant conditions are generally the result of gene loss-of-function, as with *MID1* mutations, whereas the current study points to an effect of gene over-expression, resulting from DNA hypomethylation. This would be expected to affect females, with two X-linked gene copies, more than males with a single copy, and so perhaps is an unlikely explanation for the forebrain defects in male embryos, although it could be implicated in female-specific defects.

A second possible explanation relates to the parent-of-origin inheritance of the X chromosome. Males inherit their X chromosome from their mother (X^{m}), whereas females receive an X from both parents (X^{m}, X^{p}). Following X-inactivation, females show mosaicism for X-linked gene variants, and so would have X^{m} expressed in some cells and X^{p} in others. X^{p} was found to have a higher state of global DNA methylation than X^{m} in activated CD4+ T lymphocytes, accounting for the higher X-linked gene expression observed in XY cells compared with XX cells (Golden et al., 2019). Hence, parent-of-origin effects can provide a possible mechanism by which male embryos experience higher levels of X-linked gene expression than females, which may be further exacerbated by cycloleucine or DNA methylation inhibitors.

A third possibility relates to the process of X-inactivation itself, which is known to be globally incomplete along the X chromosome. Some X-linked genes ‘escape’

inactivation, especially in the pseudo-autosomal region where there is X-Y homology (Navarro-Cobos et al., 2020). Genes that are suggested to escape XCI in mouse cells include *Mid1* and *Shroom4* (Yang et al., 2010), both of which play significant roles in neurulation. *Mid1* is required for neural tube closure in *Xenopus* (Suzuki et al., 2010) while *Shroom4*, like other family members, is an actin-binding protein with a likely role in mouse neuroepithelial apical constriction (Yoder et al., 2007). It is possible that female embryos experience twice the expression level of such X-linked genes compared with males, and this could 'buffer' females from forebrain defects, leaving males with increased susceptibility. Conversely, biallelic expression of such genes in females might predispose to the hindbrain/midbrain defect pattern. A prediction of this idea is that female heterozygotes, say for a *Shroom4* null mutation, would show a more 'male-like' regional distribution of cranial NTDs.

4.3.5 Role of protein methylation in determining female risk for cranial NTDs

Decitabine usage suggested that disrupted DNA methylation is unlikely to be responsible for the female excess in cranial NTDs. Therefore, an alternative hypothesis was examined: that protein methyltransferases are the main downstream targets mediating the sex-specific effect. Protein methylation is an epigenetic modification of the nitrogen-containing sidechains of arginine and lysine residues. Histone methylation is well known to regulate gene transcription, and underlies several inherited disorders (Fallah et al., 2020), while non-histone protein methylation can affect a wide range of protein functions (Biggar et al., 2015). In the analysis of predicted methyltransferase activities (Chapter 3), calmodulin-lysine N- methyltransferase proved particularly sensitive to cycloleucine, and showed the greatest increase in activity during MGBG-mediated rescue of female NTDs. Inconsequence, this chapter focused on SETD2-mediated tri-methyl-lysine methylation,which targets both histone and non-histone proteins (Cornett et al., 2019).

SETD2 trimethylates lysine in histone proteins (H3K36me3) and also specifically in the non-histone cytoskeletal proteins α-tubulin (a-TubK40me3) and F-actin (ActK68me3) (Seervai et al., 2020; Park et al., 2016). SETD2 is expressed during early mouse development (Brunskill et al., 2014), with a particular requirement in chick

neural crest (NC) migration (Roffers-Agarwal et al., 2021). Inactivation of the H3K36me3 lysine methyltransferase in mice (the *Hypb* mutant) produced embryonic lethality with vascular remodelling defects, and also cranial NTDs in some knockout homozygotes (Hu et al., 2010).

The Western blot analysis showed that SETD2-mediated tri-methyl-lysine methylation is significantly reduced in cycloleucine-treated female embryos, but not in males, whereas this reduction is abolished by addition of MGBG to the cultures. This may indicate a specific requirement for SAM to enable downstream protein methylation, and with a particularly severe effect in female embryos, consistent with the XCI-related 'methyl drain' hypothesis. Hence, these findings favour protein methylation over DNA methylation as likely downstream mediators of the female excess in cranial NTDs. It should be noted however that quantitative analysis of the film image may be subject limitation such as reaching the saturation level of the film if overexposed. This could however be improved by using fluorescence imaging systems, such as those used in Odyssey given it can capture a broader range of signal intensities without reaching the saturation point as quickly as film and therefore allow for accurate quantification of both low and high-intensity signals in the same image.

Clues to possible downstream proteins, whose methylation is essential for cranial neurulation, identify cytoskeletal components in particular. For example, methyl-^{14}C labelling of neurulation-stage rat embryos cultured under methionine-depleted conditions, in the absence of *de novo* protein synthesis, found actin and tubulin as among the most abundantly synthesised and methylated proteins (Moephuli et al., 1997). Indeed, actin is a methylation target of SETD2-mediated tri-methyl-lysine methylation (ActK68me3) (Seervai et al., 2020). In the present study, one of the largest changes in SETD2-mediated tri-methyl-lysine methylation occurred in a highly abundant protein of molecular weight suggestive of actin. It will be important in future work to determine whether cytoskeletal protein methylation is a key requirement for cranial neurulation.

4.3.6 Neural tube closure as a target for protein methylation defects

Protein methylation is needed for cranial neural tube closure. Rat embryos cultured on cow serum, with low methionine content, present with cranial NTDs and show a reduction in the levels of monomethylarginine, dimethylarginine, and 3-methylhistidine methylation in neural tube proteins (Coelho et al., 1990). Monomethylarginine and dimethylarginine methylation marks commonly occur on histone proteins (Paik and Kim, 1970) whereas lysine methylation marks are the major amino acid epigenetic modifications on the cytoskeletal proteins myosin (Hardy et al., 1970) and actin (Johnson et al., 1967). Tri-methyl-lysine methylation occurs in myosin near the sites for ATP hydrolysis and actin binding (Cantoni, 1975), and therefore may alter enzyme activity. In contrast, tri-methyl methylation of histidine occurs at a specific and highly conserved location on the actin molecule, indicating an important function in microfilament contraction (Uyemura and Spudich, 1978). SETD3-mediated methylation of histidine-73 affects the ATP hydrolysis rate and therefore possibly actin turnover and actin assembly dynamics (Kwiatkowski et al., 2018). Hence, reduced methylation potential in cycloleucine-treated female embryos could result in disruption of cytoskeletal protein function, as needed for the cranial neural tube to close.

Actin and other cytoskeletal proteins are known to play key roles in neural tube closure (Sawyer et al., 2009; Suzuki et al., 2012). They regulate various aspects of cell morphogenesis such as cell polarity, apical-basal elongation, and apical constriction (Colas and Schoenwolf, 2001; Davidson and Keller, 1999) which are important events in the neuroepithelium during neurulation. Moreover, actin (Sadler et al., 1982) and myosin (Lee et al., 1983) are expressed in neuroepithelial cells of the cranial neural folds and the exposure of mouse embryos to various agents which perturb cytoskeletal protein dynamics such as vinblastine (Karfunkel, 1974), diazepam (Lee et al., 1983), and the calcium blockers xylocaine, papaverine, and gallapomil (O'Shea and Kaufman, 1980, Smedley and Stanistreet, 1986) result in cranial NTDs.

NTDs were observed in rat embryos cultured in serum depleted in the SAM precursor methionine. Neuroepithelial cells exhibit disorganised actin and tubulin, and lose apical-basal polarity, with rounding of neuroepithelial cells resulting from reduced ability of cytoskeletal proteins to form focal adhesions (Moephuli et al., 1997). The

guanosine triphosphate binding protein, RhoGTPase, which induces reorganisation of actin filaments from punctate to a diffuse network of stress fibres, was implicated in this defect (Ridley et al., 1992). Interestingly, RhoGTPase requires SAM-dependent carboxy-methylation to localise properly at the inner surfaces of cell membranes (Philips et al., 1993). Hence, methionine depletion in the culture serum may have reduced SAM availability, and so downstream protein methylation.

Given the requirement for cytoskeletal dynamics in neural tube closure, actin and related proteins appear possible methylation targets that may be implicated in female preponderant cranial NTDs. However, cytoskeletal function is also required for spinal neurulation (Butler et al., 2019), and yet there is no female excess in open spina bifida (myelomeningocele). Hence, additional factor(s) must contribute to producing a female predisposition to cranial NTDs, rather than to NTDs as a whole.

4.3.7 Neural crest as a target for protein methylation defects

Cytoskeletal protein methylation is also known to be important in regulating various stages of NC cell development, specification, and migration. For example, loss of SETD2-methylation disrupts F-actin methylation in cell protrusions, leading to actin depolymerisation (reduced F/G actin ratio) and thus NC migration failure (Roffers-Agarwal et al., 2021). Moreover, chick NC cell migration requires the activity of cytoplasmic SAH hydrolase, the enzyme that breaks down SAH, the feedback inhibitor of transmethylation reactions (Vermillion et al., 2014), suggesting that methylation reactions may be needed for NC migration.

The methylome of migratory NC identified cytoskeletal proteins as abundantly methylated, and functional studies have shown that the methylation of the actin binding protein Ef1α is essential for NC cell migration (Vermillion et al., 2014). Other studies have also linked the disrupted methylation of cytoskeletal proteins in NC cells with cranial NTDs. For instance, N-cofilin mouse mutants develop cranial NTDs in which actin regulation is disrupted. Interestingly, NC cells appear unable to emigrate from the neural tube in these mutants, given their loss of polarity and absence of F-actin fibres (Gurniak et al., 2005).

4.3.8 Hypothesis: XCI-induced disruption of NC cell emigration leading to cranial NTDs

A reduced activity of downstream methylation reactions specifically in the NC may explain why a sex difference in cranial NTD susceptibility occurs in cycloleucine-treated embryos. In mammals, onset of NC emigration precedes completion of neural tube closure in the hindbrain and midbrain, but follows closure in the spinal region (Nichols et al., 1981; O'Rahilly et al., 2007). Moreover, failure of NC emigration may lead to hindbrain/midbrain exencephaly, by preventing bending of the neural folds dorsolaterally, which is the final step in cranial closure (Morriss-Kay et al., 1989). Hence, a disruption to NC migration is likely to affect cranial but not spinal neural tube closure. The forebrain appears not to form NC itself, but rather receives NC cells by forward migration from the midbrain (Morriss-Kay et al., 1991). Hence, a NC-related cytoskeletal protein methylation defect could underlie the female excess in NTDs that specifically affect the hindbrain/midbrain region, but would not explain the forebrain-predominant NTDs in males.

The findings of this chapter provide strongest support for a role of protein methyltransferases in this hypothesised mechanism, and this is reinforced by work demonstrating the importance of protein methylation in NC development (Vermillion et al., 2014). However, a role for DNA methylation is also possible, particularly as Decitabine causes midbrain/hindbrain NTDs in female embryos. De novo DNA methylation, by the DNMT3A and DNMT3B methyltransferases, are known to play a dual role in the programs governing NC development. First, DNMT3A regulates the spatial boundary between NC and neural tube progenitors by functioning as a molecular switch to repress neural markers and fates, while favouring NC gene expression and fate acquisition (Hu et al., 2012). Second, DNMT3B was found to restrict the temporal window during which progenitors in the dorsal neural tube are competent to undergo EMT and produce NC cells, with prolonged NC emigration after DNMT3B knockdown in chick embryos *(*Hu et al., 2014*).* On the other hand, conditional Cre-mediated knockout of DNMT3B in mice was found to be dispensable for NC migration (Jacques-Fricke et al., 2012*).* Hence, the role of DNMT3B in NC- related cranial NTDs requires further investigation.

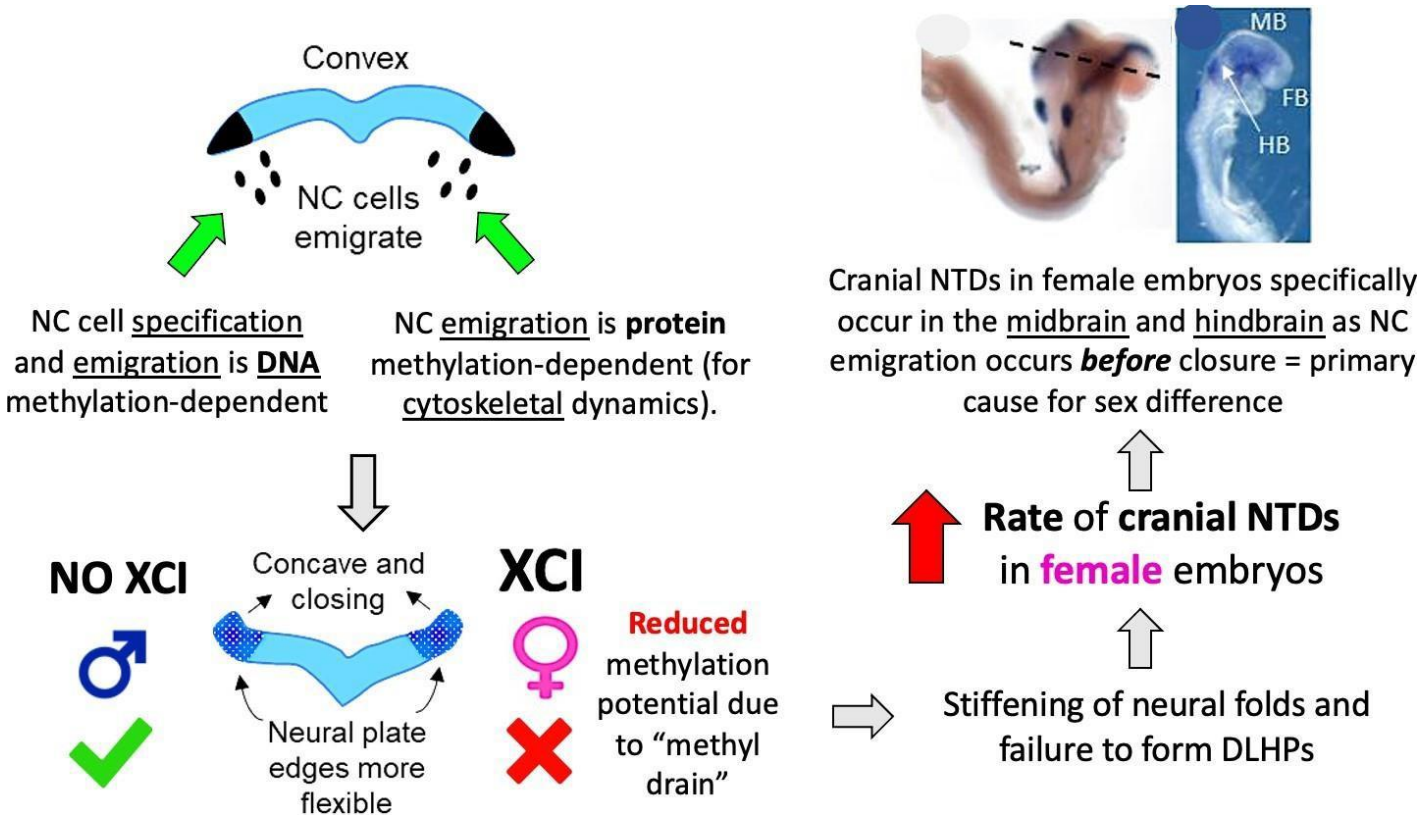

Figure 4.4. The proposed mechanism. The female excess in cranial NTDs cycloleucine causes is hypothesised to be caused by the XCI-induced disruption of NC cell emigration.

Chapter 5. Reactivating the X chromosome and risk of cranial NTDs in female embryos

5.1 Introduction

In Chapter 3, treatment of embryos with cycloleucine, with or without MGBG, was able to modulate the sex ratio, as well as altering the overall frequency of cranial NTDs. The female excess among cranial NTDs, resulting from inhibition of the methylation cycle by cycloleucine, was abolished by maintaining SAM in the methylation cycle, through MGBG action. These findings are consistent with the hypothesis that a 'methyl sink' exists in female embryos, which causes them to be at higher risk of failed cranial neurulation than males (Juriloff & Harris, 2012). This hypothesis proposes that the relative shortage of methyl groups results from the requirement to inactivate, and maintain inactivity, of an X chromosome in every female cell. In the present chapter, an attempt was made to reactivate the inactive X chromosome in female embryos, to test the prediction that this should overcome the female excess in cranial NTDs, by reducing the requirement for methyl groups for XCI.

The process of XCI involves epigenetic changes that maintain dosage compensation of X-linked genes in females. The adverse effect of gene dosage imbalance between X chromosome and autosomes is evidenced by homozygous deletion of *Xist*, the master gene regulator of XCI. When confined to the embryonic lineage, *Xist* loss causes a severe reduction in fitness and survivability of female mice (Yang et al., 2016). The initial phase of random XCI (see Section 1.6.8) involves the upregulation of the long non-coding RNA *Xist* gene product from the maternal or paternal X chromosome (Brockdorff et al., 2011; Lee et al., 2011; Pollex et al., 2012). Once upregulated, *Xist* RNA coats the entire X chromosome from which it is expressed, and initiates a cascade of events that establish the process of XCI by excluding RNA polymerase II, gaining repressive H3KK27me3 methylation marks, and recruiting

structural chromosomal epigenetic protein complexes (Brockdorff et al., 2011; Lee et al., 2011; Pollex et al., 2012).

XCI then transitions into the maintenance phase, which is mediated by accumulation of histone variant macroH2A1 and the gain of DNA methylation at CpG islands. These are extremely stable epigenetic and molecular modifications which result in heritable gene silencing. The maintenance phase of XCI is marked by the resistance to X chromosome reactivation (XCR) upon deletion of *Xist* (Costanzi and Pehrson 1998; Gendrel et al., 2012; Grant et al., 1992; Wutz et al., 2000) which suggests that, although *Xist* is essential for XCI initiation, it becomes dispensable for later stages of the silencing process. Hence, different molecular processes and repressive chromatin marks mediate and regulate the different stages of XCI (Wutz et al., 2000; Csankovszki et al., 2001).

The possibility of reactivating the silenced X chromosome represents a possible therapy to overcome female-specific X-linked conditions that are caused by malfunctional or missing X-linked proteins. Indeed, the process of XCI can be reversed, for example to reset cellular identity to the pluripotent state in ‘cellular reprogramming’ (Mak et al., 2004; Okamoto et al., 2004; Maherali et al., 2007). Hence, the modifications that underlie the maintenance phase of XCI are not ‘locked’ in position and can be overcome. Various pharmacological and genetic approaches are known to overcome XCI and restore X-linked gene expression. Use of the DNA methylation inhibitor 5-azacytidine together with an *Xist* anti-sense oligonucleotide led to increased expression of the X-linked-*Mecp2* gene in a mouse model of Rett syndrome (Carrette et al., 2018), while Decitabine plus a ribonucleotide reductase inhibitor induced expression of a silenced X-linked reporter gene (Minkovsky et al., 2015).

Despite the many repressive chromatin factors that are implicated in maintaining the inactive X, interference with DNA methylation has proven most effective in overcoming gene silencing (Gendrel et al., 2012; Csankovszki et al., 2001; Blewitt et al., 2008). Mouse-human or hamster-human somatic hybrids, deficient in X-linked hypoxanthine-

guanine phosphoribosyltransferase (HPRT), and containing a structurally normal inactive human X chromosome, can form HPRT+ve colonies when treated with 5-azacytidine (Venolia et al., 1982). Similarly, 5-azacytidine treatment of hybrid HPRT-deficient *Mus musculus* × *M. caroli* lines causes the $HPRT^{+}$ allele on the inactive *M. caroli* X to become reactivated (Graves et al., 1982). In these studies, the mode of action of 5-azacytidine in causing XCR is thought to be caused by inducing changes at the level of DNA given the fact that cell lines treated with DNA from an inactive X chromosome are not able to transform HPRT (Venolia et al., 1982). Interestingly*, the* transformed HPRT+ donor cells have also been shown to be able to grow for a number of generations in HAT-selective media even in the absence of 5-azacytidine findings which suggest that 5-azacytidine-modification of DNA and the induced-XCR likely results in a stable, long-lasting, and heritable changes in gene expression. The treatment of 5-azacytidine has also shown to result in the demethylation of cytosine residues at the 5 prime CpG island of other X chromosome-linked genes such as phophoglycerate-kinase-3 and glucose-6-phosphate dehydrogenase (Pfeifer et al., 1990) whilst also being able to cause under-condensation of the inactive X (Jones et al., 1982) and alter the replication timing of the entire inactive X chromosome from late to early – findings which collectively suggest that 5-azacytidine treatment does not only cause gene-specific reactivation but is likely to result in chromosomal wide reactivation (Gregory et al., 2008).

DNA methylation is concentrated in CpG islands on the inactive X and occurs specifically at the promoter regions of genes, in contrast to the intragenic (‘gene body’) and intronic CpGs that are methylated on the active X chromosome (Gendrel et al., 2012; Lock et al., 1987; Hellman et al., 2007; Weber et al., 2005). This suggests that DNA methylation may directly inhibit X-linked gene expression on the inactive X. Methylation of CpG islands is established by the de novo methyltransferase DNMT3B and subsequently propagated by the maintenance methyltransferase DNMT1 (Csankovszki et al., 2001 Gendrel et al., 2012; Sado et al., 2000). Thus, the ability of cytosine analogue inhibitors such as 5-azacytidine and Decitabine to reactivate X-linked gene expression is likely the result of their incorporation into DNA and the resultant inhibition of DNMT1 activity (Jones et al., 1980).

The purpose of this chapter was to co-treat embryos with cycloleucine and Decitabine, with the aim of partially or completely reactivating the inactive X chromosome in cells of female embryos. If XCI-related methyl group usage underlies the female excess in cycloleucine-induced cranial NTDs, then X-reactivation would be predicted to specifically rescue female embryos compared with males. In addition to performing this experiment, several approaches were adopted to test whether Decitabine treatment is indeed effective in X-reactivation in neurulation-stage embryos.

5.2 Results

5.2.1 Exposure of cycloleucine-treated embryos to Decitabine reduces the frequency of cranial NTDs

This experiment was performed some months after the studies in Chapter 3, and so cycloleucine-only (10 mM) cultures were performed again, to check on the rate of cranial NTDs. This gave a 61.5% rate (8 NTDs among 13 embryos) with no additional developmental abnormalities. Since this was close to the NTD rate of the original cycloleucine study (Table 3.1), the effect of Decitabine co-treatment was compared with the full set of cycloleucine-treated embryos (n = 108) from the original study, in order to increase statistical power.

As both cycloleucine and Decitabine caused cranial NTDs when individually administered in embryo culture (Tables 3.1 and Table 4.2, respectively), it was initially predicted that co-treatment would produce an enhanced NTD frequency compared with the single agents. However, a striking biphasic dose-response relationship was observed (Table 5.1; Figure 5.1) in which the NTD rate fell from 0 to 0.05 μM Decitabine, and then rose to 0.1 μM. At 0.05 μM Decitabine, NTD rate was significantly lower than at 0 μM (i.e. cycloleucine alone) and also significantly lower than at 0.1 μM($p = 0.006$ and 0.016 respectively; chi-square tests). There was no significant difference in NTD rate between 0 μM and 0.1 μM Decitabine ($p = 0.316$).

Hence, low concentrations of Decitabine protect embryos from cycloleucine-induced cranial NTDs, although the concentration window for this ‘rescue’ effect is narrow (0.025 to 0.05 μM), and corresponds to a dose range that produced no adverse embryonic effects, including no NTDs, when embryos were treated with Decitabine alone (Table 4.1).

5.2.2 The female excess in cycloleucine-induced cranial NTDs is abolished by Decitabine co-treatment

The sex ratio was determined in embryos co-treated with 10 mM cycloleucine and 0.05 μM Decitabine (i.e. the 'rescuing' concentration), compared with the previously identified (Chapter 3) sex ratio of embryos treated with 10 mM cycloleucine alone (Figure 5.2). Among female embryos co-treated with Decitabine + cycloleucine, the NTD rate was 24.3% (9/37), compared with 68.4% (39/57) in cycloleucine alone, a highly significant difference ($p < 0.001$). By contrast, the NTD rate in co-treated male embryos was 50% (17/34), not significantly different from the rate of 45.1% (23/51) in cycloleucine alone ($p = 0.66$). Hence, female embryos are selectively rescued from cycloleucine-induced NTDs by co-treatment with low-dose Decitabine.

Considering the proportions of embryos with NTDs in Decitabine + cycloleucine cultures (Figure 5.2), females made up 34.6% and males 65.4%, a significant difference ($p = 0.015$) from the 62.9% female: 37.1% male ratio among NTDs in cycloleucine-only cultures. Hence, addition of Decitabine results in a reversal of the cranial NTD sex ratio compared with cycloleucine-only cultures, although this is solely due to the reduction in affected females, as the NTD rate in males was not altered.

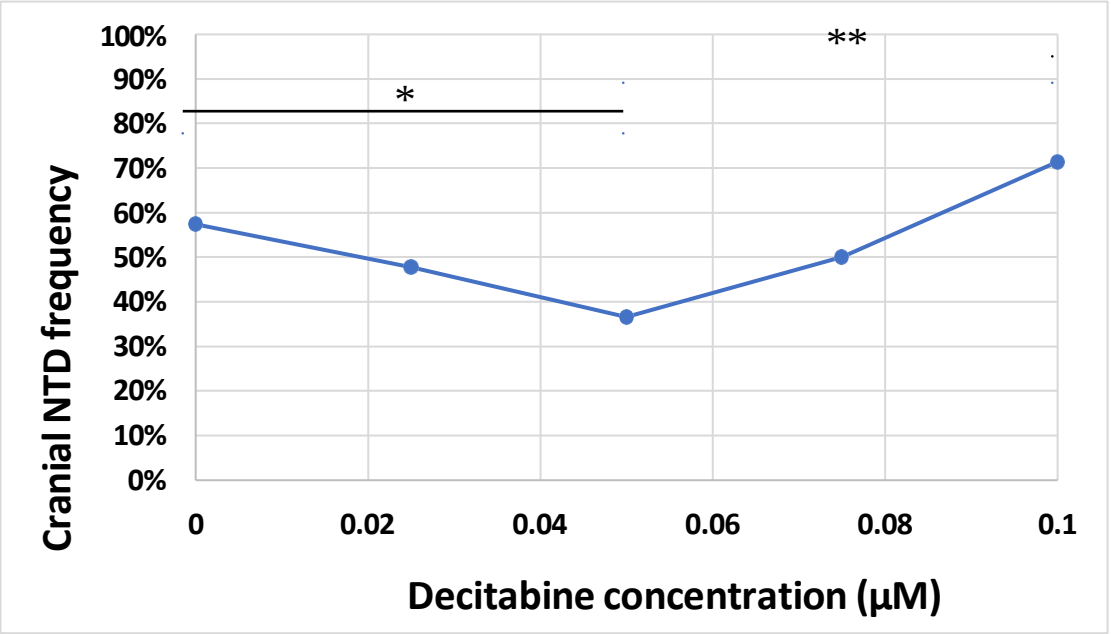

Figure 5.1. Biphasic response of cranial NTD frequency to co-treatment with 10 mM cycloleucine and increasing concentrations of Decitabine. Cranial NTD rate varies significantly with Decitabine concentration ($p = 0.04$; 5 x 2 Chi-squared test of total data set). In pairwise comparisons (2 x 2 Chi-squared tests), NTD frequency is reduced significantly with 0.05 µM Decitabine compared with cycloleucine alone (* $p = 0.006$), while NTD frequency increases significantly from 0.05 to 0.1 µM Decitabine (** $p = 0.016$).

Decitabine conc. (μM)	Cycloleucine conc. (mM)	No. of embryos	Yolk sac circulation	Crown-rump length (mm)	No. of embryos with failed axial rotation (%)	No. of somites	No. of embryos with cranial NTDs (%)
0.0	0.0	10	3.00 ± 0.00	2.68 ± 0.21	0 (0)	20.8 ± 0.10	0 (0)
0.0	10	108	2.79 ± 0.15	2.57 ± 0.26	0 (0)	20.3 ± 0.23	62 (57.4)
0.025	10	23	2.69 ± 0.08	2.59 ± 0.21	0 (0)	20.6 ± 0.18	**11 (47.8)**
0.05	10	71	2.73 ± 0.09	2.61 ± 0.18	0 (0)	19.8 ± 0.32	**26 (36.6)***
0.075	10	16	2.63 ± 0.11	2.46 ± 0.16	0 (0)	19.3 ± 0.26	**8 (50.0)**
0.1	10	14	2.53 ± 0.08	2.23 ± 0.38	0 (0)	18.3 ± 0.58	**10 (71.4)**

Table 5.1. Growth and development of CD1 mouse embryos cultured in the presence of cycloleucine and Decitabine. Data for cycloleucine-only cultures (second row) are reproduced from Table 3.1. Co-treating embryos with cycloleucine and Decitabine does not significantly impair embryonic development as judged by yolk sac circulation, crown-rump length, axial rotation or somite number, when compared with cycloleucine-only or PBS control embryos (top two lines; $p > 0.05$, as tested by 1-way ANOVA). A biphasic effect of increasing Decitabine concentration on cranial NTDs is seen, in which 47.8% of embryos were affected at the lowest dose level, 0.025 μM, a further reduced rate of 36.6% was seen at 0.5 μM (* $p = 0.006$ compared with 0 μM), while at higher doses the rate of cranial NTDs rose again, with no significant difference in NTD rate between 0 μM and 0.1 μM ($p = 0.316$). Hence, cranial NTDs are rescued in embryos treated with 0.05 μM Decitabine + cycloleucine compared with cycloleucine alone. Values for yolk sac circulation, somite number and crown-rump length are mean ± SEM. Data for failed axial rotation and cranial NTDs are presented as the number of embryos with percentage values in parentheses.

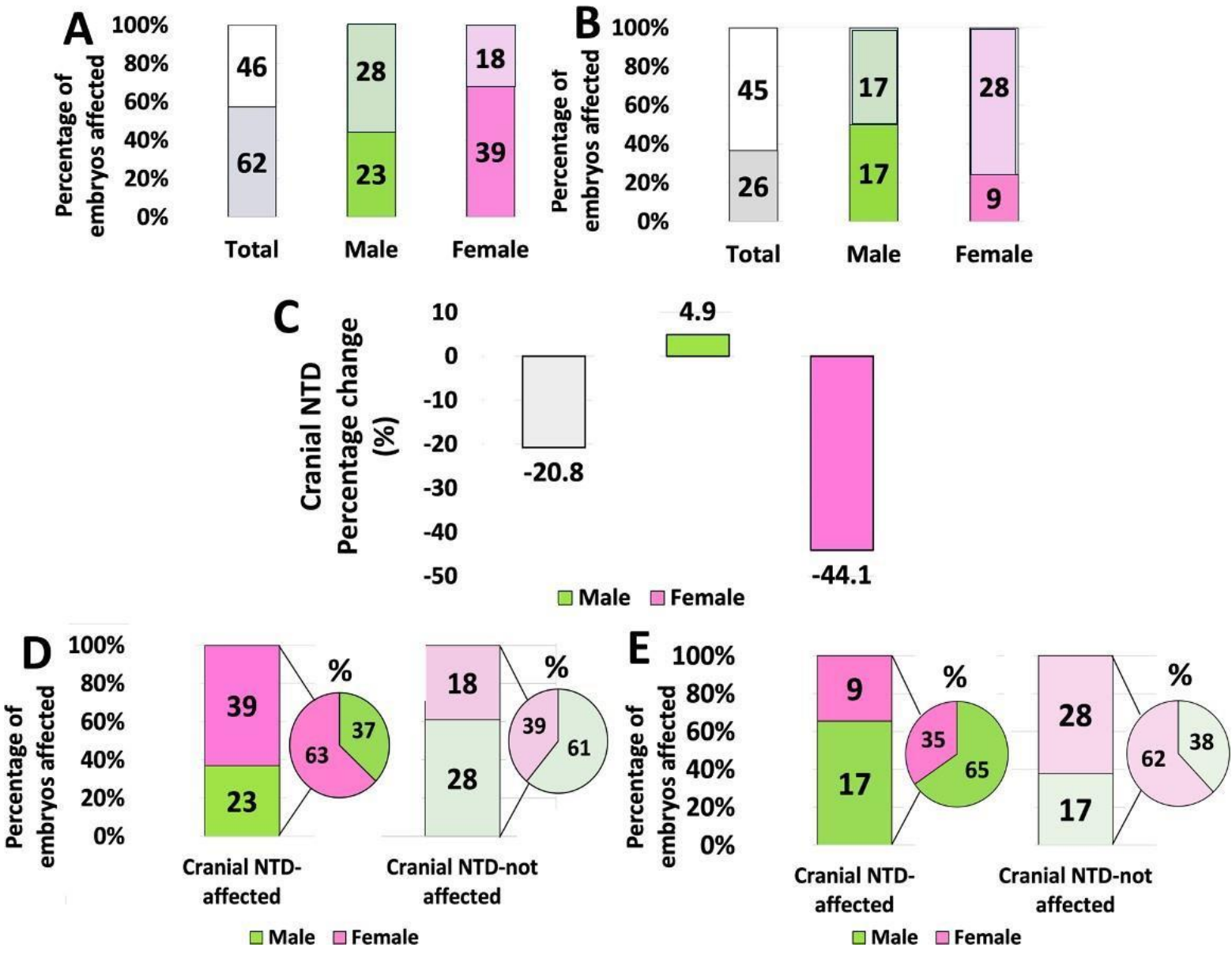

Figure 5.2. Decitabine abolishes the female excess in cycloleucine-induced cranial NTDs. **(A, B)** Distribution of embryos with (filled sectors) or without (no fill) cranial NTDs when treated with 10 mM cycloleucine alone (A, data from Figure 3.3) or 0.05 μM Decitabine + 10 mM cycloleucine (B). Embryo numbers are shown on bars. The proportion of cranial NTDs is significantly reduced in female embryos exposed to Decitabine ($p < 0.001$) whereas there is no change in proportion of male embryos with cranial NTDs ($p = 0.66$). **(C)** Changes in cranial NTD rate with addition of Decitabine which is significant for total NTDs (grey; $p = 0.006$), and females but not males. **(D, E)** The distribution of embryos with (dark bars) or without (light bars) cranial NTDs when treated with cycloleucine alone (D) and Decitabine + cycloleucine (E). Addition of Decitabine reverses the sex ratio of embryos in each category ($p = 0.015$ with NTDs; $p = 0.028$ without NTDs). Pie charts represent the proportion and thus percentage of male and female embryos as extrapolated from the numerical embryo values.

5.2.3 Two embryonic phenotypes with a skewed sex ratio after Decitabine treatment

The next step was to ask whether Decitabine may rescue female cranial NTDs by inducing reactivation of an X chromosome. In Chapter 4, embryos were treated with a range of Decitabine concentrations, and analysis of embryonic parameters for the pooled embryos at 0.2 μM showed overall growth and developmental retardation (Table 4.2). However, re-analysis of these data showed that two dramatically different embryonic phenotypes were present, in almost equal proportions. Just over half of the embryos (16/28; 57.1%; Figure 5.3A, B) showed signs of severe embryonic toxicity. There was perturbed embryonic growth and developmental arrest as shown by a significantly reduced yolk sac circulation and failure of yolk sac to expand, a significantly reduced crown-rump length, with embryos having less than half the normal length, a significantly reduced somite number, and almost complete failure to undergo axial rotation. In contrast, the other sub-group of 0.2 μM Decitabine-treated embryos (12/28; 42.9%) showed no significant developmental abnormalitiescompared with PBS controls (Figure 5.3A, B).

Assessment of sex among the embryos cultured at 0.2 μM Decitabine showed a striking correlation with developmental phenotype, with females making up the majority (81.3%; 13/16; Figure 5.3C) of embryos with the abnormal developmental profile, whereas males made up the majority of the normally developing embryos (66.7%; 8/12; Figure 5.3C). This significant sex difference ($p = 0.019$) is a striking demonstration of the effect of DNA methylation inhibition, with one possible explanation being partial reactivation of the X chromosome in the cells of female embryos. Severe embryonic toxicity has been reported when XCI is disrupted in early development, as a result of failure of the dosage-compensation process that XCI normally provides. In particular, it was shown that extraembryonic tissues with two active X chromosomes, owing to an Xist mutation, fail to sustain the embryo, leading to early lethality (Marahrens et al., 1997). Since whole embryo culture depends pivotally on yolk sac viability for health of the embryo itself, then prevention of XCI

maintenance in yolk sac endoderm could have led to the severely compromised female embryonic development. Indeed, failure of yolk sac circulation and expansion was observed in the 0.2 μM Decitabine cultures (Figure 5.3A, B).

A

Decitabine conc. (μM)	No. of embryos	Yolk sac circulation	Crown-rump length (mm)	No. of embryos with failed axial rotation (%)	No. of somites	No. of embryos with cranial NTDs (%)
0	20	3.00 ± 0.00	2.72 ± 0.14	0 (0)	20.7 ± 0.2	0 (0)
0.2	12	2.81 ± 0.08	2.41 ± 0.24	1 (8.3)	20.3 ± 1.2	9 (0)
0.2	16	0.50 ± 0.50***	0.61 ± 0.35***	15 (93.4)***	8.54 ± 2.5***	-

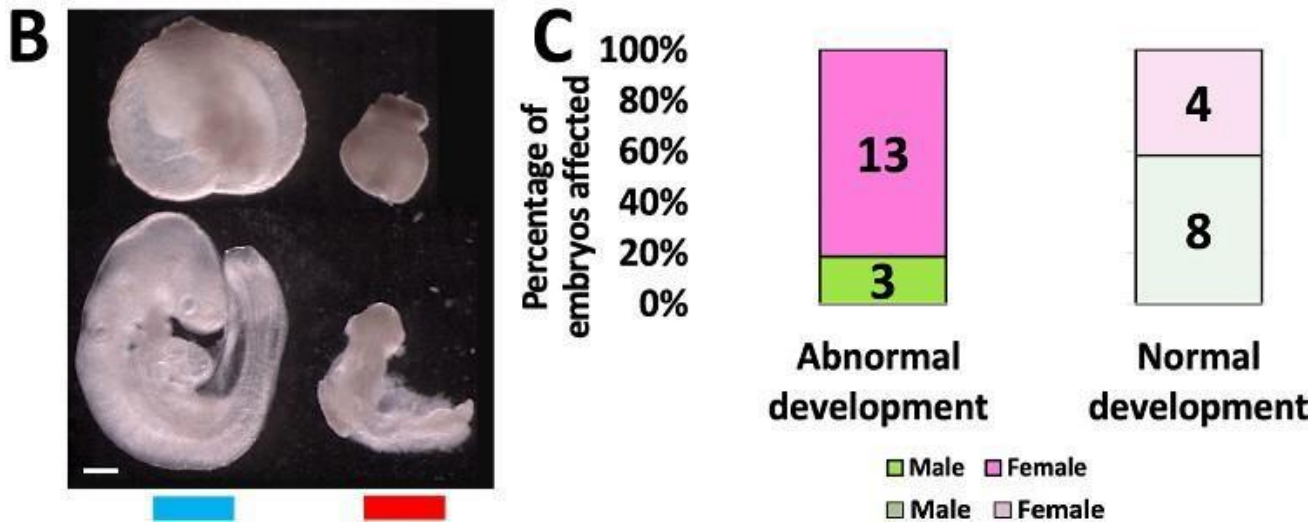

Figure 5.3. Decitabine exposure results in a sex difference embryonic development. (A) Growth and development of CD1 embryos treated with 0.2 μM Decitabine alone. Two embryonic sub-groups were apparent: over half the embryos (red, bottom row) showed signs of severe toxicity and failed embryonic development. All developmental parameters were significantly reduced compared to PBS-treated control embryos (top row: 0 μM Decitabine). The other embryos treated with 0.2 μM Decitabine developed normally, with no significant differences from PBS controls, and no evidence of NTDs (blue, middle row). *** signifies $p < 0.001$, as tested by Student's t test for somite number and Z-test for all other developmental parameters. **(B)** Embryos of the two developmental outcomes after treatment with 0.2 μM Decitabine. Top images: embryos enclosed in yolk sac; bottom images: embryos after removal of yolk sac. Those on the left (blue) appear normal whereas embryos on the right (red) are severely abnormal. **(C)** Distribution by sex of embryos that developed normally and abnormally in 0.2 μM Decitabine. There is a significant sex difference ($p = 0.019$; as assessed by Fisher's exact test) with female embryos making up majority of embryos (81%; 13/16) that show perturbed embryonic development. Values for yolk sac circulation, somite number and crown-rump length are given as mean ± SEM. Data for failed axial rotation and cranial NTDs are presented as the number of embryos with percentage values in parentheses. Scale bar in B: 200 μM

5.2.4 Assessment of Barr bodies as an indication of XCI status in Decitabine-treated embryos

When XCI is fully established, the inactive X chromosome exhibits a conformational change in chromatin structure whereby the active nuclear compartment collapses and the inactive X chromosome becomes highly folded and compacted to form a densely staining structure known as the Barr body or 'sex chromatin' (Barr, 1949; Dyer et al., 1985). Many cytological studies have taken advantage of this phenomenon, with Barr body counts as a measure and indication of the status of XCI. In the present study, Barry body analysis was used to investigate the effect that Decitabine may have on reversal of XCI.

Several experiments were conducted to establish the Barr body method for use with cultured mouse embryos (see detailed method in Chapter 2). In keeping with previous experience (Capel et al., 2008), it was found that amnion gave the most reproducible results, in contrast to embryonic tissues which proved hard to disaggregate for single cell analysis. Toluidine blue (1%) was the best stain, of several that were tested, while uncoated slides with a hydrophobic border gave the best localised cell spreading. Having developed the method, amnion cell spreads from male and female embryos were prepared and inspected by three trained and blinded observers, to arrive at criteria which could most effectively identify Barr bodies. These criteria were: (i) a densely and darkly stained structure, larger than 0.8 × 1.1 µm, and situated at the periphery of the nuclear membrane; (ii) present only in nuclei that appeared approximately circular in appearance, with a length:width ratio of 1 and that did not share any boundaries with other nuclei (Figure 5.4A, B).

Subsequent Barr body analysis was performed by at least two observers blinded to sex and treatment group of the embryos. Female embryos treated with 0.05 µM Decitabine (either alone or with cycloleucine) showed a significantly reduced ($p < 0.001$) proportion of cells positive for a Barr body (10.15$\pm$ 2.1. %), compared with PBS-treated (24.81$\pm$ 6.8%) and cycloleucine-only treated (25.3$\pm$7.9%) embryos (Figure

5.4C). By contrast, amnion cells from male embryos in the PBS control and cycloleucine-only treatment groups showed a ‘background’ Barr body count of 2-5%, which was not significantly altered by addition of Decitabine ($p = 0.18$). These findings are consistent with a partial reactivation of the X chromosome by Decitabine in female embryos. Moreover, they suggest that almost all female embryos exhibit some degree of X-reactivation, given the minimal overlap of data points between the PBS/cycloleucine groups and the Decitabine + cycloleucine group. On the other hand, the proportion of cells showing X-reactivation seems to vary between Decitabine-treated female embryos, with some showing ‘male-like’ values for % Barr bodies, and some showing much higher values.

A

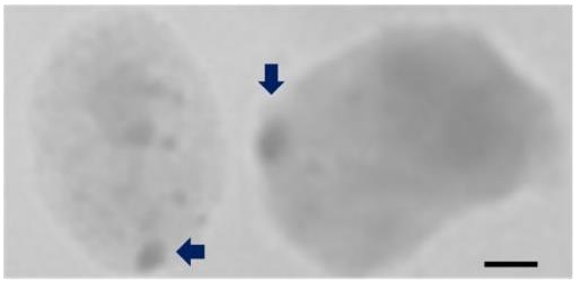

B

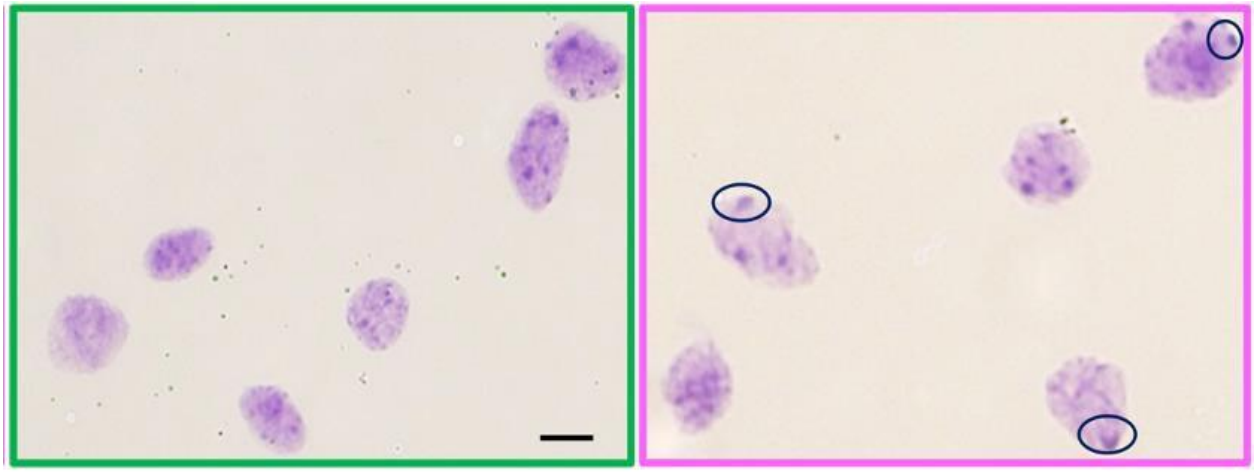

Male Female

C

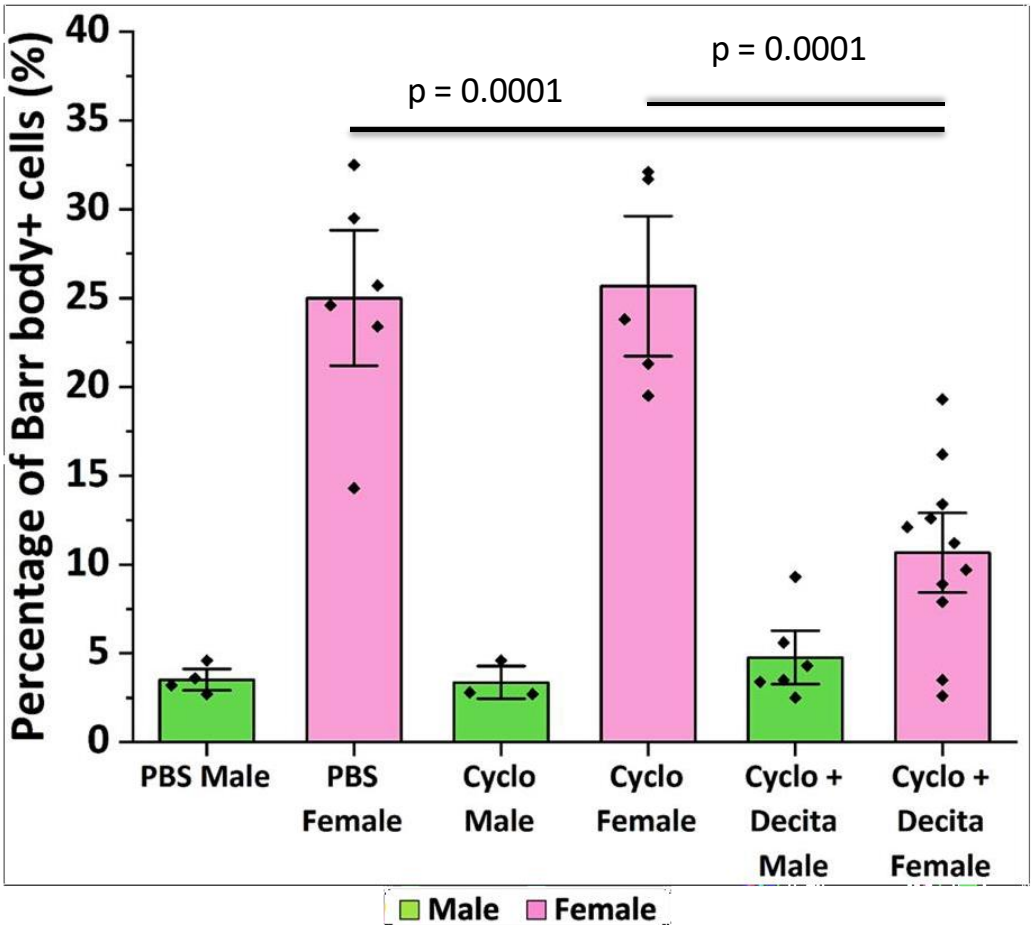

Figure 5.4. Decitabine treatment leads to a reduced proportion of cells positive for a Barr body in female embryos. (A) Grey-scale image of two nuclei to show location and staining of Barr bodies (arrows). Scale bar: 2 μm. **(B)** Representative images of amnion cell spreads from Decitabine-treated female (left) and male (right) embryos. Barr bodies are circled and are seen only in female cells. Note the peripheral position of Barr bodies within nuclei, which distinguishes them from other stained chromatin structures which are generally separate from the nuclear membrane. Images taken at x40 magnification; scale bar: 10 μm. **(C)** Percentage of total amnion cells positive for a Barr body in female (pink) and male (green) embryos in the three treatment groups (as assessed in 120 nuclei). Addition of Decitabine to cycloleucine-treated female embryos results in a significant reduction in % Barr body positive cells, compared with PBS control ($p < 0.001$; Student's t-test) and cycloleucine-only treated females ($p < 0.001$; Student's t-test) as assessed in 120 nuclei. Cells from male embryos show background (2-5% positive) Barr body % values, with no significant effect of Decitabine treatment. Each data point represents the mean value for an individual embryo. Error bars represent mean ± SEM.

5.2.5 Decitabine treatment results in a non-sex specific increase in autosomal gene expression

If cytosine analogue inhibitors such as Decitabine cause X chromosome reactivation by being incorporated into DNA and the resulting in inhibition of DNMT1 activity (Jones et al., 1980) a prediction would be that Decitabine treatment would result in an increase in gene expression as a result of inhibiting DNA methylation. Quantitative reverse transcriptase (qRT) PCR was performed, using whole embryo homogenates. One question was how to normalise gene expression during the qRT-PCR assays. Initially, *Gapdh* and *β-actin* were used, but this gave inconsistent results, with variability between samples and experiments. Given the widespread role of DNA methylation in transcriptional repression, Decitabine was thought likely to activate most genes, making 'housekeeping' genes inappropriate for normalisation. In consequence, experiments were performed using 28S rRNA, which is not affected by methylation and therefore should not exhibit altered expression in Decitabine-treated embryos.

Plots of relative expression of both the autosomal genes glycine decarboxylase (Figure 5.5A; *Gldc*) and grainyhead-like 3 (Figure 5.5B; Grhl3) against embryo sex show increased expression treated with Decitabine (+cycloleucine) compared with PBS control (Figure5.5). This increase is seen in both sexes, likely reflecting an overall reduction in DNA methylation, which generally serves to inhibit gene expression. Despite the increase, there was no selective and specific increase in relative expression of autosomal genesin female embryos. These findings provide support for the idea that the mode of actionof the cytosine analogue inhibitor, Decitabine is likely as a result of its incorporation into DNA and the resultant inhibition of DNMT1 activity (Jones et al., 1980) which results in an increase in gene expression. Moreover, the non-sex-specific increase in autosomal gene expression likely suggests that the specific rescue of female embryosis unlikely due to an increase in autosomal gene expression.

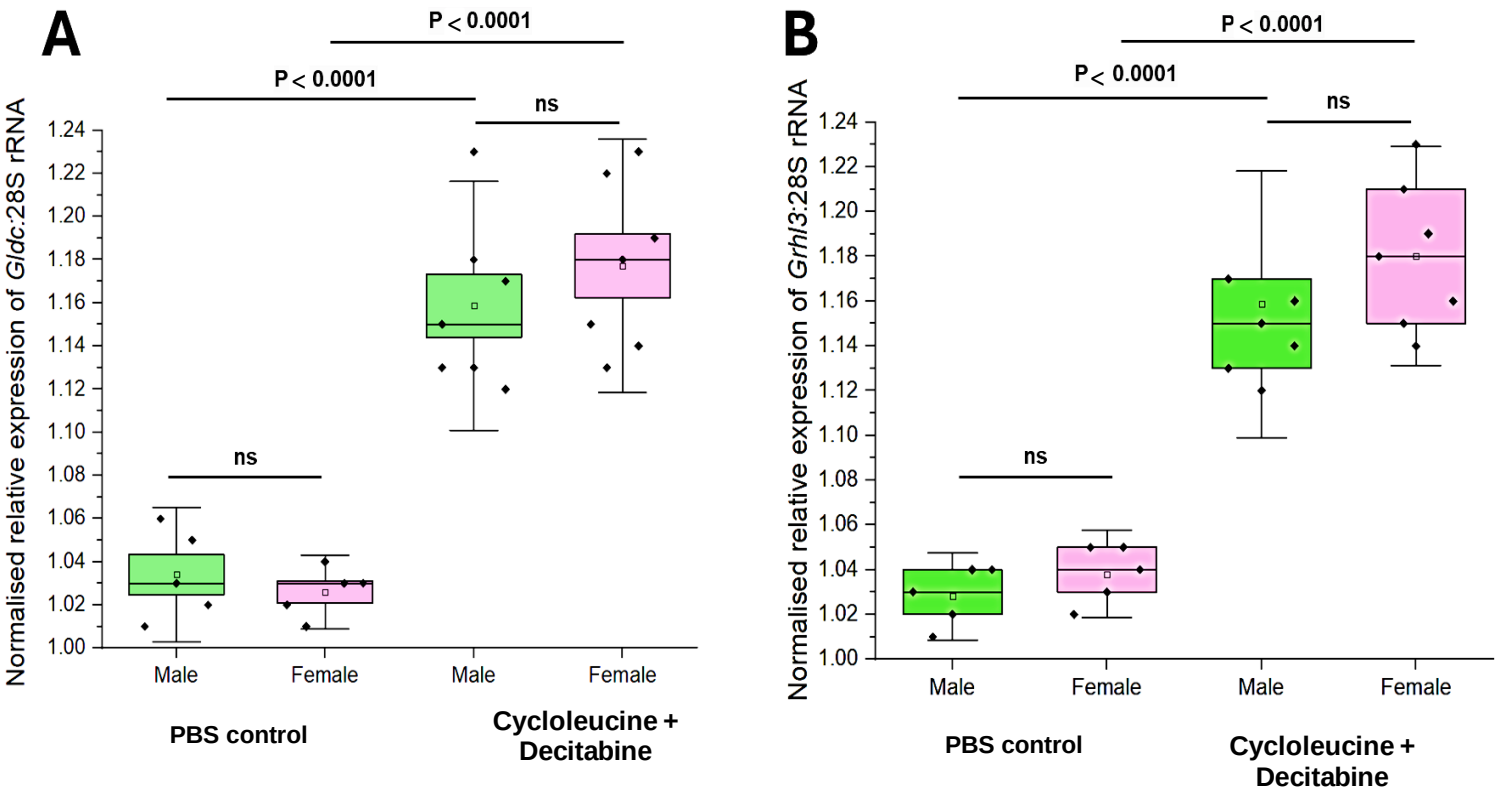

Figure 5.5. Effect of Decitabine on autosomal gene expression in male and female embryos. (A-B) Expression of *Gldc* (A), *Grhl3* (B) as assessed by qRT- PCR in in male (green) and female (pink) embryos in PBS and treated with Decitabine + cycloleucine. Both autosomally linked genes show significantly increased relative expression in female and male embryos treated with Cycloleucine + Decitabine when compared to PBS controls (as assessed by Student's t-test). Relative gene expression does not differ significantly between Decitabine + cycloleucine treated female and male embryos (as assessed by Student's t-test). Data points: individual embryos that were stage-matched; square: mean values; error bars: SD

5.2.6 Decitabine results in a female-specific increase in X-linked gene expression

The findings of female-specific embryonic toxicity after 0.2 μM Decitabine, and the reduction in Barr body count after 0.05 μM Decitabine treatment, are both consistent with partial reactivation of the X chromosome by Decitabine in female embryos. A further prediction would be that Decitabine-treated female embryos should exhibit specifically increased expression of X-linked genes when compared with non-Decitabine-treated female embryos, or male embryos of any treatment group.

Three X-linked genes were chosen for analysis: *Hprt*, *Mecp2* and *G6pdx* (Figure 5.6A). All were previously found to be re-expressed in studies of X-reactivation and therefore appeared viable candidates for assessing potential X-linked gene re-expession in Decitabine-treated embryos. Quantitative reverse transcriptase (qRT) PCR was performed, using whole embryo homogenates. Plots of relative expression of the three X-linked genes against embryo sex and treatment group show increased expression of all genes in embryos treated with Decitabine (+/-cycloleucine) compared with PBS control and cycloleucine-only cultures (Figure 5.6B-D). This increase is seen in both sexes, likely reflecting an overall reduction in DNA methylation, which generally serves to inhibit gene expression. Strikingly, however, there was a selective and specific increase in relative expression of all three X-linked genes in female embryos, in contrast to the much smaller increase in males (Figure 5.6B-D). These findings provide further support for the hypothesis that Decitabine partially reactivates the X chromosome in female embryos, and that this effect may underlie its ability to rescue female embryos from cycloleucine-induced cranial NTDs.

Relative expression of all three X-linked genes increased to a comparable level in Decitabine + cycloleucine co-treated female embryos ($p > 0.05$ between genes; 1-way ANOVA; Figure 5.6E). This suggests that Decitabine-induced X chromosome reactivation is not locus-specific, but likely acts broadly, at least along the region of the X chromosome where *Hprt*, *Mecp2* and *G6pdx* are located (Figure 5.6A).

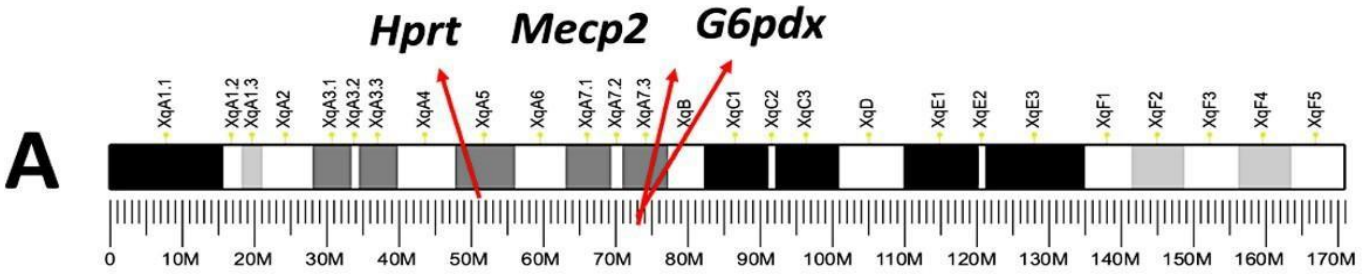
A
Hprt
Mecp2
G6pdx
XqA1.1
XqA1.2
XqA1.3
XqA2
XqA3.1
XqA3.2
XqA3.3
XqA4
XqA5
XqA6
XqA7.1
XqA7.2
XqA7.3
XqB
XqC1
XqC2
XqC3
XqD
XqE1
XqE2
XqE3
XqF1
XqF2
XqF3
XqF4
XqF5
0
10M
20M
30M
40M
50M
60M
70M
80M
90M
100M
110M
120M
130M
140M
150M
160M
170M

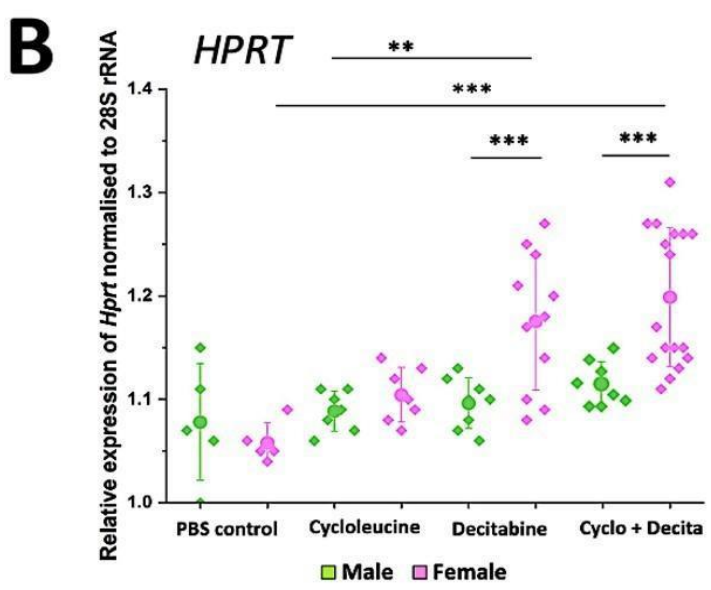
B
HPRT
Relative expression of Hprt normalised to 28S rRNA
**
***
***
***
1.0
1.1
1.2
1.3
1.4
PBS control
Cycloleucine
Decitabine
Cyclo + Decita
Male
Female

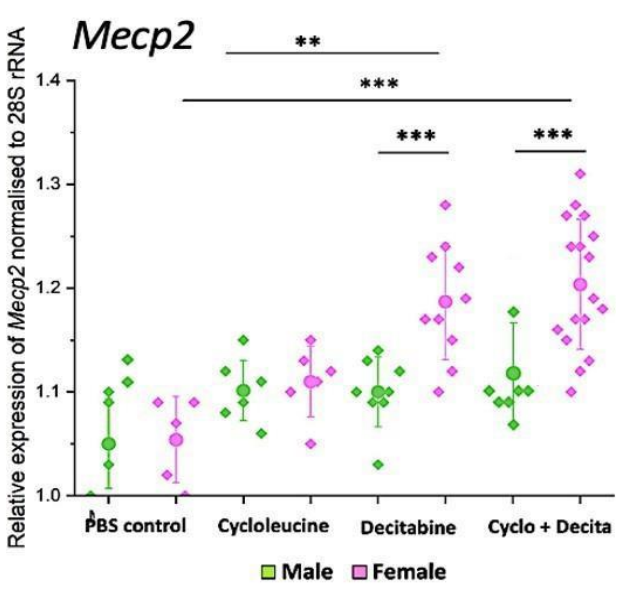
C
Mecp2
Relative expression of Mecp2 normalised to 28S rRNA
**
***
***
***
1.0
1.1
1.2
1.3
1.4
PBS control
Cycloleucine
Decitabine
Cyclo + Decita
Male
Female

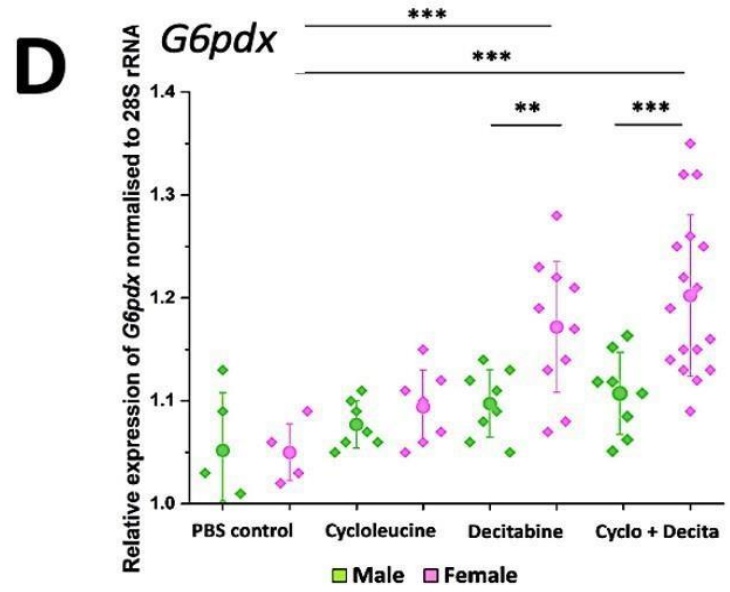
D
G6pdx
Relative expression of G6pdx normalised to 28S rRNA
***
***
**
***
1.0
1.1
1.2
1.3
1.4
PBS control
Cycloleucine
Decitabine
Cyclo + Decita
Male
Female

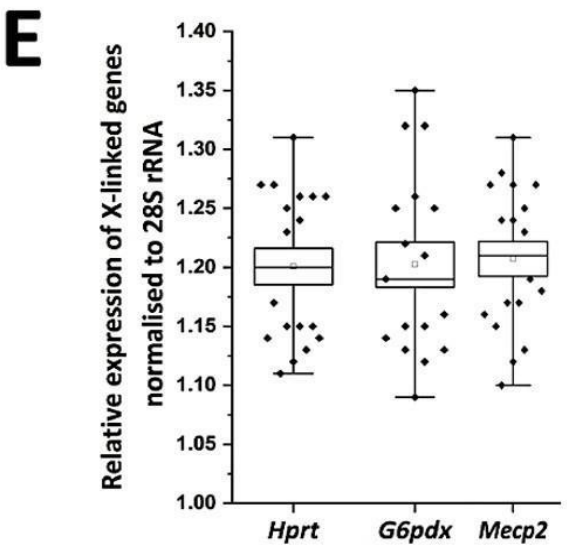
E
Relative expression of X-linked genes normalised to 28S rRNA
1.00
1.05
1.10
1.15
1.20
1.25
1.30
1.35
1.40
Hprt
G6pdx
Mecp2

Figure 5.6. Effect of Decitabine on X-linked gene expression in male and female embryos. (A) Diagram of mouse X chromosome (centromere to left) to show location of the three X-linked genes whose embryonic expression was assessed. **(B-D)** Expression of *Hprt* (B), *Mecp2* (C) and *G6pdx* (D) as assessed by qRT-PCR in in male (green) and female (pink) embryos treated with (left to right): PBS, cycloleucine-only, Decitabine-only and Decitabine + cycloleucine. All three X-linked genes show significantly increased relative expression in female embryos treated with Decitabine (+/- cycloleucine). Relative gene expression does not differ significantly between female cycloleucine-only and PBS control embryos, nor between males of any treatment groups. Data points: individual embryos; large data points: mean values; error bars; ** $p < 0.01$; *** $p < 0.001$; Student's t-tests. **(E)** Relative expression of all three X-linked genes in Decitabine + cycloleucine co-treated embryos. There are no significant differences between the genes. Data points: individual embryos that were stage-matched; circles: mean values; error bars: percentile ranges.

5.2.7 Correlation between NTD phenotype and X-linked gene expression level after Decitabine rescue

Decitabine resulted in the female-specific rescue of cranial NTDs in cycloleucine-treated embryos (Figure 5.2), and caused a female-specific increase in X-linked gene expression (Figure 5.5 B-D). This raised the possibility that the magnitude of the gene expression response of individual embryos (a possible indicator of the completeness of X reactivation between embryonic cells) might be related to developmental outcome, in terms of whether an NTD is present or not. To test this hypothesis, relative gene expression values in each sex/treatment group combination were separated into upper and lower 50% of values (Figure 5.6).

Comparing these sub-groups for proportion of NTDs revealed a significant difference for the *Hprt* and *Mecp2* genes among female embryos treated with Decitabine + cycloleucine. Data for *G6pdx* showed a similar trend but did not reach statistical significance. In contrast, Decitabine-only-treated female embryos, and males of both treatments, showed no significant difference in proportion of NTDs between upper and lower 50% sub-groups (Figure 5.6). Hence, specifically in the Decitabine 'rescue' group, female embryos that do not present with cranial NTDs cluster together and express the highest levels of X-linked gene expression, whereas female embryos with cranial NTDs cluster together and express the lowest levels of X-linked gene expression. These findings provide strong evidence that Decitabine reactivates the X chromosome in female embryos, and that the completeness of this reactivation is key to whether or not embryos are rescued from cycloleucine-induced NTDs.

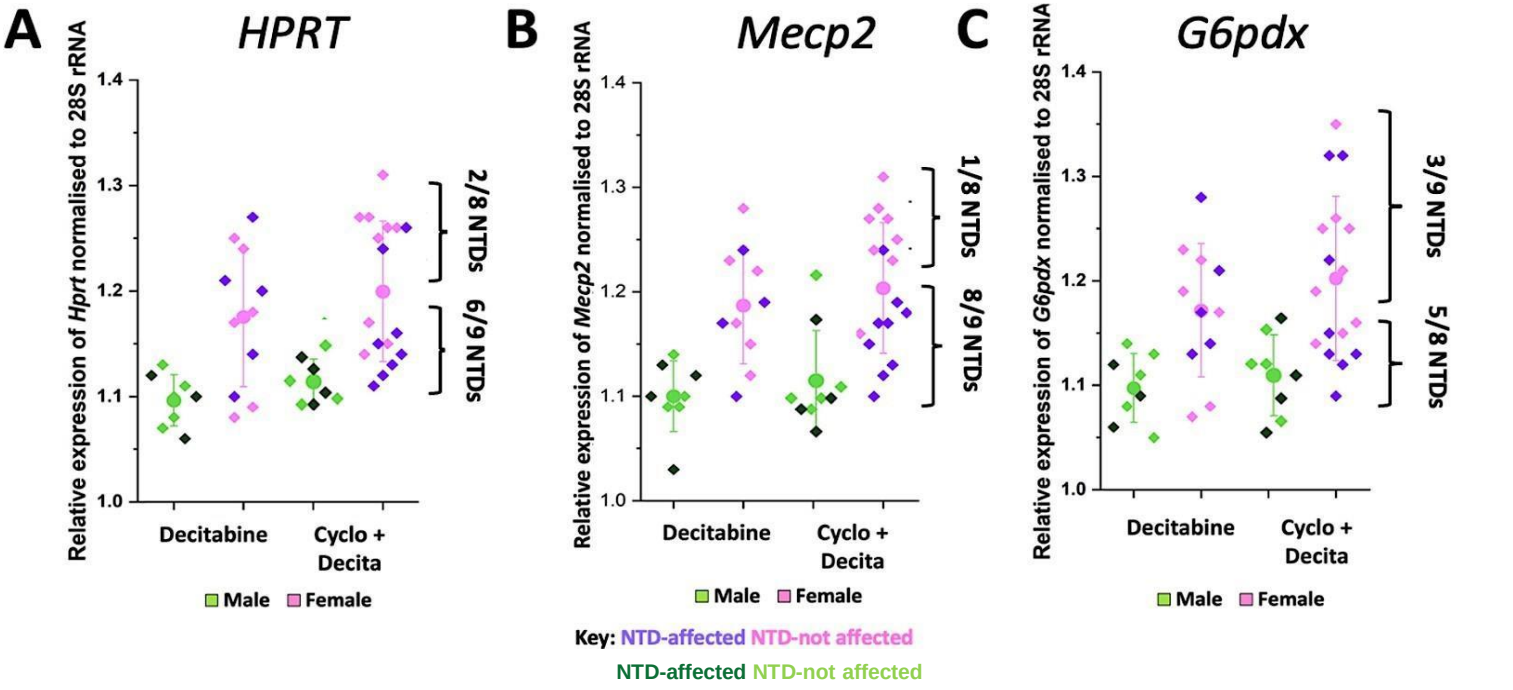
A
HPRT
Relative expression of Hprt normalised to 28S rRNA
1.4
1.3
1.2
1.1
1.0
Decitabine
Cyclo + Decita
Male
Female
2/8 NTDs
6/9 NTDs
B
Mecp2
Relative expression of Mecp2 normalised to 28S rRNA
1/8 NTDs
8/9 NTDs
C
G6pdx
Relative expression of G6pdx normalised to 28S rRNA
3/9 NTDs
5/8 NTDs
Key: NTD-affected NTD-not affected
NTD-affected NTD-not affected

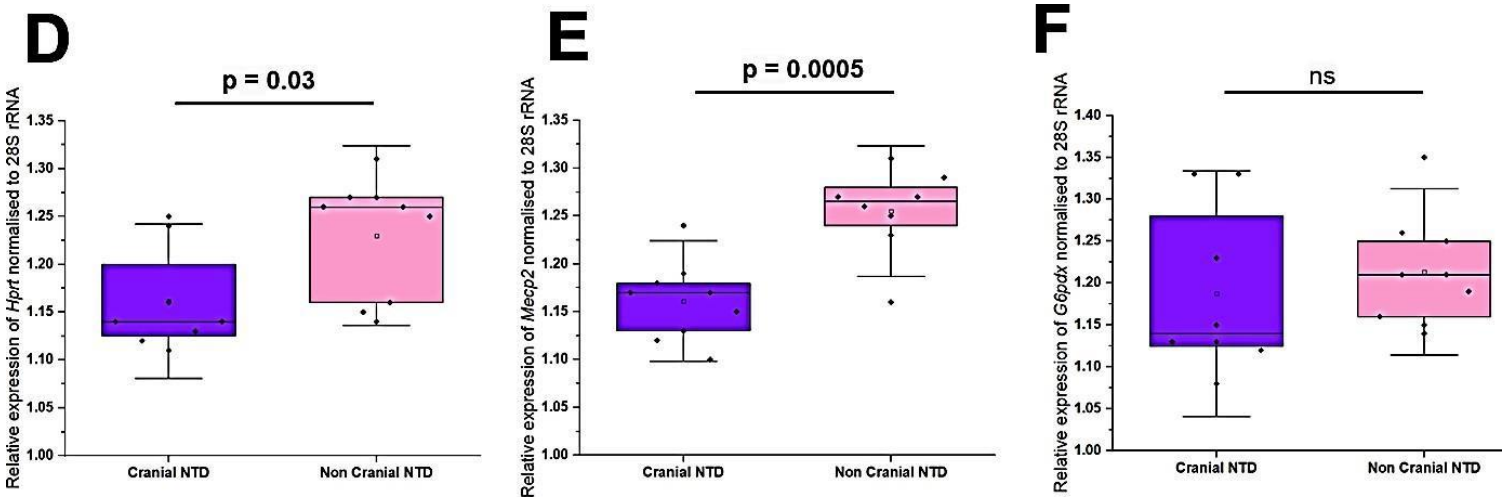
D
p = 0.03
Relative expression of Hprt normalised to 28S rRNA
1.35
1.30
1.25
1.20
1.15
1.10
1.05
1.00
Cranial NTD
Non Cranial NTD
E
p = 0.0005
Relative expression of Mecp2 normalised to 28S rRNA
F
ns
Relative expression of G6pdx normalised to 28S rRNA
1.40

Figure 5.7. Correlation between embryonic phenotype and relative expression of the X-linked genes: *Hprt* (A), *Mecp2* (B) and *G6pdx* (C). Data shown are for Decitabine-only and Decitabine + cycloleucine treatment groups. For statistical analysis, data points within each sex/treatment combination were separated into upper and lower 50% of relative gene expression values, as illustrated by the brackets for the Decitabine + cycloleucine female groups. For *Hprt* (A) and *Mecp2* (B), there is a significant difference in NTD proportion (affected vs unaffected embryos) between upper and lower 50% sub-groups, specifically among Decitabine + cycloleucine-treated female embryos ($p < 0.001$ and$p < 0.001$ respectively; Fisher exact tests). A similar trend is discernible for *G6pdx* (C), but the difference does not reach statistical significance ($p = 0.07$). In contrast, female embryos treated with Decitabine alone, and males of both treatments, show no significant difference in NTD proportion between upper and lower 50% sub-groups. Hence, a normal embryonic phenotype correlates with higher X-linked geneexpression level in females where Decitabine has 'rescued' a proportion of embryos from cycloleucine-induced NTDs. **(D-F)** Comparison of *Hprt* (**D**), *Mecp2* (**E**) and *G6pdx* (**F**) in Decitabine + cycloleucine treated female embryos that do and do not present with a cranial NTD. Analysis reveals a significant increase in the level of *Hprt* and *Mecp2* in female embryos that are 'rescued' but not for G6dpx (as assessed by student's t test). Each dot represents an individual embryo, with darker shades indicating cranial NTD-affected embryos and lighter shades showing unaffected embryos.

5.3 Discussion

In this chapter, embryos were cultured in Decitabine plus cycloleucine, with striking and unexpected findings. Although Decitabine is a potent inhibitor of DNA methylation, and causes cranial NTDs when administered alone to embryos in culture, it proved to have a protective effect at low dose levels against NTDs. This was seen in two ways: first, through the biphasic dose-response effect of Decitabine on total NTD rate in embryos exposed to cycloleucine and, second, in the specific rescue of female, but not male, embryos from cycloleucine-induced cranial NTDs. Since Decitabine was previously shown to induce reversal of XCI (Carrette et al., 2018), it was hypothesised that the female-specific rescue of NTDs in this study was due to partial reactivation of the inactive X chromosome by Decitabine. Subsequent experiments provided three lines of evidence in support of this X-reactivation hypothesis.

5.3.6 Differential toxicity of Decitabine for female and male embryos

A dose of Decitabine (0.2 μM) led to sub-lethal toxicity in embryo culture, but on careful examination of the data was found to produce two different embryonic phenotypes with a strong correlation with embryo sex. More than half of the embryos, of which 81% were female, exhibited severe developmental abnormalities including growth cessation, axial rotation defects and failure to develop somites. The remaining embryos, of which 67% were male, developed normally, with no differences from PBS-treated controls. The predominantly female growth arrest in this experiment was associated with defects of yolk sac development, with no functional blood circulation and failure of the yolk sac to expand. Embryo culture relies on the ‘histiotrophic’ mode of embryonic nutrition, in which nutrients and waste products are exchanged across the yolk sac (Lloyd et al., 1985). This is the main mode of embryonic nutrition during the period of neural tube closure, before the chorio-allantoic placenta becomes functional (D'Souza et al., 2021). If yolk sac function is compromised, the embryo exhibits growth and developmental retardation and, ultimately, death (Brent et al., 1990). It may be significant, therefore, that improper balancing of X-linked gene

dosage by germline deletion of *Xist* in the extraembryonic tissues, including trophoblast and yolk sac endoderm, was shown to result in early embryonic lethality (Marahrens et al., 1997). A likely explanation for the 'dual phenotype' seen after 0.2 μM Decitabine, therefore, is reactivation of the X chromosome in the yolk sac of female embryos leading to nutritional failure and embryo toxicity.

5.3.7 Reduction in Barr body count in female cells after Decitabine

If Decitabine reactivates an X chromosome, it was hypothesised that the proportion of cells with a Barr body, which represents the heterochromatic inactive X, would be reduced in female but not male embryos. Using amnion cell spreads from cultured embryos, this prediction was confirmed, with significantly fewer Barr body positive cells in female embryos after Decitabine treatment. In this analysis, males were scored as positive for a Barr body in 3-5% of cells, whereas in reality males never exhibit an inactive X chromosome. This 'false-positive' Barr body count was taken as a limitation of the scoring system, and the value of Barr body positive cells in male embryos was subtracted from other experimental groups, to internally control for background.

Conversely, the proportion of Barr body positive cells in female embryos was scored as around 25%, for PBS control and cycloleucine-treated groups, whereas a score of 100% might be expected given that all female cells exhibit XCI. Other authors (Capel et al., 2008) state that: "Barr bodies are visible in ~ 50-60% of the cells in an XX embryo" and a "5% error rate [is] associated with this technique". The reason for the present work scoring fewer than half the expected proportion of female cells as positive may include several factors. Although Barr bodies usually appear at the periphery of the nucleus, a minority can also be found in other parts of the nucleus, such as the nucleolus (Klinger et al., 1957) or cytoplasm. They can also vary in shape: while the 'typical' Barr body is plano-convex or wedge-shaped, with the plane side resting against the nuclear membrane and the convex part pointing toward the cytoplasm, Barr bodies in the centre of the nucleus can appear rectangular, spherical, biconvex or triangular, depending on location within the nucleus.

In the present study, a conservative approach was taken to scoring Barr bodies, for example only counting structures with a specific size threshold, at the periphery of the nucleus, and this would have under-estimated the total Barr body count. Importantly, the same selection criteria were used for all treatment groups, with Barr body scoring carried out as a double-blind trial involving several different lab personnel. This gives confidence that, as a comparative measure, the Barr body method gave informative data in this research. To obtain a more detailed analysis of the effect Decitabine has on the inactive X chromosome, for example to assess whether the inactive X chromosome is partially or completely reactivated, a more detailed assessment of Barr body size, staining intensity and/or changes in position could be undertaken. Others have used specific markers such as immunostaining for macroH2A1 to provide this information (Costanzi et al., 1998).

5.3.8 Enhanced X-linked gene expression in female embryos with cranial NTDs after Decitabine

A third line of evidence consistent with induction of X chromosome reactivation by Decitabine in female embryos came from an assessment of X-linked gene expression using qRT-PCR. This revealed a specific increase in expression of three X-linked genes in female embryos co-treated with Decitabine and cycloleucine, whereas Decitabine-treated male embryos showed significantly less enhancement of X-linked gene expression. In PBS control and cycloleucine-only cultures, female and male embryos showed similar gene expression levels. Strikingly, two subgroups could be identified among the Decitabine-treated females: those lacking a cranial NTD (‘rescued’) showed the highest levels of X-linked gene expression, whereas those with a cranial NTD (‘non-rescued’) had lower gene expression levels. By contrast, co-treated male embryos showed no correlation between NTD phenotype and X-linked gene expression level. These findings strongly suggest that the degree of X reactivation, as reflected by the magnitude of gene expression increase, determines whether female embryos develop an NTD or not. That is, when a larger proportion of

embryonic cells undergo reversal of XCI, the level of overall X-linked gene expression is greater, the ‘methyl drain’ is minimised, and cranial neural tube closure is rescued. Conversely, a smaller X reactivation effect may be insufficient to diminish the female-specific methylation deficiency, and so the risk of cranial NTDs persists.

5.3.9 p53-related hypothesis to explain the female excess in cranial NTDs

The work of Delbridge *et al*. (2019) proposes that failure of XCI in female embryos may be a possible mechanism underlying the increased risk of cranial NTDs in females. According to this idea, biallelic and therefore unbalanced expression of X- linked genes would occur in female cells, leading to abnormal neural tube closure. Theauthors used *p53* (*Trp53*) mutant mice in which partially penetrant cranial NTDs occur in homozygotes, with a female excess (Armstrong et al., 1995). A co-existing mutationin the pro-apoptotic Bim gene was included, which gave 100% penetrant NTDs. Then neural tube samples were assessed for X-inactivation markers *Xist* and H3K27me3, while the X-linked genes *Huwe1* and *Usp9x* were assessed for biallelic expression. Embryos lacking p53 contained fewer cells showing X-inactivation and greater biallelic X gene expression than controls, while p53 protein was found to bind directly to the X-inactivation centre, providing a mechanism for this effect on XCI in mutant embryos (Delbridge et al., 2019).

While this study provides a possible mechanism for the female excess in p53 mutant NTDs, it does not explain the more general finding of female preponderant exencephaly in other mouse mutant strains, where p53 is not mutant. It is possible that p53 defects occur downstream of these other genes, but such a highly gene- specific mechanism seems unlikely to explain the generality of sex differences in cranial NTDs, including in humans. Moreover, the findings from the present study argue against this as a general mechanism, as co-treatment with Decitabine rescued female embryos, concomitantly with a higher (presumably biallelic) level of X-linked gene expression, which Delbridge et al (2019) consider to predispose to NTDs. An

enhancement of the present work would be to include analysis of mono-allelic versus biallelic expression of X-linked genes which was achieved by fluorescence in situ hybridization on interphase nuclei, in the Delbridge et al study.

5.3.10 XCI escapee genes as an explanation for the female excess in cranial NTDs

Another possible explanation for the female excess in cranial NTDs concerns genes that escape XCI, and so are biallelically expressed in all females. Examples of XCI escapee genes that may also play a role in cranial neural closure include *Mid1* and *Shroom4* (Yang et al., 2010). *Mid1* encodes a ubiquitin E3 ligase and is required for neural tube closure in *Xenopus* with deletion of the *Mid1* causing destabilisation and disorganisation of microtubules, and disruption of neuroepithelial apical-basal polarity (Suzuki et al., 2011). *Mid1* is also essential in neural crest migration in chick whereby it degrades protein phosphatase 2A (Latta et al., 2012). *Shroom4*, like other family members, is an actin binding protein with a likely role in neuroepithelial apical constriction (Yoder et al., 2007), a cellular event needed for bending of the neural folds. In Chapter 4, it was suggested that biallelic expression of such genes might protect female embryos against the forebrain NTDs that characterise male embryos. However, the enhanced expression of these escapee genes could predispose female embryos to failed cranial neural tube closure, compared with males where mono-allelic expression would always occur. According to this idea, Decitabine usage would be expected to increase the expression of XCI escapee genes even further, and potentially result in an increased rate of cranial NTDs in female embryos. This is contrary to the findings of the present study, where Decitabine rescued female NTDs, and so the role of XCI escapee genes in predisposing females to cranial NTDs is not supported by the data.

Chapter 6. General Discussion

Sex differences in disease frequency and severity are common, and can provide information on pathogenic mechanisms, as well as having health care implications. While direct or indirect effects of the sex hormones are often implicated, it is striking that a sex bias can also occur in clinically important birth defects that arise before the stage of gonad development or onset of sex steroid secretion. Understanding how such early arising malformations affect the sexes differentially may provide significant insight into developmental and preventive mechanisms.

A well-known example of a sex-biased birth defect is the cranial NTD anencephaly (with its developmental forerunner exencephaly), a severe brain defect that results from failed cranial neural tube closure in the third week post-conception. Prolonged exposure of the neural tissue to amniotic fluid leads to progressive degeneration, with lethal consequences by birth. Anencephaly affects ~ 0.2-5 per 1000 births (0.5/1000 in UK), depending on geographical location (Zaganjor et al., 2016), with highest numbers in developing countries (Berihu et al., 2018). It is a major cause of stillbirth or pregnancy termination after prenatal diagnosis (Johnson et al., 2012). Cranial NTDs have been found to occur more commonly in females than in males with human studies having shown females to be 1.5-2 times more often affected by than males. In mice, exencephaly is also known to occur more commonly in females in genetic strains with partially penetrant cranial NTDs. Hence, female excess in cranial NTDs may be a general mammalian phenomenon.

6.1 Testing the “methyl sink” hypothesis

The focus of the current PhD thesis was to test a prominent hypothesis that seeks to explain the female excess in cranial NTDs (Juriloff & Harris, 2012). This focuses on the process of X chromosome inactivation (XCI) whereby the extensive use of methyl groups needed to silence the X chromosome in every cell of the developing female embryo is proposed to create an epigenetic “methyl sink”, that disrupts and puts other cellular methylation-dependent processes at risk of failing. Cranial neural tube closure

is likely methylation-dependent and occurs after XCI has taken place, making this a prime candidate for effects of the “methyl sink”.

To begin with, an in vitro whole embryo culture model was established, in which methyl group availability was modulated. Methyl group deficiency was induced in normal CD1 embryos by 24 h culture (E8.5-9.5) in the presence of cycloleucine, an inhibitor of the enzyme methionine adenosyltransferase (MAT). MAT inhibition reduces the cellular levels of SAM, the major methyl donor for methylation of DNA, RNA, lipid and protein molecules. The findings in Chapter 3 revealed that the addition of cycloleucine at 10 mM resulted in female embryos being significantly more often affected (68%; 39/57) than male (45%; 23/51) embryos. Hence, a non-genetic influence on methyl group availability can induce female-preponderant cranial NTDs in wildtype embryos. To test whether SAM depletion was responsible for this effect, cycloleucine-treated embryos were co-treated with MGBG, a SAM decarboxylase inhibitor, which preserves the pool of endogenous SAM for methylation donation, at the expense of polyamine synthesis (Chapter 3). MGBG-treatment rescued cranial NTDs in cycloleucine-treated embryos in a dose-dependent way: 1 μM (no effect) to 5 μM (100% rescue), with no detectable toxicity. At 2 μM, MGBG reduced the overall cranial NTD rate to 29% (30/103), more than halving the cranial NTDs rate in females (22%; 10/46) but with no significant effect on males (35%; 20/57). This specific rescue of females by ‘sparing’ SAM is as predicted by the methylation XCI hypothesis of female predisposition to cranial NTDs.

An important aspect of this study is that, whereas previously a female excess in mouse cranial NTDs was found exclusively in genetic NTD models, here an environmental influence on wild-type development was also shown to produce a sex difference in exencephaly rates. Moreover, the environmental agent, cycloleucine, was specifically chosen to diminish methyl group availability, an approach that would not be easily achieved using genetic tools. For example, knockout of the mouse *Mat2A* gene, which encodes extra-hepatic MAT enzyme, is lethal prenatally although the stage of death is not clear (https://www.mousephenotype.org/data/genes/MGI:2443731).

6.2 Relative merits of embryo culture versus in vivo dosing

Assessment of somite number, degree of axial rotation, developmental progression, and protein content showed that development and growth of embryos can be closely similar in culture and in vivo, both in rats and mice (New, 1978; Sadler, 1979). Assessment of somite number, degree of axial rotation, developmental progression, and protein content showed that development and growth of embryos can be closely similar in culture and in vivo, both in rats and mice (New, 1978; Sadler, 1979).

The use of whole embryo culture for teratogen studies is beneficial in terms of the 3Rs aims of Replacement, Reduction and Refinement of animal experiments (Culshaw et al., 2019). In particular, embryo culture avoids the need to dose pregnant females with a teratogen. Moreover, a single litter of embryos can be assigned to several treatment groups in culture, whereas the unit of in vivo teratogenesis is the pregnant female, raising the issue of inter-female differences. On the other hand, embryo culture removes the maternal environment and so is a simplified model of prenatal development. Nevertheless, embryonic development in culture and in vivo have been shown to be closely parallel in both mouse and rat embryos over the early organogenesis period, e.g. E8.5 to E9.5 (New, 1978; Sadler, 1979). In the present study, for example, embryos with 5-7 somites at the start of culture progressed to 18-21 somites after 24 hr culture, representing an increase of at least one somite per 2 hr, as observed in vivo. This suggests that ex vivo culture experiments were representative of in vivo embryonic development in the present research. Other advantages of embryo culture in this study included:

1. Accessibility and visualisation of embryos was possible throughout cranial neural tube closure, which would not be the case in vivo.

2. Selection of embryo suitability for experiments was possible, for example allowing only embryos within a specific somite range to be cultured. This ruled out the possibility that the partial penetrance of cranial NTDs was the result of developmental differences between embryos in different litters in vivo.

3. The ex vivo approach ensured that the final concentration of the drug reaching the embryo was precisely controlled, given that every embryo had an equal opportunity to take the drug up from the culture serum. In vivo this might be influenced by factors such as position of the embryo within the uterus.

4. With application of drugs in vivo, maternal metabolism, especially in the liver, can lead to rapid turnover and so limited availability to embryos, making it difficult to control the final concentration of the drug. This is not the case when using an ex vivo approach.

6.3 The protective effect of folic acid on NTDs may converge with the "methyl sink" hypothesis

Further evidence a role of for the XCI epigenetic "methyl sink" hypothesis comes from the possible interface between folic acid supplementation and downstreammethylation reactions. Maternal folic acid supplementation has shown to reduce the occurrence and recurrence of NTD-affected pregnancies (MRC Vitamin Study Research Group, 1991, Eichholzer et al., 2006). Moreover, evidence from population-based studies in South America (Poletta et al., 2018) and China (Liu et al., 2018), andcase-control studies in the US (Shaw et al., 2020) have shown a greater preventive effect of folic acid in overcoming anencephaly in females when compared to males. Given the multibranched nature of folate one-carbon metabolism reactions (Blom et al., 2006), it is possible that one way in which folic acid nutrition may reduce the rate of cranial NTDs is via the increased shunting of one-carbon units to the methylation cycle, and thereby stimulation of downstream cellular methylation reactions (Blom et al., 2006).

Supporting evidence for this idea comes from the female preponderance in cranial NTDs being more pronounced in regions where the birth prevalence of anencephaly is high (Carter, 1974; Borman et al., 1986; Seller, 1987). Such geographical regions usually have no folic acid fortification or multivitamin nutritional programmes, and so the female excess particularly correlates with a lack of folate-mediated prevention.

However, folic acid is an un-methylated, synthetic form that needs to be converted to THF, and then 5-methylTHF with gain of a methyl group, to become active. In contrast, the naturally occurring folate, 5-methylTHF, and the one carbon donor betaine both donate methyl groups directly to homocysteine, forming methionine. It is possible, therefore, that 5-methylTHF (marketed as Metafolin), and choline the precursor of betaine, may be more bio-available alternatives to folic acid for NTD prevention (Obeid et al., 2013) and specifically to prevent female anencephaly, which represents almost two-thirds of all anencephalic cases.

It should be noted, however, that excessive methylation cycle stimulation may be detrimental: treating embryos with excess methionine can suppress the methylation cycle, cause a reduction in the SAM/SAH ratio, and lead to cranial NTDs (Dunlevy et al., 2006). Hence, methionine is contraindicated as a protective agent. Excess methionine results in a build-up of homocysteine which in turn increases SAH levels, given that the kinetics of the SAH hydrolase enzyme favours SAH synthesis. Active removal of homocysteine is needed to maintain flux through the methylation cycle. Importantly, the SAM/SAH ratio is not only important for regulating methylation but also influences flux through the interlinked folate cycle, since SAM inhibits the functionof the 5,10-methylene tetrahydrofolate reductase enzyme (MTHFR; EC1.7.99.5) (Kutzbach and Stokstad, 1971). An increase of SAH levels compared to SAM increases MTHFR activity, driving the production of 5-methyl THF for the remethylationof homocysteine to methionine. However, this depletes the availability of 5,10- methylene THF, the MTHFR substrate, for reactions in the folate cycle including the de novo synthesis of dTMP and purines. This can inhibit DNA synthesis and limit cellproliferation, and may explain why excess levels of methionine result in cranial NTDs.

6.4 Polyamine synthesis appears dispensable for normal development at neurulation stages

Polyamines are polycationic compounds that play important regulatory roles in various cellular processes such as: growth, proliferation, and differentiation. The intracellular levels of polyamines change throughout the cell cycle (Friedman et al., 1972; Bachrach et al., 1973) with intracellular pools increasing most drastically during the S,

G_2 and M phases of the cell cycle (Heby et al., 1973; Heby and Russell, 1973). This suggests the importance of polyamines for DNA replication and cell division. Indeed, polyamines are known to play a key role in early embryogenesis: for example, the highest order polyamine putrescine, undergoes a rapid increase in abundance immediately prior to, during and after implantation (Fozard et al., 1980). MGBG, an inhibitor of spermidine and spermine synthesis, results in developmental quiescence at the 8-cell or morula stage before cavitation can take place to form the blastocyst (Alexandre et al., 1979; Zwierzchowski et al., 1986). Moreover, embryos homozygous for loss of SAMDC, the enzyme which synthesises spermine and spermidine (Heby, Marton, Wilson & Gray, 1977) die early in development, between E3.5 and E5.5, prior to implantation (Nishimura et al., 2002), and with reduced cell proliferation. Collectively, these studies suggest that polyamine synthesis and availability is essential for early embryonic development and that any perturbation in the availability or synthesis of polyamines can result in developmental arrest.

It was striking, therefore, that the addition of MGBG to neurulation-stage embryo cultures (Chapter 3) did not result in any obvious growth abnormalities or disrupted embryonic development, such as cranial NTDs. This may suggest that the role of polyamines in development is time- and stage-dependent. However, the mode of action of MGBG in specifically blocking spermidine and spermine synthesis is well documented, with MGBG having been used and applied in both cell and embryo culture experiments. Moreover, the present study used MGBG up to 10 µM, which is the same dose that inhibited preimplantation development in vitro (Zwierzchowski et al., 1986). Several possible explanations can be suggested for these unexpected findings with MGBG in the present study:

1. Polyamines may not be required or utilised at the neurulation stage of embryonic development. This seems unlikely as polyamines appear to have an obligatory link to cell proliferation (Mandal et al., 2013).

2. There may be an ‘alternative’ route of polyamine synthesis at neurulation stages. The rate-limiting enzymes in polyamine biosynthesis are SAMDC (inhibited by MGBG)

and ornithine decarboxylase (ODC). SAMDC converts SAM to spermidine and spermine, whereas ODC converts L-ornithine to putrescine, which can then be converted to spermidine and spermine (Chapter 1, Figure 1.3) SAMDC is already active at preimplantation stages, whereas ODC shows a rise in activity from gastrulation onwards in mice and chick (Fozard et al., 1980; Löwkvist et al., 1980). Hence, ODC may compensate for SAMDC inhibition by MGBG at neurulation stages, whereas it is unable to do so earlier, leading to the preimplantation developmental arrest observed with MGBG (Alexandre et al., 1979; Zwierzchowski et al., 1986).

3. It is possible that putrescine, the precursor of spermidine and spermine, has a specific role in development that is not fulfilled by spermidine and spermine, whose synthesis is blocked by MGBG. Fillingame et al. found that MGBG treatment of proliferating lymphocytes caused 50% inhibition of [3H]-thymidine incorporation, but the level of inhibition increased to 75% when putrescine accumulation was also inhibited (Fillingame et al., 1975). It remains to be determined whether putrescine has a separate function from spermidine and spermine, or can simply make good their shortage after MGBG treatment.

4. MGBG may be unable to deplete the pools of endogenous polyamines, as a result of the long half-lives of these compounds (Russell et al., 1970). Addition of MGBG to L1210 leukemia cells resulted in a decline of spermidine and spermine levels within 4 hours, but spermidine and spermine were still present in significant amounts even after 24 hours of administration (Pleshkewych et al., 1980).

5. The inhibitory effect of MGBG may be short-lived and/or reversible, and can even result in a paradoxical increase in SAMDC activity (Fillingame et al., 1973; Holtta et al., 1973; Pegg et al., 1973; Pegg et al., 1974). This has been attributed to MGBG binding to and stabilising SAMDC against proteolytic attack and thus resulting in reversible inhibition of SAMDC.

Polyamine analysis was not a goal in the present study, and so no measurements of polyamine levels were made, which is a limitation of the work. Such analysis would be

valuable in future. In addition, it might be informative to treat E8.5 embryos with an ODC inhibitor, such as difluoromethylornithine (DFMO), which blocks putrescine synthesis (Poulin et al., 1992). Alone or in combination with MGBG, this should have adverse effects on embryonic development, if polyamines are essential for growth at neurulation stages. Unlike MGBG, however, DFMO would not be expected to rescue cycloleucine-induced NTDs, as it should not replenish SAM levels. On the contrary, it might induce a compensatory increase in SAMDC activity, to produce spermidine and spermine, which might diminish available SAM for transmethylation reactions, and potentially cause cranial NTDs, especially in females.

6.5 Limitations of the study

As a model system, the experimental approach of whole embryo culture used throughout this thesis presents with many benefits (as outlined in section 6.2) but is also liable to some potential drawbacks. For instance, cranial neurulation stage embryos were explanted and grown in rat serum which itself is an undefined media. That is, the make-up and concentrations of the various metabolites, nutrients and growth factors that constitute the serum remains unknown. Therefore, it is plausible that inconsistencies and differences in the make-up of the serum itself may be a factor that may contribute to or affect embryonic development in our study. It should be noted however that several steps and considerations were taken to minimise this effect. First, in each experiment conducted a control group was also cultured parallel to the teratogen-based culture to assess any differences serum quality may cause. In no control embryo was embryonic viability, growth or developmental progression (as assessed by parameters outlined in the Methods section 2.2.3) disrupted or different from one another which suggest that the serum itself is unlikely to be a factor that causes the differences in embryonic development or cranial NTDs that are observed. Second, to better control serum consistency the serum used throughout this thesis was only collected from adult male rats to reduce hormonal-dependent differences that may influence and alter metabolite and nutrient concentration in the serum as may be the case if adult female rats were used. Thirdly, upon collection and preparation of serum all serum was pooled together and then aliquoted as either 2 ml or 3 ml aliquot

with the pooling of serum likely helping to reduce batch-batch variation if any existed. Fourthly, all E8.5 embryos cultured were done so with the same volume of serum per embryo that was 0.75 ml of serum per embryo (four embryos were cultured in 3 ml of serum) to ensure that consistency was obtained and differences in embryonic development was not due to the availability and access of embryos to the metabolites and nutrients present in the serum. Although the use of rat serum for whole embryo culture is a potential source of limitation in this study several measures were taken to ensure the serum itself was not a factor contributing to the results obtained. Translationally, it is important to note that human pregnancy itself also presents as an undefined culture process given that women who become pregnant do not routinely undergo any biochemical or metabolic profiling until much later in pregnancy and certainly most often after the 3-4th week post conception when the neural tube has already formed. Thus, as a model system the use of whole embryo culture in rat serum may be sufficient to recapitulate embryonic development as would be expected to occur in normal human pregnancy.

Another caveat of using the whole embryo culture approach is the explant of embryos from the pregnant dam and hence the removal of the maternal environment during the stage of cranial neural tube closure. As a result, it is unknown how the different teratogens and inhibitors used in this study would affect embryonic development in vivo at the same doses used. It is possible that maternal metabolism may alter the metabolic form or dose of the drug used and therefore how translatable the findings of this study are for in vivo development remains unclear. In addition to this, removal of embryos from the maternal environment also means it is difficult to assess the impact various treatment and supplementation strategies may have on reducing or rescuing cranial NTDs. For instance, MTHFR null embryos do not present with cranial NTDs despite having impaired methylation cycle activity. It is thought that this is a result of the maternal circulation providing sufficient provision of methyl groups such as methionine or from other methyl group donors such as betaine or dimethylglycine to the neurulating embryo. If MTHFR null embryos however were grown in culture it is likely that they would not be able to successfully close their cranial neural tube given they supply of methyl groups would not be sufficient to support cranial neural tube closure and hence show that different phenotypes may exist in the same genetic

knockout model in vivo or if embryos are grown in culture. An additional factor to consider is that in our model the only way to rescue cycloleucine-induced cranial NTDs was to use the SAMDC inhibitor, MGBG and therefore to maximise endogenous use of SAM for methylation reactions at the expense of polyamine synthesis. Other methyl group donors such as betaine although theoretically may have been able to overcome cycloleucine-induced cranial NTDs the inability of neurulation-stage embryos to utilise the methyl group from betaine as a result of not expressing the BHMT enzyme provide a further limitation of using an ex vivo whole embryo culture approach as this would likely not be the case in vivo given maternal supply of methyl groups may be sufficient to protect embryos from cycloleucine-induced cranial NTDs. Thus, the removal of the maternal environment in an ex vivo whole embryo culture approach has limitations in allowing assessment of potential strategies to overcome cranial NTDs.

Furthermore, the use of the non-mutant CD1 mouse strain in this study may also have some limitation. In human pregnancy, NTDs likely arise as a result of an accumulation of various interacting predisposing genetic and environmental factors which ultimately increase the susceptibility of an NTD affected pregnancy. The use of the wildtype CD1 mouse strain may therefore not recapitulate the true extent of the incidence, severity and sex ratio of cranial NTDs that may be caused by cycloleucine if a genetic mouse strain that is predisposed to cranial NTDs was used. It is possible that a much lower dose may be needed to have the same effect given that the genetic mouse strain may be sensitised to develop cranial NTDs. As a result, the generalisability of the findings from this study to reflect the population-level risk of having an NTD-affected pregnancy may be questioned.

6.7 Future directions

6.7.1 To assess whether the number of X chromosomes and XCI is related to the sex difference in cranial NTD rate

If the process of XCI and the epigenetic “methyl sink” hypothesis is the underlying cause of the increased risk of female developing cranial NTDs, then the rate of cranial NTDs in aneuploid embryos would be expected to follow a specific pattern of cranial NTDs. Males with Klinefelter syndrome (47, XXY) undergo XCI on one X chromosome, like XX females, whereas females with Turner syndrome (45, XO) have no XCI, like XY males. Given the rarity of these syndromes, it is unclear whether anencephaly rates differ from XX and XY levels in humans. However, mice with 41, XXY or 39, XO chromosomes can be produced using the XY* genetic system, based on the B6Ei.LT-Y(IsXPAR;Y)Ei/EiJ strain of mice (JAX, 002021). A variant Y* chromosome with altered centromere position leads to an increased rate of meiotic nondisjunction. The XY* system is often combined with the Four Core Genotypes (FCG) system to distinguish effects of X/Y chromosomal composition, from Sry-determined male gonadal status (Arnold et al., 2020). XXY* mice produced in this way have many features of humans with Klinefelter syndrome, and undergo XCI (Werler et al., 2011) while XO mice are models of Turner syndrome.

To assess whether the number of X chromosomes and XCI is related to the sex difference in cranial NTD rate, the XY* strain from JAX has been imported. XY* studs

will be mated with XX females to produce both XXY* and monosomy X (strictly XY*^{X}) embryos and XX and XY littermates will serve as controls. Like CD1 embryos in Chapter 3, these embryos will also be cultured in cycloleucine to induce cranial NTDs by depleting the pool of SAM availability . If XCI is the critical factor imparting a high risk of cranial NTDs in females, then XXY* male embryos would be expected to show show a similar rate of cranial NTDs as XX females, while the rate of cranial NTDs in XO females should resemble the rate found in XY males, an experimental set up that would uncouple the process of XCI from embryonic sex and directly assess it to cranial NTD risk.

6.7.2 To test the possible neural crest mechanism of XCI-predisposed female brain defects.

The hindbrain/midbrain pattern of cranial NTDs in cycloleucine-treated female embryos coincides with findings that: (i) DNA and protein methylation are required for neural crest emigration (Vermillion et al., 2014; Hu et al., 2012) (ii) pre-closure NC migration occurs specifically in hindbrain and midbrain regions and (iii) failure of neural crest emigration can lead to hindbrain/midbrain cranial NTDs, by preventing ‘dorsolateral bending points’ in the neural plate, which bring the neural fold tips together in the midline. Thus, it is hypothesised that the female-specific requirement in cranial neurulation relates to a dependence of neural crest emigration on DNA or protein methylation and this produces cranial NTDs specifically in the hindbrain/midbrain region because this is the only neural tube region where neural crest emigration occurs before closure.

Male and female embryos will be cultured in the presence of cycloleucine and stopped 8-12 hours before cranial neural tube closure is complete in order to allow comparison of cycloleucine-treated male and female embryos at an early stage of cranial NTDs development. To test the neural crest cell hypothesis, whole mount in situ hybridisation or immunohistochemistry, for markers such as FoxD3 and ErbB2, which are expressed by neural crest cells prior to and during emigration will be carried out to reveal whether the onset of neural crest emigration is delayed or diminished particularly in female embryos as predicted by the NCC hypothesis. If these results

reveal significant findings, then cycloleucine-treated embryos expressing *Wnt1*^{Cre} and R26R-EYFP or mTmG, which provides a fluorescent reporter for neural crest migration, will also be used in order to provide semi-quantitative comparisons of neural crest numbers. In addition, the neural fold tips from the open hindbrian/midbrain could also be dissected and explanted into culture on a fibronectin substrate, to allow neural crest to emigrate away over a 24-48 h period. This method would allo neural crest cell number to be precisely determined (using Wnt1^{Cre}/mTmG fluorescence as neural crest marker) and neural crest cell migration dynamics, could be studied by live time-lapse imaging these cultures.

6.7.3 **Molecular basis of methylation effects in sex specific cranial NTDs***.*

DNA methylation. Overall DNA methylation will be compared between female and male embryos after cycloleucine culture, with or without MGBG rescue. To do this, gene-specific methylation differences between sexes may initially be conducted using a methylation microarray which has comprehensive coverage of CpG islands and other genomic methylation target sites. The analysis may indicate global effects or may pinpoint specific candidate regions, from the position of differentially methylated single nucleotide polymorphisms in putative regulatory regions. Candidate genes with differential methylation between females and males, with/without cranial NTDs, could then be identified and assessed further for embryonic expression by qRT-PCR, in situ hybridisation and/or immunohistochemistry, and top priority candidates considered for functional analysis.

Protein methylation. In order to assess the specific proteins and protein sites or residues which show differential methylation patterns in cycloleucine-treated female embryos, Western blot analysis for the SETD2 trimethylation mark will be extended specifically for embryonic hindbrain/midbrain extracts (Seervai et al., 2020). Particular proteins of interest could be further analysed by identification of methylated peptides using mass spectrometry-based analysis using time-of-flight mass spectrometers dedicated for peptide discovery. Given actin is a specific protein of interest, attempts could be made to localise SETD2 and trimethylated F-actin using anti-SETD2 and anti-Me3K40 methyl-tubulin antibodies (Seervai et al., 2020), together with phalloidin to

identify F-actin and comparisons between between male and female embryos, cultured with cycloleucine +/- MGBG, could be assessed. These experiments may help indicate whether differences in actin methylation in neuroepithelium and/or neural crest cells exist and correlate with female predisposition to hindbrain/midbrain defects. If positive results emerge, a SETD2 floxed mouse could be obtained and mated with $Sox1^{Cre}$, $Pax3^{Cre}$ or $Wnt1^{Cre}$ to conditionally delete SETD2 in the cranial neuroepithelium or neural crest cells prior to cranial neural tube closure in order to assess the important cell specific site in which SETD2 methylation may be important for the process of cranial neural tube closure.

Appendix

In addition to the experiments completed and reported in the main body of the thesis other preliminary experiments were also conducted.

Experiment 1. Assessing whether cycloleucine treatment results in cranial NTDs in other wildtype mouse strains.

Results

C57/BL6 embryos were treated with cycloleucine and cultured in rat serum for the period of cranial neural tube closure (E8.5-E9.5) using the whole embryo culture system (New DAT, 1978).

PBS was used as a vehicle control and embryos from within litters were allocate according to size/stage to make sure groups are balanced and to minimise any effect of litter-to-litter variation.

At the end of the culture period, embryos were harvested and assessed for cranial NTDs and scored for other developmental parameters including measures of embryo viability, embryonic growth, and development progression whilst the yolk sac was removed and used to determine embryonic sex by genomic PCR. Embryos were obtained from 10 litters.

Cycloleucine-treatment does not perturb embryonic viability or embryonic growth in C57/BL6 mouse embryos

Exposure to cycloleucine at concentrations of up to 2 mM did not adversely affect embryonic viability as indicated by the mean yolk sac circulation scores at the end of the culture period which did not differ significantly between cycloleucine-treated and PBS-control embryos (Figure A1). Crown-rump length (measure of growth) and number (measure of developmental progression) and occurrence of axial rotation were also not adversely affected in embryos cultured with cycloleucine
Figure A1). Hence, treating embryos with cycloleucine up to 15 mM does not have

detectable embryotoxic effects.

Cycloleucine causes cranial NTDs in C57/BL6 mouse embryos

All embryos cultured from E8.5 for 24 h in the presence of cycloleucine progressed past the 18-somite developmental stage (Figure A1A), at which cranial neural tube closure is normally complete in C57/BL6 mouse embryos. Hence all embryos in this experiment could be assessed for cranial NTDs.

The treatment of embryos with cycloleucine resulted in a dose-dependent increase in cranial NTDs (Figure A1A). A significant proportion of cycloleucine-treated embryos exhibited cranial NTDs: 33.3% at 1.50 mM ($p < 0.05$, tested by Z-test) and 60.7% at 2 mM ($p < 0.05$) when compared to PBS control embryos (Figure A1A).

Since cycloleucine-treated embryos treated with up to 2 mM cycloleucine did not exhibit developmental or growth abnormalities (Figure A1A), these findings suggest that failure to close the cranial neural folds is a specific effect of cycloleucine, and not as part of a non-specific influence on development or growth.

Cycloleucine treatment results in an increase trend of cranial NTDs in C57/BL6 mouse embryos

To detect a possible sex difference in the rate of cranial NTDs, cycloleucine at 2 mM was used as this gave an NTD rate of ~ 50% (Figure A1B). Hence, any increase or decrease in NTD rate in females versus males should be detectable. The overall cranial NTD rate at 2 mM cycloleucine was 60.7% (17/28; Figure A1B), with female embryos (65%% NTDs; 11/17) significantly more often affected than male embryos (35% NTDs; 6/17; Figure A1B). Although this did not result in a significant sex difference perhaps due to the number of embryos assessed there did appear to be a trend towards an increase in the rate of cranial NTDs in female embryos ($p = 0.4$; 2x2 Fisher Exact Test).

A

Cycloleucine (mM)	No. of embryos	Yolk sac circulation	Crown-rump length (mm)	No. of embryos with failed axial rotation (%)	No. of somites	No of embryos with cranial NTDs (%)
0.00	12	3.00 ± 0.00	2.17 ± 0.34	0 (0)	19.4 ± 0.3	0 (0)
0.50	8	3.00 ± 0.00	2.12 ± 0.21	0 (0)	18.9 ± 0.4	0 (0)
1.00	10	3.00 ± 0.00	2.01 ± 0.43	0 (0)	18.8 ± 0.4	1 (10.0)
1.50	12	2.86 ± 0.12	2.06 ± 0.37	0 (0)	19.1 ± 0.3	4 (33.3)**
2.00	28	2.65 ± 0.10	1.97 ± 0.24	0 (0)	19.2 ± 0.4	17 (60.7)***
5.00	8	-	-	-	-	-
10.00	6	-	-	-	-	-

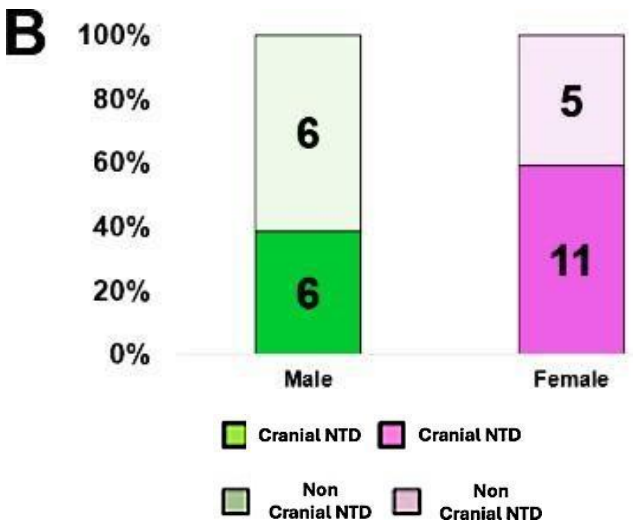

Figure A1. (A) Growth and development of C57/BL6 mouse embryos cultured in the presence of cycloleucine. Non-viable embryos were identified by the absence of yolk sac circulation. Values for yolk sac circulation, somite number and crown-rump length are given as mean ± SEM. No significant difference between the developmental parameters assessed are found between cycloleucine-treated and PBS control embryos (0 mM; $p > 0.05$, as tested by Student's t-test). Data for failed axial rotation and cranial NTDs are presented as the number of embryos with percentage values in parentheses. Cycloleucine-treatment results in a significant increase in the rate of cranial NTDs; ** indicates $p < 0.0001$, as tested by Z-test. **(B)** Cycloleucine-treatment results in a trend towards a female excess in cranial NTDs. The colours in the stacked bar charts represent cranial NTD-affected embryos and the numerical values the number of embryos.

Experiment 2

To test the idea that cycloleucine causes cranial NTDs in CD1 mouse embryos by inhibiting the production of SAM and therefore disrupting downstream transmethylation reactions it was hypothesised that supplying cycloleucine-treated embryos with sufficient levels of SAM would overcome the inhibitory effect of cycloleucine and reduce the incidence of cranial NTDs observed with cycloleucine. Another prediction of the rescue experiment would be that if cycloleucine causes the female excess in cranial NTDs by exaggerating the natural difference in methyl group availability between male and female embryos and as a result putting female embryos at an even greater 'methylation deficit' then supplementing cycloleucine-treated embryos with exogenous SAM would result in a greater reduction in the rate of cranial NTDs in female embryos when compared to male embryos.

Results

CD1 embryos were treated with exogenous SAM for 24 h in whole embryo culture from E8.5 to E9.5. PBS served as vehicle control and embryos from within litters were allocate according to size/stage to ensure groups were balanced and to minimise effects of litter-to-litter variation. Embryos were obtained from 12 litters.

At the end of the culture period, embryos were harvested and assessed for cranial NTDs and scored for other developmental parameters including measures of embryo viability, embryonic growth, and development progression. The yolk sac was removed and used to determine embryonic sex by genomic PCR.

Supplementing embryos with exogenous SAM results in severe embryonic toxicity

Culture of embryos for 24 h with SAM resulted in dose-dependent toxicity. At doses up to 0.05 mM, exogenous SAM did not reveal any adverse effects as shown by the measures of viability, growth and developmental progression, compared with PBS-treated control embryos (0 mM; Table A1). By contrast, in the dose range 1-5 mM, exogenous SAM showed significantly reduced viability (yolk sac circulation), growth

(crown-rump length) and developmental progression (axial rotation and somite number) compared with PBS controls (Table A1).

SAM (mM)	No. of embryos	Yolk sac circulation	Crown-rump length (mm)	No. of embryos with failed axial rotation (%)	No. of somites	No of embryos with cranial NTDs (%)
0.00	16	3.00 ± 0.00	2.34 ± 0.28	0 (0)	19.7 ± 0.2	0 (0)
0.05	6	2.50 ± 0.50	2.16 ± 0.31	0 (0)	19.3 ± 0.3	0 (0)
1.00	8	1.88 ± 0.11**	1.69 ± 0.23*	1 (13)*	17.2 ± 0.4**	0 (0)
2.00	14	1.62 ± 0.21**	1.43 ± 0.54**	5 (36)**	15.8 ± 0.8***	0 (0)
5.00	5	-	-	-	-	-

Table A1. Growth and development of CD1 mouse embryos cultured and supplemented with exogenous SAM. The addition of exogenous SAM resulted in a dose-dependent increase in embryonic toxicity with embryos showing no signs of embryonic viability at doses of 1 mM and above. At 1 mM the crown-rump length and somite number are already significantly impaired when compared to PBS control embryos (0 mM). At doses of 2 mM and above, no embryos developed beyond the 16-somite stage, as needed to assess for cranial NTDs. There is a significant difference in all developmental parameters between embryos supplemented with exogenous SAM and PBS control embryos at doses of 1 and 2 mM. The parameters could not be scored for embryos at 5 mM owing to the severity of abnormality. Data for failed axial rotation and cranial NTDs are presented as the number of embryos with percentage values in parentheses. Values for yolk sac circulation, somite number and crown-rump length are given as mean ± SEM. ** represents a p-value less than 0.01, and *** represents a p-value is less than 0.001 (as tested by Student's t-test for somite number and Z-test for all other parameters).

Supplementing cycloleucine-treated CD1 embryos with exogenous SAM results in severe embryonic toxicity.

Culture of cycloleucine-treated embryos for 24 h supplemented with exogenous SAM resulted in an increasing toxicity. The addition of SAM at concentrations of 0.05-1 mM, showed significantly reduced viability (yolk sac circulation), growth (crown-rump length) and developmental progression (axial rotation and somite number) compared with PBS controls (Table A2). Comparison of the addition of exogenous SAM alone (Table A1) and together when embryos are also treated with cycloleucine (Table A2) resulted in a more severe embryotoxicity as shown by the comparison of 0.05 mM dose of SAM (Table A2 vs Table A1).

The critical issue in this experiment was whether the addition of exogenous SAM could overcome cranial NTDs causes. However, embryos that were treated with cycloleucine and supplemented with SAM at a dose previously found to not be embryotoxic (0.05 mM; Table A1) resulted in a severe toxicity when added in conjunction with cycloleucine (0.05 mM; Table A2). At no dose of co-treatment were embryos able to progress beyond the 16-somite stage, when normal cranial closure is complete, and so no assessment of whether the addition of SAM can overcome cycloleucine-induced cranial NTDs could be made.

Cycloleucine (mM)	SAM (mM)	No. of embryos	Yolk sac circulation	Crown-rump length (mm)	No. of embryos with failed axial rotation (%)	No. of somites	No of embryos with cranial NTDs (%)
0.00	0.00	12	3.00 ± 0.00	2.32 ± 0.24	0 (0)	19.2 ± 0.5	0 (0)
10.00	0.00	8	3.00 ± 0.00	2.18 ± 0.24	0 (0)	19.4 ± 0.3	4 (50)
10.00	0.05	10	1.20 ± 0.10***	1.31 ± 0.37***	2 (20)	14.6 ± 0.3***	-
10.00	1.00	10	0.50 ± 0.50***	1.02 ± 0.44***	6 (60)	13.3 ± 0.5***	-

Table A2. Growth and development of CD1 mouse embryos cultured with cycloleucine and supplemented with exogenous SAM. The addition of exogenous SAM to cycloleucine-treated embryos resulted in an increase in embryonic toxicity with embryos showing no signs of embryonic viability at doses of 1 mM and above. At 0.05 mM the crown-rump length and somite number are already significantly impaired when compared to PBS control embryos (0 mM). At doses of 0.05 mM SAM, no embryos developed beyond the 16-somite stage, as needed to assess for cranial NTDs. There is a significant difference in all developmental parameters between embryos supplemented with exogenous SAM and PBS control embryos at doses of 0.05 and 1 mM. Data for failed axial rotation and cranial NTDs are presented as the number of embryos with percentage values in parentheses. Values for yolk sac circulation, somite number and crown-rump length are given as mean ± SEM. ** represents a p-value less than 0.01, and *** represents a p-value is less than 0.001 (as tested by Student's t-test for somite number and Z-test for all other parameters)

SAM Rescue: Points of evaluation

The addition of exogenous SAM in our whole embryo culture system presented with a rather unexpected toxicity. However, why SAM appears to be having such a toxic effect, remains unknown. One possible explanation may be due to the experimental conditions in which whole embryo culture experiment is carried out. The ex vivo culture of embryos in our experimental system was carried out at 37°C for a period of 24 hours. According to manufacture guidelines it has been reported however that SAM is unstable with rising temperatures and humidity where a loss of 10% purity has been observed above room temperature per day, raising the possibility that temperature conditions may have also contributed to the breakdown of SAM in culture. The breakdown product of SAM, 5'-methylthio- adenosine, MTA, is a dead-end' sulphur-containing product that readily crosses the plasma membrane of mammalian cells via the nonspecific nucleoside transport system opening the possibility for cells to utilise MTA from degraded SAM. Once produced, MTA is recycled into methionine through a series of enzymatic reactions collectively known as the methionine salvage pathway. In this pathway, MTA's methylthio group and the carbon backbone of its ribose are retained and eventually transformed into methionine which upon the addition of ATP can regenerate SAM.

Possible reasons for the observed embryotoxicity of SAM:

1. MTA possesses inhibitory effects on histone methylation.

   Normal patterns of histone methylation are essential for normal embryonic development with H2K27me3 and H3K9me3 histone methylation dominating at E8.5. As a result, impaired histone methylation can have detrimental impacts on embryonic development and growth by perturbing normal gene expression such that it is possible that the toxic effects and embryonic lethality observed in SAM supplemented embryos is caused by the build-up of MTA.

2. MTA possesses inhibitory effects on the activity of SAH hydrolase.

SAH is a potent inhibitor of almost all methyltransferases given it can with high affinity, bind to the catalytic region of methyltransferase enzymes and therefore inhibit downstream transmethylation reactions. The breakdown of SAH is catalysed by the SAH hydrolase enzyme which favours the synthesis of SAH such that active removal of its breakdown products homocysteine and adenosine, are needed to prevent the build-up of SAH. As a result, any metabolite or process that has the potential to alter the equilibrium of the SAH-mediated reaction is likely to lead to catastrophic effects for the developing embryo. . As such, it is possible that the perturbed downstream methylation reactions caused by MTA-induced SAH build up is having a lethal effect of the developing embryo through inhibiting transmethylation reactions. The toxic effect of SAH can be seen in neuroblastoma cells in which when SAH hydrolase activity is inhibited these cells have an adaptive response to overcome the increased in SAH levels and its related toxicity by upregulating the synthesis of the MAT II enzyme. The increase in SAM synthesis effectively counterbalances the increase in SAH and permits cell survival.

3. MTA-mediated activation of the methionine salvage pathway, and the resultant increase in methionine availability.

Excess levels of methionine have been shown to impair methylation cycle activity and therefore impact methylation reactions (Dunlevy et al., 2006). The probable increase in methionine caused by MTA is likely to reduce the capacity of homocysteine remethylation as the product methionine would already be high within cells of the embryo. The resultant build-up of homocysteine is likely to impact the activity of SAH hydrolase and cause a concomitant increase in SAH and thus inhibition of methylation reactions as stated above. As a result, SAH induced toxicity in the embryo as observed in SAM supplemented embryos could be coming via two sources, either directly through the inhibition of SAH hydrolase MTA causes or indirectly by salvaging methionine and the resultant build of SAH due to reduced remethylation of homocysteine

4. Increased levels of homocysteine inducing a “methyl-trap” in the embryo whereby

1C units are directed for use in the methylation cycle at the expense of cytosolic 1C reactions.

The methionine/methylation and the cytosolic folate one carbon metabolism cycles are strongly intertwined with 1C flux between the two cycles being mediated by the MTHFR enzyme. MTHFR catalyses the conversion of 5,10-methyleneTHF to 5-methylTHF and therefore commits 1C units for use in methylation cycle at the expense of the folate 1C reactions in the cytoplasm. One regulator of MTHFR activity is the SAM/SAH ratio which when reduced can result in increased activity of MTHFR and therefore drive methylation reactions. The possible build of SAH in SAM treated embryos could suppress cytosolic folate one-carbon reactions such as thymidylate and purine synthesis and NADPH generation, metabolic processes essential for nucleotide biosynthesis and redox balance in cells which when disrupted may cause severe signs of toxicity and developmental arrest as normal cellular reactions needed for normal growth and development may be impaired and explain why embryos treated with SAM appeared brittle.

5. The chemical nature of SAM.

The positively charged sulfonium ion of SAM makes the three carbon atoms bonded to the sulphur atom prone to attack by nucleophile. As a result, the presence of any nucleophiles in the serum may have attacked SAM's sulfonium ion causing it to degrade. To prevent the decomposition and epimerisation of SAM it is therefore essential SAM is kept in an excess of large-size, non-nucleophilic counterions such as tosylate or sulfate which in this experiment SAM was not kept in. Moreover, the increased toxicity in cycloleucine-treated supplemented with SAM compared to embryos supplemented with SAM may be explained by the negatively charged amine group found in cycloleucine. The lone pair of electrons on the electronegative nitrogen atom may be causing cycloleucine to act as a nucleophile and thereby causing intramolecular attack on the electron deficient carbon atoms bonded to sulphur in SAM. As a result, it is likely that in the presence of cycloleucine SAM is being broken down to a greater extent and possibly at a much faster rate and hence why cycloleucine-treated embryos

supplemented with SAM showed greater signs of toxicity.

Due to these reasons and potential sources of toxicity, an alternative approach was used in our study which was to manipulate the endogenous levels of SAM in order to retain SAM in the methylation cycle at the expense of being used as a aminopropyl donor for polyamine synthesis by inhibiting the decarboxylation of SAM by co-treating cycloleucine-treated embryos with MGBG, a SAMDC inhibitor.

Additional experiments that could have been attempted to overcome SAM toxicity.

Differences in length of exposure to the breakdown products of SAM may result in differences in the toxicity levels observed. It would be predicted that embryos exposed to the toxic by-products of SAM for a shorter period would have better growth and developmental parameters compared to embryos exposed for a longer period. As such a 'serum change' method could have been whereby embryos are transferred periodically to fresh serum to overcome toxicity.

One other approach to overcome the toxicity of SAM in culture and to maximise the uptake and retention of SAM in the embryo could have been to inject SAM directly into the amniotic cavity. Amniotic cavity injections could overcome the disrupted transport across the yolk sac SAM may have given the exogenous supplementation of SAM greatly affected yolk sac circulation and integrity. Amniotic cavity injections therefore provide a possible direct route for SAM uptake in the embryo and likely without delay giving embryos the best chance to build up sufficient levels needed for a protective effect. Injections of SAM directly into the amniotic cavity could be repeated periodically to keep the levels of SAM high throughout the culture period. It is important to note however that injecting SAM directly into the amniotic cavity does have its limitations. Firstly, the insertion of the capillary needle through the yolk sac and the amnion could cause shock to the embryo and/or has the potential to damage the integrity of yolk sac and thereby disrupt the gas and nutrient exchange for the embryo, both of which could lead to embryonic death, Secondly, it would be difficult to assess the final concentration of SAM that reaches the embryo using the microinjection

technique. Usually, the injected liquid mixes with the amniotic fluid such that the final concentration of SAM taken up by embryos would be difficult to control. As a result, each embryo could potentially have a variable level of SAM that it has managed to take up, making it difficult to assess the concentration of SAM that may be needed to overcome the inhibitory effect of cycloleucine and also in interpretating results as perhaps differences in the embryos that still present with a cranial NTD and those that do not could be to the differences in the concentration of SAM that they have managed to build up intracellularly.

References

Adams RL, Fulton J, Kirk D. (1982). The effect of 5-azadeoxycytidine on cell growth and DNA methylation. Biochim Biophys Acta *697*:286–94.

Adzick, N.S., Sutton, L.N., Crombleholme, T.M., and Flake, A.W. (1998). Successful fetal surgery for spina bifida. Lancet *352*, 1675-1676.

Adzick, N.S., Thom, E.A., Spong, C.Y., Brock, J.W., 3rd, Burrows, P.K., Johnson, M.P., Howell, L.J., Farrell, J.A., Dabrowiak, M.E., Sutton, L.N., et al. (2011). A randomized trial of prenatal versus post-natal repair of myelomeningocele. N Engl J Med *364*, 993-1004.

Afman LA, Blom HJ,Drittij MJ. (2005). Inhibition of transmethylation disturbs neurulation in chick embryos. Brain Res Dev Brain Res 158: 59–65.

Alexandre, H. (1979). The utilization of an inhibitor of spermidine and spermine synthesis as a tool for the study of the determination of cavitation in the preimplantation mouse embryo. J. Embryol. exp. Morph. *53*, 145-162.

Amorim MR, Lima MA, Castilla EE, Orioli IM. (2007). Non-Latin European descent could be a requirement for association of NTDs and MTHFR variant 677C > T: a meta-analysis. Am J Med Genet A. *143A*:1726-32.

Armstrong JF, Kaufman MH, Harrison DJ. (1995). High-frequency de-velopmental abnormalities in p53-deficient mice. Curr Biol *5*:931–936.

Arnold A.P. (2020). Four core genotypes and XY* mouse models: Update on impact on SABV research. Neurosci. Biobehav. Rev., *119*; pp. 1-8

Ashe A, Morgan DK, Whitelaw NC, et al. (2008). A genome-wide screenfor modifiers of transgene variegation identifies genes with critical roles in development. Genome Biol *9*:R182

Bachrach U. (1973). Functions of Naturally Occurring Polyamines, Academic Press, New York. pp. 1-211

Barakat, T.S. (2010). X-changing information on X inactivation. Exp. Cell Res. *316*, 679–687

Barr, M., Bertram, E. (1949). A Morphological Distinction between Neurones of the Male and Female, and the Behaviour of the Nucleolar Satellite during Accelerated Nucleoprotein Synthesis. Nature *163*, 676–677.

Bedford, M.T. and Clarke, S.G. (2009). Protein arginine methylation in mammals: who, what, and why. Molecular cell, *33*(1), pp.1-13.

Berihu BA, Welderufael AL, Berhe Y, Magana T, Mulugeta A, et al. (2018). High burden of neural tube defects in Tigray, Northern Ethiopia: Hospital-based study. PLOS ONE *13*(11): e0206212

Berry, R. J., Li, Z., Erickson, J. D., Li, S., Moore, C. A., Wang, H., Mulinare, J., Zhao, P., Wong, L. Y., Gindler, J., Hong, S. X., & Correa, A. (1999). Prevention of neural-tube defects with folic acid in China. China-U.S. Collaborative Project for Neural Tube Defect Prevention. *The New England journal of medicine*, *341*(20), 1485–1490.

Biggar, K. K., & Li, S. S. (2015). Non-histone protein methylation as a regulator of cellular signalling and function. *Nature reviews.* Molecular cell biology, *16*(1), 5–17.

Blewitt ME, Gendrel AV, Pang Z. (2008). SmcHD1, containing a structural-maintenance-of-chromosomes hinge domain, has a critical role in X inactivation. Nat Genet *40*:663–669.

Blewitt ME, Vickaryous NK, Hemley SJ. (2005). An N-ethyl-N-nitro-sourea screen for genes involved in variegation in the mouse. ProcNatl Acad Sci USA *102*:7629–7634

Blom HJ, Shaw GM, den Heijer M, Finnell RH. (2006). Neural tube defects and folate: case far from closed. Nat Rev Neurosci. *7*(9):724-31.

Bond, A.M., Bhalala, O.G., and Kessler, J.A. (2012). The dynamic role of bone morphogenetic proteins in neural stem cell fate and maturation. Dev Neurobiol *72*, 1068-1084.

Borman GB, Smith AH, Howard JK. (1986). Risk factors in the prevalence of anencephalus and spina bifida in new zealand. Teratology. *33*:221–230.

Boyanapalli M, Lahoud OB, Messiaen L .(2006). Neurofibromin bindsto caveolin-1 and regulates ras, FAK, and Akt. Biochem Biophys ResCommun *340*:1200–1208.

Brockdorff N. (2011). Chromosome silencing mechanisms in X-chromosome inactivation: unknown unknowns. Development (Cambridge, England), *138*(23), 5057–5065.

Brook FA, Estibeiro JP, Copp AJ. (1994). Female predisposition to cra-nial neural tube defects is not because of a difference between the sexes in the rate of embryonic growth or development during neuru-lation. J Med Genet *31*:383–387

Broughan JM, Martin D, Higgins T, Swan G, Cullum A, Kurinczuk JJ, Draper ES, Luyt K, Wellesley DG, Stevens S, Tedstone A, Rankin J. (2023). Prevalence of neural tube defects in England prior to the mandatory fortification of non-wholemeal wheat flour with folic acid: a population-based cohort study. Arch Dis Child.

Brunskill, E.W., Potter, A.S., Distasio, A., Dexheimer, P., Plassard, A., Aronow, B.J., Potter, S.S. (2014). A gene expression atlas of early craniofacial development. Dev Biol *391*, 133-146.

Burren KA, Savery D, Massa V, Kok RM, Scott JM, Blom HJ, Copp AJ, Greene ND. (2008). Gene-environment interactions in the causation of neural tube defects: folate deficiency increases susceptibility conferred by loss of Pax3 function. Hum Mol Genet. *17*(23):3675-85.

Butler, M.B., Short, N.E., Maniou, E., Alexandre, P., Greene, N.D.E., Copp, A.J., Galea, G.L. (2019). Rho kinase-dependent apical constriction counteracts M-phase apical expansion to enable mouse neural tube closure. J Cell Sci *132*, jcs230300.

Cain, J. A., Montibus, B., & Oakey, R. J. (2022). Intragenic CpG Islands and Their Impact on Gene Regulation. Frontiers in cell and developmental biology, *10*, 832348.

Cain, J.A., Montibus, B., Oakey, R.J. (2022). Intragenic CpG Islands and Their Impact on Gene Regulation. Front Cell Dev Biol *10*, 832348.

Cantoni G. L. (1975). Biological methylation- selected aspects. *Annu. Rev. Biochem. 44*, 435–451.

Cao, R., Xie, J., & Zhang, L. (2022). Abnormal methylation caused by folic acid deficiency in neural tube defects. Open life sciences, *17*(1), 1679–1688.

Capel, B. and Batchvarov, J. (2008). Sex chromatin staining in amnion cells. CSH Protoc 2008, pdb prot. 5079.

Carballo, G.B., Honorato, J.R., de Lopes, G.P.F., and Spohr, T. (2018). A highlight on Sonic hedgehog pathway. Cell Commun Signal *16,* 11.

Carrette, L. L., Wang, C. Y., Wei, C., Press, W., Ma, W., Kelleher III, R. J., & Lee, J. T. (2018). A mixed modality approach towards Xi reactivation for Rett syndrome and other X-linked disorders. Proceedings of the National Academy of Sciences, *115*(4), E668-E675.

Carter CO. (1974). Clues to the aetiology of neural tube malformations. Dev Med Child Neurol *16*:3–15.

Carter M, Chen X, Slowinska B. (2005). Crooked tail (Cd) model ofhuman folate-responsive neural tube defects is mutated in Wnt co-receptor lipoprotein receptor-related protein 6. Proc Natl Acad Sci USA *102*:12843–12848

Carter, C. O. and Evans, K. (1973a). Spina bifida and anencephalus in Greater London. Journal of Medical Genetics, *10*, 209-234.

Carvajal-Gonzalez, J.M., Mulero-Navarro, S., and Mlodzik, M. (2016). Centriole positioning in epithelial cells and its intimate relationship with planar cell polarity. Bioessays *38*, 1234-1245.

Caudill, M. A., Wang, J. C., Melnyk, S., Pogribny, I. P., Jernigan, S., Collins, M. D., Santos-Guzman, J., Swendseid, M. E., Cogger, E. A., & James, S. J. (2001). Intracellular S-adenosylhomocysteine concentrations predict global DNA hypomethylation in tissues of methyl-deficient cystathionine beta-synthase heterozygous mice. The Journal of nutrition, *131*(11), 2811–2818.

Chatot, C. L., Klein, N. W., Clapper, M. L., Resor, S. R., Singer, W. D., Russman, B. S., Holmes, G. L., Mattson, R. H., & Cramer, J. A. (1984). Human serum teratogenicity studied by rat embryo culture: epilepsy, anticonvulsant drugs, and nutrition.Epilepsia, *25*(2), 205–216.

Chen X, Guo J, Lei Y. (2010). Global DNA hypomethylation is associated with NTD-affected pregnancy: a case-control study. Birth Defects Res A Clin Mol Teratol *88*:575–581.

Chen X, Watkins R, Delot E. (2008). Sex difference in neural tube defects in p53-null mice is caused by differences in the complement of X not Y genes. Dev Neurobiol *68*:265–273.

Chen Z, Zhang Y. (2020). Role of Mammalian DNA Methyltransferases in Development. Annu Rev Biochem. *89*:135-58.

Chureau, C. et al. (2011). Ftx is a non-coding RNA which affects Xist expression and chromatin structure within the X-inactivation center region. Hum. Mol. Genet. *20*, 705–718

Clarke S, Banfield K. (2001). S-Adenosylmethionine-dependent Methyltransferases. In: Carmel R, Jacobsen DW, editors. Homocysteine in Health and Disease. Cambridge, UK: Cambridge University Press;. p. 63-78.

Coelho CN, Klein NW. (1990). Methionine and neural tube closure in cultured rat embryos: morphological and biochemical analyses. Teratology. *42*(4):437-51.

Coelho CN, Weber JA, Klein NW, Daniels WG, Hoagland TA. (1989). Whole rat embryos require methionine for neural tube closure when cultured on cow serum. J Nutr. *119*(11):1716-25.

Colas, J.-F. and Schoenwolf, G.C. (2001). Towards a cellular and molecular understanding of neurulation. Dev. Dyn., *221*: 117-145

Constantinides, P. G., Taylor, 6. M. & Jones, P. A. (1978). Phenotypic conversion of cultured mouse embryo cells by aza pyrimidine nucleosides De&BioE. *66*, 57-71.

Copp AJ, Brook FA. (1989). Does lumbosacral spina bifida arise by failure of neural folding or by defective canalisation? J Med Genet. *26*:160–166.

Copp AJ, Clark M, Greene NDE. (2023). Morphological phenotyping after mouse whole embryo culture. Front Cell Dev Biol. *11*:1223849.

Copp, A.J. (2005). Neurulation in the cranial region – normal and abnormal. Journal of Anatomy, *207*: 623-635

Copp, A.J., and Greene, N.D. (2010). Genetics and development of neural tube defects. J Pathol *220*, 217-230.

Copp, A.J., and Greene, N.D. (2013). Neural tube defects--disorders of neurulation and related embryonic processes. Wiley Interdiscip Rev Dev Biol *2*, 213-227.

Copp, A.J., Greene, N.D., and Murdoch, J.N. (2003). The genetic basis of mammalian neurulation. Nat Rev Genet *4*, 784-793.

Copp, A.J., Stanier, P., and Greene, N.D. (2013). Neural tube defects: recent advances, unsolved questions, and controversies. Lancet Neurol *12*, 799- 810.

Cordaux, R., Batzer, M. (2009). The impact of retrotransposons on human genome evolution. Nat Rev Genet *10*, 691–703.

Cornett EM, Ferry L, Defossez PA, Rothbart SB. (2019). Lysine Methylation Regulators Moonlighting outside the Epigenome. Mol Cell. *75*(6):1092-1101.

Correa, A., Gilboa, S. M., Besser, L. M., Botto, L. D., Moore, C. A., Hobbs, C. A., Cleves, M. A., Riehle-Colarusso, T. J., Waller, D. K., & Reece, E. A. (2008). Diabetes mellitus and birth defects. American journal of obstetrics and gynaecology *199*(3), 237.e1–237.e2379.

Costanzi C, Pehrson JR. (1998). Histone macroH2A1 is concentrated in the inactive X chromosome of female mammals. Nature *393*:599–601

Costanzi, C. et al. (2000). Histone macroH2A1 is concentrated in the inactive X chromosome of female preimplantation mouse embryos. Development *127*, 2283–2289

Cowchock S, Ainbender E, Prescott G, Crandall B, Lau L, Heller R, Cederquist L. (1980). The recurrence risk for neural tube defects in the United States: A collaborative study. American Journal of Medical Genetics, *5*(3), 309–314.

Cox R, Prescott C, Irving CC. (1977). The effect of S-adenosylhomocysteine on DNA methylation in isolated rat liver nuclei. Biochim Biophys Acta. *474*(4):493-9.

Csankovszki, G., Nagy, A., & Jaenisch, R. (2001). Synergism of Xist RNA, DNA methylation, and histone hypoacetylation in maintaining X chromosome inactivation. The Journal of cell biology, *153*(4), 773–784.

Culshaw, L. H., Savery, D., Greene, N. D. E., & Copp, A. J. (2019). Mouse whole embryo culture: Evaluating the requirement for rat serum as culture medium. Birth defects research, *111*(16), 1165–1177.

Czabotar, P.E., Lessene, G., Strasser, A., and Adams, J.M. (2014). Control of apoptosis by the BCL-2 protein family: implications for physiology and therapy. Nat. Rev. Mol. Cell Biol. *15*, 49–63.

Czeizel A, & Metneki J. (1984). Recurrence risk after neural tube defects in a genetic counselling clinic. Journal of Medical Genetics, *21*(6), 413–416

Czeizel, A. E., Dudás, I., Paput, L., & Bánhidy, F. (2011). Prevention of neural-tube defects with periconceptional folic acid, methylfolate, or multivitamins?. Annals of nutrition & metabolism, *58*(4), 263–271.

Czeizel, A.E., and Dudas, I. (1992). Prevention of the first occurrence of neural-tube defects by periconceptional vitamin supplementation. N Engl J Med *327*, 1832-1835.

D'Souza, S.W., Copp, A.J., Greene, N.D. and Glazier, J.D. (2021). Maternal inositol status and neural tube defects: a role for the human yolk sac in embryonic inositol delivery?. Advances in Nutrition, *12*(1), pp.212-222.

Davidson, L. A., & Keller, R. E. (1999). Neural tube closure in Xenopus laevis involves medial migration, directed protrusive activity, cell intercalation and convergent extension. Development (Cambridge, England), *126*(20), 4547–4556.

De Cabo SF, Santos J, Fernandez-Piqueras J. (1995). Molecular and cytological evidence of *S*-adenosyl-*L*-homocysteine as an innocuous undermethylating agent in vivo. Cytogenet Cell Genet*. 71*:187–192.

de Napoles, M. et al. (2004). Polycomb group proteins Ring1A/B link ubiquitylation of histone H2A to heritable gene silencing and X inactivation. Dev. Cell *7*, 663–676

Deaton, A. M., & Bird, A. (2011). CpG islands and the regulation of transcription. Genes & development, *25*(10), 1010–1022.

Delbridge, A.R., Pang, S.H., Vandenberg, C.J., Grabow, S., Aubrey, B.J., Tai, L., Herold, M.J., and Strasser, A. (2016). RAG-induced DNA lesions activate proapoptotic BIM to suppress lymphomagenesis in p53-deficient mice. J. Exp. Med. *213*, 2039–2048.

Delbridge, Alex R.D. (2019). Loss of *p53* Causes Stochastic Aberrant X-Chromosome Inactivation and Female-Specific Neural Tube Defects. Cell Reports, Volume 27, Issue 2, 442 - 454.e5

Druker R, Whitelaw E. (2004). Retrotransposon-derived elements in the mammalian genome: a potential source of disease. J Inherit Metab Dis. *27*(3):319-30.

Dunlevy Louisa P.E., Burren Katie A., Chitty Lyn S., Copp Andrew J. and Greene Nicholas D.E. (2006). Excess methionine suppresses the methylation cycle and inhibits neural tube closure in mouse embryos, FEBS Letters, 580

Dunlevy, L.P.E., Burren, K.A., Mills, K., Chitty, L.S., Copp, A.J. and Greene, N.D.E. (2006). Integrity of the methylation cycle is essential for mammalian neural tube closure. Birth Defects Research Part A: Clinical and Molecular Teratology, *76*:544-552

Dyer, K.A., Riley, D. and Gartler, S.M. (1985). Analysis of inactive X chromosome structure by in situ nick translation. Chromosoma *92*, 209-213.

Eichholzer M, Tönz O, Zimmermann R. (2006). Folic acid: a public-health challenge. Lancet. *367*(9519):1352-61.

Elwood JM, Elwood JH. (1980). *Epidemiology of anencephalus and spina bifida.* Oxford University Press; Oxford.

Embury S, Seller MJ, Adinolfi M, et al. (1979). Neural tube defects in curly-tail mice. I. Incidence, expression and similarity to the human condition Proc Roy Soc Lond Ser B: Biol Sci *206*:85–94

Ericson, L. E. Betaine-homocysteine-methyl transferases. (1960). The methyl donor specificity of the transferase isolated from pig liver. Acta Chem. Scand. *14* 2127–2134

Eskes TK. (1998). Neural tube defects, vitamins and homocysteine. Eur J Pediatr. *157* Suppl 2:S139-41.

Fallah, M.S., Szarics, D., Robson, C.M., Eubanks, J.H. (2020). Impaired Regulation of Histone Methylation and Acetylation Underlies Specific Neurodevelopmental Disorders. Front Genet 11, 613098.

Fillingame R.H, Jorstad C.M, Morris D.R. (1975) Increased cellular levels of spermidine or spermine are required for optimal DNA synthesis in lymphocytes activated by concanavalin A. Proc. natn. Acad. Sci. U.S.A, *72*, p. 4042

Finkelstein J. D. (1990). Methionine metabolism in mammals. The Journal of nutritional biochemistry, *1*(5), 228–237.

Finkelstein J.D, Kyle W.E, Harris B.J. Methionine metabolism in mammals. (1971). Regulation of homocysteine methyltransferases in rat tissue. Arch Biochem Biophys, *146*, pp. 84-92

Finkelstein, J.D. (1998a). The metabolism of homocysteine: pathways and regulation. Eur. J. Pediatr. *157* Suppl. 2, S40-S44.

Fisher, M.C., Zeisel, S.H., Mar, M. and Sadler, T.W. (2002). Perturbations in choline metabolism cause neural tube defects in mouse embryos *in vitro*. The FASEB Journal, *16*: 619-621.

Fisher, M.C., Zeisel, S.H., Mar, M.H. and Sadler, T.W. (2001). Inhibitors of choline uptake and metabolism cause developmental abnormalities in neurulating mouse embryos. Teratology, *64*: 114-122.

Fozard, J.R., Part, M-L., Prakash, N.J., Grove, J., Schechter, P.J., Sjoerdsma, A. & Koch-Weser, J. (1980). L-Ornithine decarboxylase: an essential role in early mammalian embryogenesis. Science, N. Y. *208*, 505-508

Friso S, Choi SW. Gene-nutrient interactions and DNA methylation. J Nutr. (2002). *132*(8 Suppl):2382S-2387S.

Fujinaga M and Baden JM. (1994). Methionine prevents nitrous oxide-induced teratogenicity in rat embryos grown in culture Anesthesiology *81*:184—189

Galea, G.L., Cho, Y.J., Galea, G., Mole, M.A., Rolo, A., Savery, D., Moulding, D., Culshaw, L.H., Nikolopoulou, E., Greene, N.D.E., et al. (2017). Biomechanical coupling facilitates spinal neural tube closure in mouse embryos. Proc Natl Acad Sci USA *114*, E5177-E5186.

Gardiner-Garden, M., & Frommer, M. (1987). CpG islands in vertebrate genomes. Journal of molecular biology, *196*(2), 261–282.

Gedefaw, A., Teklu, S., & Tadesse, B. T. (2018). Magnitude of Neural Tube Defects and Associated Risk Factors at Three Teaching Hospitals in Addis Ababa, Ethiopia. BioMed research international, 2018, 4829023.

Gendrel, A. V., Apedaile, A., Coker, H., Termanis, A., Zvetkova, I., Godwin, J., Tang, Y. A., Huntley, D., Montana, G., Taylor, S., Giannoulatou, E., Heard, E., Stancheva, I., & Brockdorff, N. (2012). Smchd1-dependent and -independent pathways determine developmental dynamics of CpG island methylation on the inactive X chromosome. Developmental cell, *23*(2), 265–279.

Golden, L. C., Itoh, Y., Itoh, N., Iyengar, S., Coit, P., Salama, Y., Arnold, A. P., Sawalha, A. H., & Voskuhl, R. R. (2019). Parent-of-origin differences in DNA methylation of X chromosome genes in T lymphocytes. Proceedings of the National Academy of Sciences of the United States of America, *116*(52), 26779–26787.

Golding J. (1982). Evidence for an environmental aetiology for anencephalus. In: Persaud TVN, ed. Advances in the study of birth defects. Vol 7. New York: Alan R Liss,19-45.

Goto, Y. (2002) Differential patterns of histone methylation and acetylation distinguish active and repressed alleles at X-linked genes. Cytogenet. Genome Res. *99*, 66–74

Grant M, Zuccotti M, Monk M. (1992). Methylation of CpG sites of two X-linked genes coincides with X-inactivation in the female mouse embryo but not in the germ line. Nat Genet *2*:161–166

Greene NDE, Leung KY, Gay V, Burren KA, Mills K, Chitty LS, Copp AJ. (2016). Inositol for prevention of neural tube defects: a pilot randomised controlled trial. British Journal of Nutrition. *115*:974-83.

Greene, N. D., & Copp, A. J. (1997). Inositol prevents folate-resistant neural tube defects in the mouse. Nature medicine, *3*(1), 60–66

Greene, N.D., Stanier, P., and Copp, A.J. (2009). Genetics of human neural tube defects. Hum Mol Genet *18*, R113-129.

Grillo MA, Colombatto S. (2005). S-adenosylmethionine and protein methylation. Amino Acids. *4*:357-62.

Gurniak, C. B., Perlas, E., & Witke, W. (2005). The actin depolymerizing factor n-cofilin is essential for neural tube morphogenesis and neural crest cell migration. Developmental biology, *278*(1), 231–241.

Halloran KM, Stenhouse C, Wu G, Bazer FW. (2021). Arginine, Agmatine, and Polyamines: Key Regulators of Conceptus Development in Mammals. Adv Exp Med Biol. *1332*:85-105.

Hardy M, Harris I, Perry SV, Stone D. (1970). Epsilon-N-monomethyl-lysine and trimethyl-lysine in myosin. Biochem J *117*: 44P–45P

Harper, M.I. et al. (1982). Preferential paternal X-inactivation in extra-embryonic tissues of early mouse embryos. J. Embryol. Exp. Morphol. *67*, 127–135

Harris, M.J., and Juriloff, D.M. (2007). Mouse mutants with neural tube closure defects and their role in understanding human neural tube defects. Birth Defects Res A Clin Mol Teratol. *79*, 187-210.

Harris, M.J., and Juriloff, D.M. (2010). An update to the list of mouse mutants with neural tube closure defects and advances toward a complete genetic perspective of neural tube closure. Birth Defects Res A Clin Mol Teratol *88*, 653-669.

Hartwig JH, Thelen M, Rosen A. (1992). MARCKS is an actin filament crosslinking protein regulated by protein kinase C and calcium-calmodulin. Nature *356*:618–622

Hartz CS, Schalinske KL. (2006). Phosphatidylethanolamine N-methyltransferase and regulation of homocysteine. Nutr Rev. *64*(10 Pt 1):465-7.

Hasenpusch-Theil, K., Magnani, D., Amaniti, E. M., Han, L., Armstrong, D., & Theil, T. (2012). Transcriptional analysis of Gli3 mutants identifies Wnt target genes in the developing hippocampus. Cerebral cortex (New York, N.Y. : 1991), *22*(12), 2878–2893.

Heard E, Clerc P, Avner P. (1997). X-Chromosome inactivation in mammals. Annu Rev Genet 31: 571–610

Heard, E. (2001). Methylation of histone H3 at Lys-9 is an early mark on the X chromosome during X inactivation. Cell *107*, 727–738

Heby O, Marton LJ, Wilson CB, Gray JW. (1977). Effect of methylglyoxal-bis (guanylhydrazone), an inhibitor of spermidine and spermine synthesis, on cell cycle traverse. Eur J Cancer (*9*):1009-17.

Heby O, Russell D.H. (1973). Changes in polyamine metabolism in tumor cells and host tissues during tumor growth and after treatment with various anticancer agents. Polyamines in Normal Neoplastic Growth, Raven Press, New York, pp. 221-237

Heby O, Sarna G.P, Marton L.J. Omine M, Perry S, Russell D. H. (1973). Polyamine content of AKR leukemic cells in relation of the cell cycle. Cancer Res., *33*, pp. 2959-2964

Hellman A, Chess A. (2007). Gene body-specific methylation on the active X chromosome. Science. *315*:1141-3.

Holmberg, J., Clarke, D.L., and Frisen, J. (2000). Regulation of repulsion versus adhesion by different splice forms of an Eph receptor. Nature *408*, 203-206.

Hölttä E, Sinervirta R, Jänne J. (1973). Synthesis and accumulation of polyamines in rat liver regenerating after treatment with carbon tetrachloride. Biochem. Biophys. Res. Commun. *54*, pp. 350-357

Honarpour, N., Gilbert, S.L., Lahn, B.T., Wang, X., and Herz, J. (2001). Apaf1 deficiency and neural tube closure defects are found in fog mice. Proc Natl Acad Sci USA. *98*, 9683-9687.

Hu M, Sun XJ, Zhang YL, Kuang Y, Hu CQ, Wu WL, Shen SH, Du TT, Li H, He F, Xiao HS, Wang ZG, Liu TX, Lu H, Huang QH, Chen SJ, Chen Z. (2010). Histone H3 lysine 36 methyltransferase Hypb/Setd2 is required for embryonic vascular remodeling. Proc Natl Acad Sci USA. *107*(7):2956-61.

Hu N, Strobl-Mazzulla P, Sauka-Spengler T, Bronner ME. (2012). DNA methyltransferase3A as a molecular switch mediating the neural tube-to-neural crest fate transition. Genes Dev. *26(*21):2380-5.

Hu, N., Strobl-Mazzulla, P.H., Simoes-Costa, M., Sanchez-Vasquez, E., Bronner, M.E. (2014). DNA methyltransferase 3B regulates duration of neural crest production via repression of Sox10. Proc Natl Acad Sci USA. *111*, 17911-17916.

Huang, Y., Lin, S., Jin, L., Wang, L., & Ren, A. (2019). Decreased global DNA hydroxymethylation in neural tube defects: Association with polycyclic aromatic hydrocarbons. Epigenetics, *14*(10), 1019–1029.

Huynh, K.D. and Lee, J.T. (2003). Inheritance of a pre-inactivated paternal X chromosome in early mouse embryos. Nature *426*, 857–862

Isono K, Nemoto K, Li Y. (2006). Overlapping roles for homeodomain-interacting protein kinases Hipk1 and Hipk2 in the mediation of cell growth in response to morphogenetic and genotoxic signals. Mol Cell Biol *26*:2758–2771

Jabbour E, Issa JP, Garcia-Manero G, Kantarjian H. (2008). Evolution of decitabine development: accomplishments, ongoing investigations, and future strategies. Cancer. *112*(11):2341-51

Jacques-Fricke BT, Roffers-Agarwal J, Hussein AO, Yoder KJ, Gearhart MD, Gammill LS. (2021). Profiling NSD3-dependent neural crest gene expression reveals known and novel candidate regulatory factors. Dev Biol. *475*:118-30.

Jacques-Fricke, B.T., Roffers-Agarwal, J., Gammill, L.S. (2012). DNA methyltransferase 3b is dispensable for mouse neural crest development. PLoS One 7, e47794.

Janerich, D. T., & Piper, J. (1978). Shifting genetic patterns in anencephaly and spina bifida. *Journal of medical genetics*, *15*(2), 101–105.

Jin B, Robertson KD. (2013). DNA methyltransferases, DNA damage repair, and cancer. Adv Exp Med Biol. *754*:3-29.

Johnson P, Harris CI, Perry SV. (1967). 3-methylhistidine in actin and other muscle proteins. Biochemical Journal. *105*, 361–370.

Johnson, C. Y., Honein, M. A., Dana Flanders, W., Howards, P. P., Oakley, G. P., Jr, & Rasmussen, S. A. (2012). Pregnancy termination following prenatal diagnosis of anencephaly or spina bifida: a systematic review of the literature. Birth defects research. Part A, Clinical and molecular teratology, *94*(11), 857–863.

Jones PA, Taylor SM, Mohandas T and Shapiro LJ. (1982). Cell cycle-specific reactivation of an inactive X-chromosome locus by 5-azadeoxycytidine. Proc Natl Acad Sci USA, *79*(4):1215–1219.

Jones PA, Taylor SM. (1980). Cellular differentiation, cytidine analogs and DNA methylation. Cell. *20*(1):85-93.

Juriloff DM, Harris MJ. (2000). Mouse models for neural tube closure defects. Hum Mol Genet. *9*(6):993-1000.

Juriloff, D.M. and Harris, M.J. (2012). Hypothesis: The female excess in cranial neural tube defects reflects an epigenetic drag of the inactivating X chromosome on the molecular mechanisms of neural fold elevation. Birth Defects Research Part A: Clinical and Molecular Teratology, *94*: 849-855.

Juriloff, D.M., and Harris, M.J. (2018). Insights into the Etiology of Mammalian Neural Tube Closure Defects from Developmental, Genetic and Evolutionary Studies. J Dev Biol 6.

Kaniskan, H.U., Martini, M.L., Jin, J. (2018). Inhibitors of Protein Methyltransferases and Demethylases. Chem Rev *118*, 989-1068.

Kanno, T., Bucher, E., Daxinger, L., Huettel, B., Böhmdorfer, G., Gregor. Matzke, A. J. (2008). A structural-maintenance-of-chromosomes hinge domain–containingprotein is required for RNA-directed DNA methylation. Nature genetics, *40*(5), 670- 675.

Karfunkel P. (1974). The mechanisms of neural tube formation. International review of cytology, *38*(0), 245–271.

Kaslow, D.C. and Migeon, B.R. (1987). DNA methylation stabilizes X chromosome inactivation in eutherians but not in marsupials: evidence for multistep maintenance of mammalian X dosage compensation. Proc. Natl. Acad. Sci. U.S.A. *84*, 6210–6214.

Keller R. Shaping the vertebrate body plan by polarized embryonic cell movements. (2002). Science *298*:1950-4.

Kim, T.H., Goodman, J., Anderson, K.V., and Niswander, L. (2007). Phactr4 regulates neural tube and optic fissure closure by controlling PP1-, Rb-, and E2F1-regulated cell-cycle progression. Dev Cell *13*, 87-102.

Kinder, S.J., Tsang, T.E., Quinlan, G.A., Hadjantonakis, A.K., Nagy, A., and Tam, P.P. (1999). The orderly allocation of mesodermal cells to the extraembryonic structures and the anteroposterior axis during gastrulation of the mouse embryo. Development *126*, 4691-4701.

Kirke PN, Molloy AM, Daly LE, Burke H, Weir DG, Scott JM. (1993). Maternal plasma folate and vitamin B12 are independent risk factors for neural tube defects. Q J Med. *86*(11):703-8.

Kulesa, P.M., Bailey, C.M., Kasemeier-Kulesa, J.C., and McLennan, R. (2010). Cranial neural crest migration: new rules for an old road. Dev Biol *344*, 543-554.

Kutzbach C, Stokstad EL. Mammalian methylenetetrahydrofolate reductase. (1971). Partial purification, properties, and inhibition by S-adenosylmethionine. Biochim Biophys Acta. *250*(3):459-77.

Kwiatkowski, S., Seliga, A. K., Vertommen, D., Terreri, M., Ishikawa, T., Grabowska, I., Tiebe, M., Teleman, A. A., Jagielski, A. K., Veiga-da-Cunha, M., & Drozak, J. (2018). SETD3 protein is the actin-specific histidine *N*-methyltransferase. eLife, *7*, e37921

Larsen F, Gundersen G, Lopez R, Prydz H. (1992). CpG islands as gene markers in the human genome Genomics, *13*; pp. 1095-1107

Latta, E. J., & Golding, J. P. (2012). Regulation of PP2A activity by Mid1 controls cranial neural crest speed and gangliogenesis. Mechanisms of development, *128*(11-12), 560-576.

Lee J. T. (2011). Gracefully ageing at 50, X-chromosome inactivation becomes a paradigm for RNA and chromatin control. Nature reviews. Molecular cell biology, *12*(12), 815–826.

Lee TT, Karon MR. Inhibition of protein synthesis in 5-azacytidine-treated HeLa cells. (1976). Biochem Pharmacol.*25*(15):1737–42

Lee, H. Y., Kosciuk, M. C., Nagele, R. G. and Roisen, F. J. (1983). Studies on the mechanisms of neurulation in the chick: possible involvement of myosin in elevation of neural folds. *J. Exp. Zool. 225*, 449-457.

Li L.H, Olin E.J, Buskirk H.H, Reineke L.M. (1970). Cytotoxicity and Mode of Action of 5-Azacytidine on L1210 Leukemia[1]. *Cancer Res*. *30* (11): 2760–2769.

Li, E., Bestor, T.H., Jaenisch, R. (1992). Targeted mutation of the DNA methyltransferase gene results in embryonic lethality. Cell *69*, 915-926.

Liu J, Li Z, Ye R, Liu J, Ren A. (2018). Periconceptional folic acid supplementation and sex difference in prevention of neural tube defects and their subtypes in China: results from a large prospective cohort study. Nutr J. *17*(1):115.

Lloyd, J.B., Freeman, S.J. and Beck, F. (1985). Embryonic protein nutrition and teratogenesis. Biochem. Soc. Trans *13*, 82-83.

Lock, L. F., Takagi, N., & Martin, G. R. (1987). Methylation of the Hprt gene on the inactive X occurs after chromosome inactivation. *Cell*, *48*(1), 39-46.

Loenen W.A.M. *S*-Adenosylmethionine: jack of all trades and master of everything? (2006). Biochem Soc Trans 1. *34* (2): 330–333.

Lombardini JB, Burch MK, Talalay P. (1971). An enzymatic derivative double isotope assay for L -methionine. J Biol Chem. *246*(14):4465-71.

Lombardini, J.B., Talalay, P. (1970). Formation, functions and regulatory importance of S-adenosyl-L-methionine. Adv Enzyme Regul. *9*, 349-384

Löwkvist, Heby, O. & Emanuelsson. (1980). Essential role of polyamines in early chick embryo development. J. Embryol. exp. Morph. *60*, 83-92.

Lu LJW, Randerath K. (1980). Mechanism of 5-azacytidine-induced transfer RNA cytosine-5-methyltransferase deficiency. Cancer Res. *40*(8):2701–5

Lyon M. F. (1999). X-chromosome inactivation. Current biology *: CB*, *9*(7), R235–R237.

Macdonald KB, Juriloff DM, Harris MJ. (1989). Developmental study of neural tube closure in a mouse stock with a high incidence of exencephaly. Teratology *39*:195–213.

Maherali N, Sridharan R, Xie W, Utikal J, Eminli S, Arnold K, Stadtfeld M, Yachechko R, Tchieu J, Jaenisch R, Plath K, Hochedlinger K. (2007). Directly reprogrammed fibroblasts show global epigenetic remodeling and widespread tissue contribution. Cell Stem Cell. *1*:55–70

Mak, W. et al. (2004). Reactivation of the paternal X chromosome in early mouse embryos. Science *303*, 666–669

Mandal S, Mandal A, Johansson HE, Orjalo AV, Park MH. (2013). Depletion of cellular polyamines, spermidine and spermine, causes a total arrest in translation and growth in mammalian cells. Proc Natl Acad Sci USA. *110*(6):2169-74.

Maniou, E., Staddon, M.F., Marshall, A.R., Greene, N.D.E., Copp, A.J., Banerjee, S., and Galea, G.L. (2021). Hindbrain neuropore tissue geometry determines asymmetric cell-mediated closure dynamics in mouse embryos. Proc Natl Acad Sci USA 118.

Marahrens, Y., Panning, B., Dausman, J., Strauss, W., & Jaenisch, R. (1997). Xist-deficient mice are defective in dosage compensation but not spermatogenesis. Genes & development, *11*(2), 156–166.

Martin C, Zhang Y. (2005). The diverse functions of histone lysine methylation. Nat Rev Mol Cell Biol. *11*:838-49.

Massa, V., Savery, D., Ybot-Gonzalez, P., Ferraro, E., Rongvaux, A., Cecconi, F., Flavell, R., Greene, N.D., and Copp, A.J. (2009). Apoptosis is not required for mammalian neural tube closure. Proc Natl Acad Sci USA *106*, 8233-8238.

Massarwa, R., and Niswander, L. (2013). In toto live imaging of mouse morphogenesis and new insights into neural tube closure. Development *140*, 226-236.

Matsuda M and Keino H. (1994). An Open Cephalic Neural Tube Reproducibly Induced by Cytochalasin D in Rat Embryos in vitro. Zoological Science *11*: 547-553

Matsuda M, Yasutomi M. (1992). Inhibition of cephalic neural tube closure by 5-azacytidine in neurulating rat embryos in vitro. Anat. Embryol*. 185*:217–23.

Matsuda M. (1990). Comparison of the incidence of 5-azacytidine-induced exencephaly between MT/HokIdr and Slc:ICR mice. Teratology. *41*:147-54.

Mazzio, E. A., & Soliman, K. F. (2012). Basic concepts of epigenetics: impact of environmental signals on gene expression. Epigenetics, *7*(2), 119–130.

McLaughlin, M.E., Kruger, G.M., Slocum, K.L., Crowley, D., Michaud, N.A., Huang, J., Magendantz, M., and Jacks, T. (2007). The Nf2 tumor suppressor regulates cell-cell adhesion during tissue fusion. Proc Natl Acad Sci USA *104*, 3261-3266.

Mietton, F. et al. (2009). Weak but uniform enrichment of the histone variant macroH2A1 along the inactive X chromosome. Mol. Cell. Biol. *29*, 150–156

Minkovsky, A., Sahakyan, A., Bonora, G., Damoiseaux, R., Dimitrova, E., Rubbi, L., Pellegrini, M., Radu, C. G., & Plath, K. (2015). A high-throughput screen of inactive X chromosome reactivation identifies the enhancement of DNA demethylation by 5-aza-2'-dC upon inhibition of ribonucleotide reductase. Epigenetics & chromatin, *8*, 42.

Missmer, S. A., Suarez, L., Felkner, M., Wang, E., Merrill, A. H., Jr, Rothman, K. J., & Hendricks, K. A. (2006). Exposure to fumonisins and the occurrence of neural tube defects along the Texas-Mexico border. Environmental health perspectives, *114*(2), 237–241.

Moephuli, S.R., Klein, N.W., Baldwin, M.T., Krider, H.M. (1997). Effects of methionine on the cytoplasmic distribution of actin and tubulin during neural tube closure in rat embryos. Proc. Natl. Acad. Sci. USA *94*, 543-548.

Momparler RL, Momparler LF, Samson J. (1984). Comparison of the antileukemic activity of 5-aza-2'-deoxycytidine, 1-ß-D-arabinofuranosyl-cytosine and 5- azacytidine against L1210 leukemia. Leukemia Res. *8*:1043–9.

Monkhorst, K. et al. (2008). X inactivation counting and choice is a stochastic process: evidence for involvement of an X-linked activator. Cell *132*, 410–421

Moretti, M. E., Bar-Oz, B., Fried, S., & Koren, G. (2005). Maternal hyperthermia and the risk for neural tube defects in offspring: systematic review and meta- analysis. Epidemiology (Cambridge, Mass.), *16*(2), 216–219.

Morris-Wiman, J., and Brinkley, L.L. (1990). Changes in mesenchymal cell and hyaluronate distribution correlate with in vivo elevation of the mouse mesencephalic neural folds. Anat Rec *226*, 383-395.

Morriss-Kay and Tan, (1987). Mapping cranial neural crest cell migration pathways in mammalian embryos. Trends Genet., 3, pp. 257-261

Morriss-Kay GM. (1981). Growth and development of pattern in the cranial neural epithelium of rat embryos during neurulation. J Embryol Exp Morphol. *65* (Suppl.):225-41.

Morriss-Kay, G., and Tuckett, F. (1985). The role of microfilaments in cranial neurulation in rat embryos: effects of short-term exposure to cytochalasin D. J Embryol Exp Morphol *88*, 333-348.

Morriss-Kay, G., Tuckett, F. (1991). Early events in mammalian craniofacial morphogenesis. J. Craniofac. Genet. Dev. Biol *11*, 181-191.

Morriss-Kay, G.M., Tuckett, F. (1989). Immunohistochemical localisation of chondroitin sulphate proteoglycans and the effects of chondroitinase ABC in 9- to 11- day rat embryos. Development *106*, 787-798.

MRC Vitamin Study Research Group. (1991). Prevention of neural tube defects: Results of the Medical Research Council Vitamin Study. MRC Vitamin Study Research Group. Lancet *338*:131–137

Mukhopadhyay, P., Seelan, R.S., Rezzoug, F., Warner, D.R., Smolenkova, I.A., Brock, G., Pisano, M.M., Greene, R.M., (2017). Determinants of orofacial clefting I: Effects of

5-Aza-2'-deoxycytidine on cellular processes and gene expression during development of the first branchial arch. Reprod Toxicol *67*, 85-99.

Murdoch, J.N., and Copp, A.J. (2010). The relationship between sonic Hedgehog signaling, cilia, and neural tube defects. Birth Defects Res A Clin Mol Teratol *88*, 633-652

Naggan, L. and MacMahon, B. (1967). Ethnic differences in the prevalence of anencephaly and spina bifida in Boston, Massachusetts. New England Journal of Medicine, *277*, 1119-1123.

Nakatsu, T., Uwabe, C., and Shiota, K. (2000). Neural tube closure in humans initiates at multiple sites: evidence from human embryos and implications for the pathogenesis of neural tube defects. Anat Embryol (Berl) *201*, 455-466.

Navarro-Cobos, M. J., Balaton, B. P., & Brown, C. J. (2020). Genes that escape from X-chromosome inactivation: Potential contributors to Klinefelter syndrome. American journal of medical genetics. Part C, Seminars in medical genetics, *184*(2), 226–238.
NEW, D. A. (1978). Whole-embryo culture and the study of mammalian embryos during organogenesis. Biol Rev Camb Philos Soc, *53*, 81-122.

NEW, D.A.T. (1978). Whole-Embryo Culture And The Study Of Mammalian Embryos During Organogenesis. Biological Reviews, *53*: 81-122

Newell-Price J, Clark A.J.L ,King P. DNA methylation and silencing of gene expression. (2000). Trends Endocrinol. Metab., *11* (4) pp. 142-148

Nichols, D.H. (1981). Neural crest formation in the head of the mouse embryo as observed using a new histological technique. J. Embryol. Exp. Morphol. *64*, 105-120.

Nikolopoulou, E., Galea, G.L., Rolo, A., Greene, N.D., and Copp, A.J. (2017). Neural tube closure: cellular, molecular and biomechanical mechanisms. Development *144*, 552-566.

Nikolopoulou, E., Hirst, C.S., Galea, G., Venturini, C., Moulding, D., Marshall, A.R., Rolo, A., De Castro, S.C.P., Copp, A.J., and Greene, N.D.E. (2019). Spinal neural tube closure depends on regulation of surface ectoderm identity and biomechanics by Grhl2. Nat Commun *10*, 2487.

Nishimura K., Nakatsu F., Kashiwagi K., Ohno H., Saito T., Igarashi K. (2002). Essential role of S-adenosylmethionine decarboxylase in mouse embryonic development. *Genes Cells. 7*:41–47

O'Carroll D, Erhardt S, Pagani M, Barton SC, Surani MA, Jenuwein T. (2001). The polycomb-group gene Ezh2 is required for early mouse development. Mol Cell Biol. *21*(13):4330-6

O'Rahilly, R., and Muller, F. (2002). The two sites of fusion of the neural folds and the two neuropores in the human embryo. Teratology *65*, 162-170

O'Rahilly, R., Muller, F. (2007). The development of the neural crest in the human. J Anat *211*, 335-351.

O'Shea, K. S., & Kaufman, M. H. (1980). Neural tube closure defects following in vitro exposure of mouse embryos to xylocaine. The Journal of experimental zoology, *214*(2), 235–238.

O'Connor, L., Strasser, A., O'Reilly, L.A., Hausmann, G., Adams, J.M., Cory, S., and Huang, D.C.S. (1998). Bim: a novel member of the Bcl-2 family that promotes apoptosis. EMBO J. *17*, 384–395.

O'Neill, L.P. (2008). Differential loss of histone H3 isoforms mono-, di- and tri-methylated at lysine 4 during X-inactivation in female embryonic stem cells. Biol. Chem. *389*, 365–370

Obeid R, Holzgreve W, Pietrzik K. (2013). Is 5-methyltetrahydrofolate an alternative to folic acid for the prevention of neural tube defects? J Perinat Med. *41*(5):469-83.

Okamoto I, Otte AP, Allis CD, Reinberg D, Heard E. (2004). Epigenetic dynamics of imprinted X inactivation during early mouse development. Science. *303*:644–649.

Okano M, Bell DW, Haber DA, Li E. (1999). DNA methyltransferases Dnmt3a and Dnmt3b are essential for de novo methylation and mammalian development. Cell. *99*(3):247-57

Oommen A.M, Griffin, J.B, Sarath G, Zempleni J. Roles for nutrients in epigenetic events. (2005) J. Nutr. Biochem, *16*, pp. 74-77

Paik WK, Kim S. (1971). Protein Methylation: Enzymatic methylation of proteins after translation may take part in control of biological activities of proteins. Science *174*,114-119

Park, I.Y., Powell, R.T., Tripathi, D.N., Dere, R., Ho, T.H., Blasius, T.L., Chiang, Y.C., Davis, I.J., Fahey, C.C., Hacker, K.E. and Verhey, K.J. (2016). Dual chromatin and cytoskeletal remodeling by SETD2. Cell, *166*(4), pp.950-962

Pegg, A. E. & Jefferson, L. S. (1974). Effect of methylglyoxal bis(guanylhydrazone) on *S*-adenosylmethionine decarboxylase in the isolated perfused rat liver. FEBS Lett. *40*, 321-324

Pegg, A. E., Corti, A. & Williams-Ashman, H. G. (1973). Paradoxical enhancement of S-adenosylmethionine decarboxylase in rat tissues following administration of the

specific inhibitor methyl glyoxal bis(guanylhydrazone). Biochem. Biophys. Res. Commun. *52*, 696-701

Pendeville H, Carpino N, Marine JC, Takahashi Y, Muller M, Martial JA, Cleveland JL. (2001). The ornithine decarboxylase gene is essential for cell survival during early murine development. Mol Cell Biol. *21*:6549-58.

Pfeifer, G. P., Steigerwald, S. D., Hansen, R. S., Gartler, S. M., & Riggs, A. D. (1990). Polymerase chain reaction-aided genomic sequencing of an X chromosome-linked CpG island: methylation patterns suggest clonal inheritance, CpG site autonomy, and an explanation of activity state stability. Proceedings of the National Academy of Sciences of the United States of America, *87*(21), 8252–8256.

Philips, M. R., Pillinger, M. H., Staud, R., Volker, C., Rosenfeld, M. G., Weissmann, G., & Stock, J. B. (1993). Carboxyl methylation of Ras-related proteins during signal transduction in neutrophils. Science (New York, N.Y.), *259*(5097), 977–980.

Plath, K. (2003). Role of histone H3 lysine 27 methylation in X inactivation. Science *300*, 131–135

Plath, K. et al. (2004). Developmentally regulated alterations in Polycomb repressive complex 1 proteins on the inactive X chromosome. J. Cell Biol. *167*, 1025–1035

Pleshkewych, A., Kramer, D.L., Kelly, E. and Porter, C.W. (1980). Independence of drug action on mitochondria and polyamines in L1210 leukemia cells treated with methylglyoxal-bis (guanylhydrazone). Cancer research, *40*(12), pp.4533-4540.

Poletta FA, Rittler M, Saleme C, Campaña H, Gili JA, Pawluk MS, Gimenez LG, Cosentino VR, Castilla EE, López-Camelo JS. (2018). Neural tube defects: Sex ratio changes after fortification with folic acid. PLoS One. *13*(3):e0193127.

Pollex, T., & Heard, E. (2012). Recent advances in X-chromosome inactivation research. Current opinion in cell biology, *24*(6), 825-832.

Poulin R, Lu L, Ackermann B, Bey P, Pegg AE. (1992). Mechanism of the irreversible inactivation of mouse ornithine decarboxylase by alpha-difluoromethylornithine. Characterization of sequences at the inhibitor and coenzyme binding sites. J Biol Chem. *267*(1):150-8.

Pyrgaki, C., Trainor, P., Hadjantonakis, A.K., and Niswander, L. (2010). Dynamic imaging of mammalian neural tube closure. Dev Biol *344*, 941-947.

Quaderi, N. A., Schweiger, S., Gaudenz, K., Franco, B., Rugarli, E. I., Berger, W., Feldman, G. J., Volta, M., Andolfi, G., Gilgenkrantz, S., Marion, R. W., Hennekam, R. C., Opitz, J. M., Muenke, M., Ropers, H. H., & Ballabio, A. (1997). Opitz G/BBB syndrome, a defect of midline development, is due to mutations in a new RING finger gene on Xp22. Nature genetics, *17*(3), 285–291.

Quere I, Paul V, Rouillac C, Janbon C, London J, Demaille J, Kamoun P, Dufier JL, Abitbol M, Chasse JF. (1999). Spatial and temporal expression of the cystathionine beta- synthase gene during early human developent. Biochem Biophys Res Commun. *254*:127-37.

Radice, G.L., Rayburn, H., Matsunami, H., Knudsen, K.A., Takeichi, M., and Hynes, R.O. (1997). Developmental defects in mouse embryos lacking Ncadherin. Dev Biol *181*, 64-78

Raj K, Mufti GJ. (2006). Azacytidine (Vidaza(R)) in the treatment of myelodysplastic syndromes. Ther Clin Risk Manag. (*4*):377-88

Renwick JH. (1972). Hypothesis: Anencephaly and spina bifida are usually preventable by avoidance of a specific but unidentified substance present in certain potato tubers. Br Jf Prev Soc Med; *26*:67-88.

Ridley, A. J., & Hall, A. (1992). The small GTP-binding protein rho regulates the assembly of focal adhesions and actin stress fibers in response to growth factors. *Cell*, *70*(3), 389–399.

Rius M, Stresemann C, Keller D. (2009). Human concentrative nucleoside transporter 1-mediated uptake of 5-azacytidine enhances DNA demethylation. Mol Cancer Ther. *8*:225–31

Robert K, Vialard F, Thiery E, Toyama K, Sinet PM, Janel N. (2003). Expression of the cystathionine b synthase (CBS) gene during mouse development and immunolocalization in adult brain. Journal of Histochemistry and Cytochemistry. *51*:363-71.

Robert, K., Chassé, J. F., Santiard-Baron, D., Vayssettes, C., Chabli, A., Aupetit, J., Maeda, N., Kamoun, P., London, J., & Janel, N. (2003). Altered gene expression in liver from a murine model of hyperhomocysteinemia. The Journal of biological chemistry, *278*(34), 31504–31511.

Roffers-Agarwal, J., Lidberg, K. A., & Gammill, L. S. (2021). The lysine methyltransferase SETD2 is a dynamically expressed regulator of early neural crest development. Genesis (New York, N.Y. : 2000), *59*(10), e23448.

Rogner, U., Spyropoulos, D., Le Novère, N. *et al.* (2000). Control of neurulation by the nucleosome assembly protein-1–like 2. Nat Genet *25*, 431–435

Rolo, A., Savery, D., Escuin, S., de Castro, S.C., Armer, H.E., Munro, P.M., Mole, M.A., Greene, N.D., and Copp, A.J. (2016). Regulation of cell protrusions by small GTPases during fusion of the neural folds. Elife 5, e13273.

Rosen, M.B., Chernoff, N. (2002). 5-Aza-2'-deoxycytidine-induced cytotoxicity and limb reduction defects in the mouse. Teratology. *65*, 180-190.

Rougeulle, C. et al. (2004). Differential histone H3 Lys-9 and Lys-27 methylation profiles on the X chromosome. Mol. Cell. Biol. *24*, 5475–5484

Russell, D.H., Medina, V.J. and Snyder, S.H., (1970). The dynamics of synthesis and degradation of polyamines in normal and regenerating rat liver and brain. Journal of Biological Chemistry, *245*(24), pp.6732-6738.

Sadler TW, Greenberg D, Coughlin P, Lessard JL. (1982). Actin distribution patterns in the mouse neural tube during neurulation Science *215*:172–174.

Sadler, T. W. (1979). Culture of early somite mouse embryos during organogenesis. J Embryol Exp Morphol, *49*, 17-25.

Sah VP, Attardi LD, Mulligan GJ, et al. (1995). A subset of p53-deficientembryos exhibit exencephaly. Nat Genet *10*:175–180

Santagati, F., and Rijli, F.M. (2003). Cranial neural crest and the building of the vertebrate head. Nat Rev Neurosci *4*, 806-818

Sawyer, J.M., Harrell, J.R., Shemer, G., Sullivan-Brown, J., Roh-Johnson, M., Goldstein, B. (2010). Apical constriction: A cell shape change that can drive morphogenesis. Dev. Biol *341*, 5-19.

Schaefer M, Hagemann S, Hanna K, Lyko F. (2009). Azacytidine inhibits RNA methylation at DNMT2 target sites in human cancer cell lines. Cancer Res. *69*:8127–32.

Schoeftner, S. (2006). Recruitment of PRC1 function at the initiation of X inactivation independent of PRC2 and silencing. EMBO J. *25*, 3110–3122

Schorah, C. (2009). Dick Smithells, folic acid, and the prevention of neural tube defects. Birth Defects Research Part A: Clinical and Molecular Teratology, *85*: 254-259.

Scott, J.M., 1999. Folate and vitamin B12. Proc. Nutr. Soc. *58*, 441-448.

Seervai H, Riyad N. H. (2002). The Huntingtin-interacting protein SETD2/HYPB is an actin lysine methyltransferase.Sci. Adv.6,eabb7854.

Seervai, R. N. H., Jangid, R. K., Karki, M., Tripathi, D. N., Jung, S. Y., Kearns, S. E., Verhey, K. J., Cianfrocco, M. A., Millis, B. A., Tyska, M. J., Mason, F. M., Rathmell, W. K., Park, I. Y., Dere, R., & Walker, C. L. (2020). The Huntingtin-interacting protein SETD2/HYPB is an actin lysine methyltransferase. Science advances, *6*(40), eabb7854.

Seller MJ, Perkins-Cole KJ. (1987). Sex difference in mouse embryonic de-velopment at neurulation. J Reprod Fertil *79*:159–161

Seller MJ. (1987). Neural tube defects and sex ratios. Am J Med Genet. *26*:699–707.

Shaw GM, Carmichael SL, Yang W, Selvin S, Schaffer DM. (2004). Periconceptional dietary intake of choline and betaine and neural tube defects in offspring. Am J Epidemiol. *160*:102–9.

Shaw GM, Velie EM & Schaffer DM. (1997). Is dietary intake of methionine associated with a reduction in risk for neural tube defect-affected pregnancies? Teratology *56*, 295±299.

Shaw GM, Yang W, Finnell RH. (2020). Male-to-female ratios among NTDs and women's periconceptional intake of folic acid. Birth Defects Research. *112*: 1187–1193.

Shoob H.D, Sargent R.G, Thompson S.J, Best R.G, Drane, J.W, Tocharoen A. (2001). Dietary methionine is involved in the etiology of neural tube defect-affected pregnancies in humans. J Nutr, *131* (10). pp. 2653-2658

Shum ASW, Copp AJ. (1996). Regional differences in morphogenesis of the neuroepithelium suggest multiple mechanisms of spinal neurulation in the mouse. Anat Embryol. *194*(1):65-73.

Sibani, S., Melnyk, S., Pogribny, I.P., Wang, W., Hiou-Tim, F., Deng, L., Trasler, J., James, S.J. and Rozen, R. (2002). Studies of methionine cycle intermediates (SAM, SAH), DNA methylation and the impact of folate deficiency on tumor numbers in Min mice. Carcinogenesis, *23*(1), pp.61-65.

Smedley MJ, Stanisstreet M. (1986). Calcium and neurulation in mammalian embryos. II. Effects of cytoskeletal inhibitors and calcium antagonists on the neural folds of rat embryos. J Embryol Exp Morphol. *93*:167-78.

Smith JL, Schoenwolf GC. (1988). Role of cell-cycle in regulating neuroepithelial cell shape during bending of the chick neural plate. Cell Tissue Res. *252*:491-500.

Smithells, R. W., Sheppard, S., Schorah, C. J., Seller, M. J., Nevin, N. C., Harris, R., Read, A. P., & Fielding, D. W. (1981). Apparent prevention of neural tube defects by periconceptional vitamin supplementation. Archives of disease in childhood, *56*(12), 911–918.

Smithells, R.W., Sheppard, S., and Schorah, C.J. (1976). Vitamin deficiencies and neural tube defects. Arch Dis Child. *51*, 944-950.

Smithells, R.W., Sheppard, S., Schorah, C.J., Seller, M.J., Nevin, N.C., Harris, R., Read, A.P., and Fielding, D.W. (1980). Possible prevention of neural-tube defects by periconceptional vitamin supplementation. Lancet *1*, 339-340.

Steegers-Theunissen RP, Boers GH, Trijbels FJ, Finkelstein JD, Blom HJ, Thomas CM, Borm GF, Wouters MG, Eskes TK. (1994). Maternal hyperhomocysteinemia: a risk factor for neural-tube defects? Metabolism. *43*(12):1475-80.

Stiefel D, Copp AJ, Meuli M. (2007). Fetal spina bifida in a mouse model: loss of neural function in utero. J Neurosurg. *106*(3 Suppl):213-21.

Sudiwala, S., Palmer, A., Massa, V., Burns, A. J., Dunlevy, L. P. E., de Castro, S. C. P., Savery, D., Leung, K. Y., Copp, A. J., & Greene, N. D. E. (2019). Cellular mechanisms underlying *Pax3*-related neural tube defects and their prevention by folic acid. Disease models & mechanisms, *12*(11), dmm042234.

Suzuki, A., Hori, T., Nishino, T., Usukura, J., Miyagi, A., Morikawa, K., & Fukagawa, T. (2011). Spindle microtubules generate tension-dependent changes in the distribution of inner kinetochore proteins. Journal of Cell Biology, *193*(1), 125-140.

Suzuki, M., Hara, Y., Takagi, C., Yamamoto, T.S., Ueno, N. (2010). MID1 and MID2 are required for Xenopus neural tube closure through the regulation of microtubule organization. Development *137*, 2329-2339.

Suzuki, M., Morita, H., Ueno, N. (2012). Molecular mechanisms of cell shape changes that contribute to vertebrate neural tube closure. Dev. Growth Diff. *54*, 266-276.
Takeuchi IK, Takeuchi YK. (1985). 5-Azacytidine-induced exencephaly in mice. J Anat. May;140 (Pt 3)(Pt 3):403-12.

Takeuchi, I.K. and Murakami, U. (1978). The preventive influence of cysteamine on the terategenic action of 5-azacytidine. Life Sciences, *23*(9), pp.897-900.

Tan SS, Williams EA, Tam PP. (1993). X-chromosome inactivation occurs at different times in different tissues of the post-implantation mouse embryo. Nat Genet *3*:170–174.

Theiler K. (1989). The House Mouse. Atlas of embryonic development.New York: Springer-Verlag. p.94.

Tian, D. et al. (2010). The long noncoding RNA, Jpx, is a molecular switch for X chromosome inactivation. Cell *143*, 390–403

Toriello, H. V., & Higgins, J. V. (1983). Occurrence of neural tube defects among first-, second-, and third-degree relatives of probands: results of a United States study. American journal of medical genetics, *15*(4), 601–606.

Ueland PM. Pharmacological and biochemical aspects of *S*-adenosylhomocysteine and *S*-adenosylhomocysteine hydrolase. (1982). Pharmacological Reviews*. 34*:223–285.

Uyemura, D. G., S. S. Brown, and J. A. Spudich. (1978). Biochemical and structural characterization of actin from Dictyostelium discoideum. J. Biol. Chem *253*:9088-9096.

Vafai SB, Stock JB. (2002). Protein phosphatase 2A methylation: a link between elevated plasma homocysteine and Alzheimer's Disease. FEBS Lett. *518*(1-3):1-4.

Van Allen, M.I., Boyle, E., Thiessen, P., McFadden, D., Cochrane, D., Chambers, G.K., Langlois, S., Stathers, P., Irwin, B., Cairns, E., et al. (2006). The impact of prenatal diagnosis on neural tube defect (NTD) pregnancy versus birth incidence in British Columbia. J Appl Genet *47*, 151-158.

Van den Veyver IB. Genetic effects of methylation diets. (2002). Annu Rev Nutr. *22*:255-82.

VanAerts LAGJM, Poirot CM, Herberts CA, Blom HJ, De Abreu RA, Trijbels JMF. (1995). Development of methionine synthase, cystathionine-b-synthase and S-adenosyl-homocysteine hydrolase during gestation in rats. J Reprod Fertil. *103*:227-32.

Venolia, L., Gartler, S. M., Wassman, E. R., Yen, P., Mohandas, T., & Shapiro, L. J. (1982). Transformation with DNA from 5-azacytidine-reactivated X chromosomes. Proceedings of the National Academy of Sciences, *79*(7), 2352-2354.

Vermillion, K. L., Lidberg, K. A., & Gammill, L. S. (2014). Cytoplasmic protein methylation is essential for neural crest migration. The Journal of Cell Biology, *204*(1), 95–109.

Wald N, Sneddon J, Densem J, Frost C, Stone R. (1991). Prevention of neural tube defects: results of the Medical Research Council Vitamin Study. Medical Research Council Vitamin Study Research Group. Lancet. *338*, 131–7.

Wallace ME, Knights PJ, Anderson JR. (1978). Inheritance and morphology of exencephaly, a neonatal lethal recessive with partial penetrance, in the house mouse. Genet Res *32*:135–149.

Wallingford JB, Niswander LA, Shaw GM, Finnell RH. (2013) The continuing challenge of understanding, preventing, and treating neural tube defects. Science. *339*(6123):1222002.

Wang L, Wang F, Guan J. (2010). Relation between hypomethylation of long interspersed nucleotide elements and risk of neural tube defects. Am J Clin Nutr *91*:1359–1367

Wang, L., Lin, S., Zhang, J., Tian, T., Jin, L., & Ren, A. (2017). Fetal DNA hypermethylation in tight junction pathway is associated with neural tube defects: A genome-wide DNA methylation analysis. Epigenetics, *12*(2), 157–165.

Weber, M., Davies, J. J., Wittig, D., Oakeley, E. J., Haase, M., Lam, W. L., & Schübeler, D. (2005). Chromosome-wide and promoter-specific analyses identify sites of differential DNA methylation in normal and transformed human cells. Nature genetics, *37*(8), 853–862.

Werler S, Poplinski A, Gromoll J, Wistuba J. (2011). Expression of selected genes escaping from X inactivation in the 41, XX(Y)* mouse model for Klinefelter's syndrome. Acta Paediatr. *100*:885–891.

Werner JM , Maraki Y. Negesse, Dominique L. Brooks, Allyson R. Caldwell, Jafira M. Johnson, Rachel M. Brewster. Hingepoints and neural folds reveal conserved features of primary neurulation in the zebrafish forebrain (2020). BioRXiv.

Wilkinson DG. (1993). Molecular mechanisms of segmental patterning in the vertebrate hindbrain and neural crest. BioEssays. *15*:499-505.

Wlodarczyk, B. J., Palacios, A. M., George, T. M., & Finnell, R. H. (2012). Antiepileptic drugs and pregnancy outcomes. American journal of medical genetics. *PartA*, *158A*(8), 2071–2090.

Wutz, A. and Jaenisch, R. (2000). A shift from reversible to irreversible X inactivation is triggered during ES cell differentiation. Mol. Cell *5*, 695–705

Xu, W., Baribault, H., and Adamson, E.D. (1998). Vinculin knockout results in heart and brain defects during embryonic development. Development. *125*, 327-337.

Yamaguchi, Y., and Miura, M. (2013). How to form and close the brain: insight into the mechanism of cranial neural tube closure in mammals. Cell Mol Life Sci *70*, 3171-3186.

Yan, L., Zhao, L., Long, Y., Zou, P., Ji, G., Gu, A., and Zhao, P. (2012). Association of the maternal MTHFR C677T polymorphism with susceptibility to neural tube defects in offsprings: evidence from 25 case-control studies. PLoS One 7, e41689.

Yang L, Kirby JE, Sunwoo H, Lee JT. (2016). Female mice lacking Xist RNA show partial dosage compensation and survive to term. Genes Dev. *30*(15):1747-60.

Yang, F., Babak, T., Shendure, J., & Disteche, C. M. (2010). Global survey of escape from X inactivation by RNA-sequencing in mouse. Genome research, *20*(5), 614–622.

Ybot-Gonzalez, P., and Copp, A.J. (1999). Bending of the neural plate during mouse spinal neurulation is independent of actin microfilaments. Dev Dyn *215*, 273-283.

Ybot-Gonzalez, P., Gaston-Massuet, C., Girdler, G., Klingensmith, J., Arkell, R., Greene, N.D., and Copp, A.J. (2007). Neural plate morphogenesis during mouse neurulation is regulated by antagonism of Bmp signalling. Development *134*, 3203-3211.

Yoder JA, Walsh CP, Bestor TH, et al. (1997). Cytosine methylation and theecology of intragenomic parasites. Trends Genet *13*:335–340

Yoder, M., & Hildebrand, J. D. (2007). Shroom4 (Kiaa1202) is an actin-associated protein implicated in cytoskeletal organization. Cell motility and the cytoskeleton,*64*(1), 49–63.

Yu Z, Bhandari A, Mannik J. (2008). Grainyhead-like factor Get1/Grhl3 regulates formation of the epidermal leading edge during eye-lid closure. Dev Biol *319*:56–67.

Zaganjor, I., Sekkarie, A., Tsang, B.L., Williams, J., Razzaghi, H., Mulinare, J., Sniezek, J.E., Cannon, M.J., and Rosenthal, J. (2016). Describing the Prevalence of Neural Tube Defects Worldwide: A Systematic Literature Review. PloS one *11*, e0151586.

Zappia V, Zydek-Cwick C.R, Schlenk F. (1969). The specificity of *S*-adenosylmethionine derivatives in methyl transfer reactions. J. biol. Chem., *244*,pp. 4499-4509

Zhao, J. et al. (2008. Polycomb proteins targeted by a short repeat RNA to the mouse X chromosome. Science *322*, 750–756

Zohn, I.E., and Sarkar, A.A. (2012). Does the cranial mesenchyme contribute to neural fold elevation during neurulation? Birth Defects Res A Clin Mol Teratol *94*, 841-848.

Zwierzchowski, L., Członkowska, M., and Guszkiewicz, A. (1986). Effect of polyamine limitation on DNA synthesis and development of mouse preimplantation embryos in vitro. Reproduction *76*, 1, 115-121